AD NUMBER

AD821541

LIMITATION CHANGES

TO:

Approved for public release; distribution is unlimited.

FROM:

Distribution authorized to DoD only; Administrative/Operational Use; OCT 1967. Other requests shall be referred to Arnold Engineering Development Center, Arnold AFB, TN.

AUTHORITY

USAEDC ltr, 12 Jul 1974

ALTITUDE TESTING OF THE J-2 ROCKET ENGINE IN PROPULSION ENGINE TEST CELL (J-4) (TESTS J4-1554-20 THROUGH J4-1554-26)

M. R. Collier and N. S. Dougherty, Jr.
ARO, Inc.

October 1967

LARGE ROCKET FACILITY
ARNOLD ENGINEERING DEVELOPMENT CENTER
AIR FORCE SYSTEMS COMMAND
ARNOLD AIR FORCE STATION, TENNESSEE

NOTICES

When U. S. Government drawings specifications, or other data are used for any purpose other than a definitely related Government procurement operation, the Government thereby incurs no responsibility nor any obligation whatsoever, and the fact that the Government may have formulated, furnished, or in any way supplied the said drawings, specifications, or other data, is not to be regarded by implication or otherwise, or in any manner licensing the holder or any other person or corporation, or conveying any rights or permission to manufacture, use, or sell any patented invention that may in any way be related thereto.

Qualified users may obtain copies of this report from the Defense Documentation Center.

References to named commercial products in this report are not to be considered in any sense as an endorsement of the product by the United States Air Force or the Government.

ALTITUDE TESTING OF THE J-2 ROCKET ENGINE IN PROPULSION ENGINE TEST CELL (J-4) (TESTS J4-1554-20 THROUGH J4-1554-26)

M. R. Collier and N. S. Dougherty, Jr.
ARO, Inc.

AF - AEDC
Arnold AFB Tenn

FOREWORD

The work reported herein was sponsored by the National Aeronautics and Space Administration (NASA), Marshall Space Flight Center (MSFC), under System 921E, Project 9194.

The results of the tests presented were obtained by ARO, Inc. (a subsidiary of Sverdrup & Parcel and Associates, Inc.), contract operator of the Arnold Engineering Development Center (AEDC), Air Force Systems Command (AFSC), Arnold Air Force Station, Tennessee, under Contract AF40(600)-1200. Program direction was provided by NASA/MSFC; engineering liaison was provided by North American Aviation, Inc., Rocketdyne Division, manufacturer of the J-2 Rocket Engine, and by Douglas Aircraft Company, manufacturer of the S-IVB stage. The testing reported herein was conducted during the period from February 18 through April 4, 1967, in Propulsion Engine Test Cell (J-4) of the Large Rocket Facility (LRF) under ARO Project No. KA1554. The manuscript was submitted for publication on June 21, 1967.

This technical report has been reviewed and is approved.

Harold Nelson, Jr.
Captain, USAF
AF Representative, LRF
Directorate of Test

Leonard T. Glaser
Colonel, USAF
Director of Test

ABSTRACT

Twenty-two start and restart transient tests of the Rocketdyne J-2 rocket engine were conducted at pressure altitudes from 95,000 to 111,000 ft in Propulsion Engine Test Cell J-4 of the Large Rocket Facility, Arnold Engineering Development Center. A flight configuration J-2 engine (S/N J-2052) and S-IVB battleship stage were used. Engine restarts were made at crossover duct and turbine hardware conditions predicted for coast periods of both one and two orbits. Engine starts were made at both S-IB/S-IVB and S-V/S-IVB predicted flight conditions. Firing durations were programmed for 5 or 30 sec, and the accumulated firing time for the test period was 352.26 sec. This test series completed the orbital restart problem investigation and demonstrated successful engine restart at simulated orbital conditions.

CONTENTS

APPENDIXES

I. ILLUSTRATIONS

Figure

Page

II. TABLES

NOMENCLATURE

A	Area
AS	Apollo Saturn
ASI	Augmented spark igniter
ECA	Electrical control assembly
E.S.	Engine start
ESCS	Engine safety cutoff system
ESTDCS	Event, start tank discharge control solenoid energized

GG	Gas generator
MFV	Main fuel valve
MOV	Main oxidizer valve
O/F	Oxidizer to fuel ratio, mixture ratio
OTBV	Oxidizer turbine bypass valve
PCC	Prechill controller
PU	Propellant utilization
RTT	Resistance temperature transducer
SAM	Stall approach monitor
STDV	Start tank discharge valve
V	Velocity
VSC	Vibration safety cutoff
W	Weight flow
Δ	Difference in two values
ρ	Density
	Other symbols are defined in Table IV.

SUBSCRIPTS

e	Exit
f	Force, fuel
m	Mass
o	Oxidizer
t	Throat

SECTION I
INTRODUCTION

The J-2 engine (S/N J-2052) test program at the Arnold Engineering Development Center (AEDC) continued during this test period on an accelerated schedule (seven-day week, three shifts) to fulfill testing requirements in support of the Saturn V/501 launch, as requested by the National Aeronautics and Space Administration, Marshall Space Flight Center (NASA/MSFC). The J-2 engine, using S-IVB battleship tankage, has been undergoing testing since July 1966 in Propulsion Engine Test Cell J-4 (Fig. 1, Appendix I) of the Large Rocket Facility (LRF). The tests reported herein, J4-1554-20 through J4-1554-26, were conducted from February 18 through April 4, 1967. Twenty-two engine starts were made at pressure altitudes ranging from 95,000 to 111,000 ft. The accumulated firing time for this report period was 352.26 sec.

These tests are a continuation of those reported in Ref. 1 in support of the Saturn V/501 launch. Earlier testing (Ref. 2) revealed excessive gas generator (GG) combustion temperatures during simulated orbital restart tests. The Saturn V first flight (AS-501) schedule was to have been impacted had this problem not been resolved in time to support the existing schedule. The test series was conducted and successfully completed without schedule impact. Based on the results of the previous tests, the following successful solutions to the problem of engine restart were made for the tests reported herein: (1) propellant utilization (PU) valve open (-29 deg) for restart as opposed to null (0 deg); (2) main oxidizer valve second stage travel timed for 1650 msec, as opposed to 1825 msec; and (3) the selection of pressures and temperatures for start gas which duplicate those expected during orbital restart, using a selected start tank vent and relief valve to limit start gas energy.

SECTION II
APPARATUS

2.1 TEST ARTICLE

The test article was a J-2 rocket engine (S/N J-2052), designed and developed by Rocketdyne Division of North American Aviation, Inc., and an S-IVB battleship stage designed and developed by Douglas Aircraft Company. The fluid-dynamic characteristics of the test stage are identical

to the S-IVB flight vehicle. The J-2 rocket engine is a multiple-restart engine that utilizes liquid oxygen (LO_2) and liquid hydrogen (LH_2) as propellants and is designed to be used individually or in clusters. Thrust rating of the engine is 225,000 lb_f at an oxidizer-to-fuel mixture ratio (O/F) of 5.5. A cutaway view of the test article is presented in Fig. 2. Figure 3 shows the basic components of the J-2 engine.

The major engine components at the beginning of this test period are shown in Table I (Appendix II). All engine configuration changes accomplished during this test period are presented in Tables II and III. Thrust chamber heater blankets (P/N 105906 through 105906-15) were installed prior to this test series and consisted of 16 sections of film-type, electrical heating elements applied to the thrust chamber between the throat and nozzle exit; the blankets were covered with aluminum foil secured with an overlay of wire mesh. The blankets were subsequently insulated externally with Larodyne® and aluminum foil over the Larodyne; each entire segment consisted of heater blankets, Larodyne insulation, and aluminum foil, and a band of wire mesh to secure the aluminum foil and Larodyne. Figure 4 shows the engine before and after thrust chamber heater blanket installation and insulation.

2.1.1 J-2 Rocket Engine

The J-2 rocket engine (Ref. 3, Fig. 3), features the following major components:

1. a regeneratively fuel-cooled, tubular-wall, bell-shaped thrust chamber (Fig. 5) with a throat area (A_t) of 170.4 $in.^2$ and an expansion ratio (A_e/A_t) of 27.1. Thrust chamber length (from the injector flange to nozzle exit) is 107 in.
2. a concentric-orificed, porous-faced thrust chamber injector (Fig. 6). Orifice areas for fuel and oxidizer injection are 25 and 16 $in.^2$, respectively. Fuel flow through the porous face of the injector is three to four percent of thrust chamber fuel flow rate.
3. an augmented spark igniter assembly (ASI) (Fig. 7) to which fuel and oxidizer are routed and ignited at engine start to provide ignition energy for main chamber propellants.
4. a fuel turbopump which is composed of a two-stage turbine-stator assembly, an inducer, and a seven-stage, axial-flow pump. The pump is self-lubricated and nominally produces a head rise of 35,517 ft of hydrogen (H_2) at a flow rate of 8414 gpm for a rotor speed of 26,702 rpm at rated conditions.

5. an oxidizer turbopump which is composed of a two-stage turbine-stator assembly and a single-stage centrifugal pump. The pump is self-lubricated and nominally produces a head rise of 2117 ft of LO_2 at a flow rate of 2907 gpm for a rotor speed of 8572 rpm at rated conditions.

6. a motor-driven, PU valve (Fig. 8), mounted on the oxidizer turbopump, which bypasses LO_2 from the discharge to the inlet side of the oxidizer pump to vary mixture ratio to provide simultaneous depletion of propellants.

7. oxidizer and fuel bleed valves allow trapped gas to be expelled from the engine propellant system prior to engine start. These valves permit the propellant recirculation flow to return to the stage propellant tanks and are closed at engine start.

8. a gas generator (GG) (Fig. 9) which consists of a combustion chamber containing two spark plugs, a valve which controls the oxidizer and fuel poppets, and an injector assembly. The high-energy gases produced by the GG are routed to the fuel turbine, through the turbine crossover duct to the oxidizer turbine and are exhausted through eyelets into the thrust chamber at an area ratio (A/A_t) of approximately 11.

9. a pneumatically actuated, oxidizer turbine bypass valve (OTBV). At engine start, the OTBV is fully open, routing a large portion of fuel turbine discharge gas directly to the thrust chamber to obtain the desired O/F turbine spinup relationship. During engine acceleration to mainstage, the OTBV is closed (the valve gate contains a flow nozzle which provides a turbine power balance mechanism).

10. an integral, high-pressure gaseous hydrogen (GH_2) start tank and helium (He) control bottle. A pneumatically actuated, normally closed, start tank discharge valve (STDV), controlled by a solenoid-operated valve, permits release of the start tank GH_2 for turbine spinup during the engine start cycle. The He control bottle, located within the H_2 start tank, provides a high-pressure He supply to the engine pneumatic control system. The start tank is refilled (from fuel injector and manifold supplies) during the initial 60 sec of engine mainstage operation.

11. a pneumatically actuated, main fuel valve (MFV) which is a normally closed, butterfly-type valve.
12. a two-stage, main oxidizer valve (MOV) which is a pneumatically actuated, normally closed, butterfly-type valve. The first stage actuator positions the MOV at the 14-deg position to obtain initial main chamber ignition; the second stage actuator ramps the MOV fully open to accelerate the engine to mainstage operation. The MOV gate is pivoted offcenter (Fig. 10), providing MOV hydraulic torque in the closing direction at the 14-deg position.
13. a pneumatic control package which controls all pneumatically operated engine valves and purges.
14. an electrical control assembly (ECA) which provides the electrical logic required for proper sequencing of engine components during operation. It also provides energy for the GG and ASI spark plugs.
15. primary and auxiliary flight instrumentation packages which environmentally protect and contain sensors required to monitor critical engine parameters.

2.1.2 Vehicle Tank Pressurization

S-IVB vehicle fuel tank pressurization gas is supplied in flight by GH_2 from the engine as shown in Fig. 11. In the tests of the J-2 engine at AEDC, this engine-supplied gas for tank pressurization was not used. The gas, instead, was routed to the facility H_2 venting system through a nozzle for measurement purposes. This flow was capped off for Tests 21 through 25.

The vehicle LO_2 tank pressurization flow is supplied in flight (S-II Stage) from the engine through an engine-mounted heat exchanger as shown in Fig. 11. This flow was also capped off for Tests 20 through 26.

2.1.3 S-IVB Stage

The S-IVB battleship stage is approximately 22 ft in diameter and 49 ft long and has a maximum capacity of 46,000 lb of LH_2 and 199,000 lb of LO_2. The major components of the S-IVB stage are: (1) propellant tanks, fuel above oxidizer, separated by a common bulkhead; (2) propellant prevalves which serve as emergency engine shutoff valves and are normally closed during the recirculation chilldown procedure; (3) propellant low pressure ducts which, external to the tanks, route propellants

to the engine pump inlets; (4) propellant recirculation systems which circulate the propellants through the low-pressure ducts and turbopumps to stabilize pump temperatures near normal operating levels and thereby prevent temperature stratification in the propellant tanks prior to engine start; (5) vent and relief valve systems for both propellant tanks; and (6) a He storage system within the fuel tank (sealed and not utilized for testing at AEDC).

2.2 TEST CELL

Propulsion Engine Test Cell (J-4), Fig. 12, is a vertically oriented test unit designed for static testing large liquid-propellant rocket engines and propulsion systems at pressure altitudes of 100,000 ft. The cell is currently capable of testing engines in the 500,000-lb_f thrust class (maximum capability is 1,500,000 lb_f). The cell consists of four major components: (1) test capsule, 48 ft in diameter and 81 ft in height, situated at grade level and containing the test article; (2) spray chamber, 100 ft in diameter and 250 ft in depth, located directly beneath the test capsule to provide exhaust gas cooling and dehumidification; (3) coolant water, steam, nitrogen [gaseous (GN_2) and liquid (LN_2)], H_2 (gaseous and liquid), LO_2, and gaseous helium (GHe) storage and delivery systems for operation of the cell and test article; and (4) control building, located about 600 ft from the cell, containing test article controls, cell equipment controls, and data acquisition equipment. Exhaust machinery is connected with the spray chamber. This machinery maintains the test capsule at a pressure altitude of approximately 60,000 ft during the test period, with the exception of engine firing. During firing operations, the facility steam ejector, in conjunction with the exhaust machinery, provides a pressure altitude of 100,000 ft in the test capsule. A detailed description of the test cell is presented in Ref. 4.

The S-IVB battleship stage was installed on a support stand within the test capsule (Fig. 13), orienting the J-2 engine vertically downward on the centerline of the diffuser-steam ejector assembly. This assembly consists of a 20-ft-diam diffuser duct, 150 ft in length, containing a centerbody steam ejector. At the inlet to the diffuser is a 13.5-ft-diam diffuser insert, directly above which is a GN_2 annular ejctor. The annular ejector was provided to suppress steam recirculation into the test capsule during steam ejector shutdown. The test cell was also equipped with (1) a GN_2 purge system for continuously inerting the normal air-in-leakage of the cell; this purge is introduced at the top of the test capsule; (2) a GN_2 repressurization system for raising test cell pressure, after engine cutoff, to a level equal to spray chamber pressure and for rapid

emergency inerting of the capsule; this is also introduced at the top of the test capsule; (3) a spray chamber LN_2 supply and distribution manifold for initially inerting the spray chamber and exhaust ducting and for increasing the molecular weight of the H_2-rich exhaust products during engine operation.

2.3 INSTRUMENTATION

Instrumentation systems were provided to measure engine, stage, and facility parameters. Table IV provides a list of selected measurements. The location of selected engine and stage instrumentation used during this test series is presented in Fig. 14. The engine instrumentation was comprised of (1) flight instrumentation for the measurement of critical engine parameters and (2) facility instrumentation which was provided as backup for the flight instrumentation and to measure additional engine parameters. The flight instrumentation was provided and calibrated by the engine manufacturer; facility instrumentation was initially calibrated and periodically recalibrated at AEDC.

Pressure measurements were made using strain-gage-type pressure transducers. Temperature measurements were made using resistance temperature transducers (RTT) and a combination of copper-constantan, iron-constantan, and Chromel®-Alumel® thermocouples. Oxidizer and and fuel turbopump shaft speeds were sensed by magnetic pickup. Fuel and oxidizer flow rates to the engine were measured by turbine-type flowmeters which are an integral part of the engine. The propellant recirculation flow rates were monitored with turbine-type flowmeters provided in the supply lines by the S-IVB stage manufacturer. Engine side loads were measured with dual-bridge, strain-gage-type load cells which were laboratory calibrated prior to installation. Vibrations produced during engine operation were measured by accelerometers mounted in the vertical plane on the oxidizer dome and in the horizontal planes on the turbopumps. Primary engine and stage valves were instrumented with linear potentiometers and limit switches.

The data acquisition systems were calibrated by (1) precision electrical shunt resistance substitution for the pressure transducers, load cells, and RTT units, (2) voltage substitution for the thermocouples, (3) frequency substitution for shaft speeds and flowmeters, and (4) frequency voltage substitution for accelerometers.

The types of data acquisition and recording systems used during this test period were (1) a multiple-input digital data acquisition system (Microsadic®) scanning each parameter at 40 samples per second and

recording on magnetic tape, (2) single-input, continuous-recording FM systems recording on magnetic tape, (3) photographically recording galvanometer oscillographs, (4) direct-inking, null-balance potentiometer-type X-Y plotters and strip charts, and (5) optical data recorders. Applicable systems were calibrated prior to each test (atmospheric and altitude calibrations). Television cameras, in conjunction with video tape recorders, were used to provide visual coverage during an engine firing, as well as replay capability for rapid examination of unexpected events.

SECTION III
CONTROL SEQUENCE

Control of S-IVB battleship stage, J-2 engine, and test cell systems during the terminal countdown was centrally provided from the test cell control room. The less-critical facility, stage, and certain J-2 engine functions were manually controlled. Other functions were programmed to the facility countdown sequencer which provided (1) verification of the readiness of critical systems to proceed with engine firing and (2) a necessary time display for integrating the manual operations into the countdown. The critical engine and stage operations were controlled by a facility logic network which interconnected the required systems to start and shut down the engine safely. The facility control logic was activated at T - 0.5 sec (sequencer time) by the sequencer. The facility and engine controls are briefly described in the following sections.

3.1 FACILITY CONTROL LOGIC

The facility logic was an electrical control network designed to interconnect the engine control system, major stage systems, the engine safety cutoff system (ESCS), observer cutoff circuits, and the countdown sequencer. A diagram of the facility control logic is shown in Fig. 15. The primary functions normally performed by the facility logic were to:

1. ascertain facility and engine systems ready to test,
2. open stage propellant prevalves,
3. shutoff stage propellant recirculation pumps and close recirculation valves,
4. apply start signal to engine control logic, and

5. initiate facility systems shutdown at expiration of sequencer-programmed run duration - this involved closing the prevalves and initiating facility-supplied engine purges.

The countdown sequencer was programmed to function with the facility logic as follows:

1. at T - 1 sec, verify systems ready, or stop countdown;
2. at T - 0.5 sec, apply firing command to facility logic;
3. at T - 0 sec, stop sequencer countdown until either (a) the facility logic started the engine to yield STDV solenoid energized or (b) an engine safety cutoff was obtained: if (a), the sequencer resumed counting for the preset length of run and applied an engine cutoff signal at expiration of run duration as well as initiated facility systems shutdown sequence; if (b), the sequencer initiated facility systems shutdown sequence.

The time between "fire" command and engine start varied (as a function of prevalve opening time); it was nominally 8 sec.

A modification to the facility logic[1] was performed to meet requirements to simulate the engine first-burn start sequence on S-V/S-IVB (flight 501). This modification, called the "auxiliary" logic, was to simulate the following sequence:

Time, sec	Event
T_4	S-V/S-II Engine Cutoff
$T_4 + 0.2$	Command S-IVB/S-V Prevalves Open
$T_4 + 1.0$	S-V/S-IVB Engine Start
$T_4 + 1.4$	Shutdown Oxidizer Recirculation Pump
$T_4 + 2.2$	Shutdown Fuel Recirculation Pump

The modifications were accomplished (Fig. 15) and utilized initially on Tests -17A and -17C (Ref. 1). A test safety feature was also provided for the auxiliary logic to prevent STDV opening, if both stage prevalves

[1]The normal facility logic closely simulated prevalve sequencing on S-V/S-IVB (flight 501) engine restart.

were not fully open (the signal to energize the STDV solenoid would produce an automatic engine cutoff in this case).

Automatic engine cutoff circuitry was provided in the facility logic (sequence monitor or start "OK" timer expiration) as well as in the ESCS. The ESCS monitored engine vibration and GG outlet temperature. Engine vibration, sensed by accelerometers mounted on the oxidizer dome, was required to sustain a level equal to or greater than ±150 g's for 150 msec to produce an engine cutoff. Prior to Test 24 this time was increased to 200 msec. The GG outlet temperature was required to exceed 2000°F (effective 0.8 sec after mainstage solenoid energized) to produce an engine cutoff. This limit was changed to 2200°F (effective 0.7 sec after mainstage solenoid energized) prior to Test 17. An engine cutoff was also produced if GG outlet temperature (a) exceeded 1450°F, effective 3.5 sec after mainstage solenoid energized or (b) failed to achieve 250°F by 0.8 sec after mainstage solenoid energized. An additional cutoff circuit was added during the test series. Titled stall approach monitor (SAM), this system monitored fuel flowmeter output to provide cutoff at flowmeter speeds less than 95 cps for a 55-msec period after mainstage control solenoid energized plus 135 msec.

3.2 ENGINE SEQUENCE

3.2.1 Engine Start Sequence

An engine schematic and an engine starting sequence diagram are presented in Figs. 11 and 16, respectively. Initiation of engine start start command (facility initiated) activates the engine start module which simultaneously opens the He control valve, the ignition phase control valve, and energizes the ASI and GG spark plug exciters. The STDV delay timer is also energized at engine start command. The He control valve initiates filling of the pneumatic accumulator, closes the propellant bleed valves, and purges the oxidizer dome and GG oxidizer injector manifold through the purge control valve. The ignition phase solenoid opens the ASI oxidizer valve and the main fuel valve, and supplies pressure to the inlet port of the sequence valve located within the MOV first stage actuator. With the ASI oxidizer valve and the main fuel valve open, propellants flow under static head to the ASI chamber and are ignited. If the main fuel valve is 90-percent open, a sequence valve supplies pressure to the STDV solenoid control valve.

A normal engine sequence will continue with the opening of the STDV and the energizing of the ignition phase timer (440-msec timer), if the

following conditions exist: (1) the main fuel valve and fuel sequence valve are open, (2) proper fuel quality at the injector is verified by a fuel injection temperature below -150°F, (3) STDV control timer has expired (640-msec[2] timer initiated at engine start), and (4) the fuel lead timer has expired. With these four conditions satisfied, the STDV opens to release GH_2 to the fuel and oxidizer turbines. Once the ignition phase timer has expired, the STDV is closed by de-energizing the control solenoid, a 3.3-sec spark plug de-energize timer is activated, and the mainstage control module is energized. If ASI ignition has not been detected (ASI ignition detect probe), upon expiration of the ignition phase timer, engine cutoff will occur. After the mainstage control module is energized, the mainstage control valve opens, venting He pressure from the MOV closing actuator and the opening port of the purge control valve. The purge control valve closes, and the oxidizer dome and GG oxidizer purges are terminated. Opening pressure is applied to the MOV actuators, and the MOV first atage opens. A sequence valve in the MOV supplies pressure to open the GG control valve and to close the OTBV. Fuel and oxidizer flow to the GG are controlled by poppets in the GG control valve that open sequentially to provide a fuel lead. Gases generated are directed in series to the fuel and oxidizer turbines. The second stage of the MOV is sequenced to start opening approximately 0.6 sec after the mainstage control valve is opened. The second stage valve ramp time is controlled by venting closing pressure through an orificed check valve. As the propellant turbopumps approach steady-state operation, the "mainstage OK" signal is generated by an oxidizer injector pressure switch and steady-state engine operation follows. If the mainstage OK signal has not been initiated before expiration of the sparks de-energize timer, engine cutoff will occur. The time from engine start command to mainstage OK signal is primarily dependent upon the fuel lead time; the relative time between engine starting events may be obtained from Fig. 17a.

3.2.2 Engine Shutdown Sequence

A cutoff signal simultaneously de-energizes the control solenoids for closing the mainstage and ignition phase control valve and energizes the He control de-energize timer. Opening control pressure for the MOV actuator, ASI oxidizer valve, and main fuel valve is vented. Pressure is supplied to close the MOV, to open the purge control valve, to close the ASI oxidizer valve, to close the main fuel valve, and to open the fast shutdown control valve. Oxidizer dome and GG oxidizer line purges begin upon decay of the thrust chamber and GG pressures below the He control pressure. With the exception of the normally open propellant bleed

---

[2]A replacement ECA was installed following Test 20 which had a 1000-msec STDV control timer.

valves and the OTBV, all valves are normally closed. Expiration of the He control de-energize timer closes the He control valve, venting control system pressure through the oxidizer dome and GG oxidizer purge lines. Once He control pressure decays to actuation pressure of the purge control valve, the valve closes to stop the purges. Closing pressure of the propellant bleed valve is bled off through the MFV closing vent port, and these valves open under spring pressure. The engine cutoff sequence is presented in Fig. 17b.

SECTION IV
PROCEDURE

Preoperational procedures were begun several hours prior to each test. All consumable storage systems were replenished, and engine inspections and leak checks were conducted. Propellant tank pressurants and engine pneumatic and purge gas samples were taken to ensure that specification requirements were met. (Chemical analysis of propellants was provided by the propellant suppliers.) Facility sequence, engine sequence (see Tables V and VI), and engine abort checks were conducted within a 24-hr time period before an engine firing to verify the proper sequence of events. The abort checks consisted of electrically simulating engine malfunctions to verify the occurrence of an automatic engine cutoff signal. Engine and facility sequence checks consisted of verifying the timing of all engine and facility valves and events to be within specified limits. Engine drying procedures recommended by the manufacturer were performed. A final engine sequence check was conducted immediately preceding each test period.

Oxidizer dome, GG oxidizer injector, and thrust chamber jacket purges were initiated prior to evacuating the test cell (engine purges required for a typical test period are presented in Table VII). Upon completion of instrumentation calibrations at atmospheric conditions, the test cell was evacuated to approximately 0.5 psia with the exhaust machinery, instrumentation calibrations at altitude conditions were conducted, and a cell air in-leakage evaluation was subsequently performed. Immediately prior to loading propellants on board the vehicle, the cell and exhaust-ducting atmosphere was inerted with approximately 20,000 lb of N_2 to reduce the O_2 content to less than 4.9 percent by volume (lower flammability limit of H_2-O_2-N_2 mixtures). At this same time, the cell N_2 purge was initiated at a rate equivalent to the cell air inleakage multiplied by 3.2. This cell purge (6 to 10 lb/sec) continuously inerted the air leaking into the cell for the duration of the test period. The vehicle propellant tanks were then loaded to the 30 percent level (a test safety maximum), and the remainder of the terminal countdown was conducted. A typical terminal countdown is presented in Ref. 2.

Engine restart tests were conducted at a time determined by observation of turbine crossover duct temperatures after first-burn engine cutoff to achieve crossover duct temperature requirements at engine start. Secondary requirements for the restart tests were dry, low-pressure propellant ducts prior to initiation of propellant recirculation. Helium purges were connected to both fuel and oxidizer low-pressure ducts for drying immediately after first-burn engine cutoff. Normally, however, the ducts were dry within 15 min after first-burn cutoff and the duct purges were not required. During this test series, turbine crossover duct, closing control line to the MOV second stage actuator, and pneumatic control package, low-temperature conditioning became a requirement on some firings. The crossover duct was chilled internally by the introduction of cold He through an instrumentation fitting; the MOV closing control line and the pneumatic package were externally chilled with He. The GG oxidizer supply line was also conditioned externally with 40 to 60°F N_2 during Test 26. Since the line was relatively long, a shroud was installed to contain the gas as shown in Fig. 18. Conditioning with these systems normally began about 1 hr prior to engine start; the conditioning systems were shut down 30 to 60 sec prior to engine start. The ASI fuel supply line was conditioned, beginning with Test 24, to simulate ullage motor heating. Heater tape was used to provide the required temperatures on the lower two-thirds and upper one-third of the line, separately.

SECTION V
RESULTS AND DISCUSSION

5.0 GENERAL

Earlier testing of the J-2 engine at AEDC (Refs. 1 and 2) isolated and verified the existence of an orbital restart problem of excessive GG temperature because of the warm turbine hardware condition following the engine first burn. The primary objective of the series of tests included in this report was to verify that the solutions selected and/or contemplated for Saturn V/501 were adequate to achieve successful J-2 engine restart in orbit. Specific objectives by test number are listed in Table VIII. Although not all these tests were specifically Saturn V/501 restart oriented, all of the test results are related to expected flight profile predictions for the 500 series Saturn V flights.

A test matrix specifying required starting conditions is presented in Table IX. The test conditions, results, and selected engine parameters measured for each test are shown in Table X. Altitudes shown in this table are pressure altitudes (geometric) from Ref. 5. Pump inlet and start

tank conditions for each test are shown plotted on safe starting maps in Figs. 19 and 20. General test results are presented in Table XI. The results discussed in succeeding paragraphs are of specific tests which were selected as best illustrating the points of discussion.

5.1 ENGINE RESTART

5.1.1 Gas Generator Overtemperature

Altitude restart GG overtemperatures first occurred during Tests 11B (Ref. 2) and 13B (Ref. 1), which were both terminated by the ESCS. The suspected restart problem was verified to exist with the overtemperature condition (2410°F at cutoff) experienced during Test 13B. These high temperatures were caused by several factors, which are discussed in subsequent paragraphs of this section.

5.1.1.1 Gas Generator Temperature Initial Peak

The initial temperature peak was primarily affected by the following conditions:

(a) Thrust Chamber Tube Temperature - Colder temperatures cause higher GG temperature peaks because of reduced fuel system resistance. Lowered resistance, in effect, reduces main chamber flow blockage and results in reduced fuel flow to the GG during transient operation. The resulting higher GG O/F ratio increases temperature.

(b) Crossover Duct and Turbine Temperature - Warmer crossover duct and turbine temperatures cause higher GG temperature peaks because of energy transfer between the duct/turbines and the start gas. The higher energy transfer from warmer duct temperatures results primarily in a faster LO_2 pump spinup, higher LO_2 pump discharge pressure, and therefore, higher GG O/F ratio.

(c) Start Gas Energy - Start gas energy level affects both fuel and oxidizer pump spinup for start tank discharge. Succeeding paragraphs will show that changes in oxidizer pump spinup are primarily caused by start gas temperature. Oxidizer pump spinup, for a given crossover duct temperature, is shown to increase with colder start gas temperature. Fuel pump spinup is shown to increase with higher start gas pressure. Variations in start gas total energy were achieved by changes

in both pressure and temperature that, for some tests, showed no effect on peak GG temperature. Higher energy achieved by decreasing temperature (providing greater mass at constant pressure) increases GG peak temperature because of the start gas-crossover duct temperature relationship.

5.1.1.2 Gas Generator Temperature Overshoot

The GG temperature overshoot (second peak) is primarily a function of the main oxidizer valve timing. The MOV plateau time (time at the 14-deg position) varies with second stage opening time which is controlled by a thermostatic orifice (S-IVB application) in the closing control pressure side of the valve. Colder MOV components and control gases also lengthen valve opening time. The MOV plateau time is also a function of hydraulic torque which, because of valve geometry, creates a closing force on the valve when the valve is at the 14-deg position.

The overshoot temperature is reduced if the MOV leaves the plateau earlier because the MOV restricts oxidizer flow to the main chamber, forcing more oxidizer to the GG until it begins the second stage ramping movement and relieves the restriction.

5.1.2 Restart Problem Solutions Demonstrated

Comparison of data from Tests 13B and 25D shows the results of the solutions that were made to solve the problem of the GG overtemperature. These solutions incorporated for test 25D were:

1. The propellant utilization valve positioned in the full-open position as opposed to the null- or zero-deg position for engine start. (Figure 21 shows PU valve position as a function of engine mixture ratio.)
2. Sizing of the MOV closing control orifice to provide a 1650 msec dry sequence ramping time as opposed to 1825 msec.
3. Selection and use of a start tank vent and relief valve with a low specification relief setting to limit start gas energy. (Figure 20 shows the upper relief limit of the selected valve imposed on the safe starting map for the J-2 start tank gas.)

The crossover duct and turbine temperature conditions for Test 25D were those expected for orbital restarts 90 min after first burn (a one-orbit coast period).

Conditions at ESTDCS for Tests 13B and 25D were:

	Test 13B	Test 25D
Start Tank Pressure, psia	1359	1323
Temperature, °F	-218	-217
Total Energy, Btu	2974	2904
LO_2 Pump Inlet Pressure, psia	41.2	41.4
Temperature, °F	-291	-295.4
Fuel Pump Inlet Pressure, psia	36.1	37.2
Temperature, °F	-421.2	-419.9
Thrust Chamber Temperature, °F	-167	-239
Fuel Lead Time, sec	4.7	8.0
Crossover Duct Temperature, °F	233	185
LO_2 Turbine Inlet Temperature, °F	292	323
MOV Closing Control Line Temperature, °F	---	-140
Pneumatic Control Package Temperature, °F	---	-140
PU Valve Position	Null	Open
MOV Dry Sequence Time (Nominal), msec	1810	1650

Start transient comparisons of these two tests are shown in Fig. 22. The lower GG temperature overshoot during Test 25D resulted from lower GG oxidizer injection pressure because of the lower oxidizer pump discharge pressure. The GG temperatures during Test 25D were 2150 and 2180°F, peak and overshoot, respectively.

Comparison of these two tests shows the total effectiveness of the above-listed solutions to the overtemperature problem. The effects of the three solutions are discussed in the following paragraphs of this section. It is shown that for successful engine restart with the elevated turbine hardware temperatures expected for flight that the open PU valve solution had a large effect in alleviating the problem and that the selected start tank vent and relief valve and MOV reorificing solutions proved to be relatively ineffectual.

5.1.3 Temperature Peak Comparisons

5.1.3.1 Cold Thrust Chamber Effects

Colder thrust chamber temperatures can be expected to increase the GG temperature peak, all other factors being equal. This is illustrated in Fig. 23 which is a comparison of the results of Tests 23C and 24A. Average thrust chamber temperatures at ESTDCS were 140°F colder during Test 23C than during Test 24A. The other variables affecting GG temperature can be seen from Table X to agree closely for these two tests, with the exception of pump inlet pressures. Pump inlet conditions are shown (Section 5.1.3.4) to have little effect on first peak temperatures. Pump inlet differences, though small, for these two tests would be expected to lower slightly the peak temperature measured during Test 24A. The peak GG temperature difference shown for the 140°F thrust chamber temperature difference was 480°F. Figure 23 shows, that, for this thrust chamber temperature difference (ΔT), the fuel pump discharge pressure and speed were increased for Test 24A because of increased thrust chamber resistance. The result of this higher fuel pump discharge pressure was a lower oxidizer-fuel pressure difference (ΔP) at the GG injector (lower O/F ratio). Warmer thrust chamber temperatures, therefore, increase resistance and lower GG peak temperatures, and cold thrust chamber temperatures increase peak GG temperatures.

5.1.3.2 Hot Crossover Duct Effects

S-IVB orbital predictions for one- and two-orbit coast periods have shown that the crossover duct could be expected to cool to temperatures of 165°F for a one-orbit coast and 125°F for a two-orbit coast. Crossover duct and turbine temperature is shown to have a significant effect on the GG temperature spike by comparison of the results of Tests 26B and 26D (Fig. 24). The comparative conditions for these two tests are:

	Test 26B	Test 26D
Crossover Duct Temperature, °F	62	145
Oxidizer Turbine Inlet Temperature, °F	77	277
Start Gas Temperature, °F	-195	-215
Start Gas Energy, Btu	2846	2868
GG Temperature Peak, °F	1950	2220

Comparisons in Table X of other variables affecting GG temperature are shown to agree closely. Although there is only a 16°F difference in thrust chamber temperatures, the colder temperature during Test 26D would be expected to increase the Test 26D temperature slightly. Crossover duct temperature does, therefore, have a major effect on GG temperature peak. The hotter crossover duct is shown in Fig. 24 to produce a higher LO_2 pump spinup on start tank discharge, thereby giving a higher LO_2 pump discharge pressure relative to fuel pump discharge pressure. The higher LO_2 pressure is then reflected in the GG injection pressures by the higher O/F ratio.

5.1.3.3 High Start Tank Energy Effects

Pump speeds on spinup are shown in Section 5.1.3.5 to vary with pressure and with increasing ΔT (crossover duct-start gas temperature). The tests conducted at AEDC to date have included simultaneous variations of both pressure and temperature of start gas and, thus, tests of constant total start gas energy with varying temperature or pressure are not available to show conclusively the effect of temperature or pressure alone on start transient pump spinup speeds. Figure 20 shows graphically that the energy difference (low during Test 25B versus high during test 23D) is achieved mainly by a change in pressure. The results of tests 25B and 23D are compared in Fig. 25 to show the effects of start tank energy on pump speeds and GG temperature peak.

Figure 25 shows a higher spinup speed for the fuel pump with very little difference in LO_2 pump speed for Tests 23D and 25B. The higher fuel pump spin speed can be attributed to the higher initial start tank gas pressure. The ΔT between crossover duct and start gas temperatures for both tests are so nearly equal that energy imparted to the start gas by the duct cannot be expected to influence LO_2 pump spinup.

Little effect can be seen from the difference of the 172-Btu higher total energy measured during Test 23D, the peak temperatures being only 102°F apart. Thrust chamber temperature can also be expected to account for a portion of the small temperature peak difference since the thrust chamber temperature was 12°F cooler during Test 23D. Test 23D, therefore, with a thrust chamber temperature equal to that of 25B, would have been expected to show a lower peak.

The variables that influenced oxidizer pump peak spin speed most were crossover duct temperature and start gas temperature. Figure 26 shows peak spin speeds attained as a function of crossover duct temperature (which relates to the energy exchange between the duct and start gas)

and PU valve position. Start tank pressures, for the data presented, varied from 1243 to 1410 psia. A part of the scatter in the data presented can probably be attributed to the variance in pressure. Attempts to normalize the data with start tank pressure were unsuccessful. A further possible influence on the data plotted in Fig. 26 is the result of the turbine wheels cooling at a slower rate than the duct (which was influenced by test cell atmosphere). Turbine temperatures (indicated by the oxidizer turbine inlet temperature probe) during some tests with high ΔT were 130°F warmer than duct temperatures; this would increase the ΔT approximately as indicated, should these temperatures be considered.

Fuel pump spin speeds corresponding to oxidizer pump peak spin speeds during start tank discharge are shown in Figs. 27 a and b. Fuel pump speeds on spinup are related in this figure to start tank pressure and to start tank energy. These two figures lead to the conclusion that the start tank-to-fuel turbine inlet duct and start tank gas energy exchange is small and has little effect on fuel pump spinup. The relationship of fuel and oxidizer pump spinup speeds has a direct bearing on GG temperature peak. Higher relative fuel pump spinup would give lower GG temperature peaks; higher relative oxidizer pump spinup would give higher GG temperature peaks. High-pressure/high-temperature start gas would, therefore, give lower GG temperature peaks than low-pressure/low-temperature start gas. It is therefore concluded that the limits provided by the selected start tank vent and relief valve cannot reduce GG temperature peaks for engine starts with start gas temperatures above -240°F. The relief valve limits shown in Fig. 20 provide lower pressure above -240°F, and this would reduce fuel pump spinup speed.

5.1.3.4 Effects of Fuel Pump Inlet Pressure

Figure 28 shows a comparison of the results of Tests 23D and 24D for the effects of pump inlet pressure. Fuel inlet pressure was 6.4 psi higher during Test 23D than during Test 24D, with LO_2 inlet pressures essentially equal for these tests. The GG temperature peak during Test 24D was 2196°F as compared with 2092°F during Test 23D. A portion of this difference can be attributed to the 16°F warmer thrust chamber during Test 23D. Pump inlet pressures, therefore, have little influence on GG temperature peak.

5.1.3.5 PU Valve Position Effects

Tests were not conducted at conditions whereby a direct comparison could be made to show only PU valve position effects on the engine

start transient. Oxidizer pump spinup speed was significantly lower for the open PU valve position when compared to the closed position, as shown in Fig. 26. The lower peak spinup speed, caused by the open PU valve, and the increased bypass flow to the inlet resulted in approximately 50 psi lower pump discharge pressure just prior to oxidizer dome prime, as shown in Fig. 22. Open PU valve provided the greatest benefit, however, in the time period between oxidizer dome prime and a chamber pressure of 550 psia. Comparison of pump discharge pressures at 1.2 sec in Fig. 22 shows open PU valve (Test 25D) oxidizer pressure to be more than 100 psi greater than for the null PU valve position (Test 13B). Fuel pump discharge pressures at this same time differed by less than 50 psi. Therefore, the open PU valve position had the most significant effect in solving the problem of GG overtemperature during engine orbital restart. The lower oxidizer pump discharge pressure attained throughout the start transient lowers both the peak and overshoot temperatures.

5.1.4 Temperature Overshoot

5.1.4.1 MOV Plateau Time Effect

The effect of MOV plateau time on GG temperature overshoot is shown in Fig. 29, a comparison of the results of Tests 25D with 26D. The GG temperature peaks for these two tests were essentially the same, and the overshoots would have agreed except that during Test 26D the MOV left the 14-deg plateau and started second-stage ramp earlier. Oxidizer flow to the GG was reduced relative to fuel flow at the start of second-stage ramp, lowering the O/F ratio and forming the overshoot peak. The overshoot peak shape was related to the second-stage ramp rate immediately after leaving the plateau. The slower the ramping rate after leaving the 14-deg plateau, the longer the overshoot temperature remains undesirably high.

5.1.4.2 Factors Affecting MOV Plateau Time

MOV plateau time (time at the 14-deg position) is influenced by several factors as follows:

(a) Hydraulic Torque - The torque attributable to valve geometry and pressure drop across the valve which tends to open or close the valve. This torque is considered for the purposes of this report to be proportional to POPD minus PC. Using these two pressures, the engine manufacturer computes hydraulic torque as

$$\text{Torque} = 0.769\ (\text{POPD} - \text{PC})\ \text{in.-lb}$$

at the 14-deg position. Hydraulic torque is, therefore, related to pump speed, thrust chamber pressure buildup, and flow across the MOV. Flow is shown in Fig. 30 to be relatively constant for the time that the MOV is at 14-deg position. Figure 31a shows hydraulic torque at the 14-deg position for Tests 21B and 23C.

(b) Pneumatic Torque - The MOV is opened from the 14-deg position by application of a regulated 400-psia opening pressure and the venting of closing control pressure through a thermostatic orifice. Figures 10 and 14 show details of the valve. (The valve is normally closed and spring-loaded.) Pneumatic (actuator applied) torque at the 14-deg position varies with the venting rate of closing pressure. This venting rate is a function of the gas and orifice temperatures. Figure 31b shows pneumatic torque for Tests 21B and 23C.

(c) Net Opening Torque - The net MOV opening torque at the time the valve leaves the plateau must equal or just exceed the torque caused by friction. Figure 32 presents the values of net opening torque computed for the time 0.05 sec prior to the valve leaving the 14-deg plateau. The values presented neglect friction effects, and the maximum value of 534 in.-lb is approximately twice the friction value expected for the valve. The scatter of the data in Fig. 32, when compared with the pneumatic and hydraulic torque plots shown in Fig. 31, leads to the conclusion that hydraulic torque is the primary variable that determines when the valve leaves the 14-deg plateau. Because of the high net torque exhibited by this particular valve, it was subsequently removed and returned to the engine manufacturer's home plant for inspection and test (reference the engine manufacturer's Failure Analysis Report No. 007921, which describes an assembly error subsequently found in this valve.)

(d) Sequenced MOV Time - This time, which is a function of the size of the closing control orifice, was changed from 1825 to 1650 msec as a solution to the GG overtemperature problem. The orifice changes the rate at which closing pressure vents from the actuator. The purpose of faster venting of this pressure was to reduce the plateau time because a faster ramp time also provides a relatively shorter plateau time. However, the effect of the reorificing solution to the overtemperature problem was compromised in the AEDC tests by the assembly error subsequently found in the MOV.

5.1.4.3 Fast and Slow Restart

Comparison of a slow and fast buildup restart are shown in Fig. 33. A faster start is characterized by faster pump spinup during start tank discharge. Faster buildup (time to 550-psia chamber pressure) is characterized by higher GG power from the higher O/F ratio and over-temperature, and faster pump speed buildup. MOV movement (plateau time and second-stage ramp rate) is shown in Fig. 33 to have a significant effect on chamber pressure buildup rate because of its effect on GG overshoot temperature while restricting oxidizer flow to the main chamber.

5.2 ONE- AND TWO-ORBIT RESTARTS

Crossover duct conditions were duplicated for a one-orbit restart during Test 25D and for a two-orbit restart during Test 25B. Figure 34 presents a comparison of start transient plots for these two tests. The conditions at ESTDCS for these two tests were:

	Test 24B	Test 25B	Test 25D
Start Tank Pressure, psia	1390	1292	1319
Temperature, °F	-220	-207	-217
Total Energy, Btu	3045	2838	2904
LO_2 Pump Inlet Pressure, psia	41.2	40.4	41.4
Temperature, °F	-295.4	-295.6	-295.4
Fuel Pump Inlet Pressure, psia	37.4	37.1	37.6
Temperature, °F	-421.7	-419.7	-419.9
Average Crossover Duct Temperature, °F	115	137	185
LO_2 Turbine Inlet Temperature, °F	226	268	323
Average Thrust Chamber Temperature, °F	-170	-277	-286
GG Peak Temperature, °F	1890	2204	2154
GG Overshoot Temperature, °F	1900	2179	2184

The warmer crossover duct during Test 25D provided faster oxidizer pump spinup and thus higher pump discharge and GG injection pressures than were recorded during Test 25B. The GG temperature peak during Test 25D was expected to exceed that during Test 25B. Oxidizer dome prime

occurred earlier during 25D; and for this reason, the GG temperature peak occurred earlier and thus at a lower level. Overshoot temperatures differed during these tests because of MOV second stage ramp rate differences just after leaving the 14-deg plateau. The faster ramping of the MOV during Test 25B provided a shorter overshoot peak duration, although the maximum overshoot temperatures were nearly equal for the two tests.

Tests 25B and 25D simulated coast period conditions for one and two orbits with the exception of thrust chamber temperature. The thrust chamber was not heated for these tests to simulate ullage motor operation. The colder thrust chamber temperatures that existed were considered to simulate the worst-case conditions for these two tests. A warmer thrust chamber has been shown (Section 5.1.3.1) to decrease peak temperature. To illustrate this effect, Test 24B, which simulated ullage motor heating by preheating the thrust chamber, had a peak GG temperature of 1890°F and an overshoot of 1900°F. The table above shows that the starting condition differences between Tests 24B and 25B were thrust chamber temperature, crossover duct and turbine temperature, and start tank pressure. All of these tended to reduce the temperature peak during Test 24B; however, the 100°F difference in thrust chamber temperature was considered to be the major contributor to the reduced peak GG temperature measured during Test 24B.

It is therefore considered that worst-case conditions for one- and two-orbit coast period restarts were simulated and satisfactorily demonstrated the effectiveness of the solutions selected for the restart problem for Saturn Flight AS-501.

5.3 THRUST CHAMBER HEATING AND FUEL LEAD CHILLDOWN

Six restart tests were conducted in this test series with the thrust chamber heated to simulate solar and ullage motor orbital restart conditions. Asymmetric heating was employed during Tests 20A, 21B, 24A, and 24B. Uniform heating was attempted during Tests 25A and 25C, but temperature targets were not met because of heater blanket thermostat malfunctions. Heating on these two tests was also asymmetric.

Temperature profiles are presented in Fig. 35 for Test 20A to show the asymmetric heating and the resulting temperature profile at ESTDCS after the fuel lead had chilled the thrust chamber. These plots show that the fuel lead (8 sec in this case) was not sufficient to cool the thrust chamber uniformly. This could have permitted fuel injection temperature OK event to have occurred early since the temperature probe was located in

the 0- to 90-deg quadrant indicated on the figures. These profiles indicate that the 0- to 90-deg quadrant could achieve a cold enough temperature (-150°F) for injection temperature OK event to occur on shorter fuel leads before the average thrust chamber temperature is at -150°F. The average of all thrust chamber thermocouple temperatures measured during Test 20A at ESTDCS was -168°F. The engine prechill controller (PCC) (fuel injection temperature OK circuitry) malfunctioned during Test 22B, and the PCC was disabled for the remaining asymmetrically heated thrust chamber tests.

5.4 GAS GENERATOR OXIDIZER QUALITY

Tests 26A and 26C were identical starting condition tests which were conducted to determine the effects of GG LO_2 supply quality on GG temperature peak and overshoot.

Prior to Test 26, a conditioning shroud was placed around the GG LO_2 supply line, and 40 to 60°F GN_2 was used to simulate sea-level, static test, GG oxidizer supply-line conditions. This purge accounted for about an 11°F supply-line temperature differential for these two tests at ESTDCS. Figures 36 and 37 show comparisons of start transient parameters and the temperature history of the GG LO_2 supply-line temperature through the start transient. The supply-line temperature differential of 11°F had little apparent effect, as shown in these figures. Figure 37 indicates that the oxidizer in the supply line for both of these tests remained gaseous during the engine start cycle.

5.5 S-V/S-IVB FIRST-BURN START COMPARISONS

5.5.1 General

Five of the 22 firings reported herein were S-V/S-IVB first-burn simulation tests. Four of the five were of 30-sec duration and included an excursion of the PU valve from the null position to the closed position (a change in mixture ratio from 5.0 to 5.5) during mainstage operation. Although the 30-sec duration firings permitted acquisition of steady-state mainstage operation performance data, the primary purpose of conducting tests of this duration was to heat the engine turbine hardware sufficiently for simulation of an orbital coast period and engine restart with elevated turbine hardware and crossover duct temperatures.

Saturn V/501 prevalve sequencing logic was duplicated for the S-IVB first-burn engine start evaluation, and engine start target conditions

were varied from test to test to explore the limits in which engine S/N J-2031 on this initial Saturn V flight will be expected to operate. Engine components which influence the engine start transient were temperature conditioned to the levels predicted in the vehicle interstage environment.

5.5.2 Fast and Slow First-Burn Start Comparisons

The results of Tests 21C and 24C illustrate the extremes of thrust chamber buildup rate observed in first-burn simulation tests in this series. Chamber pressure buildup rate during the start transient, for the purposes of this report, is compared using two definitive times:

1. Oxidizer dome prime time (when chamber pressure equals 100 psia), and
2. Chamber pressure rise time to 550 psia.

A faster start is characterized by an earlier oxidizer dome prime, and a faster buildup reaches the 550-psia level sooner.

Engine S/N J-2052 was reorificed after Test 21C, as follows, to more closely approximate the start transient characteristics of engine S/N J-2031 on vehicle AS-501.

Name	From	To	Area Increase
GG Fuel Orifice	0.482 in.	0.502 in.	8.5%
GG Oxidizer Orifice	0.269 in.	0.284 in.	11.5%
OTBV Nozzle	1.419 in.	1.520 in.	14.7%

This reorificing of the engine did not appreciably change its start transient characteristics in view of the relatively larger effects of start gas energy, turbine hardware temperature, and thrust chamber temperature. However, the OTBV exhibited an unusually fast closing time during the first firing after the reorificing (Test 22A). (The reason for this cannot be explained; the valve timing was, however, well within specification limits.)

The plots of chamber pressure versus time presented in Fig. 38 show that the buildup rate to oxidizer dome prime and to 550-psia chamber pressure was faster during Test 21C than during Test 24C. The difference in start tank energy (see Fig. 20) accounts for the difference

in these two starts. The higher initial spin speeds imparted to the turbines by the start gas during Test 21C resulted from:

1. The greater mass of H_2 contained in the start tank,
2. The higher energy available, and
3. The greater energy gain of the blowdown gas passing through the fuel turbine and crossover duct by virtue of the higher temperature differential between the crossover duct and the initial gas temperature in the start tank.

The higher initial pump speeds resulted in higher pump discharge pressures at the beginning of the ignition transient, and the oxidizer dome primed earlier.

The MOV remained on the 14-deg plateau longer on the faster start, primarily because the hydraulic torque was greater due to the oxidizer pump discharge pressure being higher. As a result, the slow chamber pressure rise rate until the MOV began its second stage ramp was more pronounced on the faster start, Test 21C.

The GG temperature rose to approximately the same initial peak level during both tests. A comparison of the gas GG injection and chamber pressure levels as the combustion process began in the GG shows that the O/F mixture ratio was nearly the same during both tests; thus, the temperature rise rates were almost identical. The lower thrust chamber temperature measured during Test 24C accounts for the reduced fuel flow to the gas generator, resulting in the same O/F ratio. At oxidizer dome prime, resistance to main chamber fuel flow increased, and more fuel flow was directed to the GG. The reduction in GG O/F ratio at oxidizer dome prime stopped the GG temperature rise. It was at this time that the initial peak temperature was reached. On the slower start, Test 24C, the MOV was subjected to a lower hydraulic torque and left the 14-deg plateau quicker. Thus, there was no temperature overshoot.

The GG temperature overshoot during Test 21C resulted from the longer time period required for the MOV to overcome the higher hydraulic torque. As the GG "bootstrap" operation began to increase the pump speeds (and discharge pressures), the MOV restricted oxidizer flow to the main chamber, thereby forcing more oxidizer to the GG until it started to ramp, relieving the restriction, and allowing the GG mixture ratio to decrease.

A comparison of the results of Tests 21C and 22A is presented in Fig. 39. Test 22A was intended to be a slow chamber pressure buildup test. Table X shows that this test actually exhibited the fastest rise to mainstage OK and to the 550-psia chamber pressure level of all the S-V/S-IVB first-burn tests in this series. Start tank energy was low for this test, 2718 Btu, only 16 Btu higher than for Test 24C. Pump inlet conditions, thrust chamber temperature at ESTDCS, and turbine hardware temperatures were nearly the same for Tests 21C and 22A. The unusually fast OTBV closing time during Test 22A resulted in the oxidizer turbine receiving more of the initial GG ignition energy, and the oxidizer pump speed curve began to converge with the Test 21C speed at about the time the OTBV was 80-percent closed.

Test 22A produced a less severe GG temperature peak. Lower hydraulic torque, coupled with a 100°F warmer MOV actuator gas temperature, resulted in a shorter MOV plateau time and thus a lower GG temperature overshoot. The shorter MOV plateau time, coupled with the faster OTBV closing time, accounted for the faster chamber pressure rise time during Test 22A than during Test 21C.

5.5.3 Flight 501 Prevalve Sequencing Effects

The objective of Test 22A was to verify the effects of AS-501 prevalve sequencing on engine start characteristics. Figure 40 shows that both pump inlet pressures were essentially stable at the start target levels approximately 0.25 sec prior to engine start. The fact that the prevalves were traveling open during the fuel lead period had no discernible effect on any aspect of the engine start transient characteristics during any of the S-IVB first-burn simulation tests of this test series at AEDC.

5.5.4 Long-Duration Propellant Soak Effects

Propellant soak times in the engine were varied from 1 hr to approximately 4-3/4 hr prior to first-burn simulation tests. Test 21A had the longest propellant soak time - 4 hr, 44 min - in an attempt to duplicate the soak time for engine S/N J-2016 during Flight AS-202 which had 4 hr, 32 min of oxidizer-in-engine time and 3 hr, 20 min of fuel-in-engine time. First-burn tests for AS-501 simulation were made with propellant soak nominal times of either 1 or 2 hr.

Comparison of the start transients on all of the first-burn simulation tests to date reveals no discernible effects from varying propellant soak time from 1 to 4-3/4 hr.

5.5.5 Engine Component Preconditioning Effects

Cold He gas was used to condition the crossover duct, the MOV closing control line, and the pneumatic control package to the temperature levels predicted for flight.

The crossover duct conditioning proved to have a significant effect on the engine start characteristics in lowering the initial LO_2 pump spinup peak. As shown in Fig. 26, the lower the crossover duct temperature with respect to the start gas temperature, the lower the LO_2 pump peak spinup speed.

Conditioning the MOV closing control line and pneumatic control package had a relatively small effect on MOV timing compared to the hydraulic torque effect; however, no tests have been conducted to date with all other variables held constant in order that the effect of MOV closing control gas temperature might be isolated.

5.6 ENGINE VIBRATION

5.6.1 Vibration History of Engine J-2052 at AEDC

Engine J-2052 has been fired under simulated altitude conditions at AEDC 47 times. Engine vibration at oxidizer dome prime in excess of 150 g was recorded during 33 of these firings. The output of two accelerometers mounted on the engine oxidizer dome (UTCD-1 and UTCD-2) was conditioned through the ESCS as VSC counts (vibration time in excess of 150 g).

It became necessary to change injectors following Test 19 because of ASI erosion during that test (Ref. 1). Twenty-six firings were made using the original injector; twenty-three of these produced VSC counts. Twenty-one firings were made using the replacement injector; ten of these produced VSC counts. Table XII contains the history of VSC count recordings for all J-2 engine firings at AEDC to date.[3] Vibration measured on these 33 firings always occurred at or near oxidizer dome prime time and was observed to dampen within a maximum period of 132 msec.

---

[3]Test 22B has been omitted from the table because ignition was not achieved on this test.

Of the 26 firings using the original injector, 22 were first-burn tests and four were engine restarts. Nineteen of these first burns and all four of the restarts produced VSC counts. Of the 21 firings using the replacement injector, six of the seven first-burn tests and only four of the 14 engine restarts had VSC counts. The low percentage of restart tests made with the replacement injector exhibiting VSC counts is attributed to the nature of the tests rather than to any significant difference between the two injectors.

The manner in which the thrust chamber was preconditioned and the duration of fuel lead were major determining factors for the presence or absence of vibration. With reference to Table XII, none of the 8-sec fuel lead restarts with thrust chamber preheating had VSC counts. Ambient thrust chamber, 8-sec fuel lead restarts showed 67 percent with VSC periods of from 3- to 21-msec duration. Tests with from 4.3- to 4.7-sec fuel lead showed 50 percent with VSC periods of from 35- to 40-msec duration. First-burn tests with from 1- to 3-sec fuel lead showed 92 percent with VSC periods of from 3- to 132-msec duration. Tests having the longest durations of excessive vibration were the 1-sec fuel lead tests.

Figure 41 shows an enlargement of the chamber pressure traces for three 1-sec fuel lead tests with vibration compared to Test 06 (the only 1-sec fuel lead test that did not produce excessive vibration.) Figure 42a shows on a more enlarged record that during the same 120-msec period (that produced VSC counts), there were oscillations in chamber pressure and indications of high-amplitude vibration on each of the engine accelerometers, both in the longitudinal and transverse axes. (The dome accelerometer UTCD-1 was mounted parallel to the engine centerline, and the turbopump accelerometers, UFPR and UOPR, were mounted perpendicular or transverse to the engine centerline.)

An amplitude versus frequency analysis of these data is presented in Fig. 42b, which shows that the excessive vibration contained several frequencies and that the predominant one was approximately 2100 cps. The oxidizer turbopump vibration contained only one frequency - 2100 cps. The fuel turbopump vibration contained several frequencies and that of 2100 cps was predominant. The 340-cps frequency present in the chamber pressure fluctuations also appeared in the dome and fuel pump vibration; the 135-in-long sensing line for the PC-2 flight transducer rendered its data meaningless for vibrational analysis.

Power spectral density analysis of the accelerometer data showed the 2100-cps frequency of vibration to contain the highest energy level, and thus identified it as the predominant frequency.

5.6.2 Injector Instability

The 2100-cps frequency which produced the high-amplitude dome prime vibration corresponds to the calculated transverse, first tangential acoustic vibration mode of combustion instability.

The basic parameters affecting the stability of the injector are the pressures, temperatures, and flow rates of the propellants at and in the injector. Although engine S/N J-2052 was not sufficiently instrumented for accurate determination of all these basic parameters, a simplified correlation may be recognized from AEDC test data for the undesirable instability which is derived as follows from an equation for propellant momentum at the injector:

$$mv = \frac{W^2}{\rho A}$$

Removing the constant area term A and taking the square root of the right-hand side of the equation, propellant momentum is represented as

$$\frac{W}{\sqrt{\rho}}$$

Since the oxidizer is a liquid at the injector, its density may be considered to remain essentially constant; thus, oxidizer momentum is represented as simply W_O, the weight flow rate, and is hereby defined as the oxidizer stability function. Since the fuel may be either liquid or gas or both at the injector, its density will vary, and fuel momentum is represented as $W_f / \sqrt{\rho_f}$, hereby defined as the fuel stability function.

Figure 43 is a map of the propellant stability functions at dome prime for the AEDC tests using propellant flow rates measured by the engine flowmeters and assuming fuel density at the pump discharge to be approximately the same at the injector. The fuel was a liquid with a density range of from 4.2 to 4.5 lb/ft^3. However, indicated fuel injection temperature (TFJ-1P) at oxidizer dome prime was always in the range of -423°F or below (off-scale for the temperature probe data reduction equation[4]) where relatively large errors in temperature measurement caused somewhat smaller errors in the determination of fuel density. Since the fuel stability function uses the square root of the fuel injection density, its denominator is roughly a constant. Stability functions for two injectors tested are shown in Fig. 43.

---

[4]See Appendix IV

5.7 COMPARISON OF AS-200 SERIES SIMULATION TESTS AND FLIGHTS

The objective of Test 21A was to perform an AS-200 series first-burn simulation test to establish a correlation between AEDC test data and flight data. The table below shows that engine start conditions were practically identical to flight AS-202 (Ref. 7). However, Fig. 44 shows that the start transient was similar to flight AS-203 (Ref. 8), primarily because of MOV timing. Significant results of Test 21A were:

1. It was the only test in this report period that exhibited a long-duration burst of VSC counts (120 msec).
2. It was the test that most nearly approached a low-level fuel pump stall in this report period.

Pertinent engine start conditions are tabulated as follows:

	(Ref. 6) J-2015 AS-201	J-2016 AS-202	J-2019 AS-203	J-2052 Test 21A
Start Tank				
Pressure, psia	1280	1270	1310	1285
Temperature, °F	-256	-170	-182	-170
Energy, Btu	2870	2760	2840	2787
LO_2 Pump Inlet Pressure, psia	40	41	41	41
Fuel Pump Inlet Pressure, psia	41	41	37	41
Thrust Chamber Temperature at E. S., °F	-195	-220	-205	-200
Oxidizer in Engine, min	---	272	316	240
Fuel in Engine, min	---	200	225	240
Thrust Chamber Chill Time, min				
3 times	(20 (19 (15	19-1/2	30	23

On the basis of data from 46 altitude firings of the J-2 engine at AEDC, 1-sec fuel lead starts, such as Test 21A, exhibit the greatest

tendency for longer duration bursts of excessive vibration and for potential low-level fuel pump stall. The AS-200 series flights utilize 1-sec fuel leads; the data imply that 1-sec duration is marginal for sufficient chilling of the thrust chamber. Two previous AEDC tests exhibited problems with the 1-sec fuel lead. The objective of Test 14 (Ref. 1) was to clear the J-2 engine first-burn application for 1-sec fuel lead with a Saturn 1B boost-phase thrust chamber warmup simulation. This was the only test where the 1-sec fuel lead was programmed after a simulated 145-sec, Saturn 1B, boost-phase warmup and the only case that the prechill controller (PCC) held the fuel lead for fuel injection temperature OK (it held an additional 0.95 sec). Test 07 (Ref. 2) was made with a 1-sec fuel lead after prechilling the thrust chamber to -70°F. It was the only test that the PCC allowed the start to proceed with the fuel injection temperature above the -150°F limit. Test 07 produced the closest approach to stall observed at AEDC - 600-gpm stall margin at oxidizer dome prime.

The AS-200 series simulation tests at AEDC have exhibited start transients very similar to those observed in the flights to date, and the data show good agreement.

5.8 FUEL PUMP STALL EVALUATIONS

Fuel pump performance during the start transient was documented for all firings, and transient pump head-flow data were compared with stall inception design data. Thrust chamber resistance to fuel flow was never high enough to produce a pump stall or a seriously "close" stall margin.

In order to compare results of tests that were expected to have a tendency toward pump stall, the term "stall margin" is defined as the ΔQ (in gpm) between the actual pump discharge flow and that which would produce stall inception at a given rpm during spinup. For the purposes of this discussion, a distinction is made between high-level and low-level pump speed stall, using 17,500 rpm as the dividing point.

Tests 21C, 25A, and 25C had as objectives the evaluation of possible low-level stall caused by high thrust chamber resistance to fuel flow. Test 21C was to be conducted with a -80 ± 10°F thrust chamber prechill and 3-sec fuel lead and with high start tank energy. Tests 25A and 25C were to incorporate uniform thrust chamber preheating to 250°F and an 8-sec fuel lead with start tank energy high during Test 25A and low during Test 25C. However, desired thrust chamber temperatures were not attained during any of these tests (see Tables IX and X). Figure 45 shows

that comfortable stall margins (1200 gpm minimum) were maintained during these tests as a result of the colder-than-planned thrust chamber temperatures. Test 21C exhibited a closer stall margin than Test 25A or Test 25C at oxidizer dome prime (approximately the 14,000 rpm level); and Test 21A, which was not anticipated to show pump stall tendencies, was closer than Test 21C. The trend of these four firings (typical of other AEDC data) is the longer the combustion instability at dome prime, the closer the approach to low-level stall. Since 1-sec fuel leads have produced the longest periods of combustion instability and the closest stall margins, fuel pump stall margin is potentially unsatisfactory for the 1-sec fuel lead application.

Test 07 produced the closest approach to stall observed to date at AEDC with a minimum low-level stall margin of 600 gpm resulting from the unusually high thrust chamber temperature, -70°F, and PCC anomaly (Fig. 46).

Only four AEDC tests have exhibited high-level stall margins of 1000 gpm or less. Tests 07 and 14 both approached within 800 gpm of stall inception at approximately 20,000 rpm, and both exhibited marginal capability of the 1-sec fuel lead for engine start with a warm thrust chamber. Although Tests 23C and 22A each exhibited stall margins of approximately 1000 gpm, as shown in Fig. 47, they illustrate the effect of MOV second stage movement on high-level stall tendency. The faster the MOV ramps, the greater the tendency toward high-level pump stall. (Note the fast MOV movements during Tests 23C and 22A shown in Figs. 33 and 39). Tests 23C and 22A were slow-starting tests with low hydraulic torque on the MOV. The faster MOV ramping movement is characteristic of a slow start and results in a lower O/F ratio in the GG (opposite extreme of a high O/F, causing GG temperature overshoot). Thus, for a slow start there is less GG power available during the high-level portion of the fuel pump spinup and an increased tendency toward high-level stall.

Pump head-flow data obtained from flight AS-202 (Ref. 7) are shown in Fig. 47 to have approached closer to high-level stall than any AEDC test to date. Comparison of other start transient variables during this flight with AEDC data reveals no obvious reason for high-level stall tendencies.

5.9 ASI TEMPERATURE

Augmented spark igniter (ASI) chamber temperature has been of interest since the engine injector was changed because of ASI port

erosion during Test 19 (Ref. 1). ASI injection and chamber pressure instrumentation were not installed for the test during which the erosion occurred, but were installed for subsequent tests. The data are presented in Fig. 48 to show the effects of pump inlet pressures on ASI injection pressures and temperatures. Comparison of pump inlet conditions shows that Test 23E was similar to Test 19 and that ASI chamber conditions could be expected to be similar, except that the ASI LO_2 orifice (0.150-in. diameter) used for all tests through 19 was replaced with one of 0.125-in. diameter for Tests 20 through 26. Test 23E shows ASI fuel injection pressure at a low level relative to ASI oxidizer injection pressure when compared with Test 24A during which a higher fuel pump inlet pressure was used. Relative ASI chamber combustion temperature of Tests 23E and 24A is indicated in Fig. 49, which shows the output of the ASI ignition detect probe amplifier. These temperatures were derived from probe characteristics of resistance versus temperature and amplifier output voltage versus probe resistance. The temperatures shown indicate a significant O/F ratio increase for Test 23E as compared to Test 24A for the 12-psi lower fuel inlet pressure, as compared to LO_2 inlet pressure. Low fuel inlet pressure was the probable cause of the erosion which occurred during Test 19; however, the LO_2 orifice size reduction lowered ASI O/F sufficiently to prevent recurrence of the erosion problem.

5.10 PREMATURE ENGINE SHUTDOWN

5.10.1 Electrical Control Assembly

Test 20 was terminated at 2.025 sec by de-energization of the ignition phase solenoid and mainstage control solenoid. Engine cutoff was subsequently activated at ESTDCS + 2.697 sec by the stall approach monitor which had been incorporated for this test, the first with thrust chamber preheating.

The failure[5] was traced to a piece of Inconel® lockwire inadvertently left inside the ECA during manufacture (resting across two printed circuit pads of the resistor board module) which caused a short-circuit in the ECA.

The ignition phase solenoid and the ECA were replaced following Test 20.

---

[5]Reference "Engine Manufacturer's Failure Analysis Report," FAR-004126.

5.10.2 Prechill Controller Anomaly

Test 22B resulted in a cutoff by the start OK timer (see Fig. 15) 13.3 sec after engine start. The fuel injection temperature OK permissive from the PCC did not occur at expiration of the 8-sec fuel lead timer. The start tank did not discharge and the mainstage control solenoid did not energize.

Fuel injection temperature recorded by TFJ-1P indicated -423°F (or below) after 6.65 sec of fuel lead had elapsed until the automatic cutoff. Two fuel injection temperature probes are used on Engine J-2052. Both are RTT's, one used for data acquisition (TFJ-1P) and the other utilized by the PCC.

Subsequent to Test 22B, a PCC system checkout was performed during which precise resistance levels were substituted for the PCC probe. This checkout revealed that the PCC would not give a fuel injection temperature OK permissive signal for a probe resistance below 3 ohms. A resistance of 3 ohms corresponds to approximately -430°F (see Appendix IV). Test 22B was the first test in the AEDC program where the fuel injection temperature was below -423°F prior to ESTDCS (or the first time that the fuel injection temperature probe outputs were on the order of 3 ohms at the time the logic allowed the PCC to sample fuel injection temperature.)

Because of this PCC anomaly, an electrical modification was made to bypass the PCC and automatically give the fuel injection temperature OK signal at expiration of the fuel lead timer for tests subsequent to Test 22B. However, as a safety precaution, the PCC was reactivated for Tests 25A and 25C because of the anticipation that an 8-sec fuel lead chilldown would not be sufficient following uniform heating of the thrust chamber to 250°F. The PCC is not a flight item; thus, the results of Test 22B, as related to the PCC anomaly, have no direct bearing on flight operations.

5.10.3 Observer Cutoff

Tests 23A was the only test to date to be terminated prematurely by an observer cutoff. This test had been scheduled for 30-sec duration with a PU valve excursion from a mixture ratio of 5.0 to 5.5 at ESTDCS + 10 sec. It was terminated by the LO_2 pump inlet "X-Y plotter" observer at ESTDCS + 3.91 sec because the LO_2 pump inlet pressure decayed below the minimum boundary for "safe" mainstage operation.

Normal LO_2 pump inlet pressure loss from the prefire set point as the pump begins its spinup is approximately 3 psi. The 3-psi pressure loss occurred during this test as usual, but the LO_2 pump inlet start requirements for this test (see Table IX) had been inadvertently established too close to the lower safe mainstage operation boundary line: $38 \begin{smallmatrix}+0\\-1\end{smallmatrix}$ psia pressure and -290.4 ± 0.4°F. The actual prefire start conditions attained, 37.5 psia and -290.2°F, were within the specified limits for this test.

5.11 STEADY-STATE PERFORMANCE

Steady-state performance data are presented in Table XIII for the 10 firings which were of 30-sec duration. The data represent performance obtained from one-sec data average (29 to 30 sec), computed using the Rocketdyne PAST 640 modification zero performance computer program. Specifically, the fuel turbine performance was examined for run-to-run deviation because of high GG outlet temperatures which were experienced. The data presented in the table show consistent performance throughout the Test 20 through 26 series. Fuel turbine efficiency total variation was only one percentage point for these tests. The engine reorificing which occurred between Tests 21 and 22 is indicated in the table by an increase of turbine weight flows and speeds and by lowered engine mixture ratio.

SECTION VI
SUMMARY OF RESULTS

During seven test periods in the Propulsion Engine Test Cell (J-4) at the Arnold Engineering Development Center, 22 altitude engine start tests of the J-2 engine were made, of which 21 were successful. Pressure altitudes at engine start ranged from 95,000 to 111,000 ft. This series of altitude start transient tests resulted in resolution of start and restart GG transient overtemperature problems encountered in earlier AEDC testing of the J-2 engine. The results of this series of tests is summarized as follows:

1. An acceptable one-orbit coast period restart was made at crossover duct and turbine hardware temperatures predicted for Saturn V/S-IVB flight. The test was made using all selected problem solutions and colder than predicted thrust chamber temperature to provide worst-case

conditions. Solutions selected for use on flight vehicle Saturn V/501 which were tested were:

(a) open PU valve position for engine restart as opposed to null position,

(b) a dry-sequenced MOV time of 1650 msec as opposed to 1825 msec, and

(c) use of a start tank vent and relief valve with low specification relief pressure setting.

2. Acceptable two-orbit coast period restarts were made at crossover duct and turbine hardware temperatures predicted for Saturn V/S-IVB flight. These tests utilized all selected solutions and colder than predicted thrust chamber temperatures to provide worst-case conditions.

3. This series of tests identified the variables which affect GG start transient temperatures. Initial peak temperature was shown to be influenced mainly by the PU valve position and thrust chamber temperature. Start tank energy, pump inlet pressures, and GG LO_2 supply line temperature effects were shown to be minor influences. Overshoot temperature was shown to be a function of MOV position. Tests for which the MOV second-stage movement began early after main chamber ignition exhibited reduced GG overshoot temperatures. From test to test, MOV second-stage movement was shown to vary significantly with variations in hydraulic torque.

4. Engine vibration associated with combustion instability during start transient was experienced during 33 of 47 engine starts at AEDC during J-2 engine testing. Instability and vibration occurred during 92 percent of all first start simulations and during 45 percent of all restarts. Significant observations about vibration during AEDC tests were:

(a) instability and vibration did not occur during any heated thrust chamber test (8-sec fuel lead);

(b) the longest periods of vibration occurred on 1-sec fuel lead tests. This correlates with Saturn IB/S-IVB first start flight data which show vibration at comparable times; and

(c) the vibration data showed that the predominant frequency was about 2100 cps caused by combustion instability.

5. Tests at starting conditions expected to provide slowest and fastest buildup were successful. Adequate fuel pump stall margin was maintained for all tests. The smallest stall margins existed for 1-sec fuel lead starts which correlate with conditions conducive to combustion instability.
6. Saturn V/501 flight prevalve sequencing was found to have no effect on engine start characteristics.
7. The test conducted to simulate AS-200 Series starts compared closely with available flight data.
8. Engine performance computations showed consistent test-to-test performance.
9. ASI erosion was not encountered during tests comparable to Test 19 (which sustained ASI erosion) when the ASI LO_2 orifice size diameter was reduced from 0.150 to 0.125 in.

REFERENCES

1. Simpson, J. N., Cantrell, F. D., and Kunz, C. H. "Altitude Testing of the J-2 Rocket Engine in Propulsion Engine Test Cell (J-4) (Tests J4-1554-12 through J4-1554-19)." AEDC-TR-67-115 (AD 820463), September 1967.
2. Muse, W. W. and Franklin, D. E. "Altitude Testing of the J-2 Rocket Engine in Propulsion Engine Test Cell (J-4) (Tests J4-1554-01 through J4-1554-11)." AEDC-TR-67-86, (AD 816454L), May 1967.
3. "J-2 Rocket Engine, Technical Manual Engine Data." R-3825-1, August 1965.
4. Test Facilities Handbook, (6th Edition). "Large Rocket Facility, Vol. 3." Arnold Engineering Development Center, November 1966.
5. Dubin, M., Sissenwine, N., and Wexler, H. "U. S. Standard Atmosphere, 1962." December 1962.
6. "J-2 Engine Performance on Saturn AS-201." Rocketdyne Division of North American Aviation, Inc., R-6750-1.
7. "J-2 Engine Performance on S-IVB Stage of Saturn Flight AS-202." Rocketdyne Division of North American Aviation, Inc., R-6750-2, October 1966.
8. "J-2 Engine Performance on S-IVB Stage of Saturn Flight AS-203." Rocketdyne Division of North American Aviation, Inc., R-6750-3, January 1967.

APPENDIXES

I. ILLUSTRATIONS
II. TABLES
III. PERFORMANCE PROGRAM EQUATIONS
IV. FUEL INJECTION TEMPERATURE DATA ACQUISITION

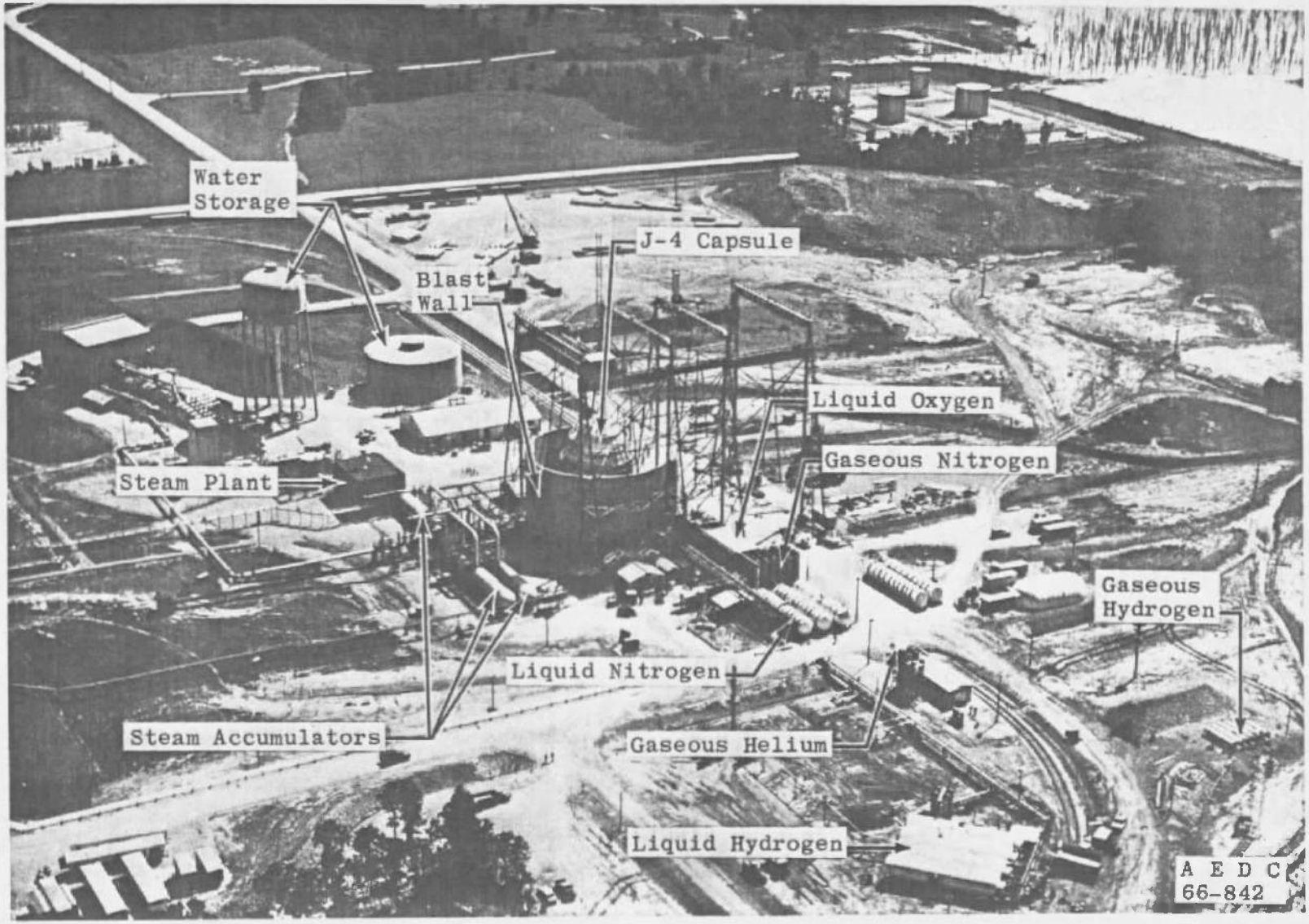

Fig. 1 Aerial View of Propulsion Engine Test Cell (J-4), LRF

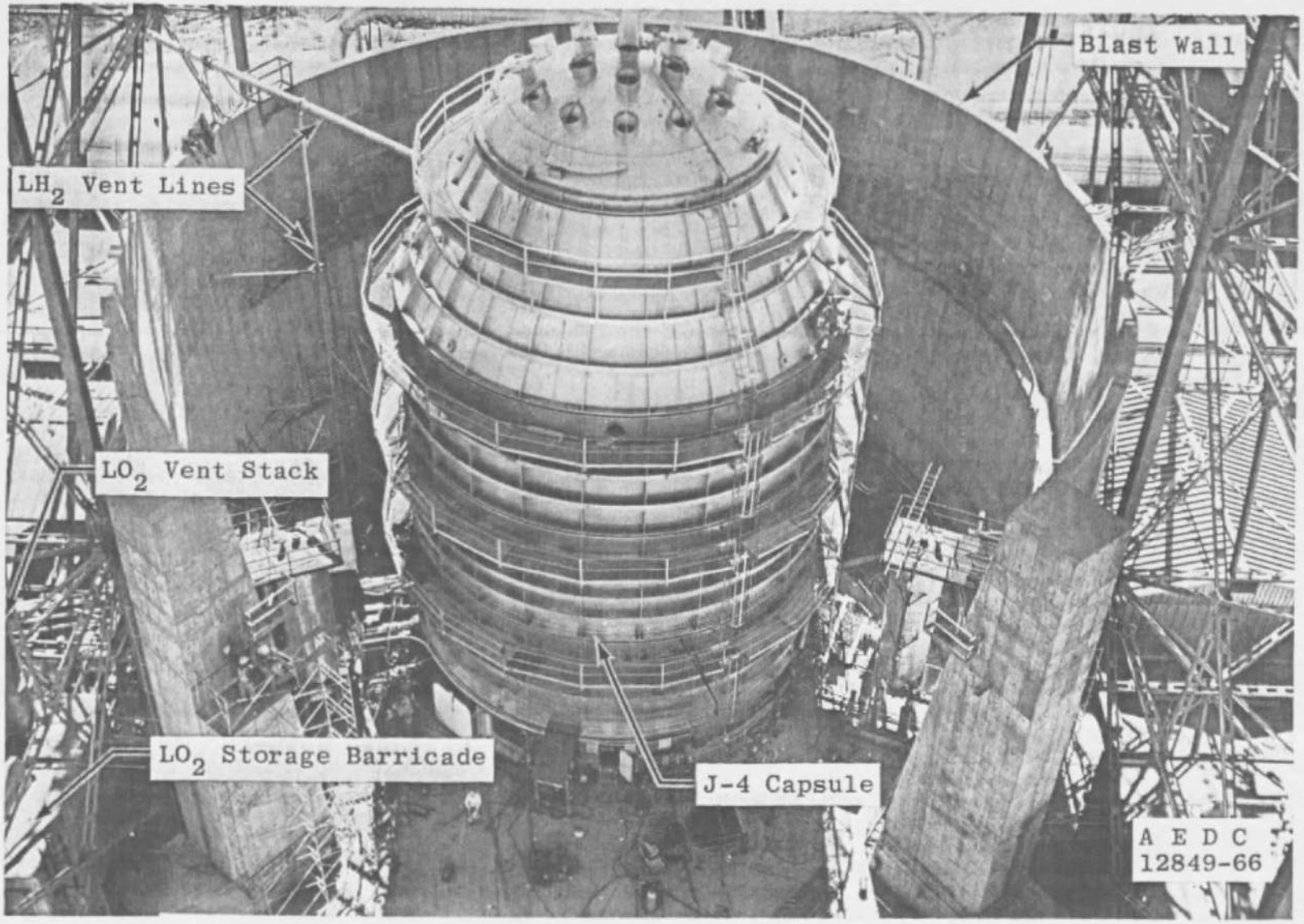

Test Cell J-4

Fig. 1 Concluded

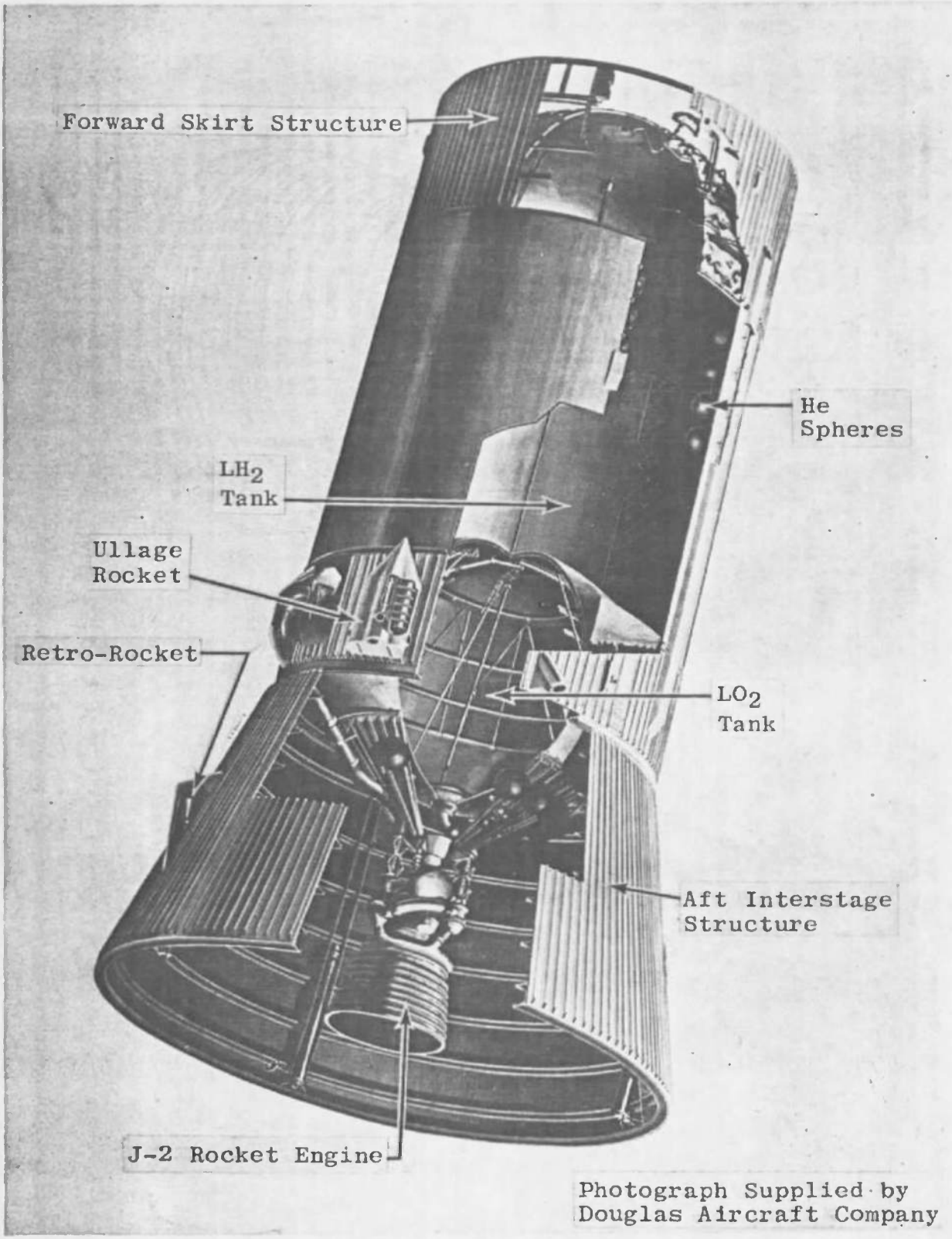

Fig. 2 Cutaway View of Saturn S-IVB Stage

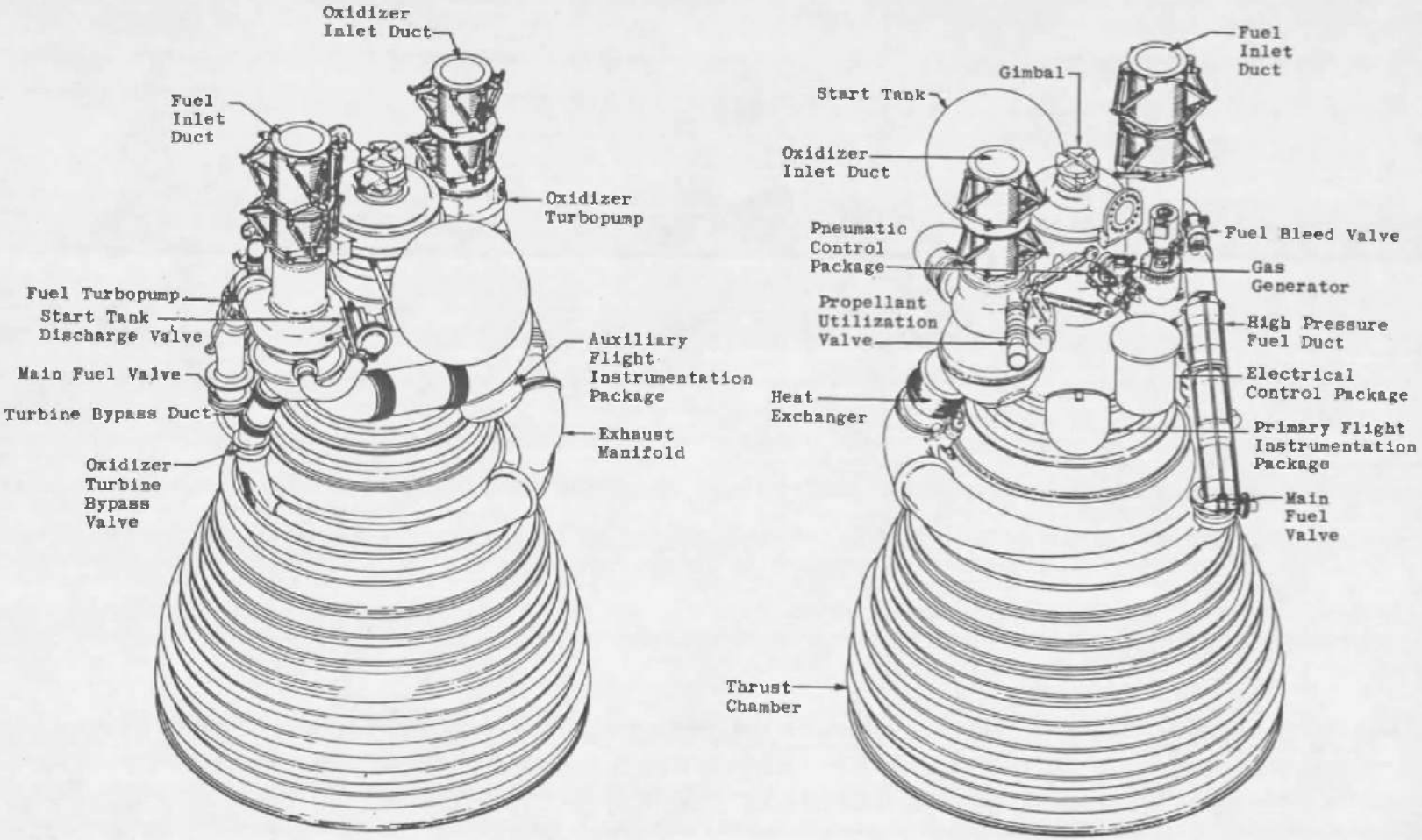

Fig. 3 J-2 Rocket Engine

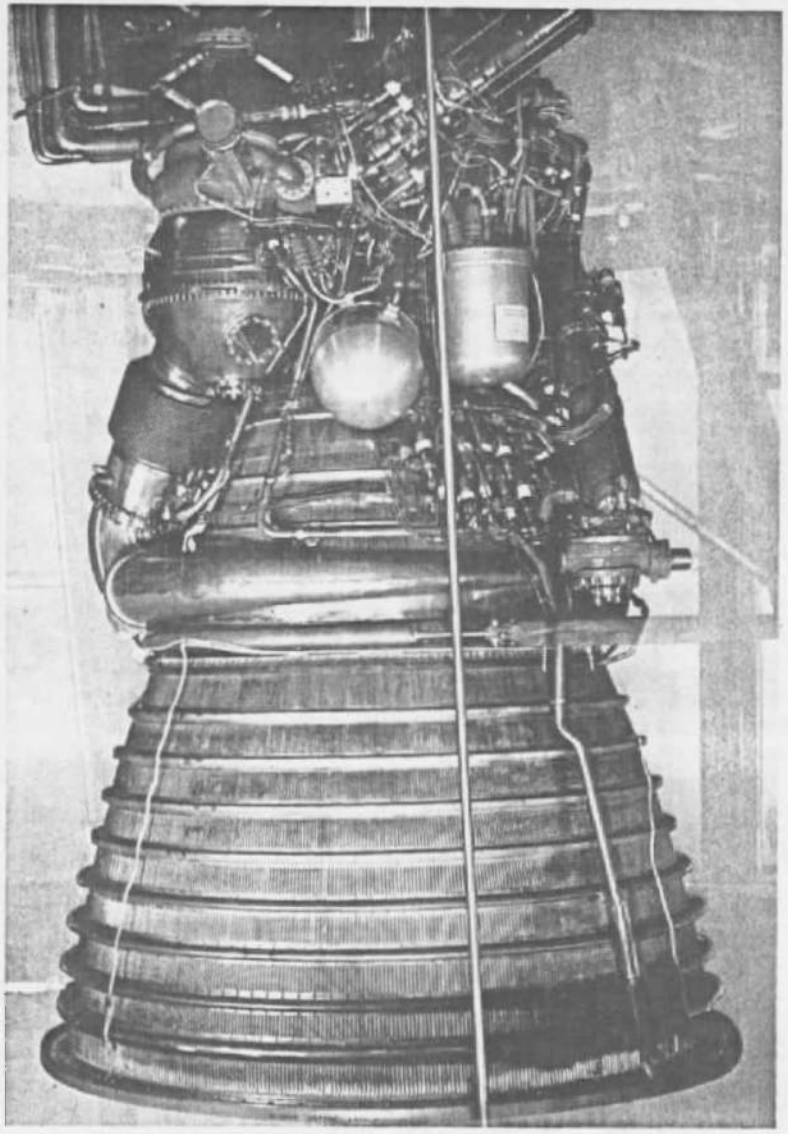

a. Before Heater Blanket Installation

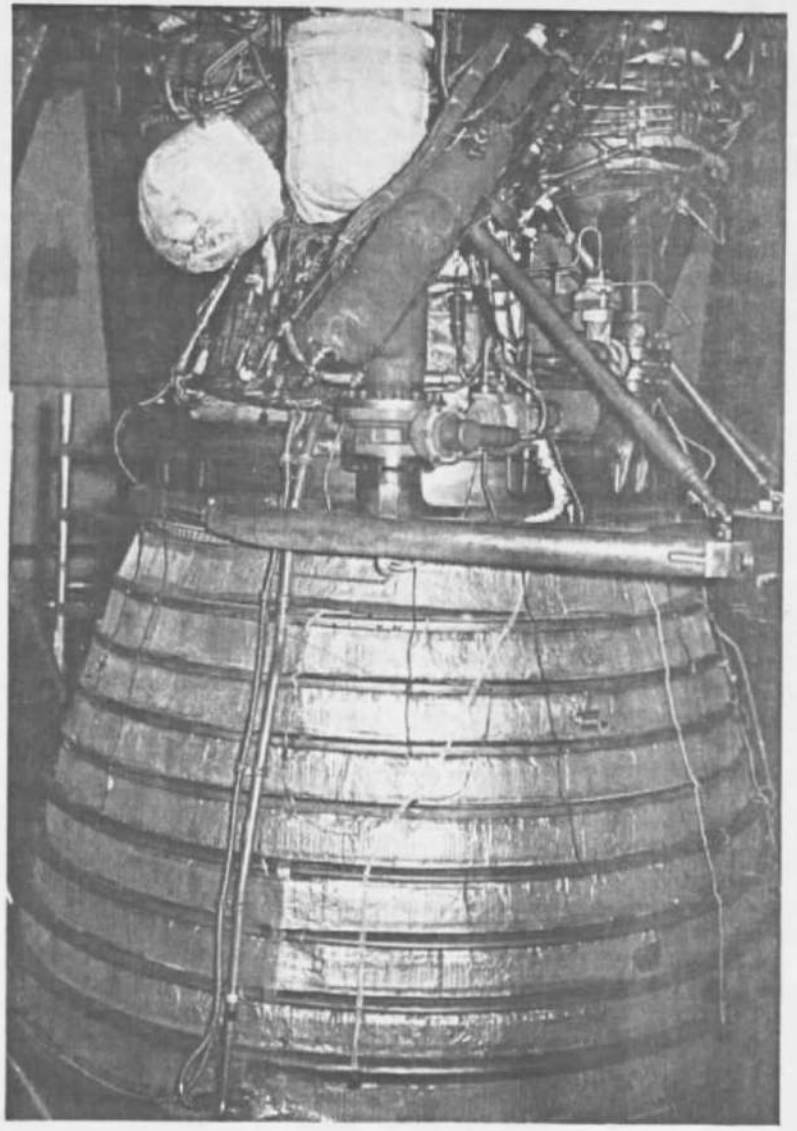

b. J-2 Engine Closeup View

Fig. 4 J-2 Engine before and after Heater Blanket Installation

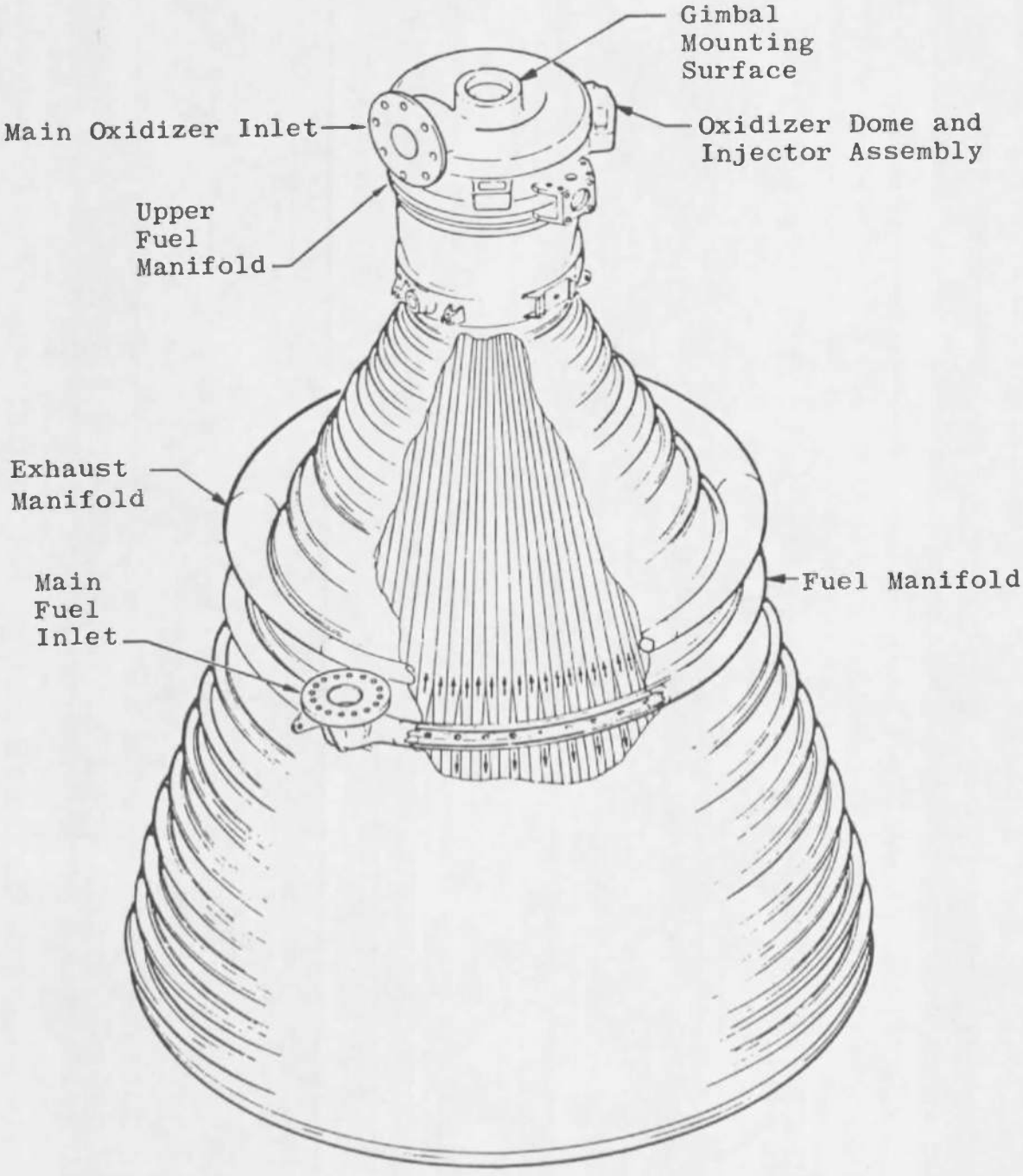

Fig. 5 J-2 Engine Thrust Chamber Details

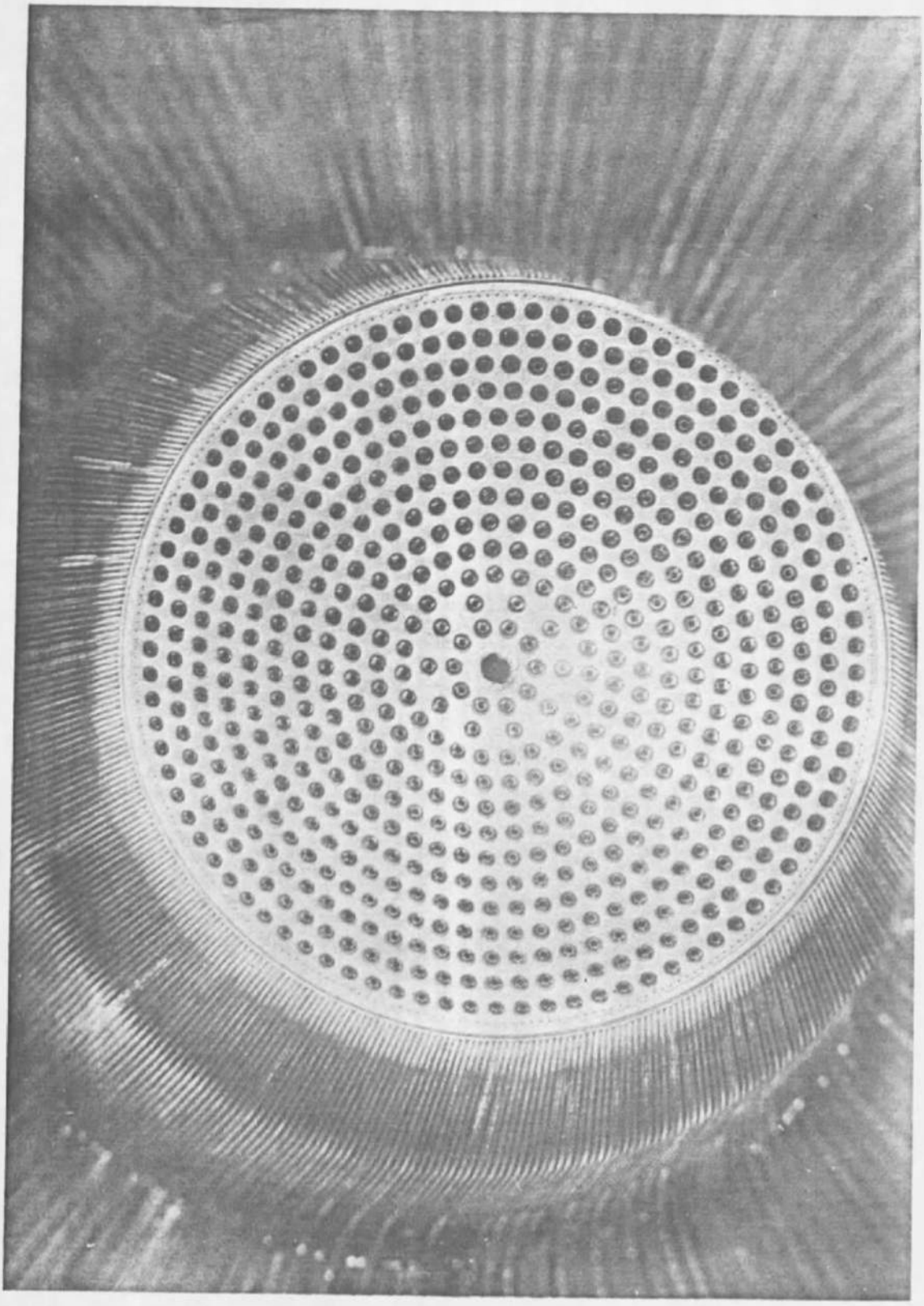

Fig. 6 J-2 Engine Injector Details

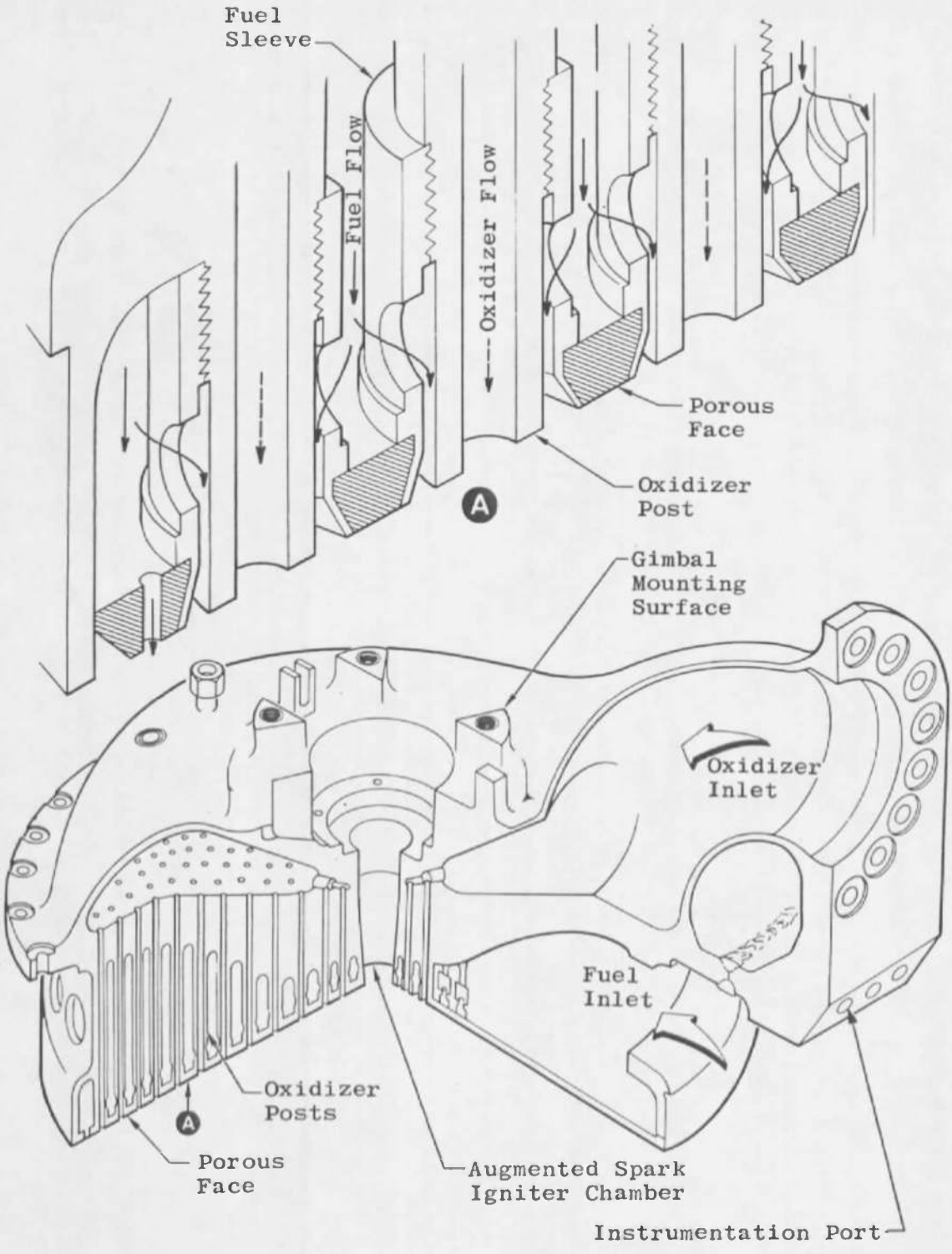

Fig. 6 Concluded

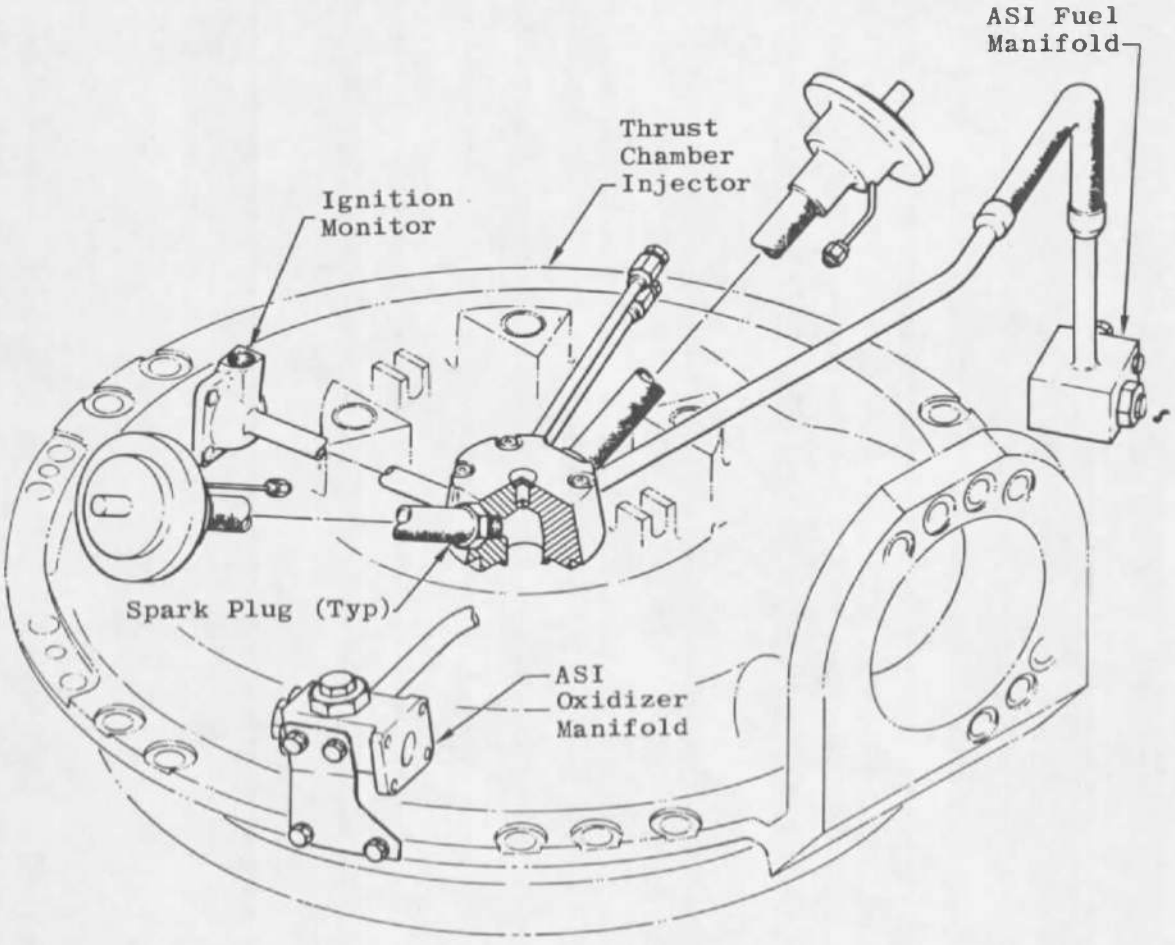

Fig. 7 Augmented Spark Igniter Unit Details

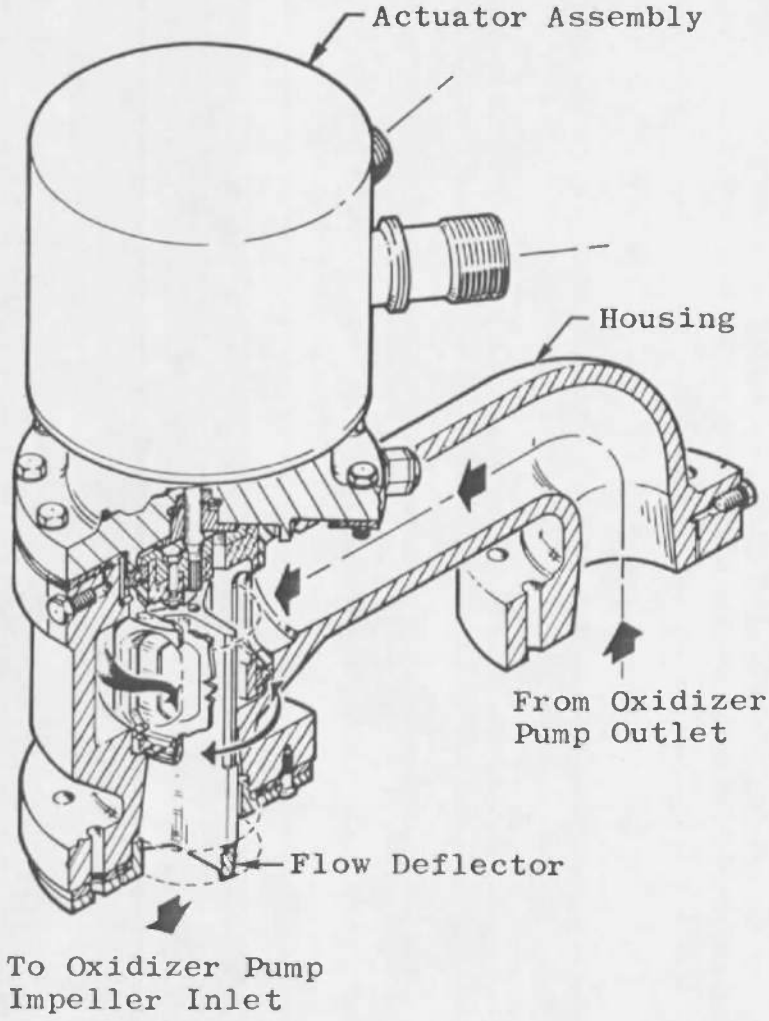

Fig. 8 Propellant Utilization Valve Details

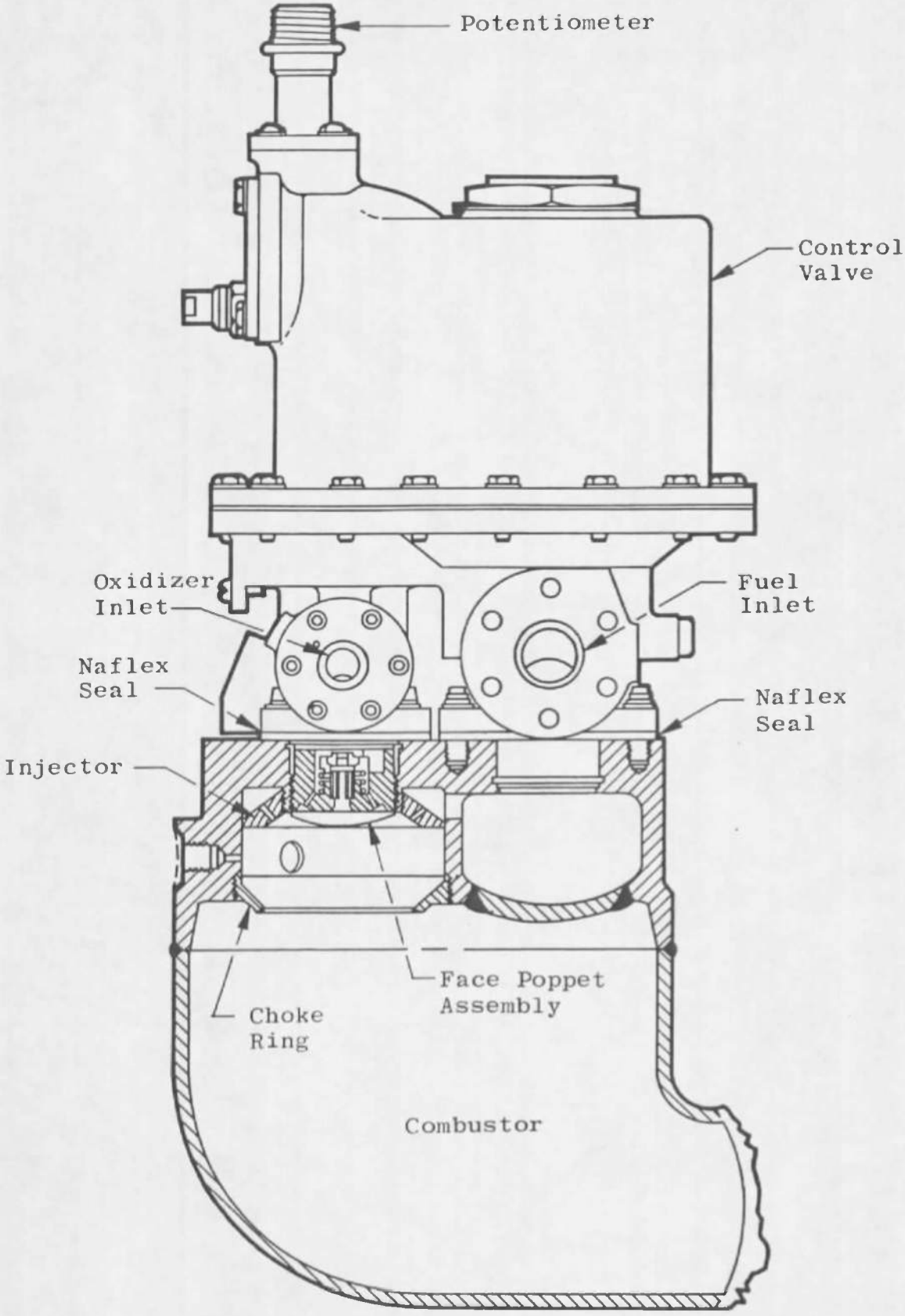

Fig. 9 Gas Generator Assembly Details

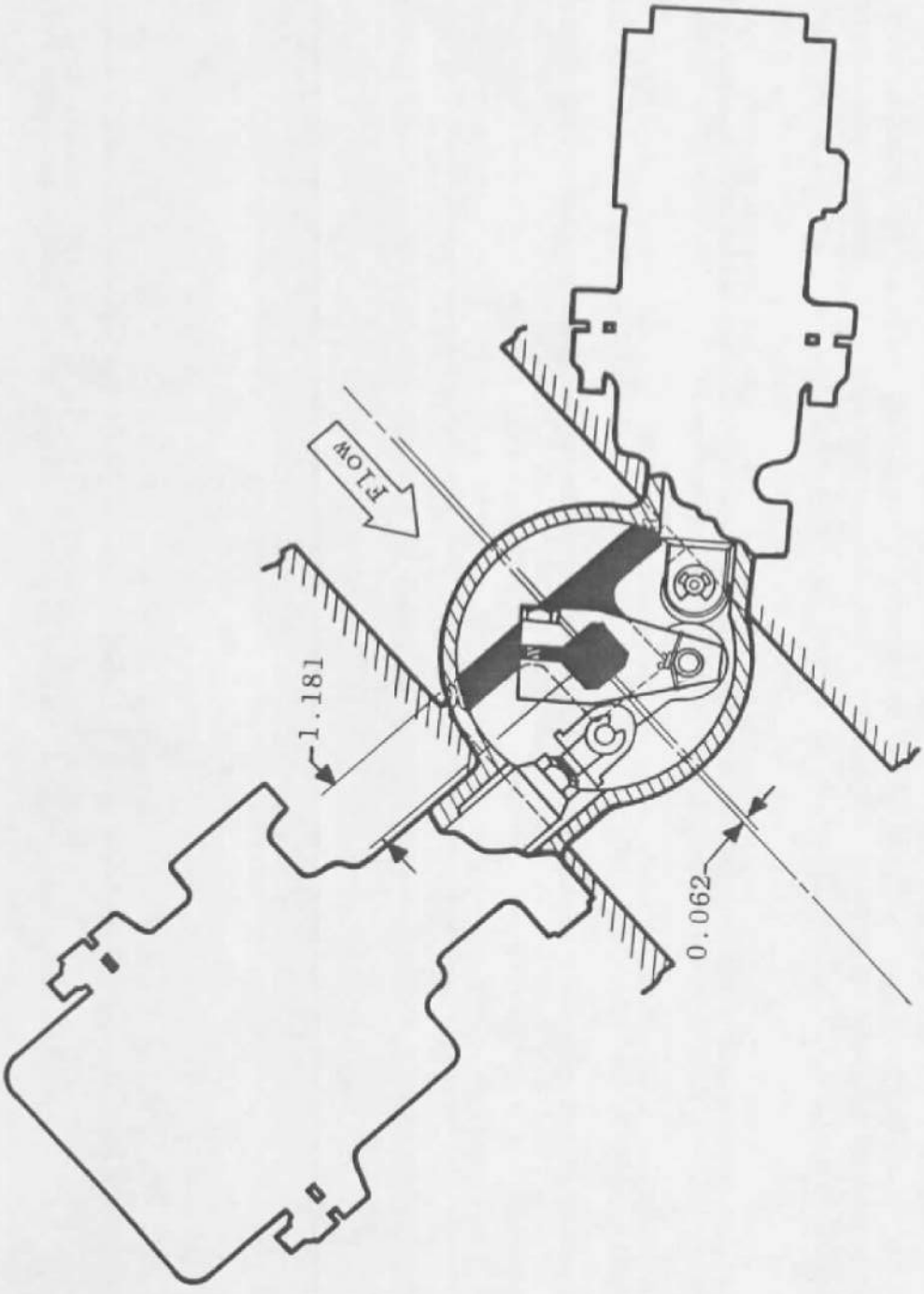

Fig. 10 Main Oxidizer Valve

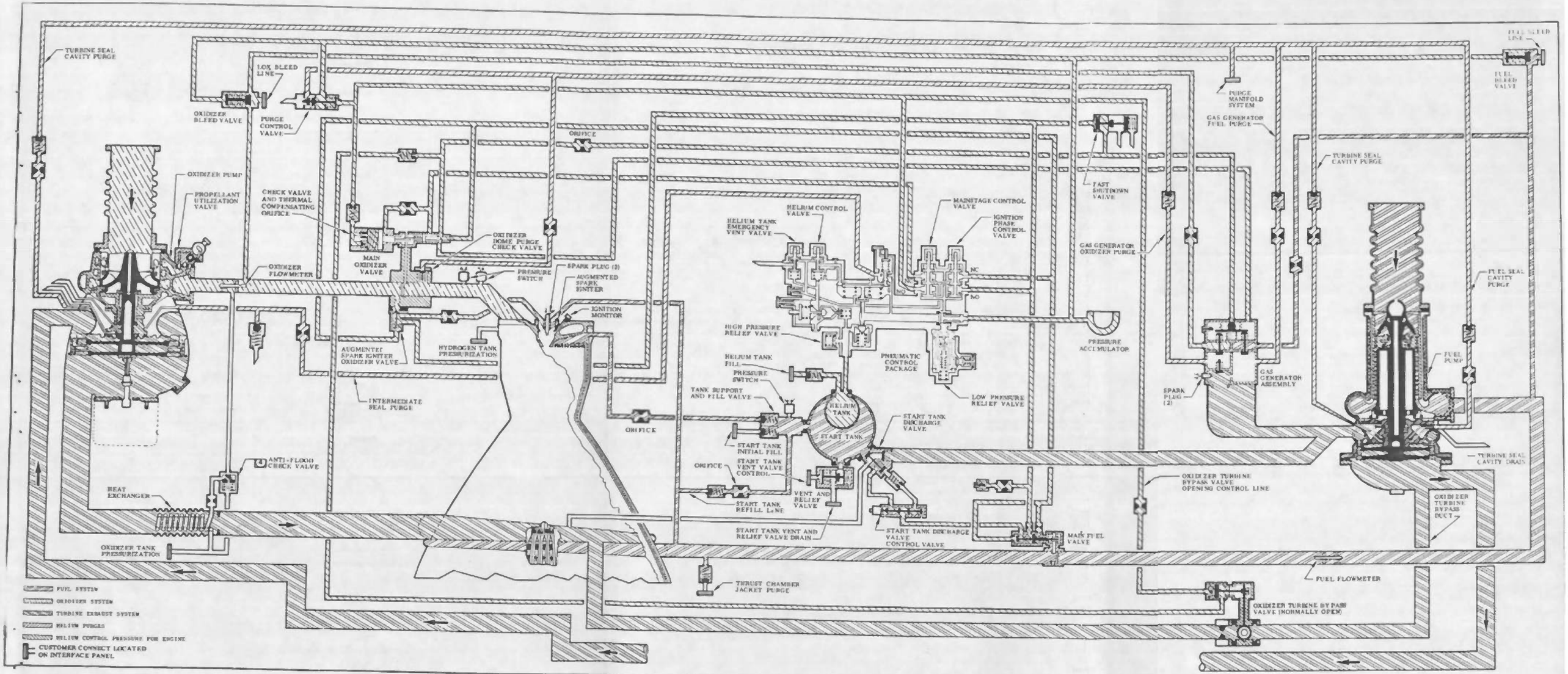

a. Detailed Schematic

Fig. 11 Mechanical Schematic of the J-2 Engine

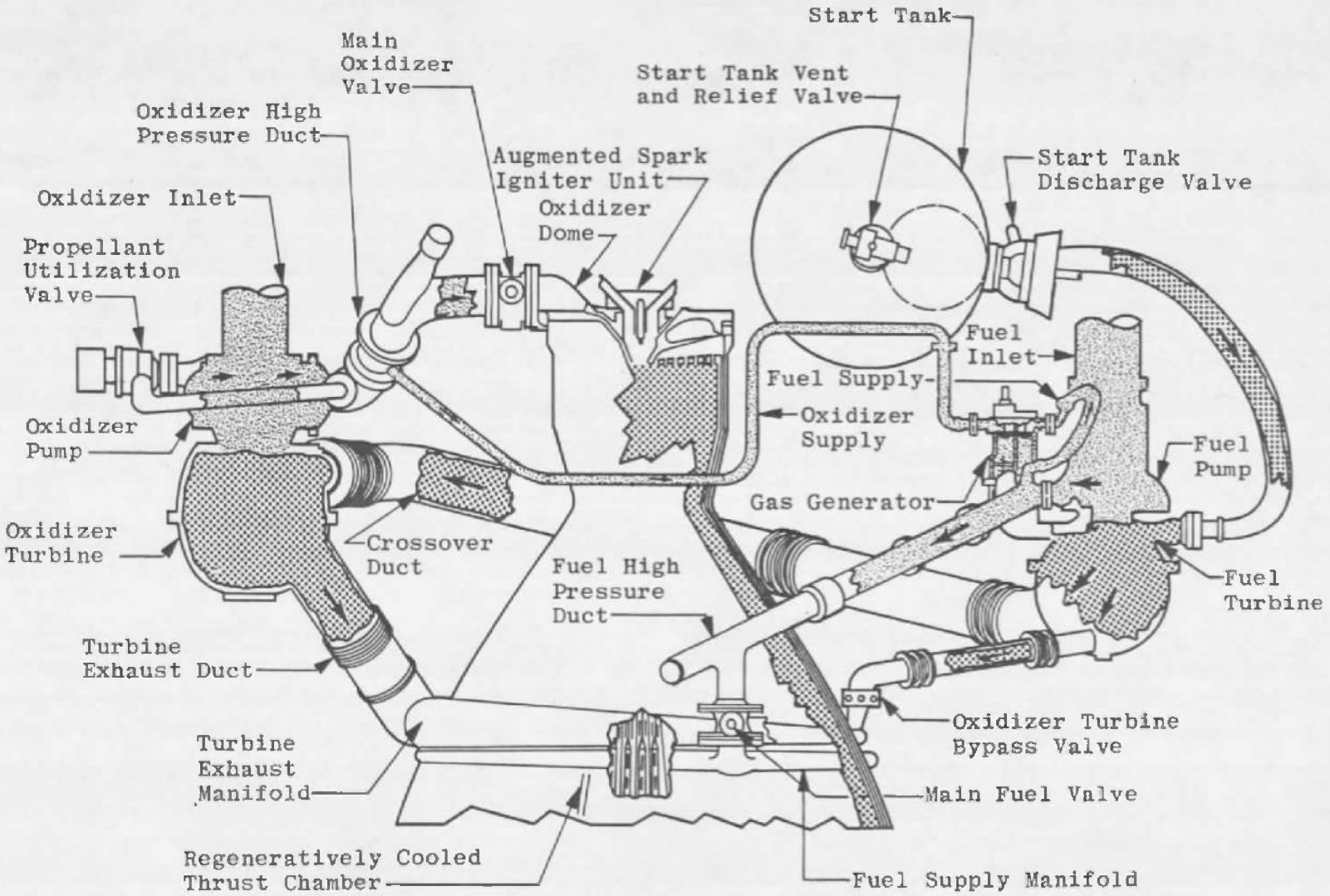

b. Simplified Propellant and Hot Gas Flow Diagram

Fig. 11 Concluded

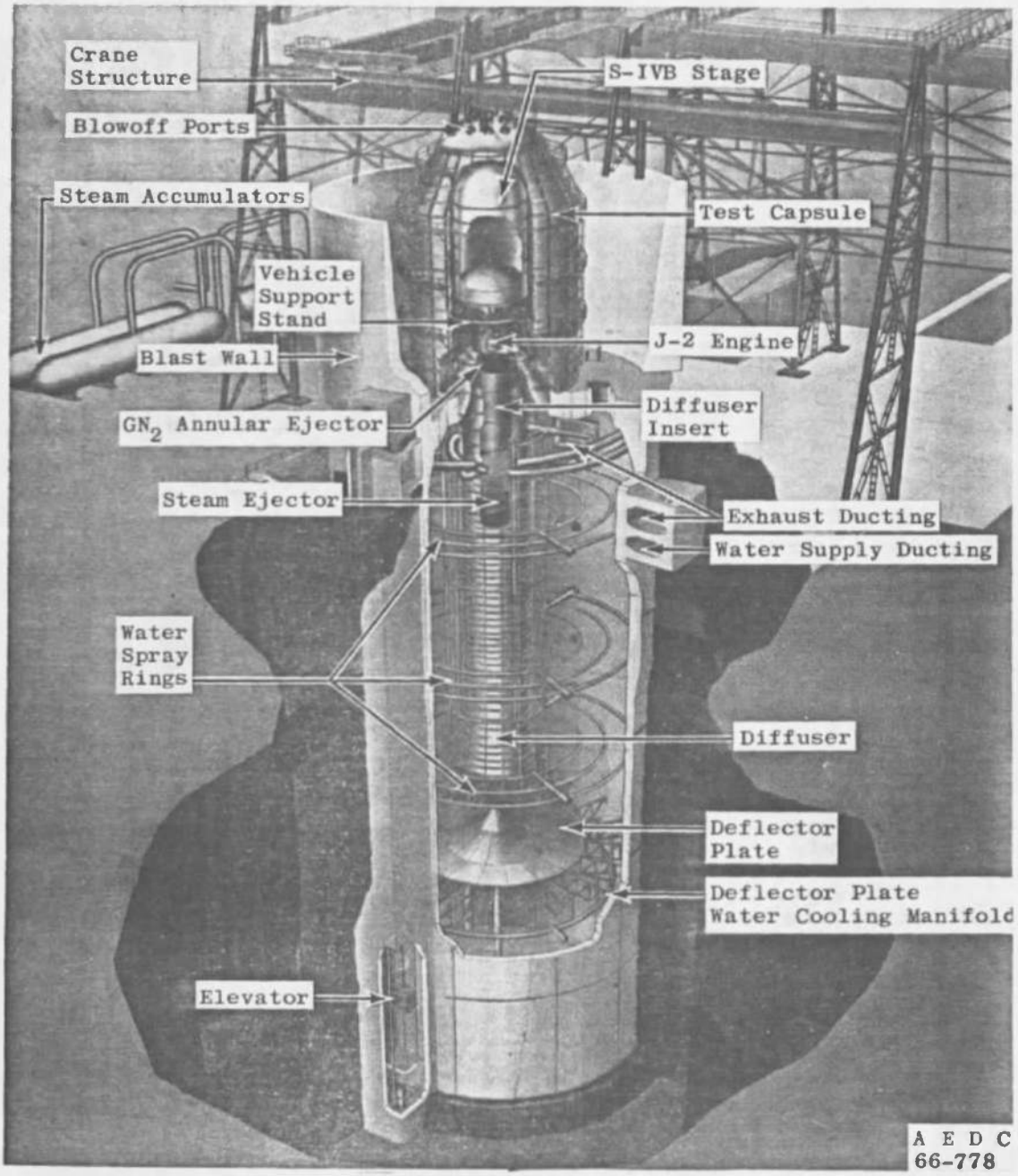

Fig. 12 Propulsion Engine Test Cell (J-4) Details

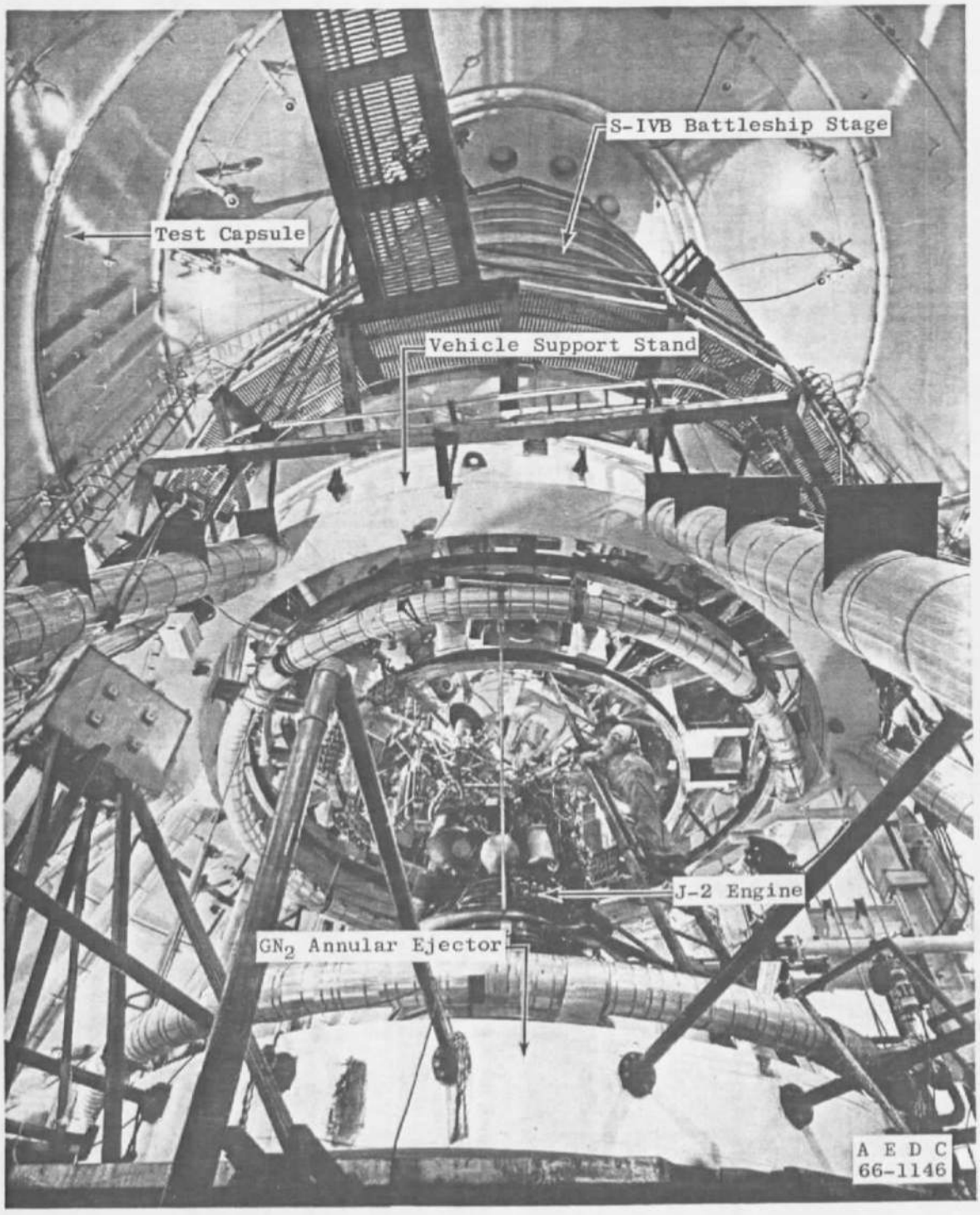

a. Test Article Installation

Fig. 13 Test Article Installation

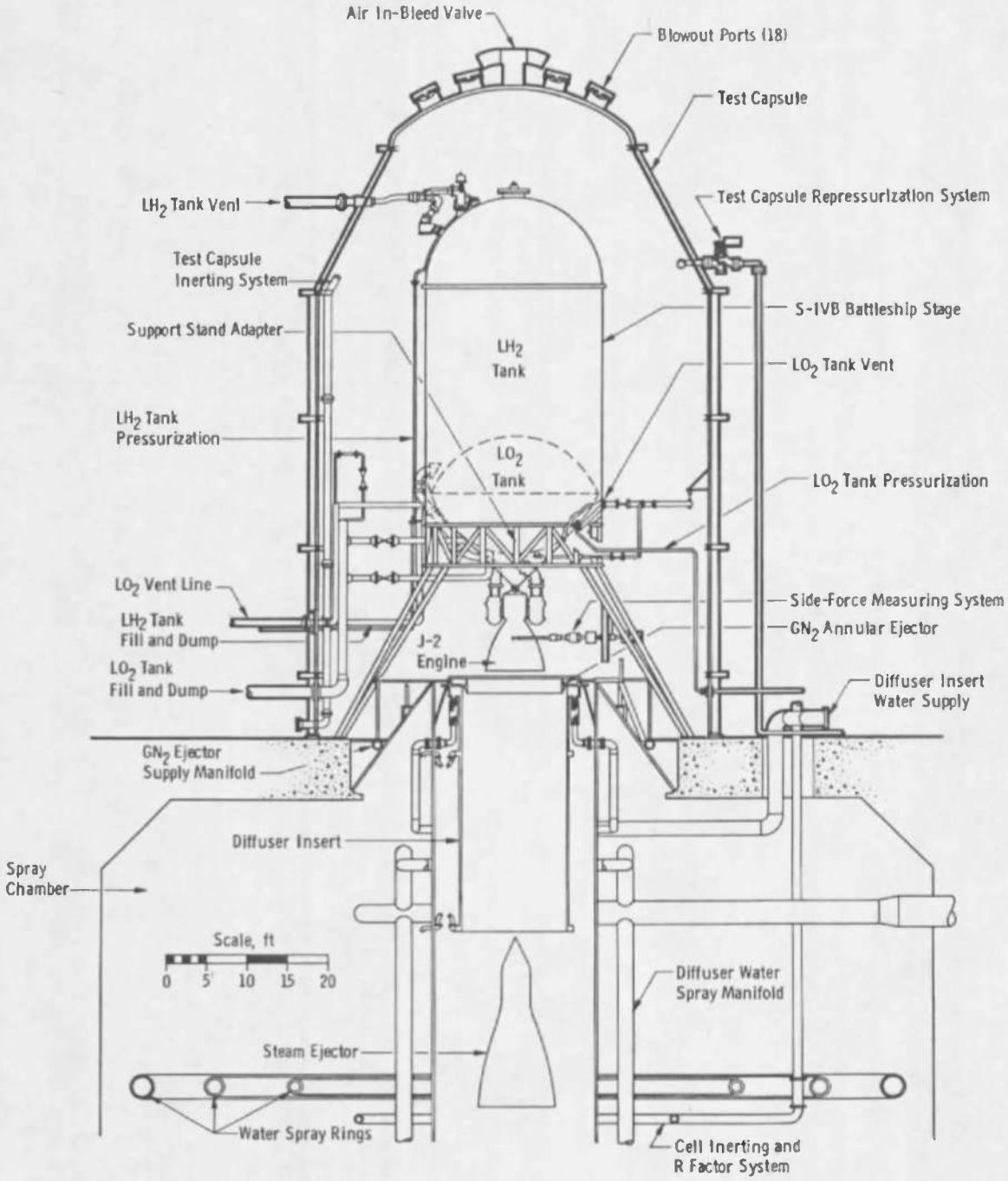

b. Test Article Installation

Fig. 13 Concluded

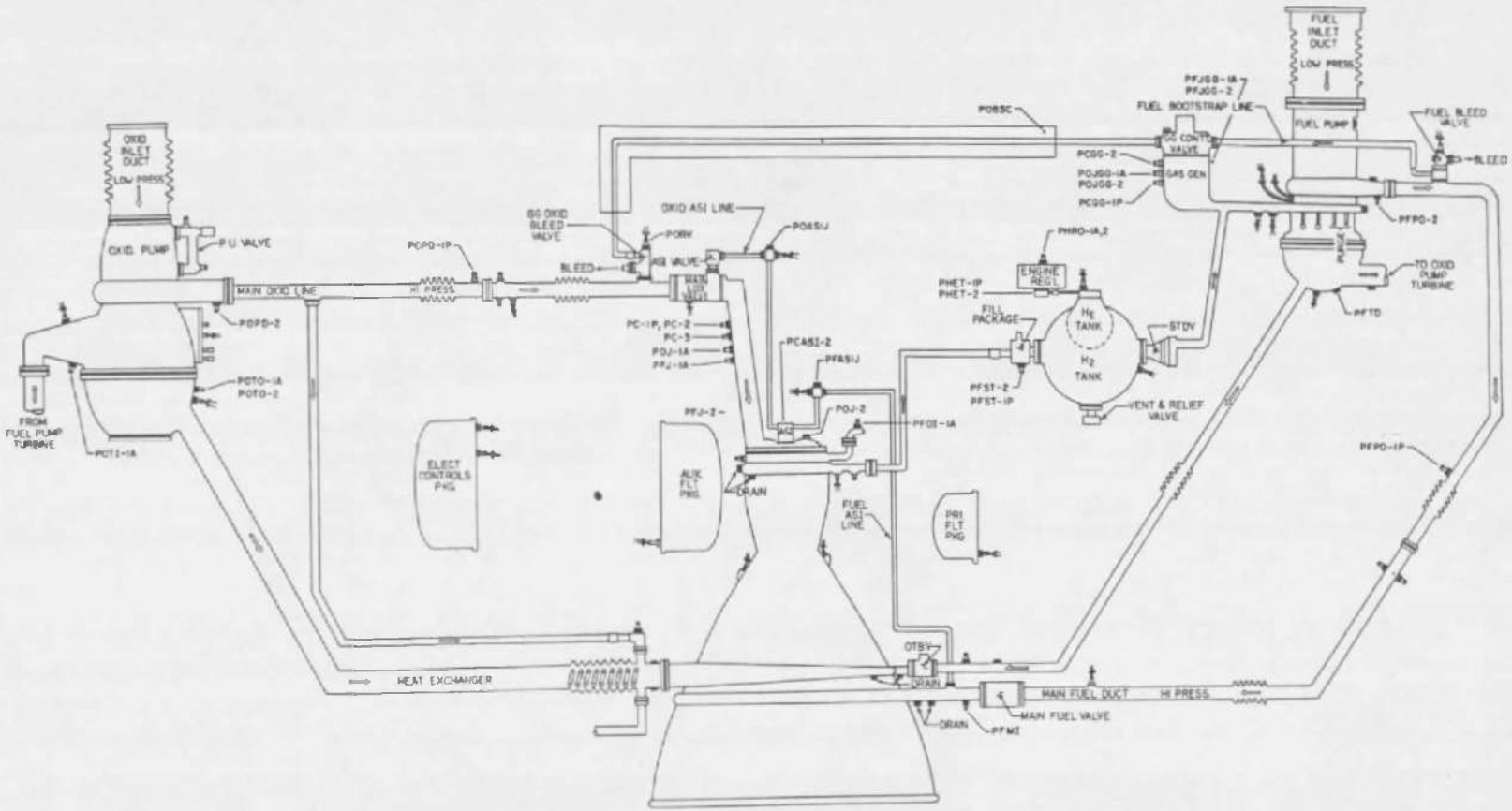

a. Engine Pressure Tap Locations

Fig. 14 Test Article Instrumentation

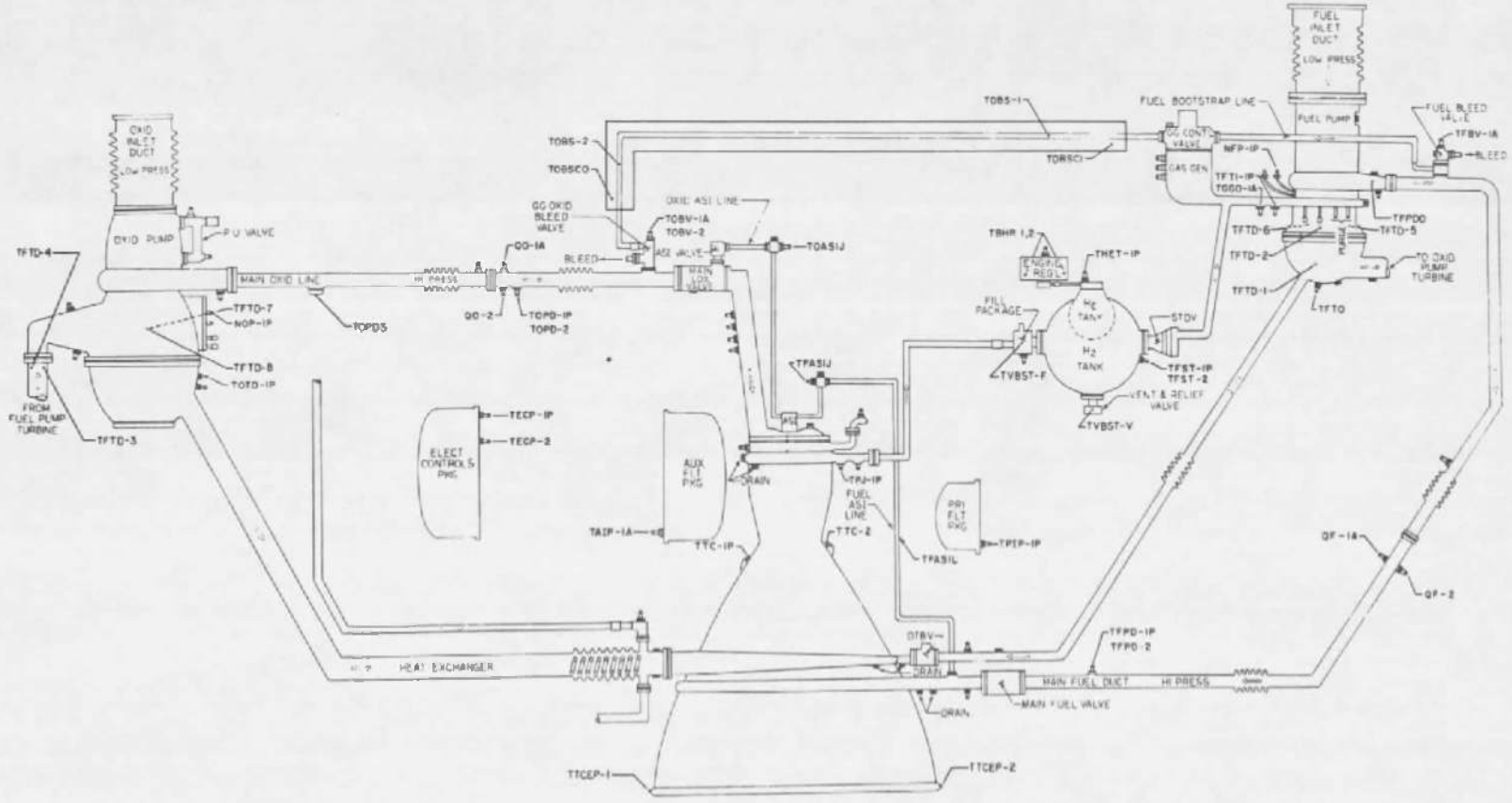

b. Engine Temperature, Flow, and Speed Instrumentation Locations

Fig. 14 Continued

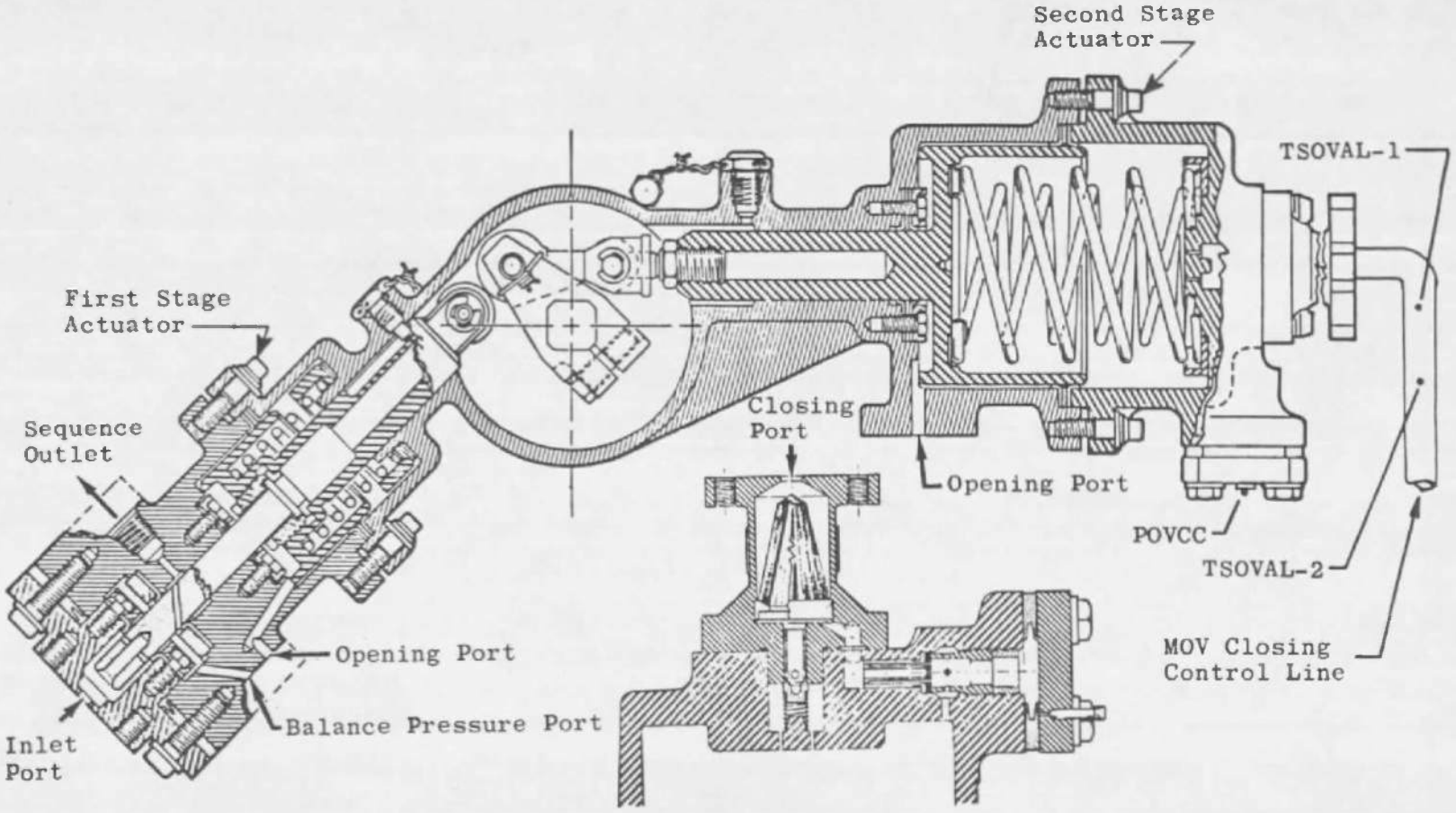

c. Main Oxidizer Valve Second Stage Actuation Instrumentation

Fig. 14 Continued

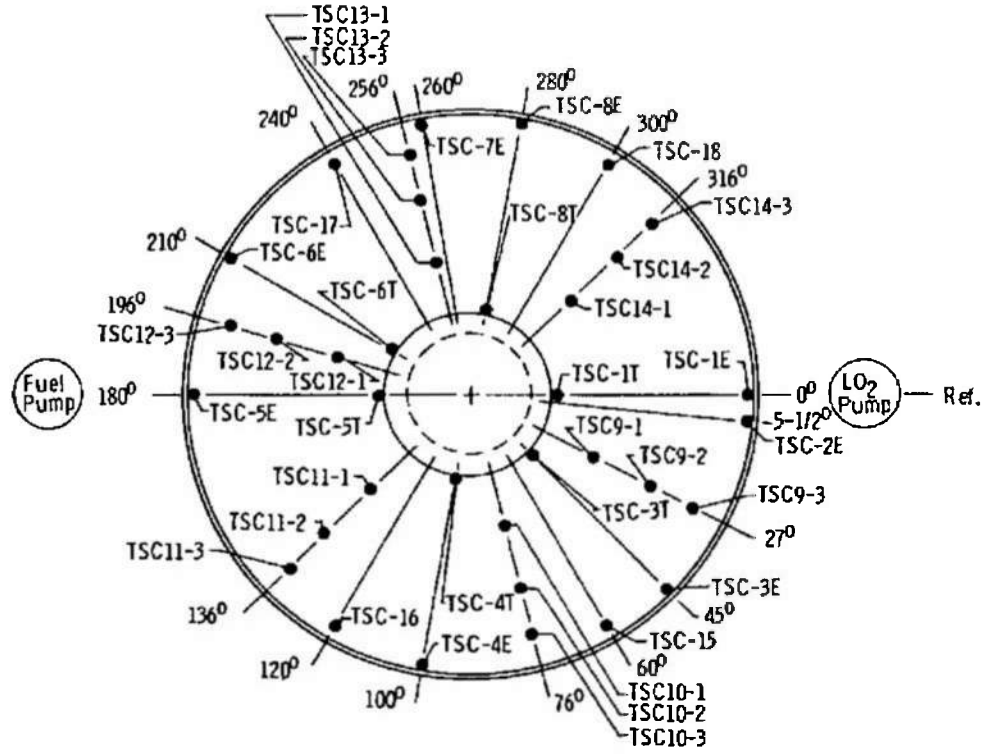

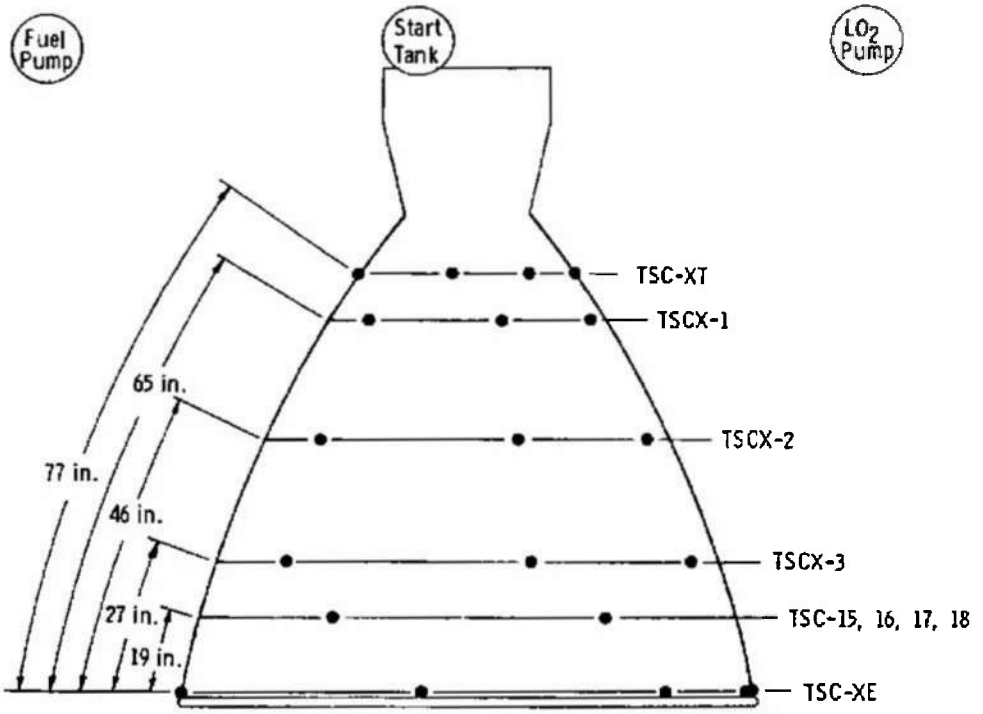

d. Thrust Chamber Skin Thermocouple Locations

Fig. 14 Continued

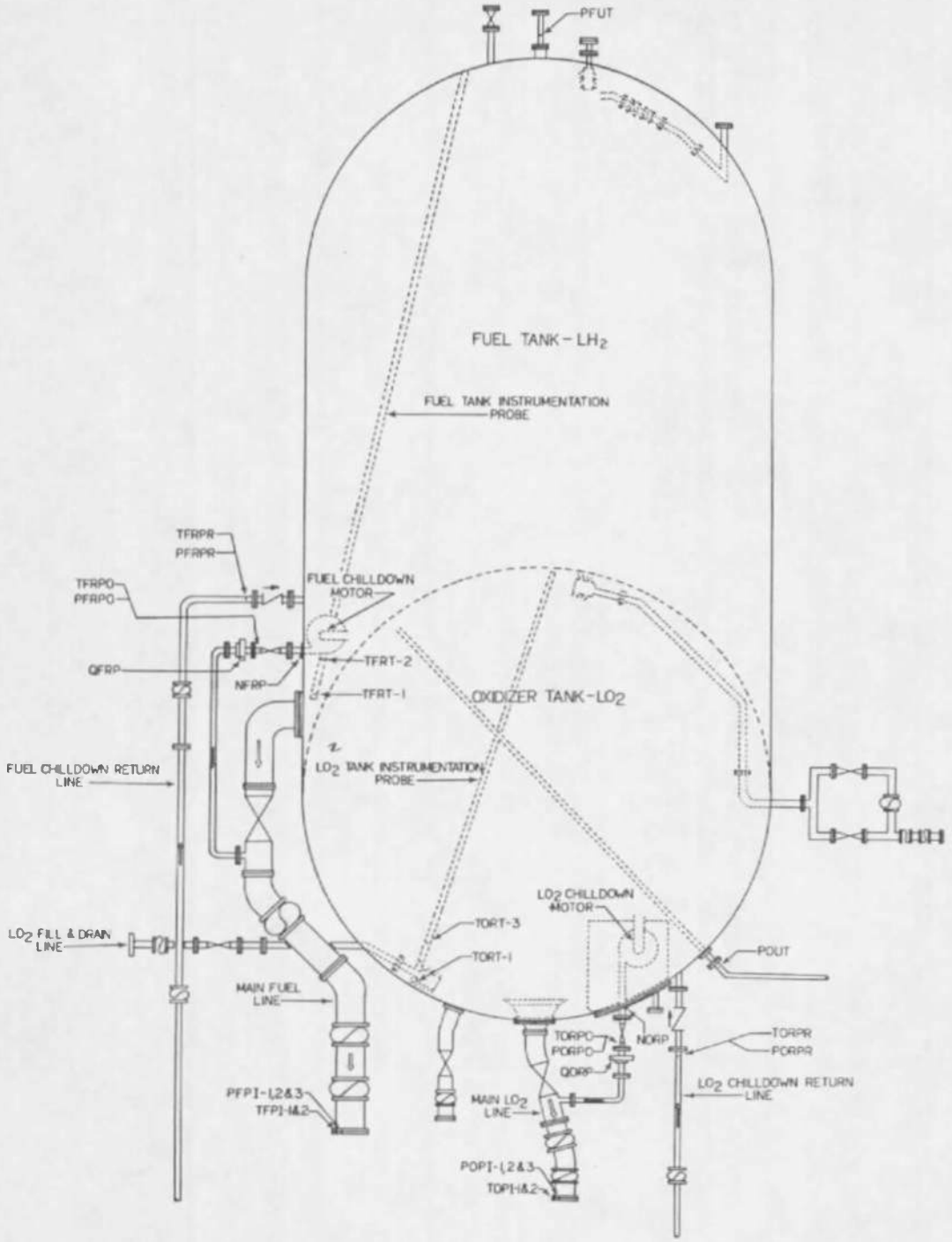

SIDE VIEW

e. S-IVB Stage Instrumentation

Fig. 14 Concluded

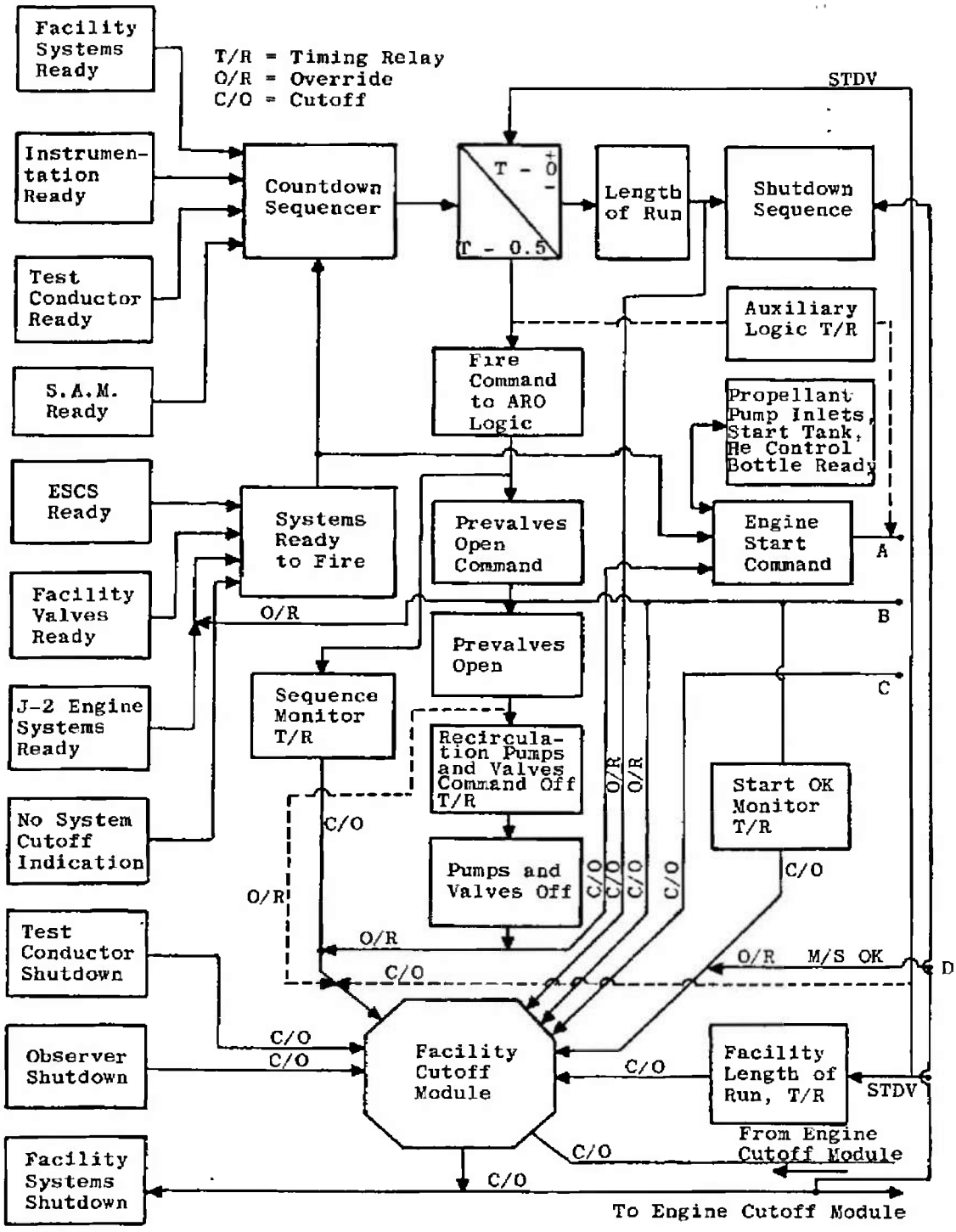

Fig. 15 Facility Logic Block Diagram

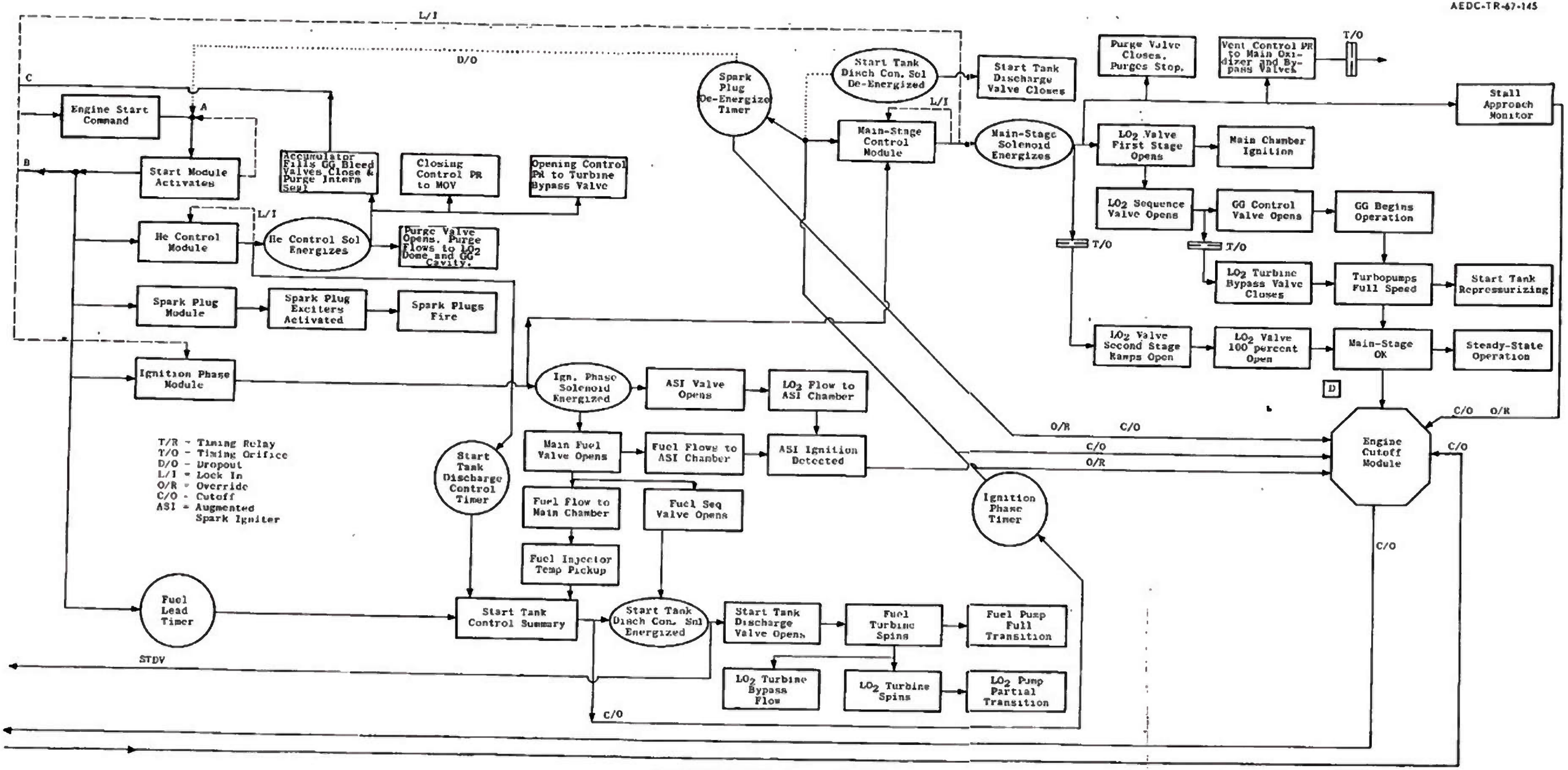

Fig. 16 Engine Starting Sequence Block Diagram

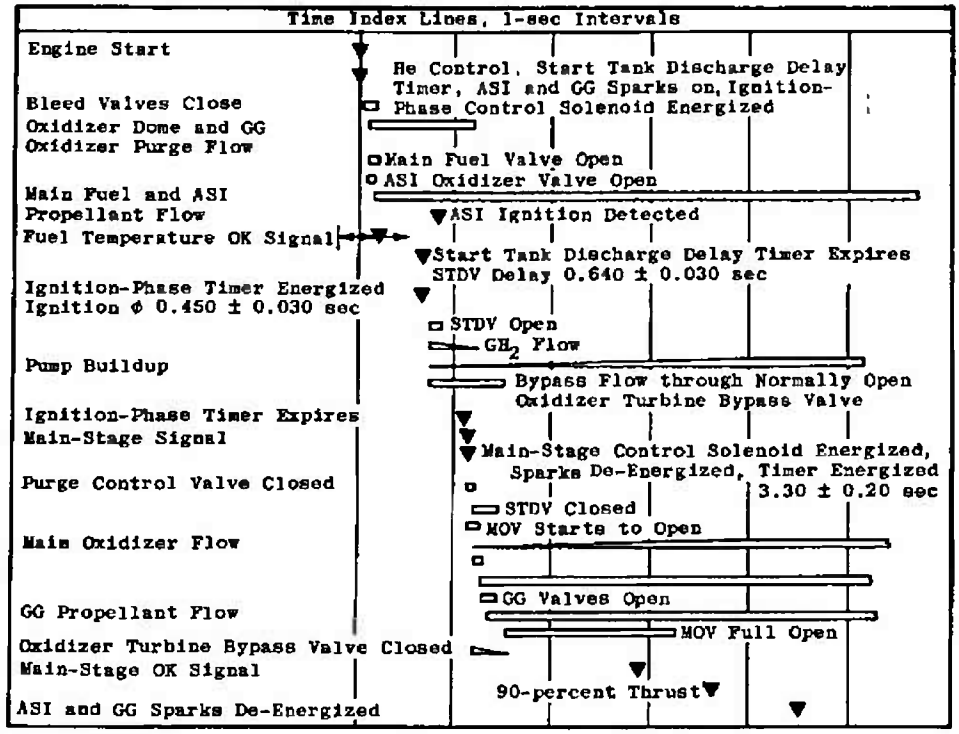

a. Start Sequence

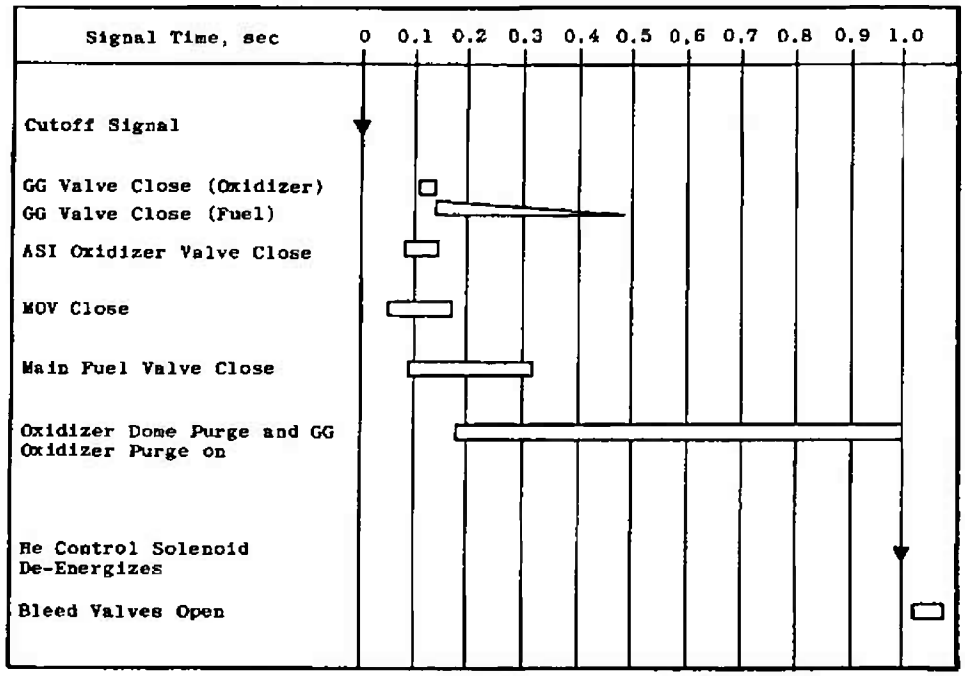

b. Cutoff Sequence

Fig. 17 Engine Start and Cutoff Sequence

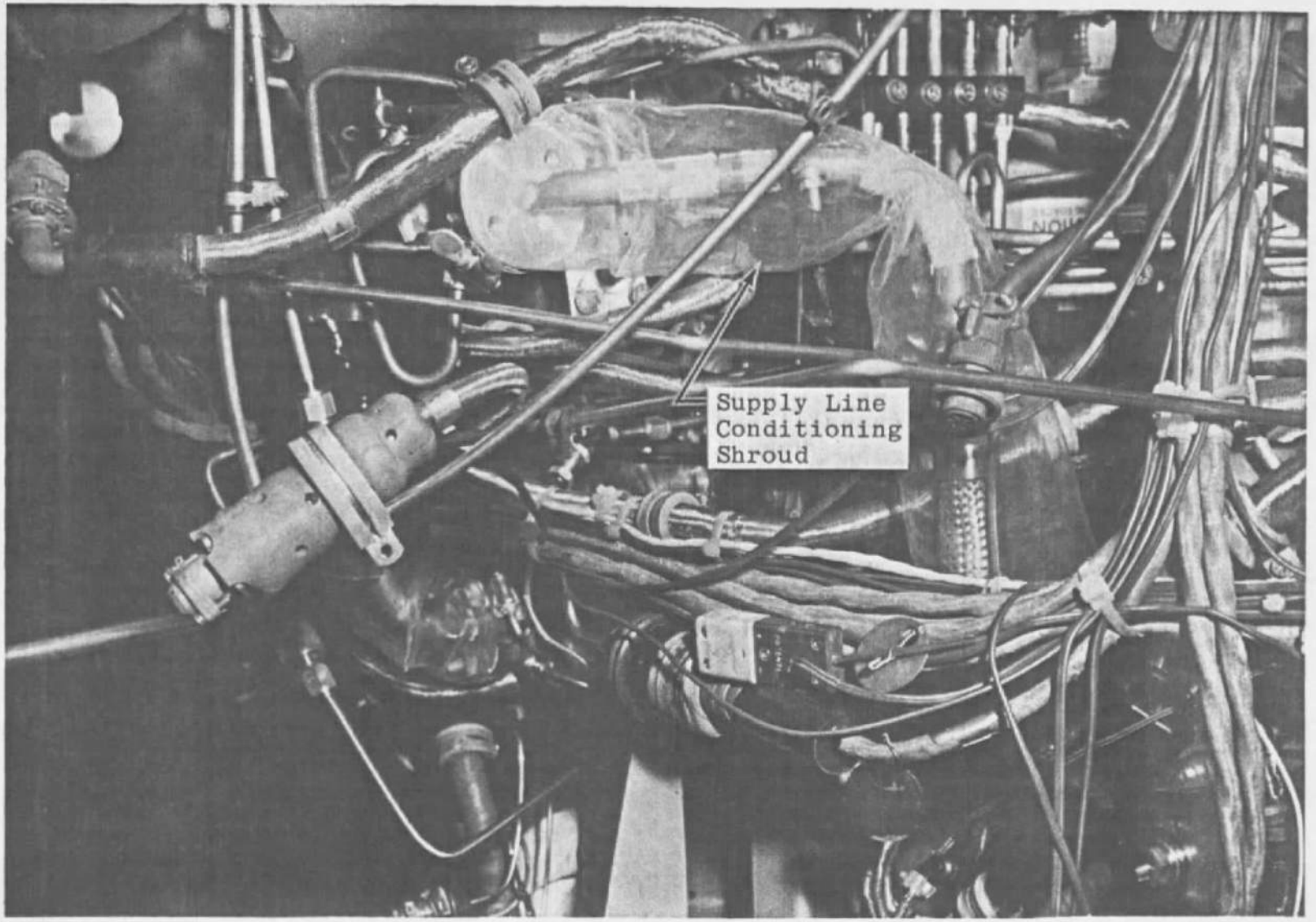

Fig. 18 Gas Generator Liquid Oxygen Supply Line Conditioning Shroud

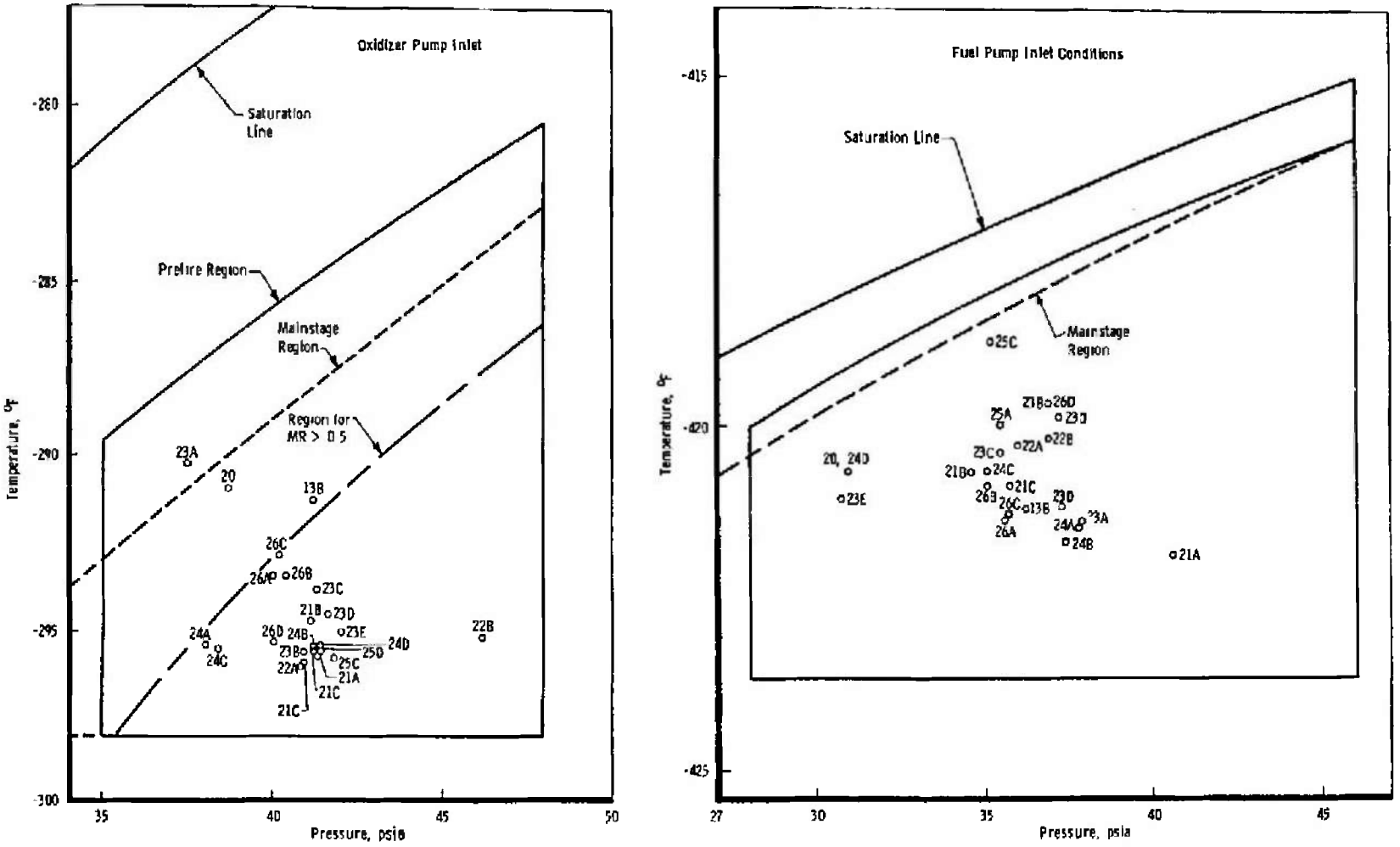

Fig. 19 Pump Inlet Conditions at Engine Start

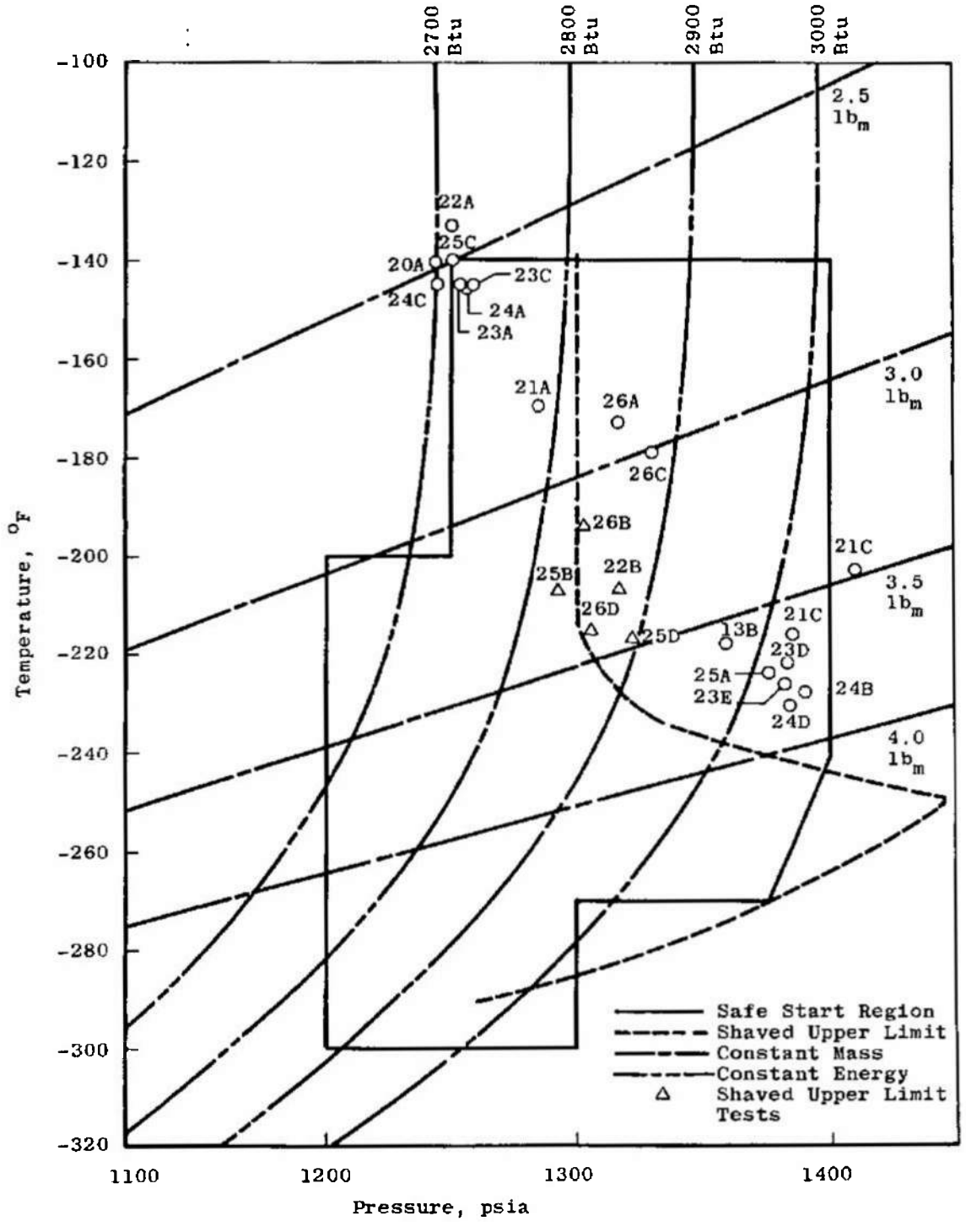

Fig. 20 Start Tank Energy Map at Engine Start

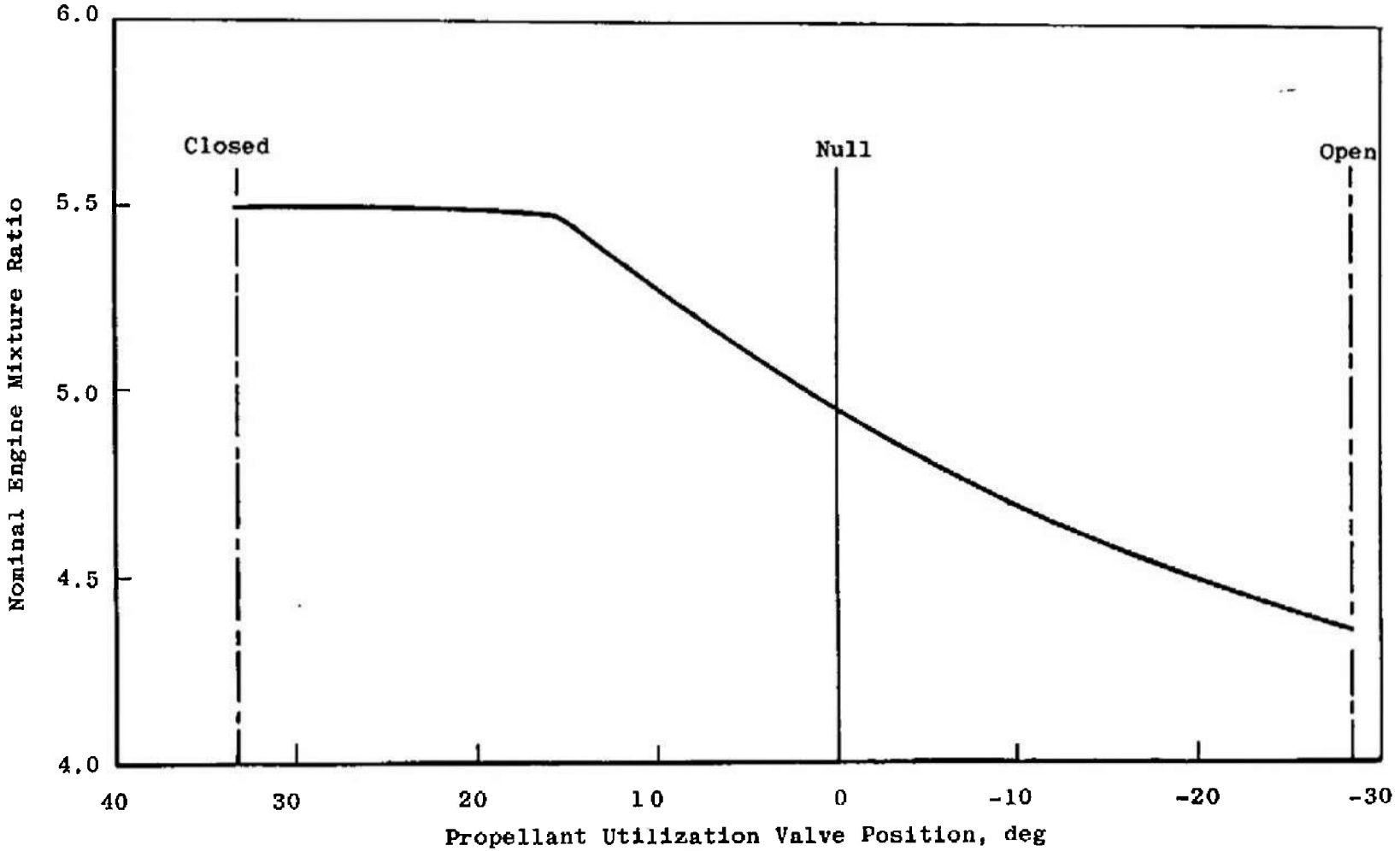

Fig. 21 J-2 Engine Nominal Mixture Ratio

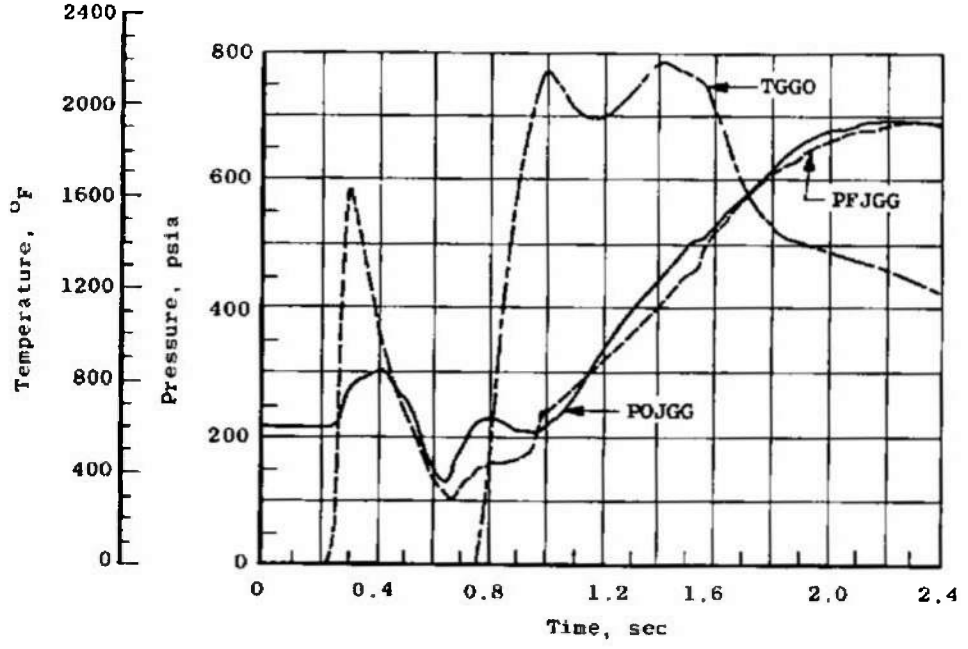

a. Gas Generator Start Transient–Test 25D

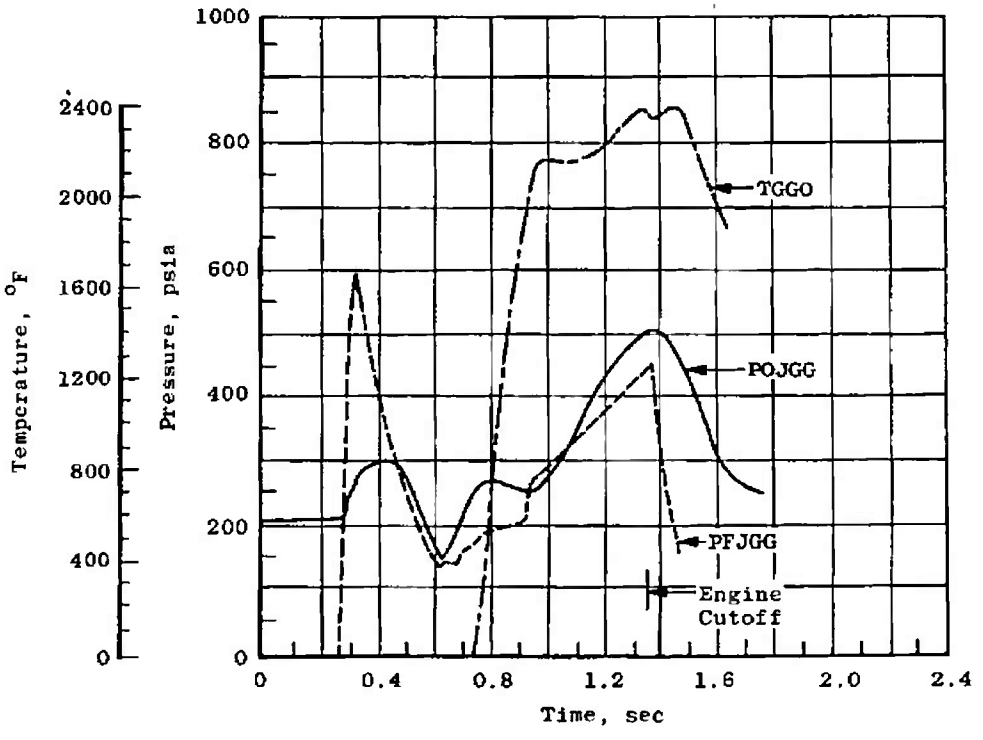

b. Gas Generator Start Transient–Test 13B

Fig. 22 Start Transient Comparisons–Tests 25D and 13B

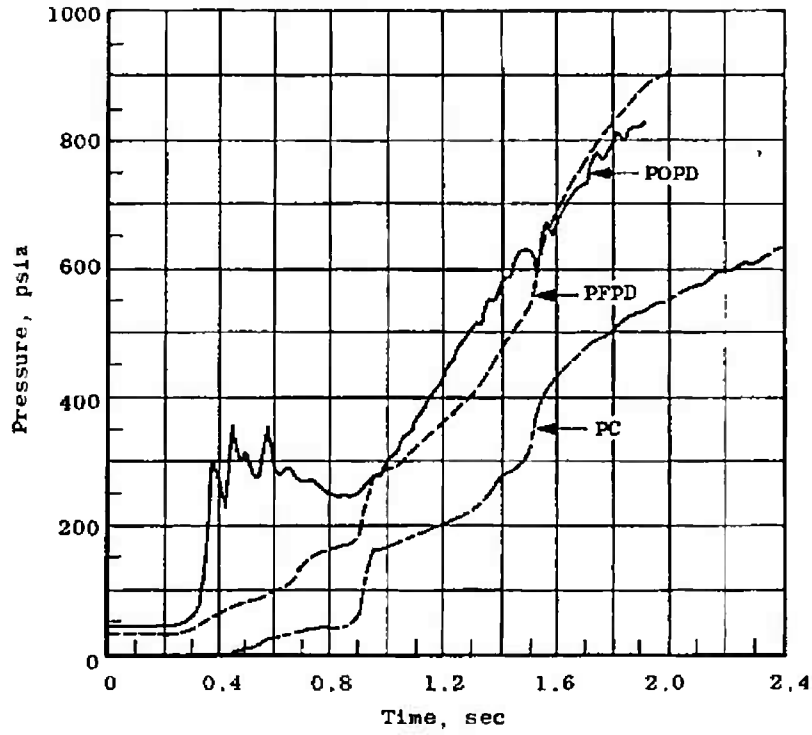

c. Main Chamber Start Transient–Test 25D

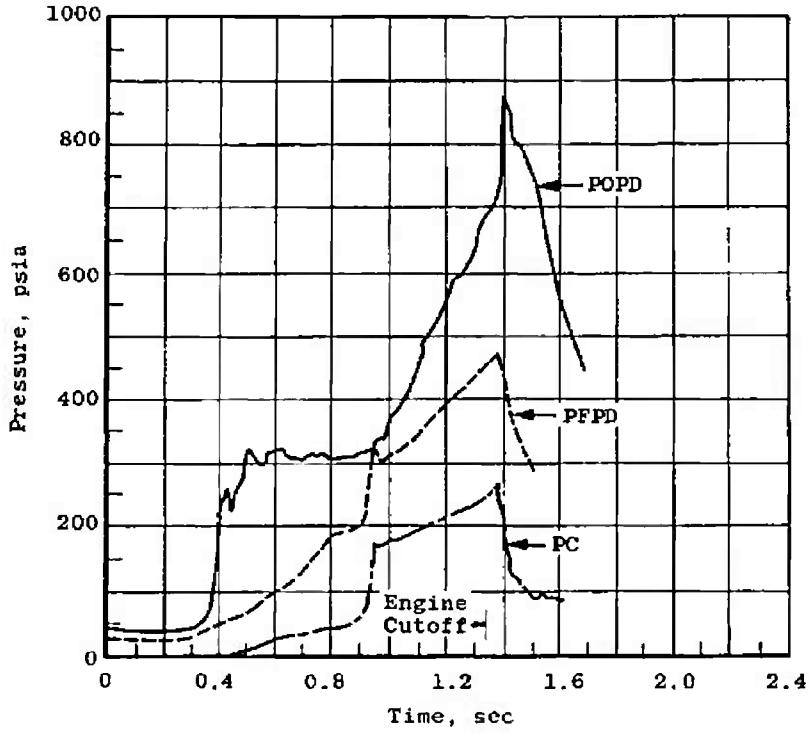

d. Main Chamber Start Transient–Test 13B

Fig. 22 Continued

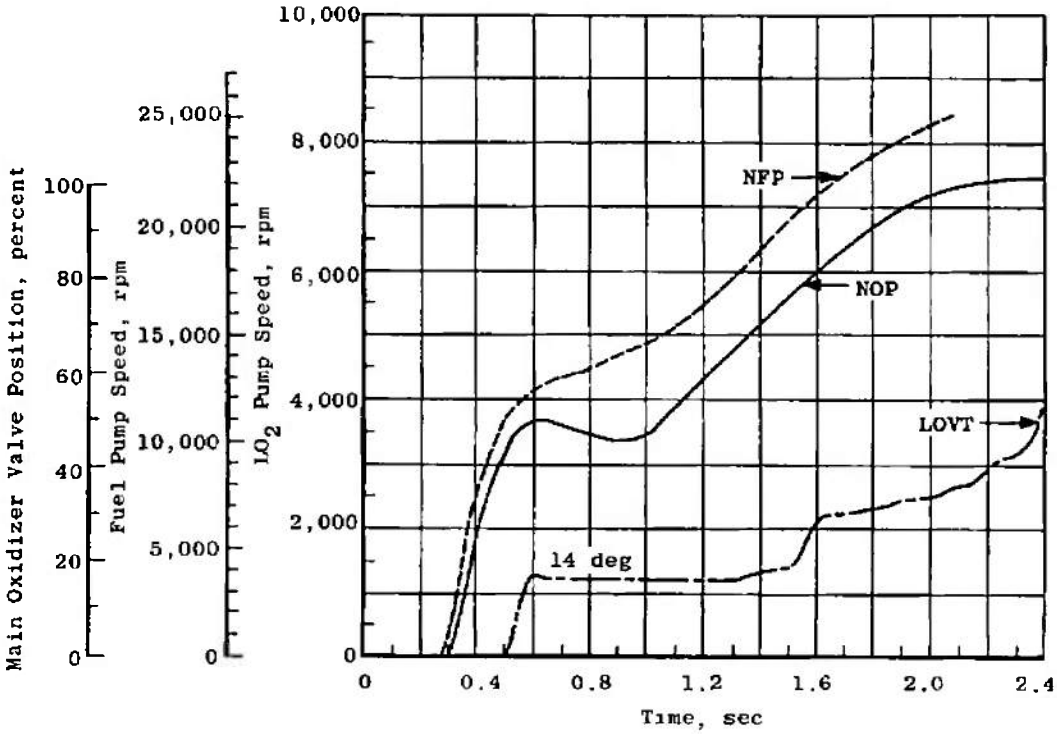

e. Pump Speeds and Main Oxidizer Valve Movement–Test 25D

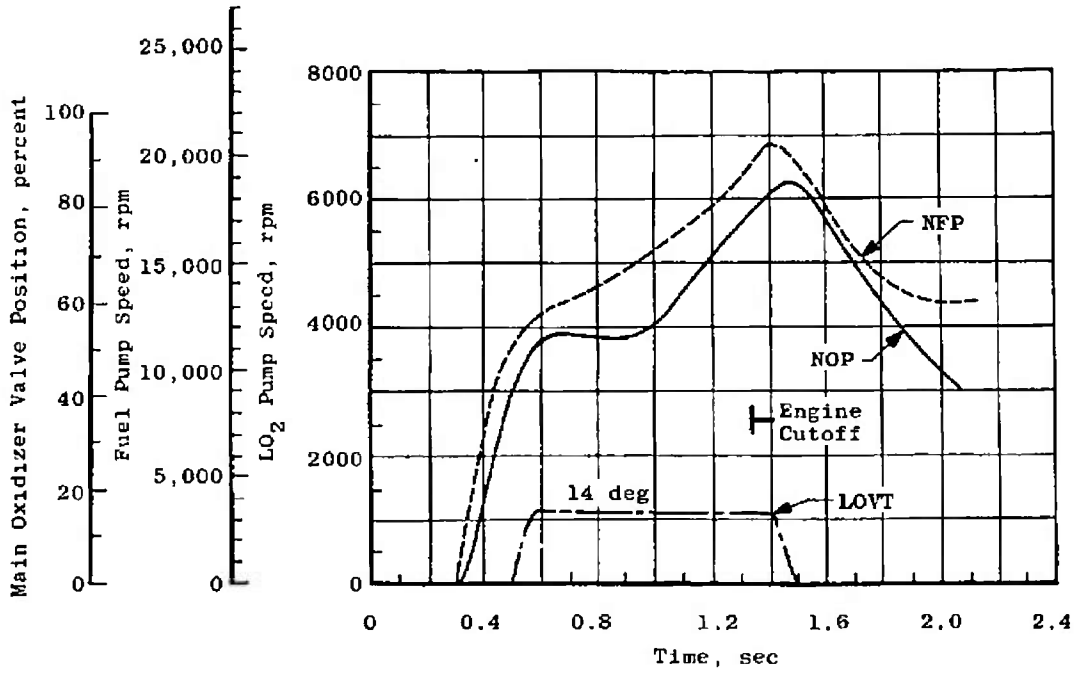

f. Pump Speeds and Main Oxidizer Valve Movement–Test 13B

Fig. 22 Concluded

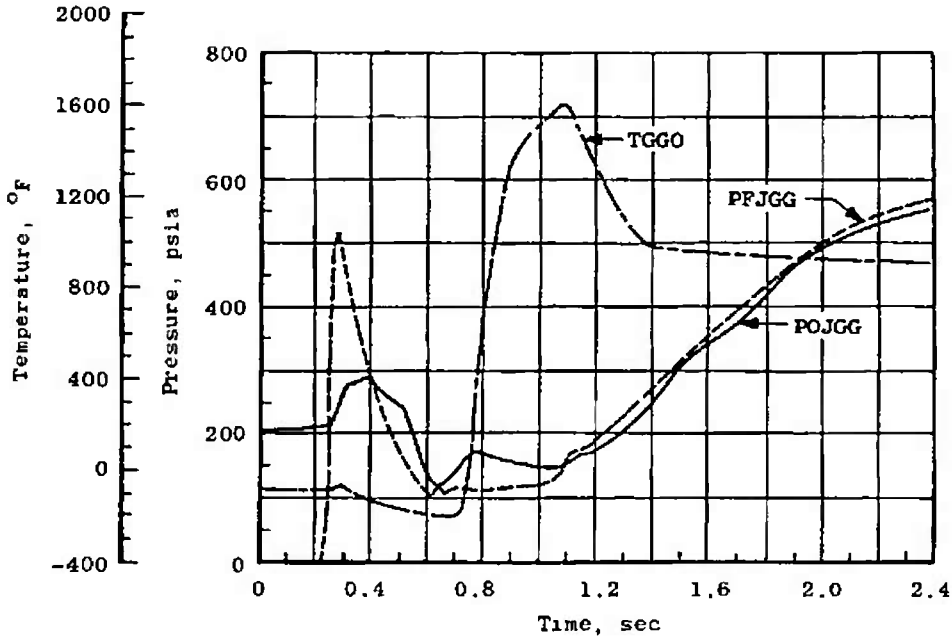

a. Gas Generator Start Transient–Test 23C

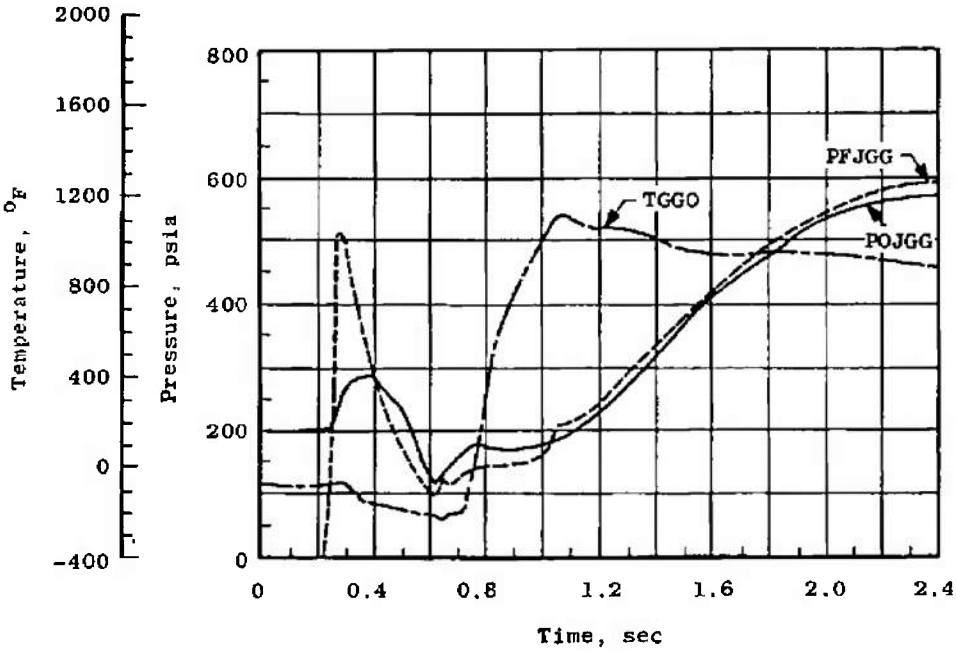

b. Gas Generator Start Transient–Test 24A

Fig. 23 Start Transient Comparisons–Tests 23C and 24A

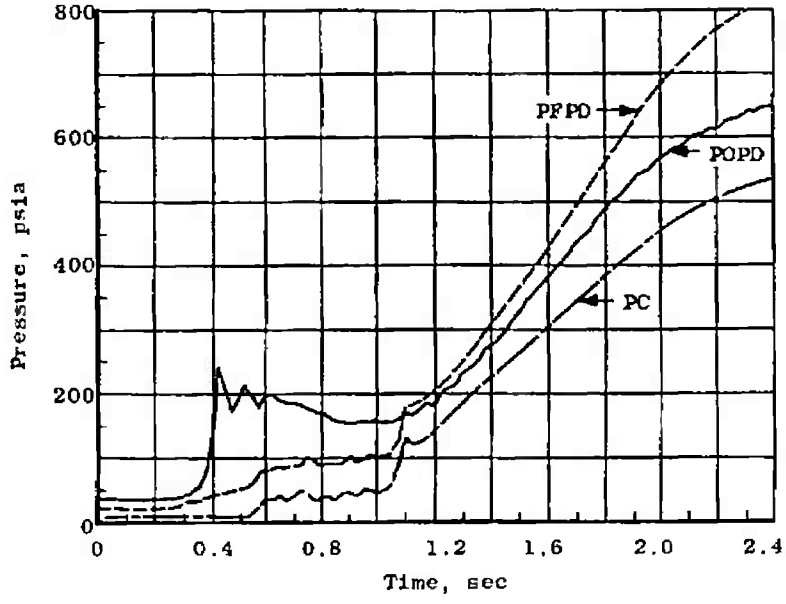

c. Main Chamber Start Transient–Test 23C

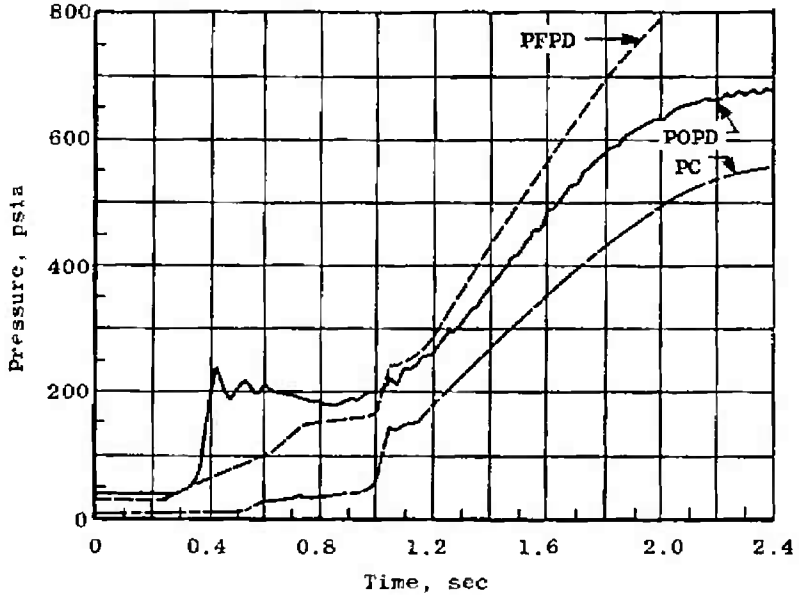

d. Main Chamber Start Transient–Test 24A

Fig. 23 Continued

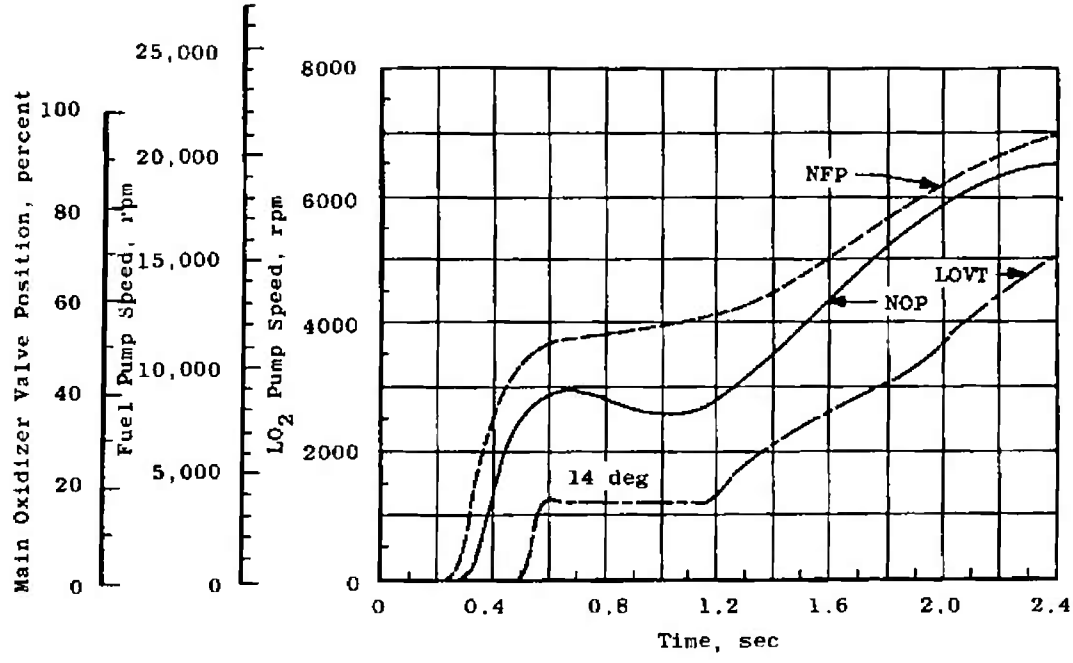

e. Pump Speeds and Main Oxidizer Valve Movement–Test 23C

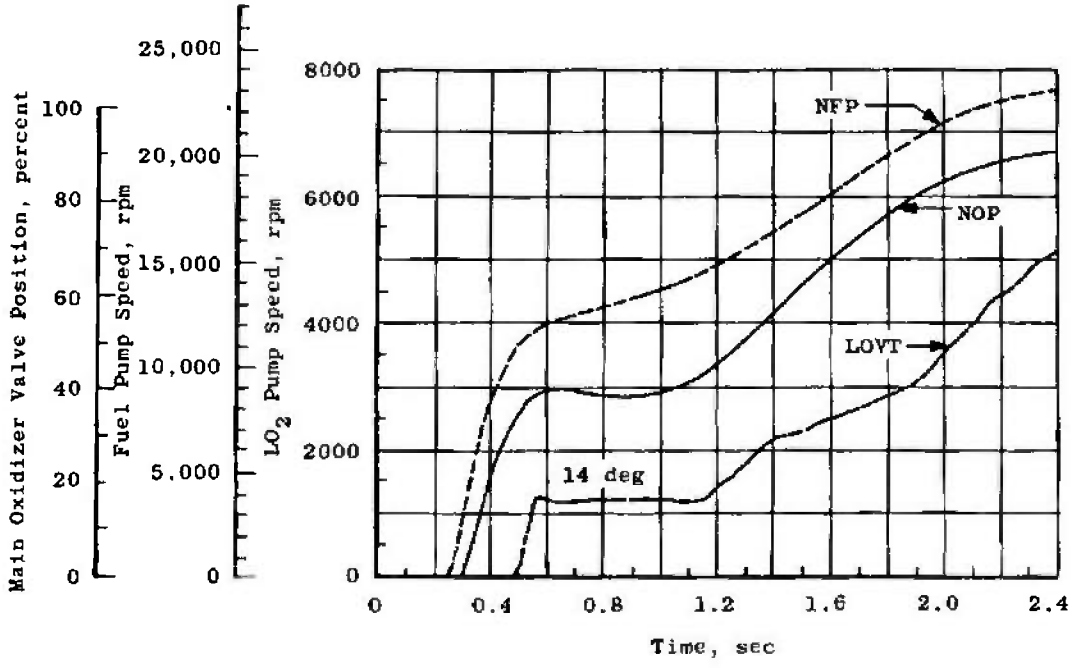

f. Pump Speeds and Main Oxidizer Valve Movement–Test 24A

Fig. 23 Concluded

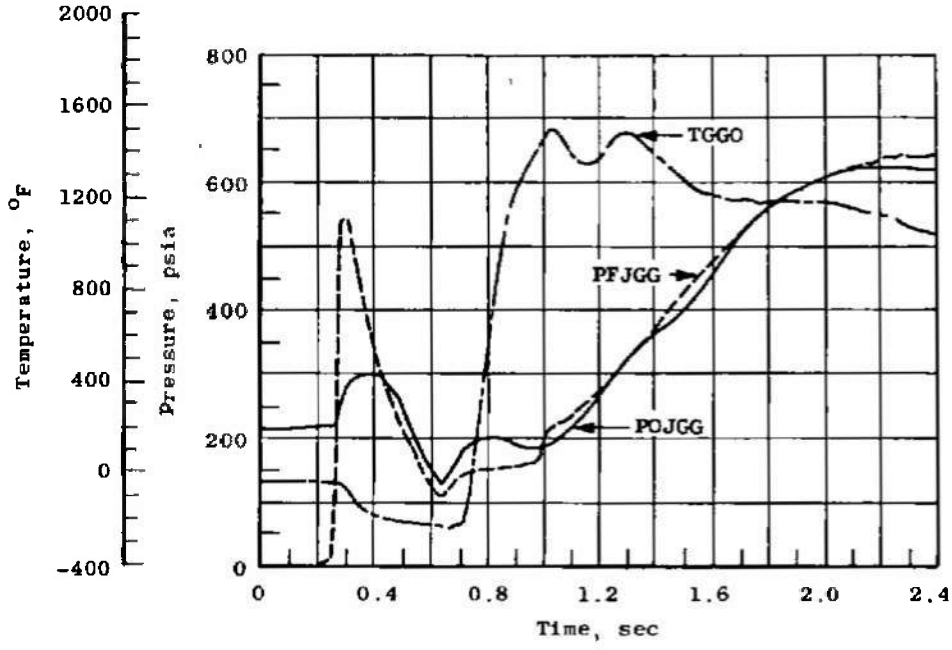

a. Gas Generator Start Transient–Test 26B

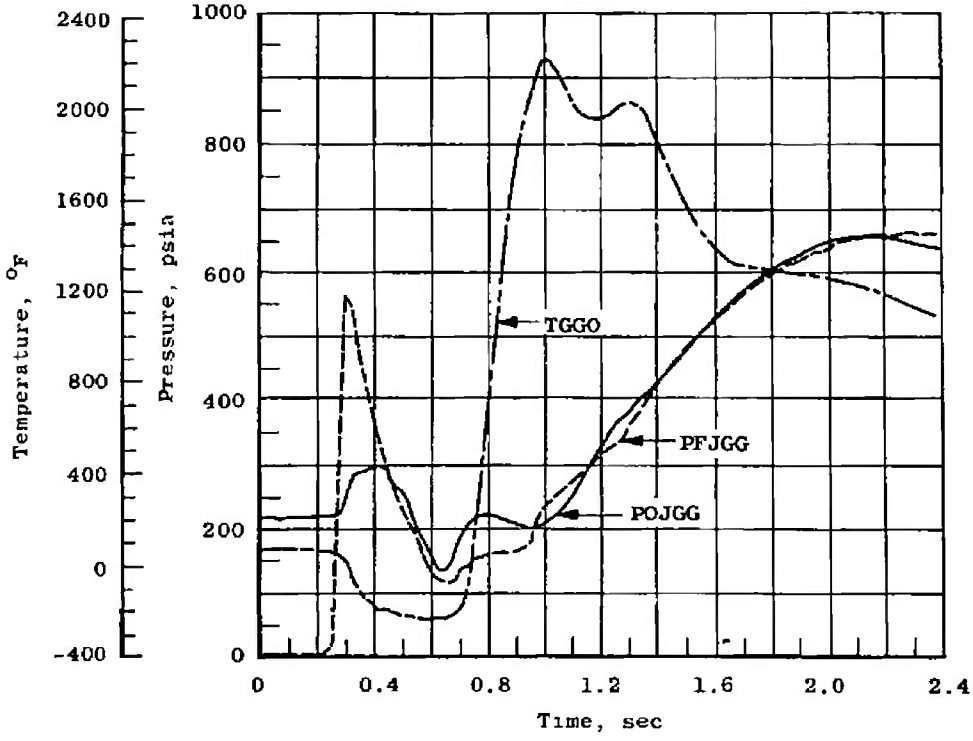

b. Gas Generator Start Transient–Test 26D

Fig. 24 Start Transient Comparisons–Tests 26B and 26D

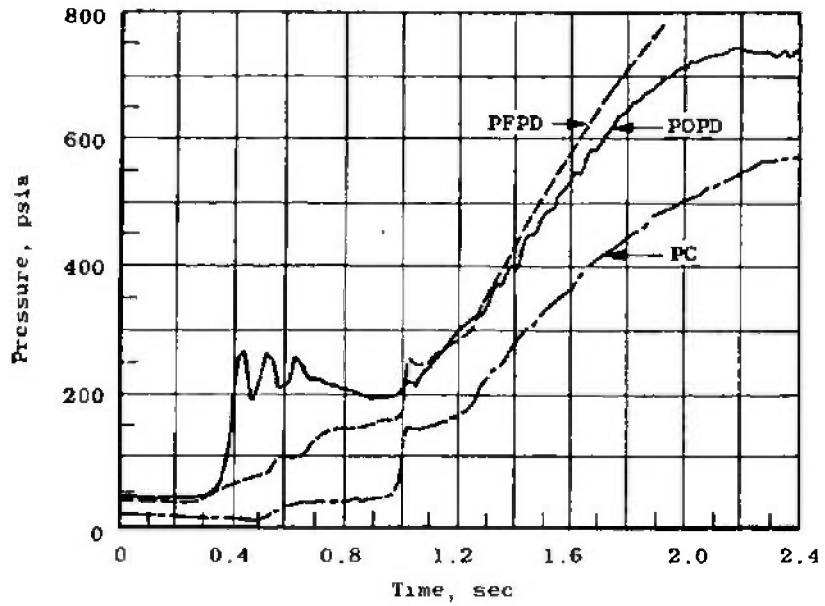

c. Main Chamber Start Transient–Test 26B

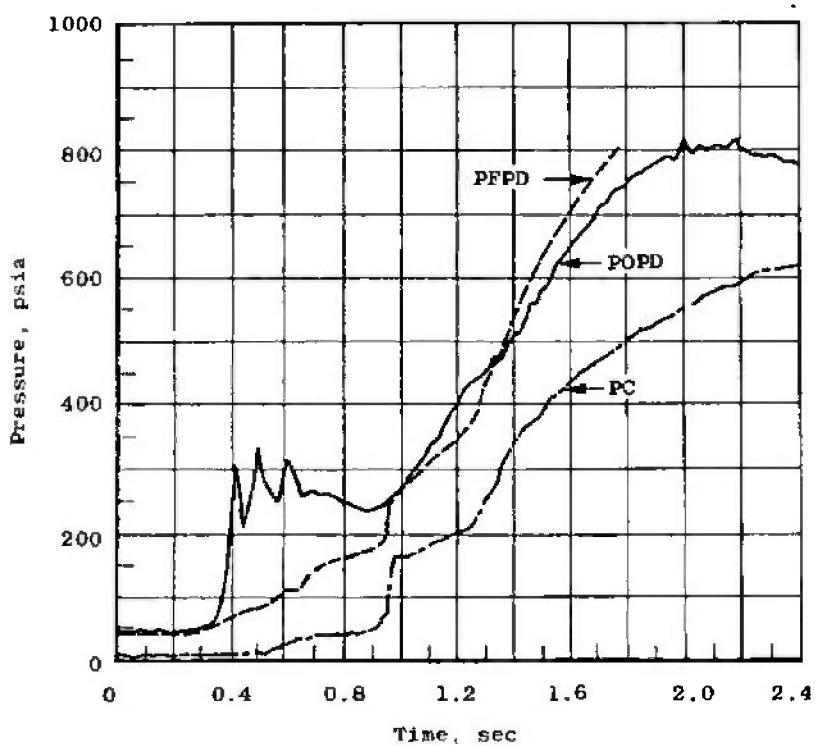

d. Main Chamber Start Transient–Test 26D

Fig. 24 Continued

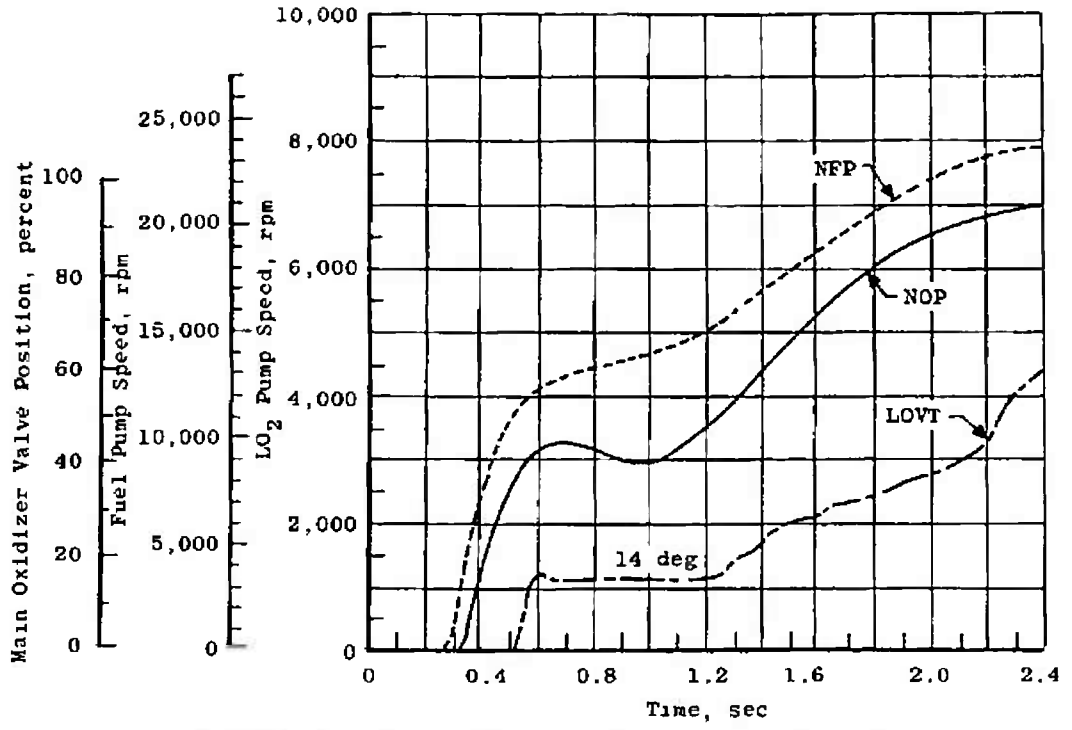

a. Pump Speeds and Main Oxidizer Valve Movement—Test 26B

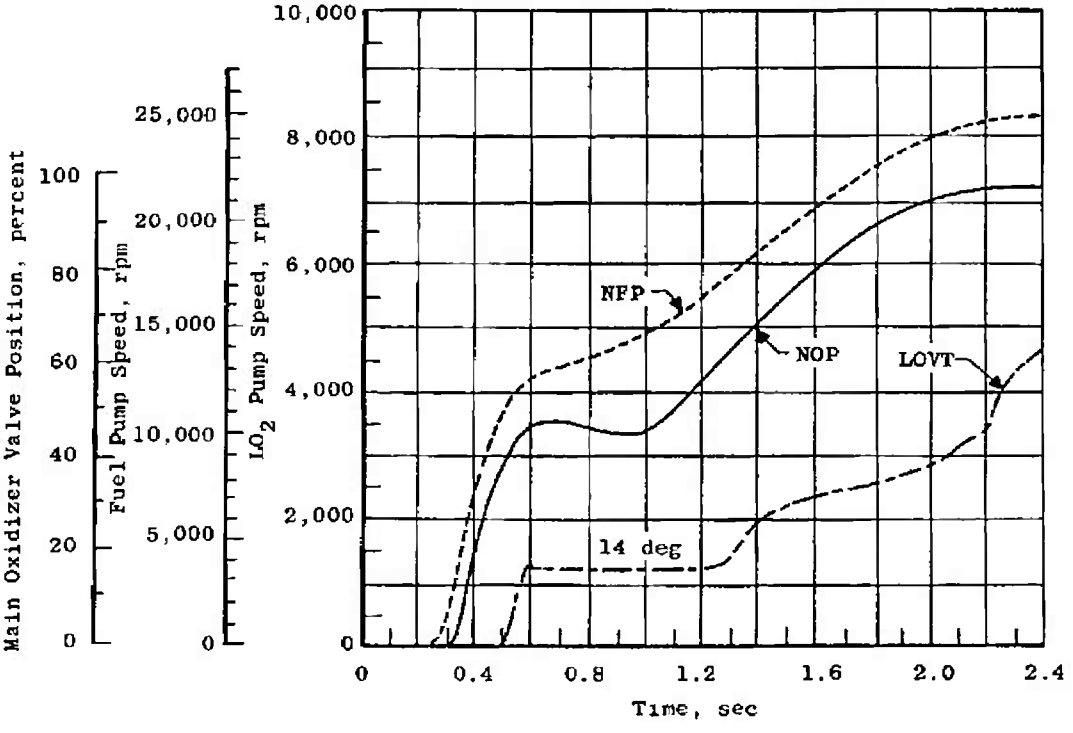

f. Pump Speeds and Main Oxidizer Valve Movement—Test 26D

Fig. 24 Concluded

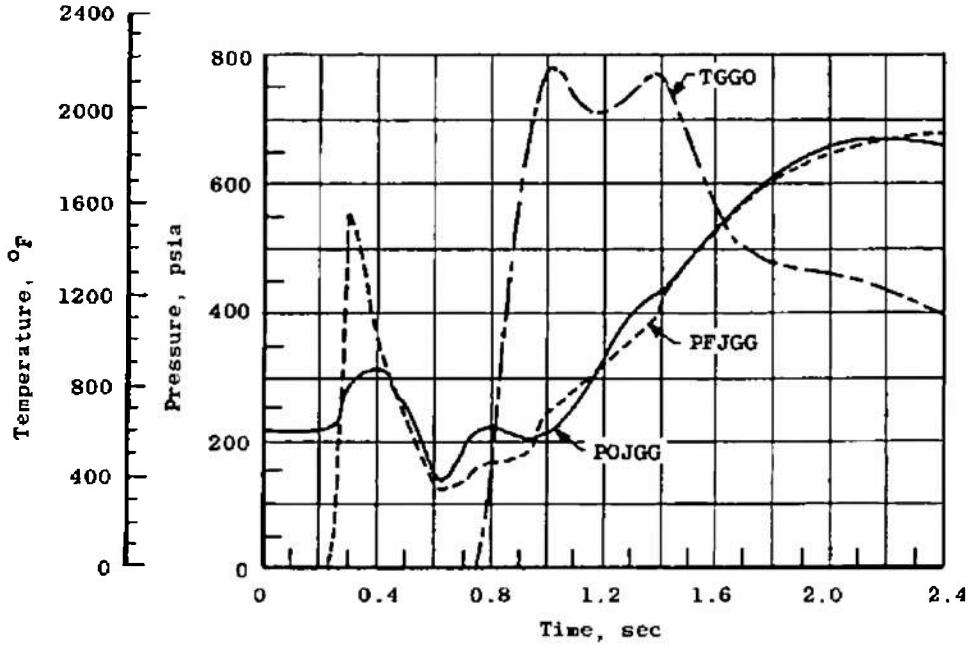

a. Gas Generator Start Transient–Test 25B

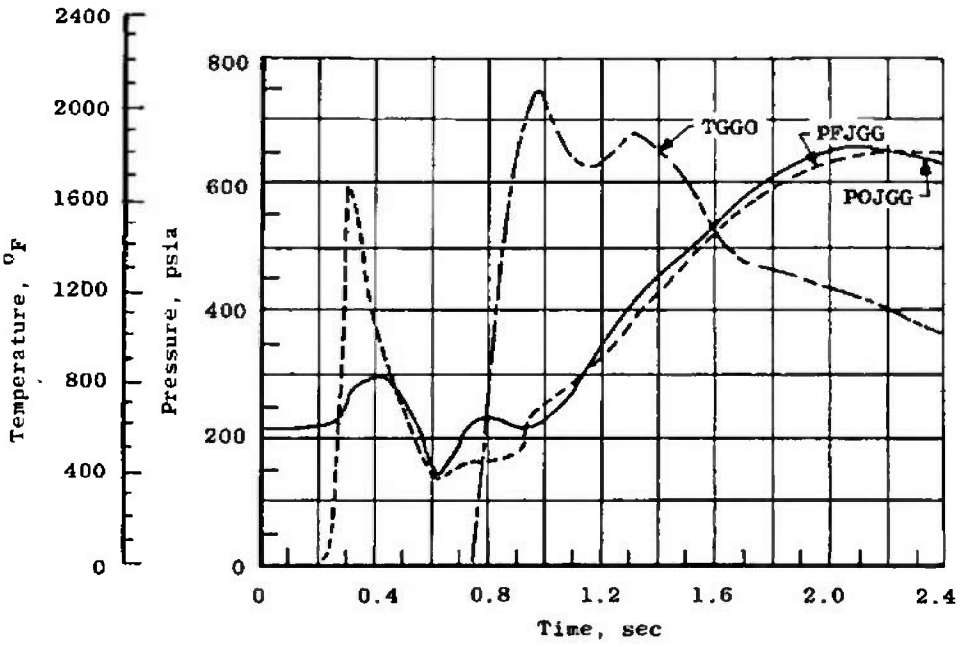

b. Gas Generator Start Transient–Test 23D

Fig. 25 Start Transient Comparisons–Tests 25B and 23D

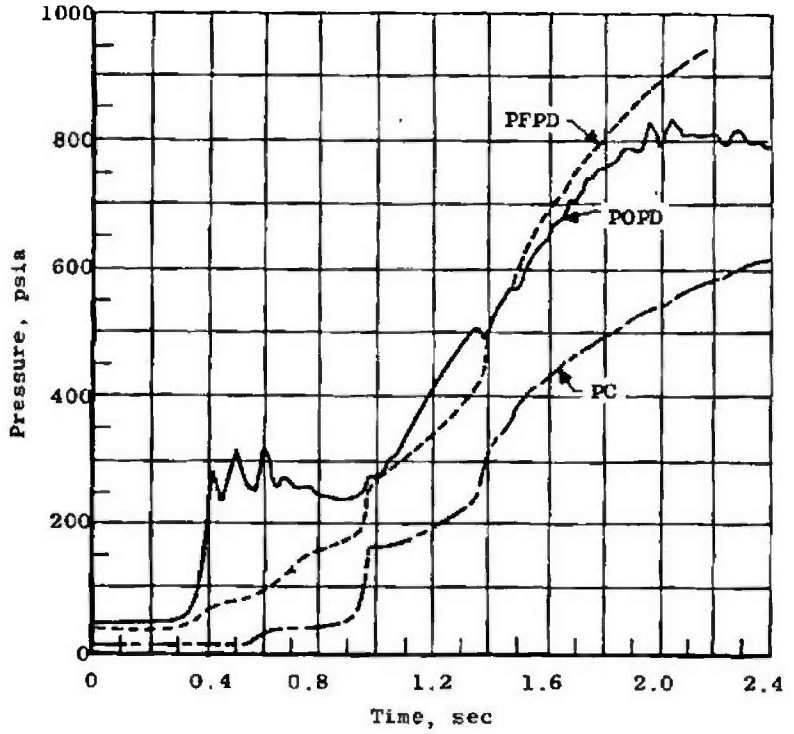

c. Main Chamber Start Transient–Test 25B

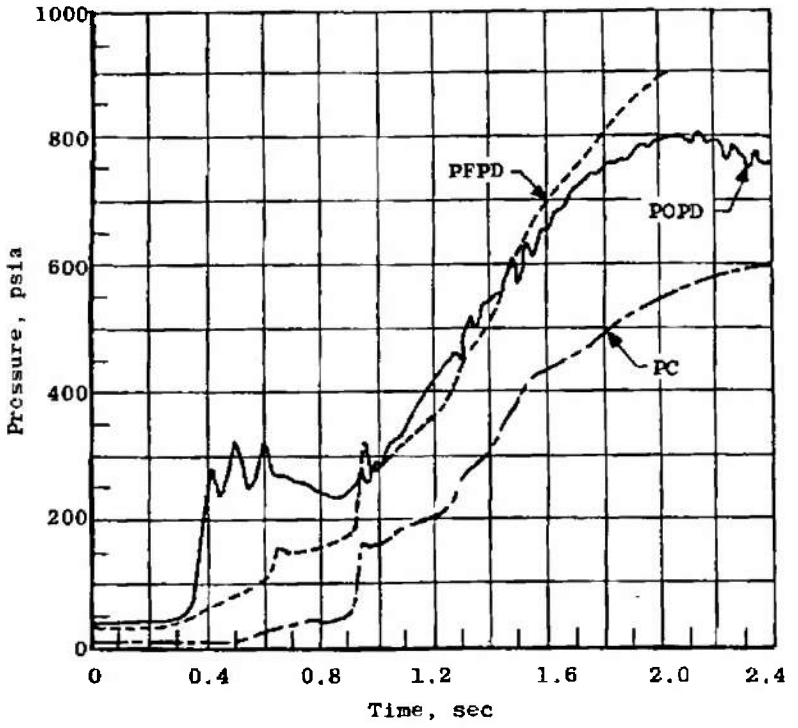

d. Main Chamber Start Transient–Test 23D

Fig. 25 Continued

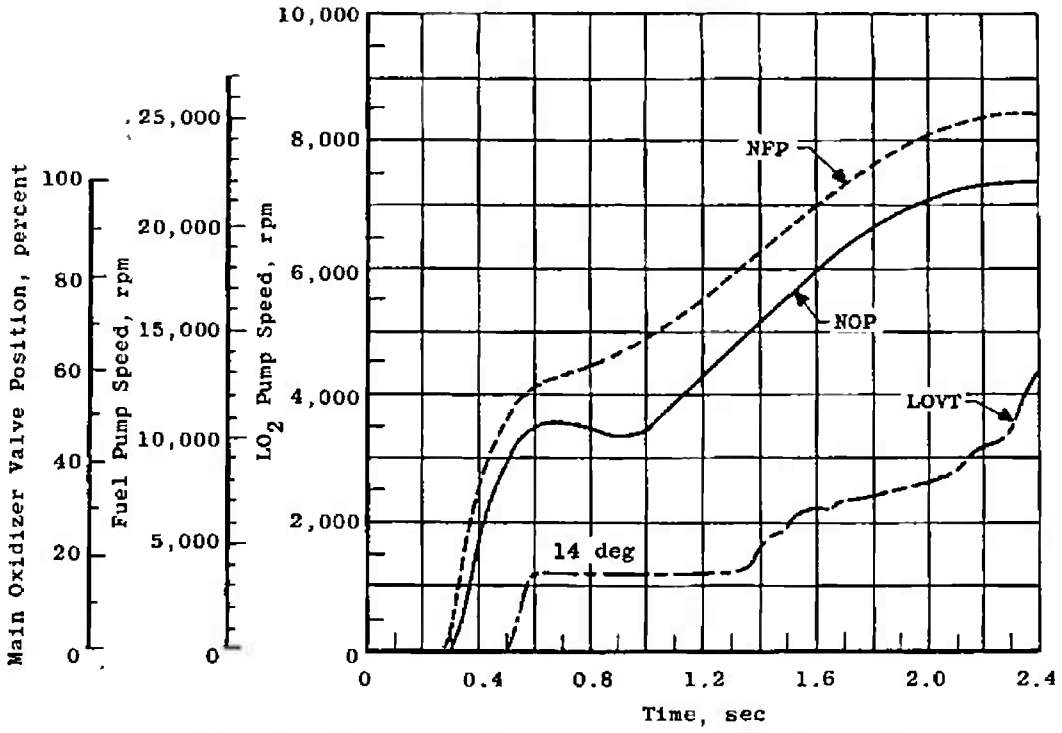

e. Pump Speeds and Main Oxidizer Valve Movement–Test 25B

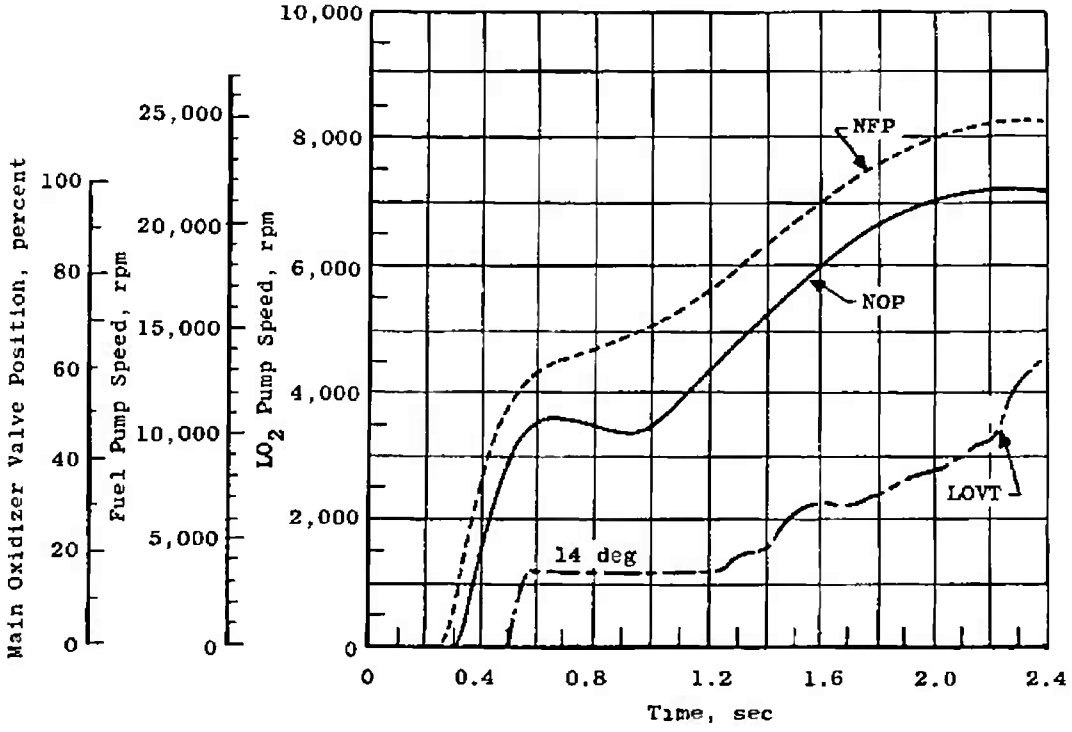

f. Pump Speeds and Main Oxidizer Valve Movement–Test 23D

Fig. 25 Concluded

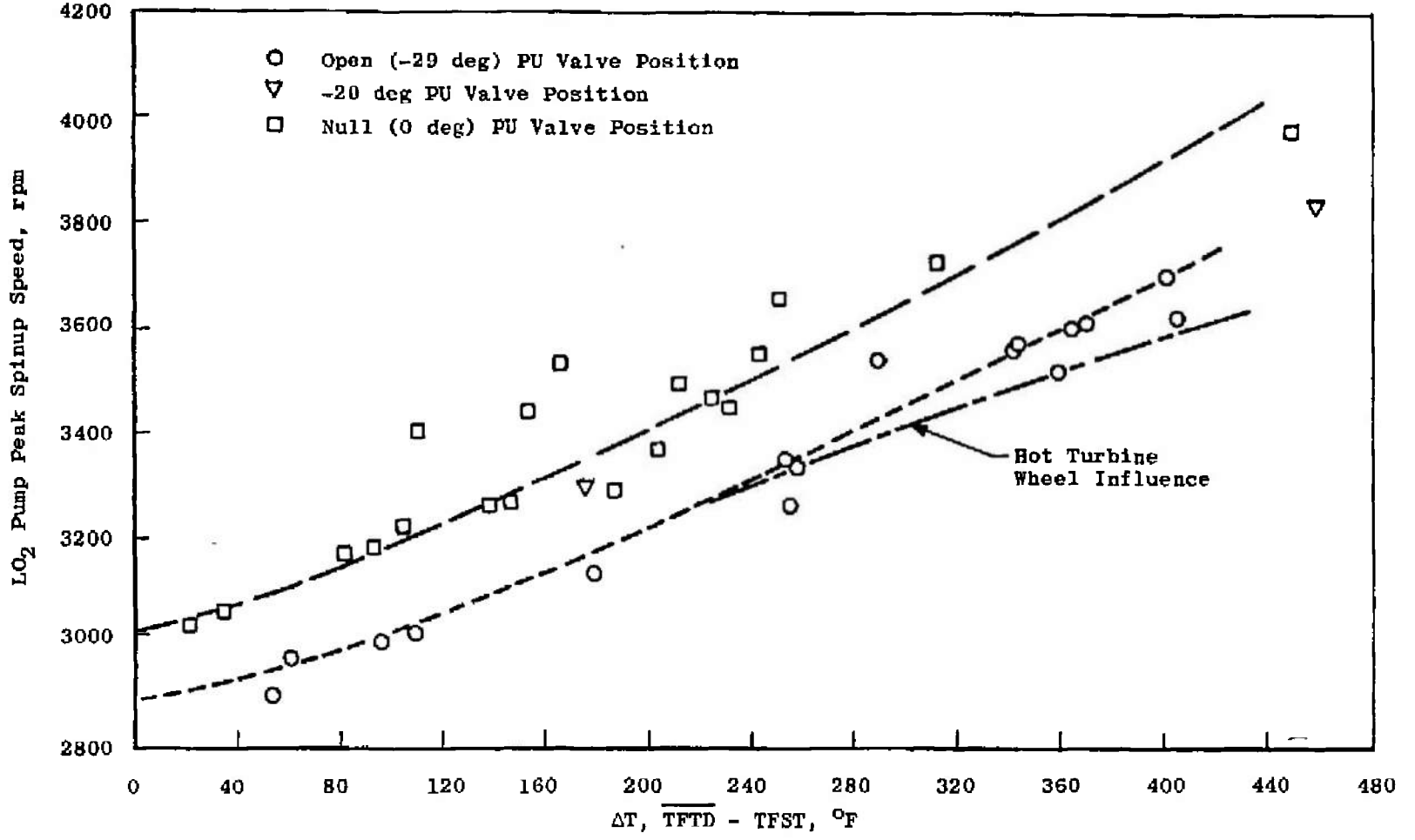

Fig. 26 Crossover Duct-to-Start Tank ΔT Effect on Liquid Oxygen Pump Spinup

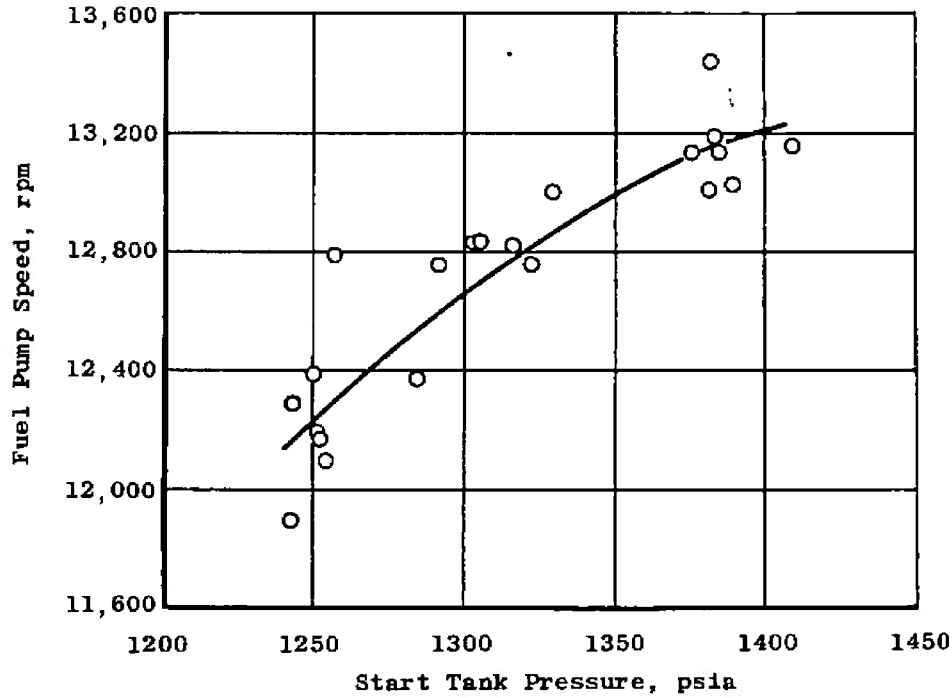

a. Start Tank Pressure Effects

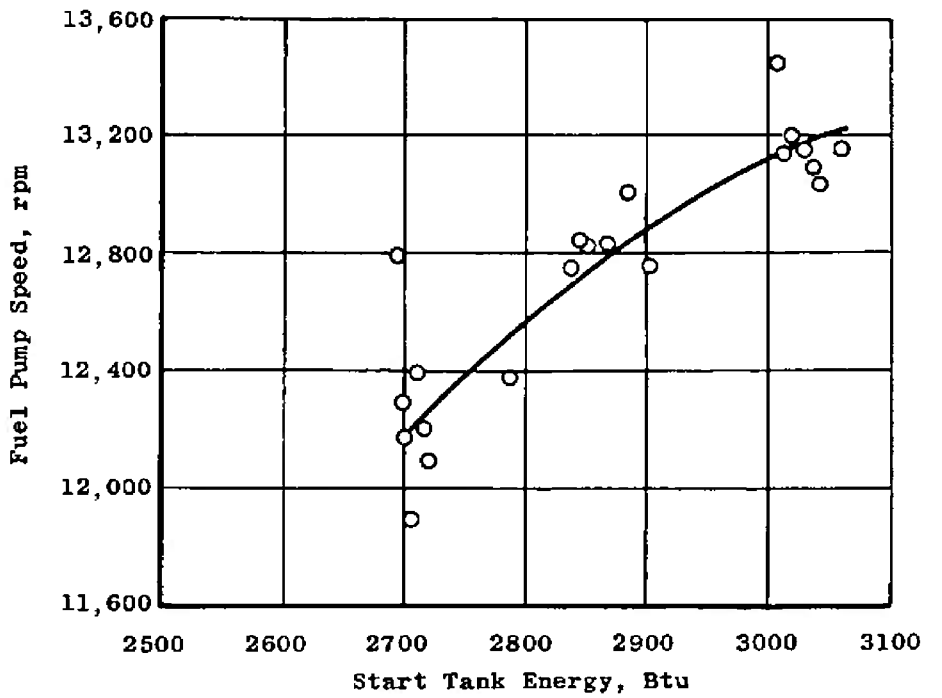

b. Start Tank Energy Effect

Fig. 27 Effect of Start Tank Conditions on Fuel Pump Spinup

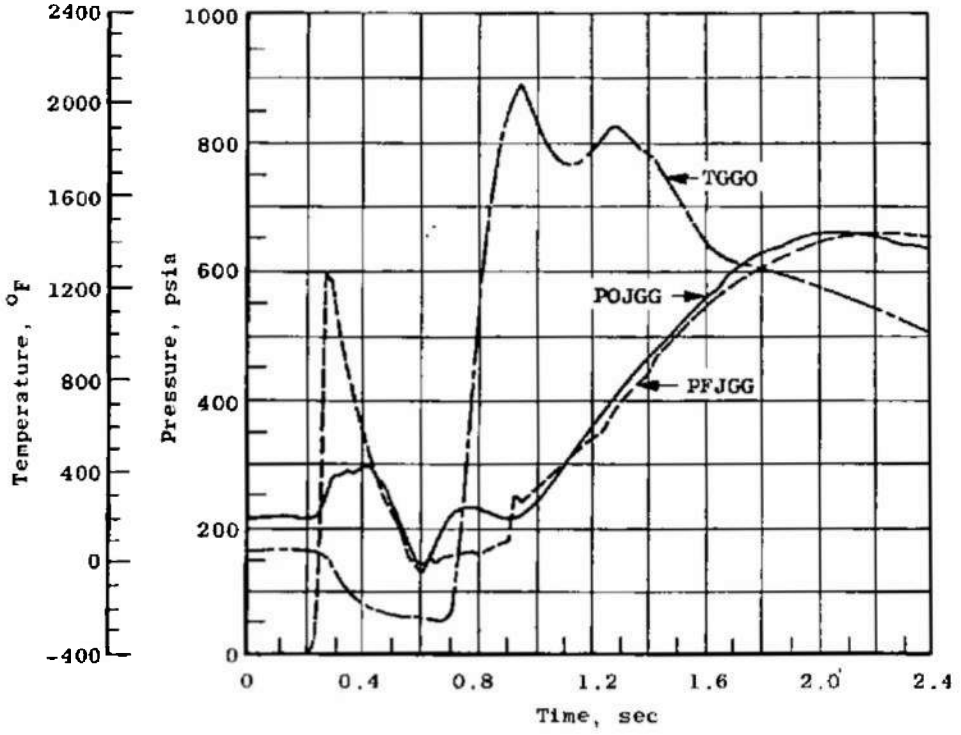

a. Gas Generator Start Transient–Test 23D

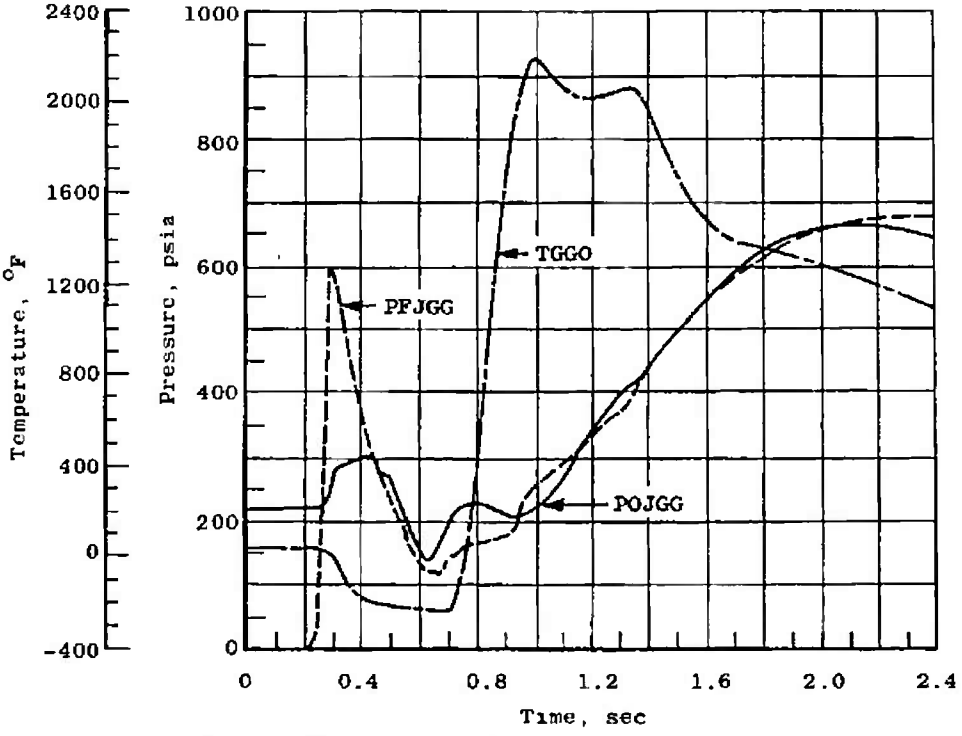

b. Gas Generator Start Transient–Test 24D

Fig. 28 Start Transient Comparisons–Tests 23D and 24D

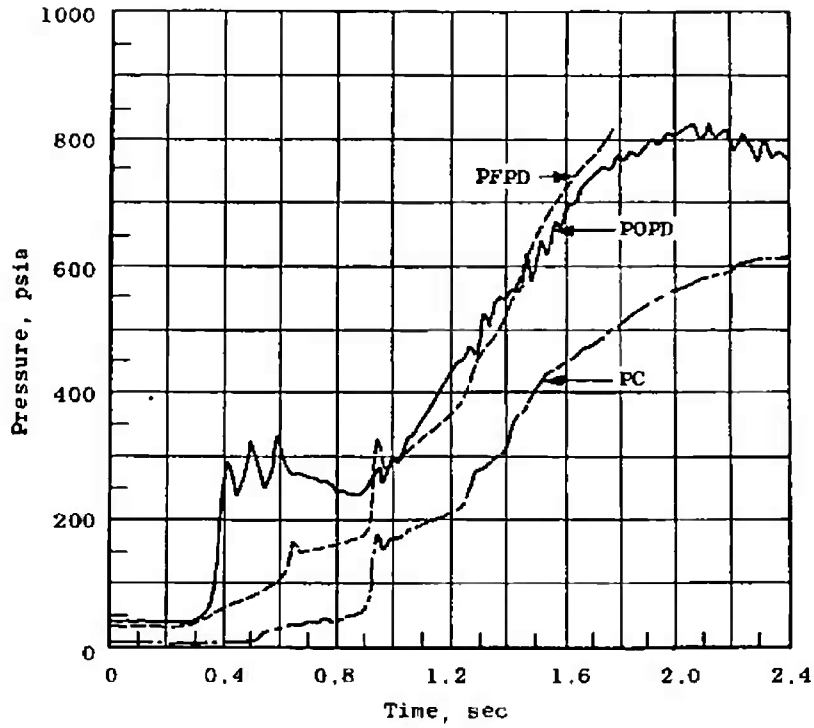

c. Main Chamber Start Transient–Test 23D

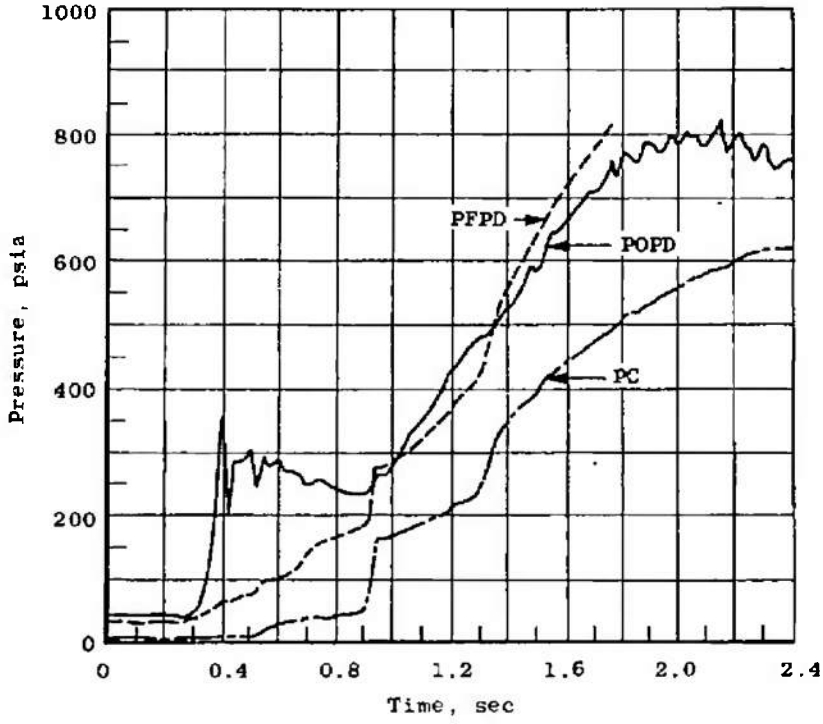

d. Main Chamber Start Transient–Test 24D

Fig. 28 Continued

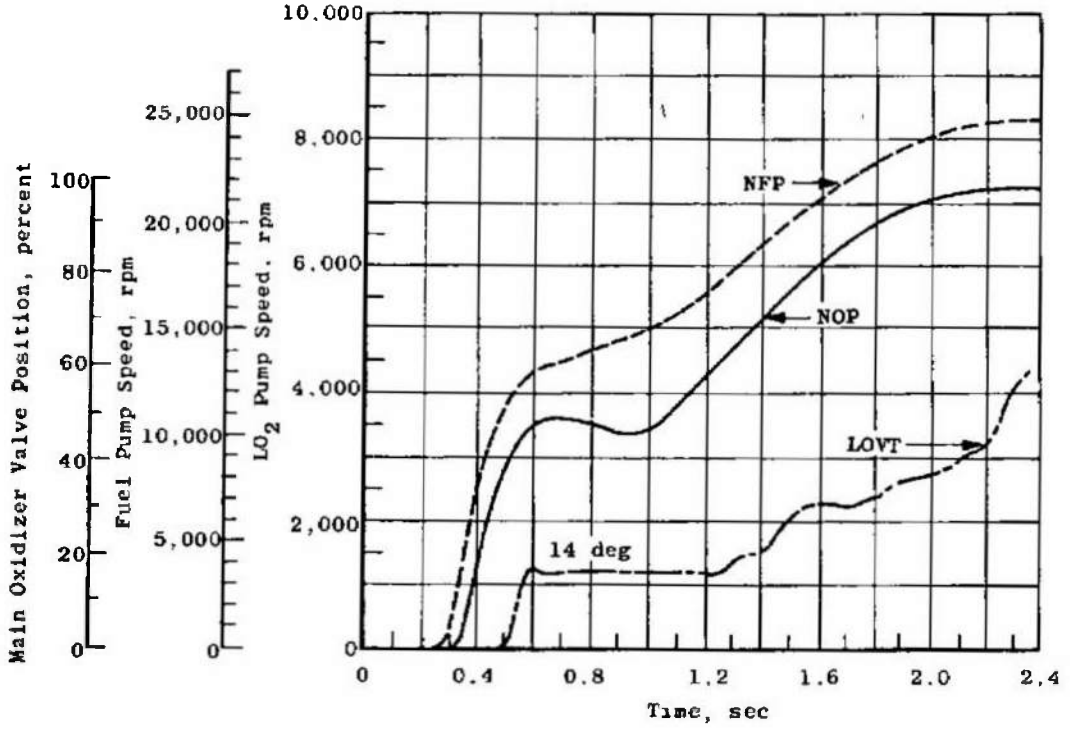

e. Pump Speeds and Main Oxidizer Valve Movement–Test 23D

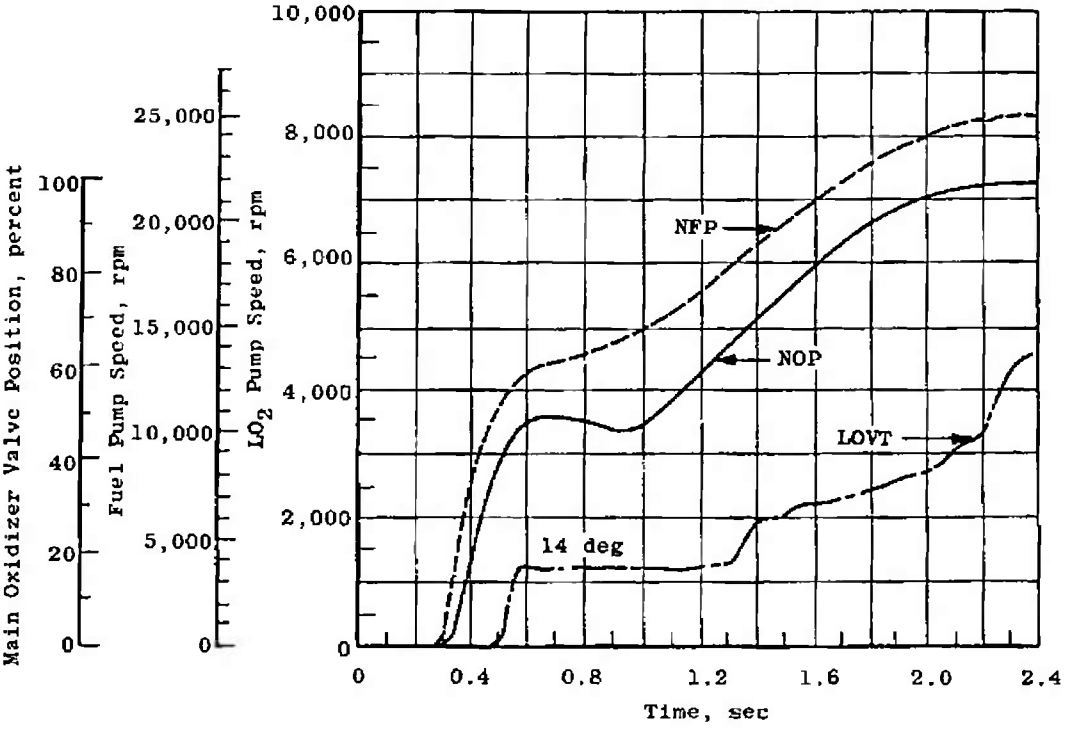

f. Pump Speeds and Main Oxidizer Valve Movement–Test 24D

Fig. 28 Concluded

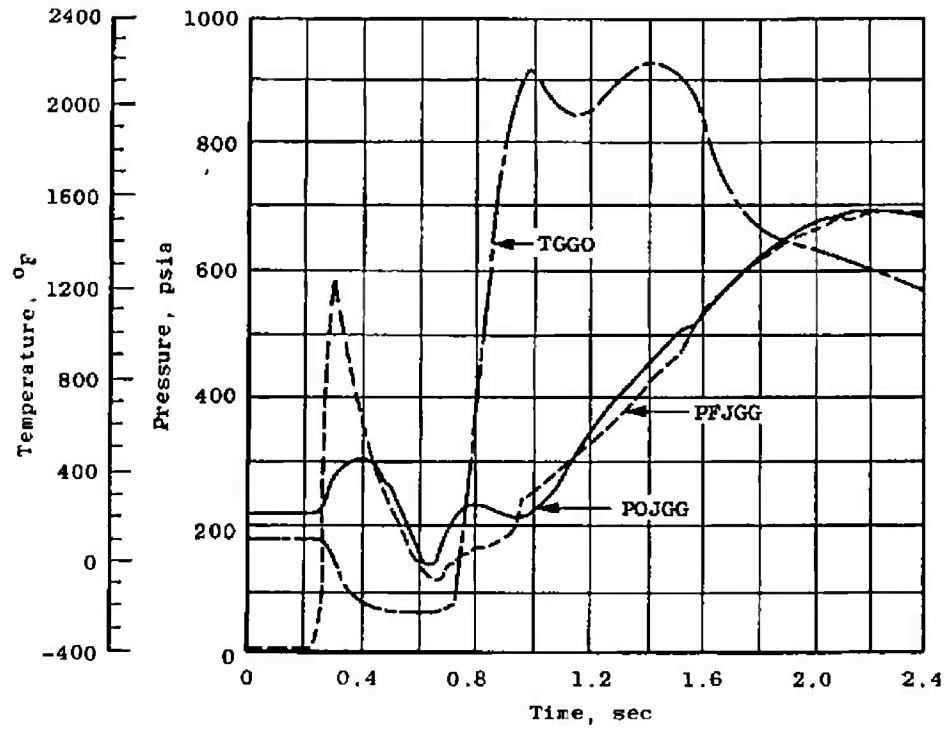

a. Gas Generator Start Transient–Test 25D

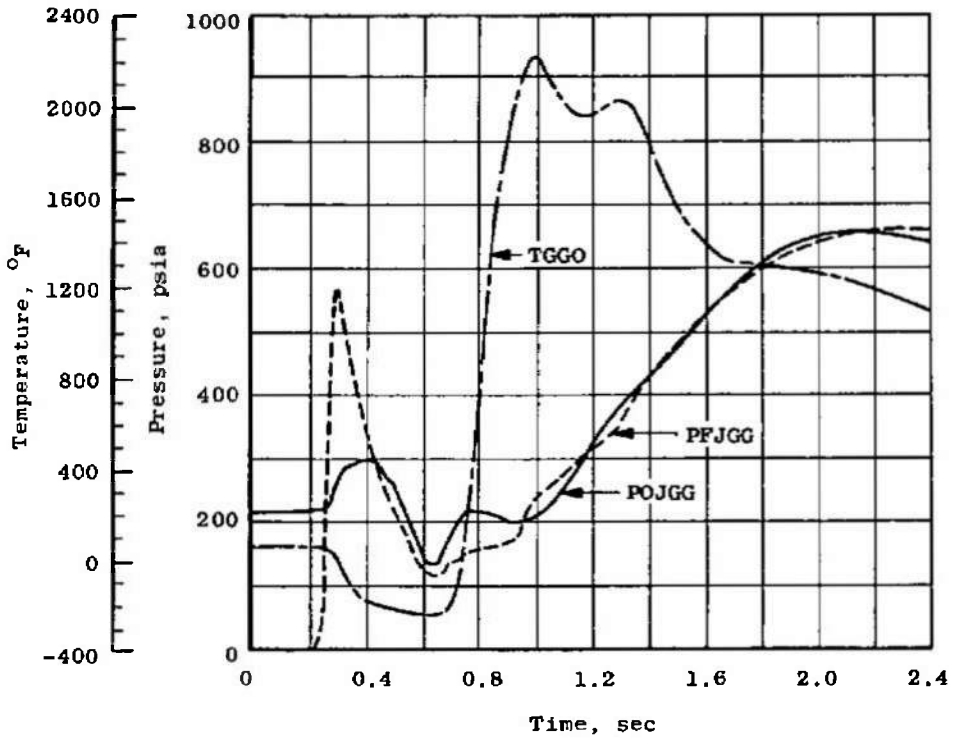

b. Gas Generator Start Transient–Test 26D

Fig. 29 Start Transient Comparisons–Tests 25D and 26D

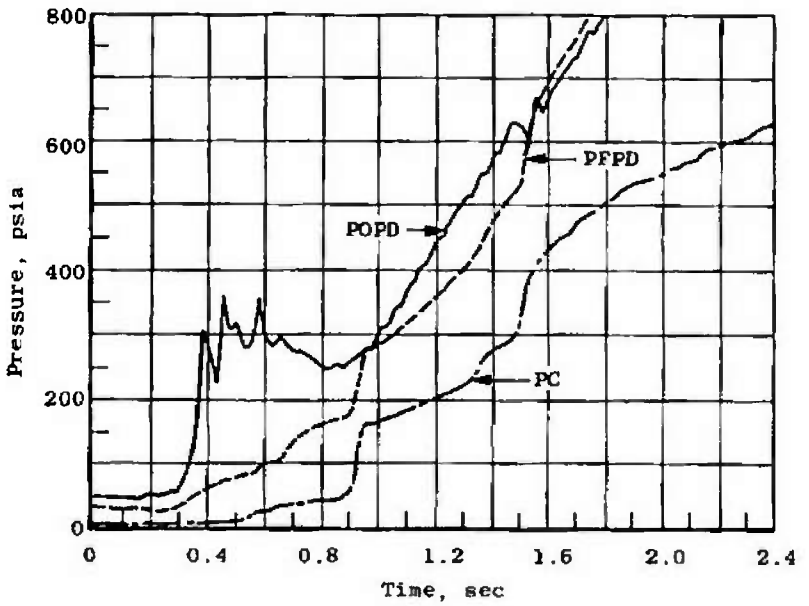

c. Main Chamber Start Transient–Test 25D

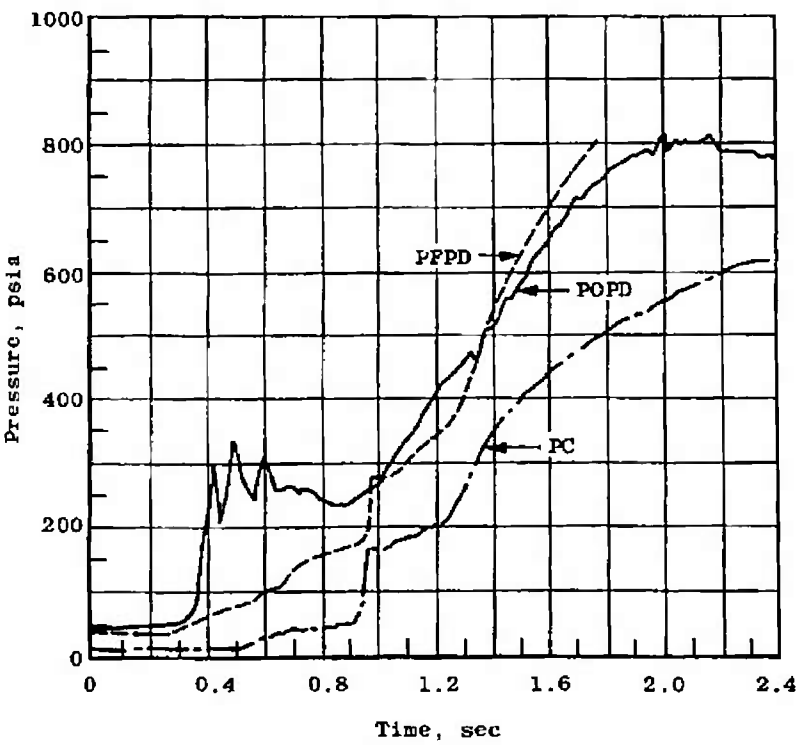

d. Main Chamber Start Transient–Test 26D

Fig. 29 Continued

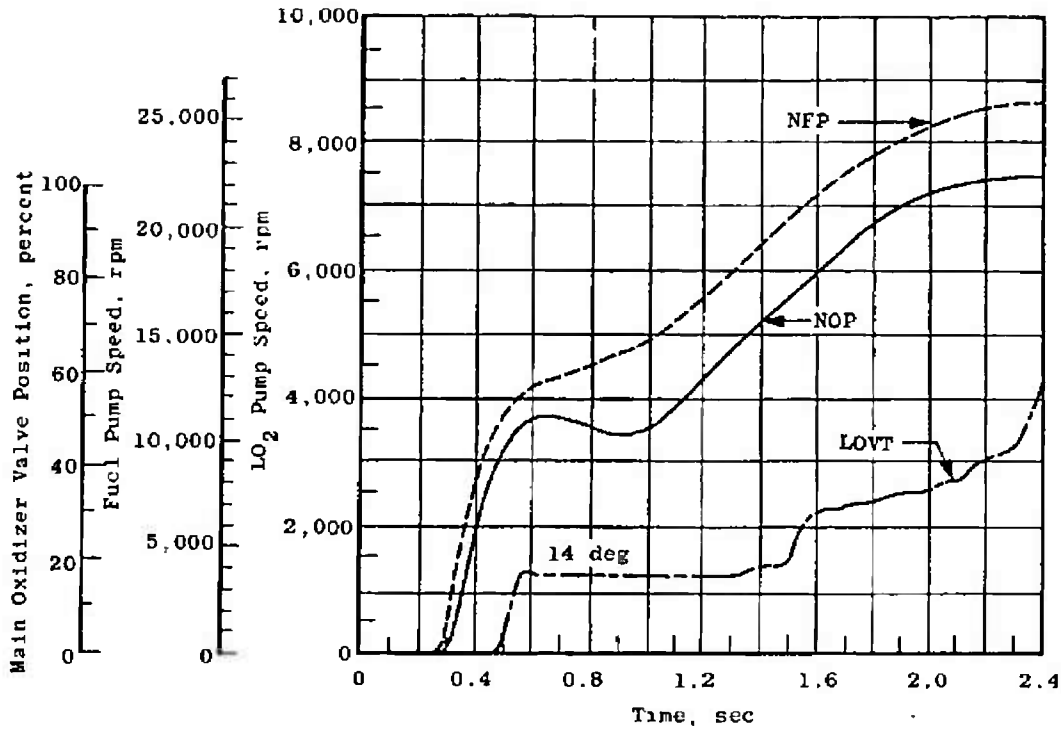

e. Pump Speeds and Main Oxidizer Valve Movement–Test 25D

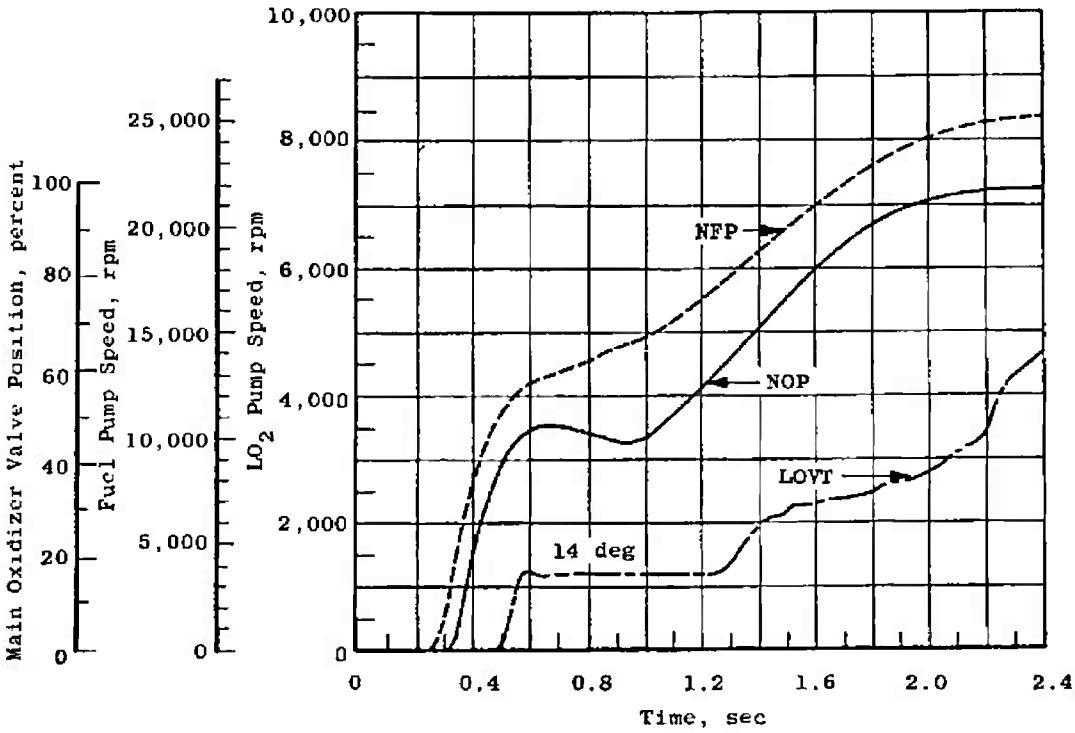

f. Pump Speeds and Main Oxidizer Valve Movement–Test 26D

Fig. 29 Concluded

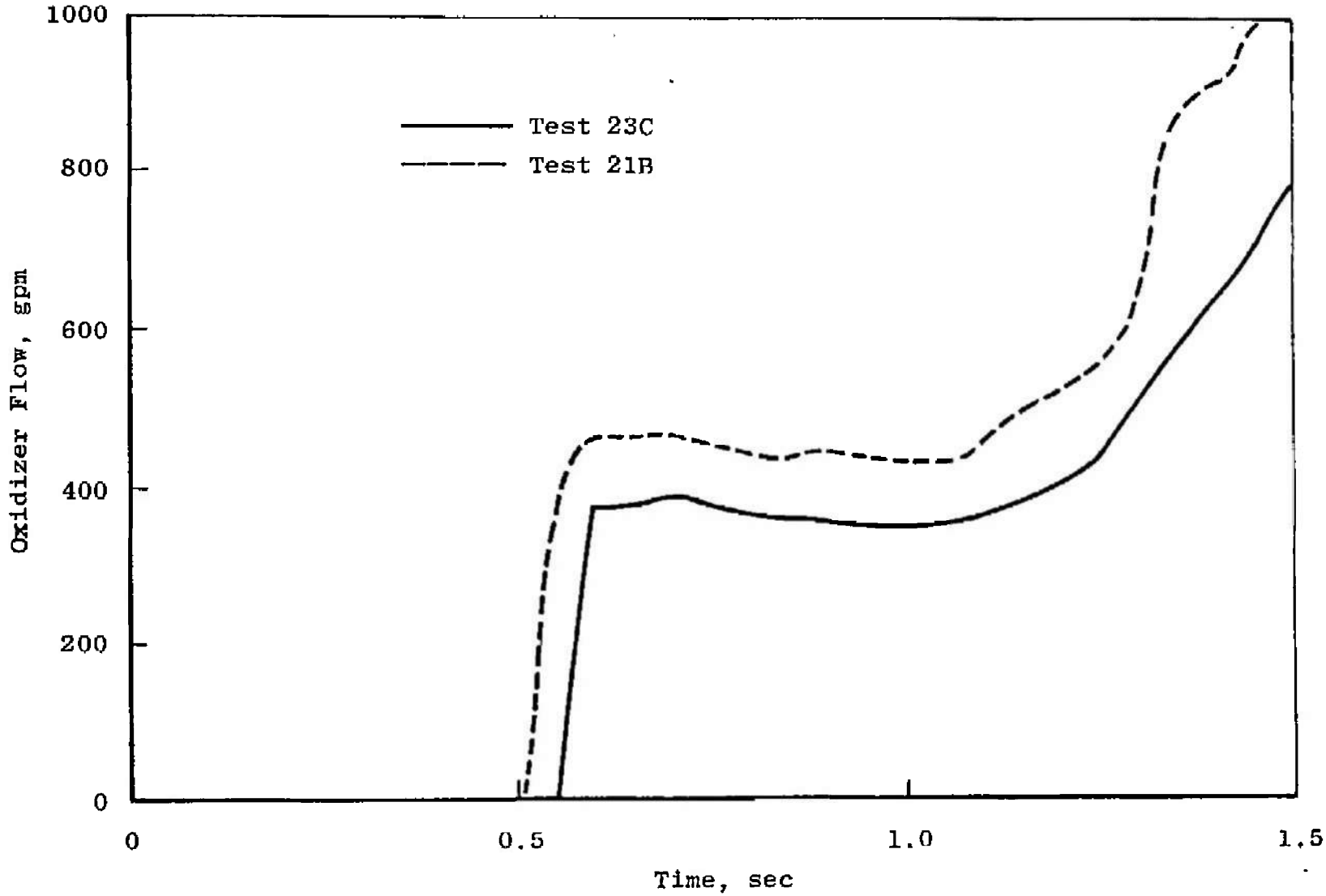

Fig. 30 Oxidizer Flow Rates–Tests 21B and 23C

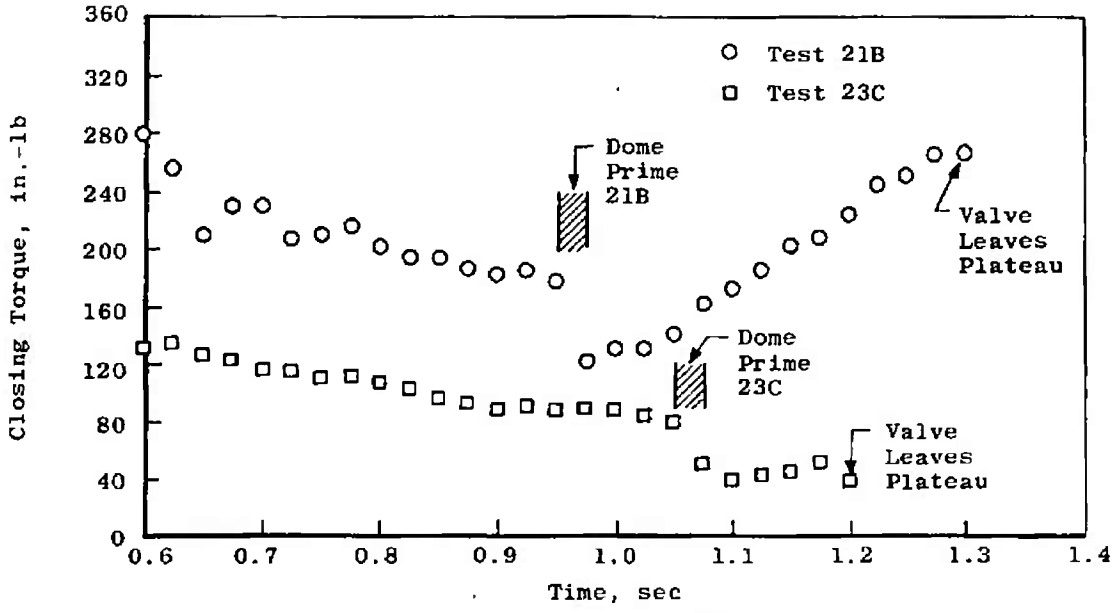

a. Main Oxidizer Valve Hydraulic Torque, Tests 21B and 23C

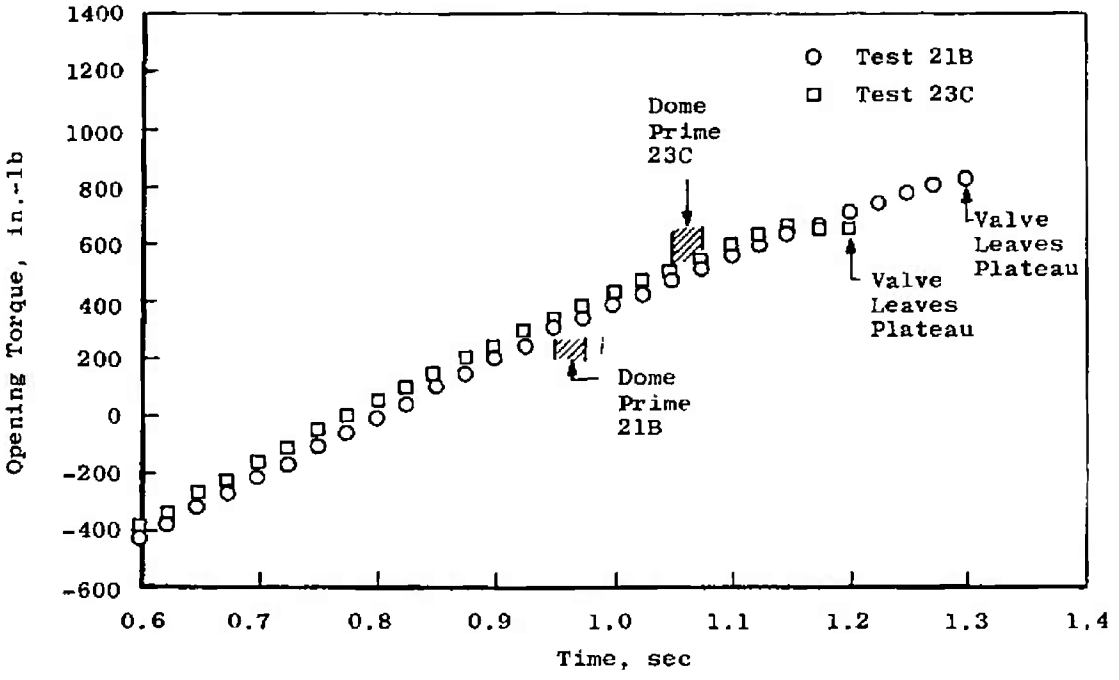

b. Main Oxidizer Valve Pneumatic Torque, Tests 21B and 23C

Fig. 31 Main Oxidizer Valve Torque Comparisons – Tests 21B and 23C

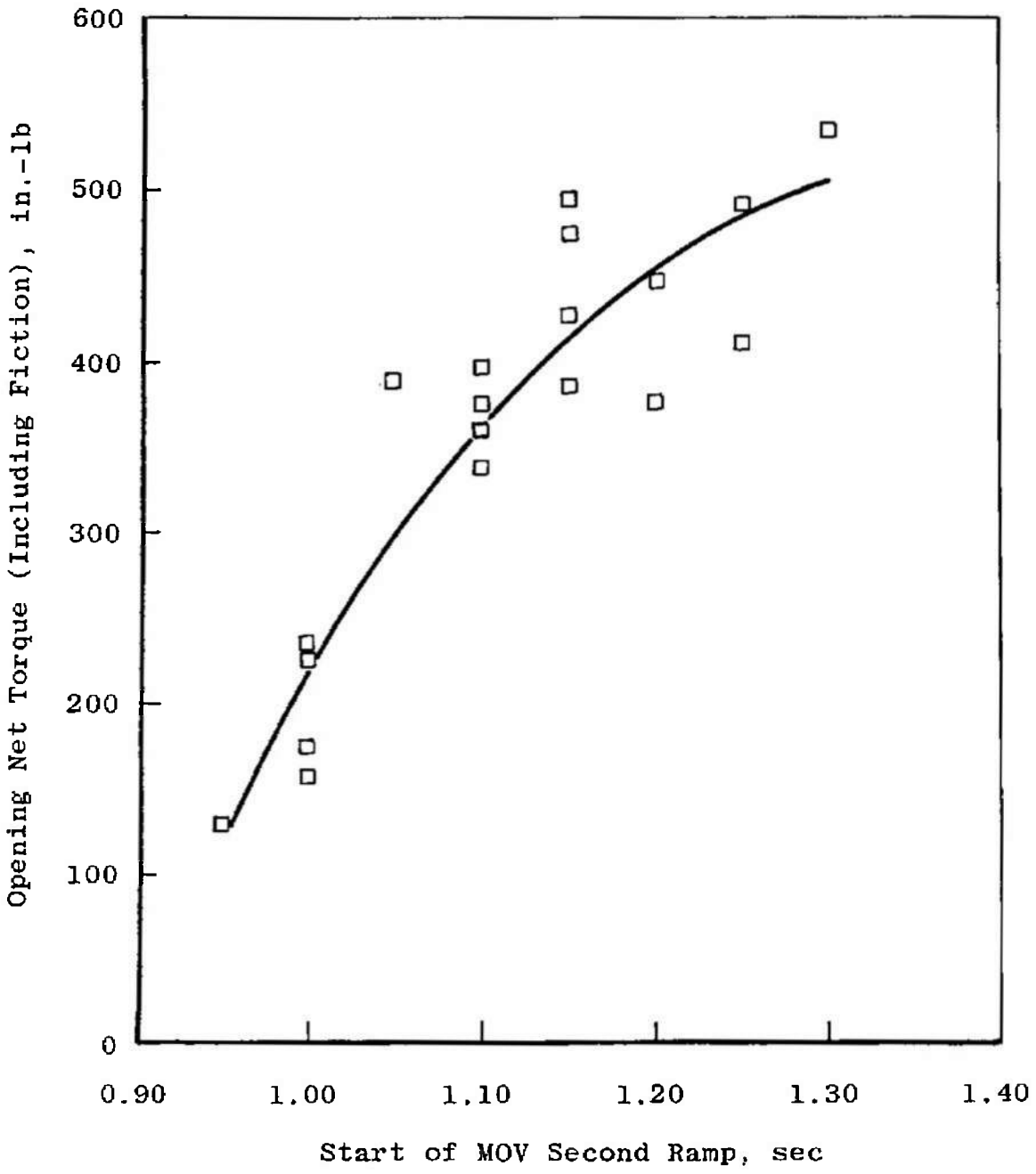

Fig. 32 Main Oxidizer Valve Net Opening Torque and Second Stage Movement Delay

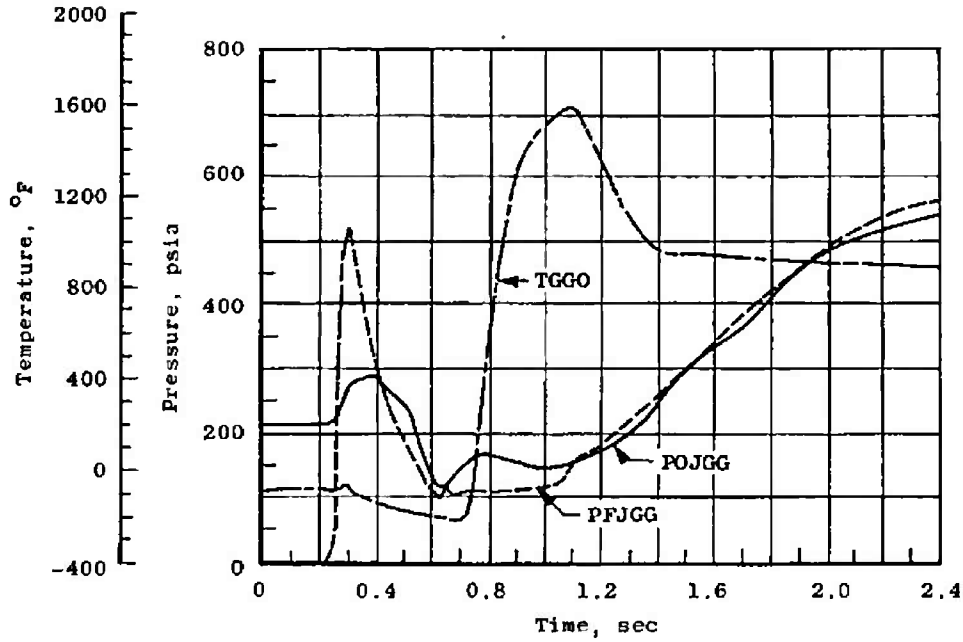

a. Gas Generator Start Transient – Test 23C

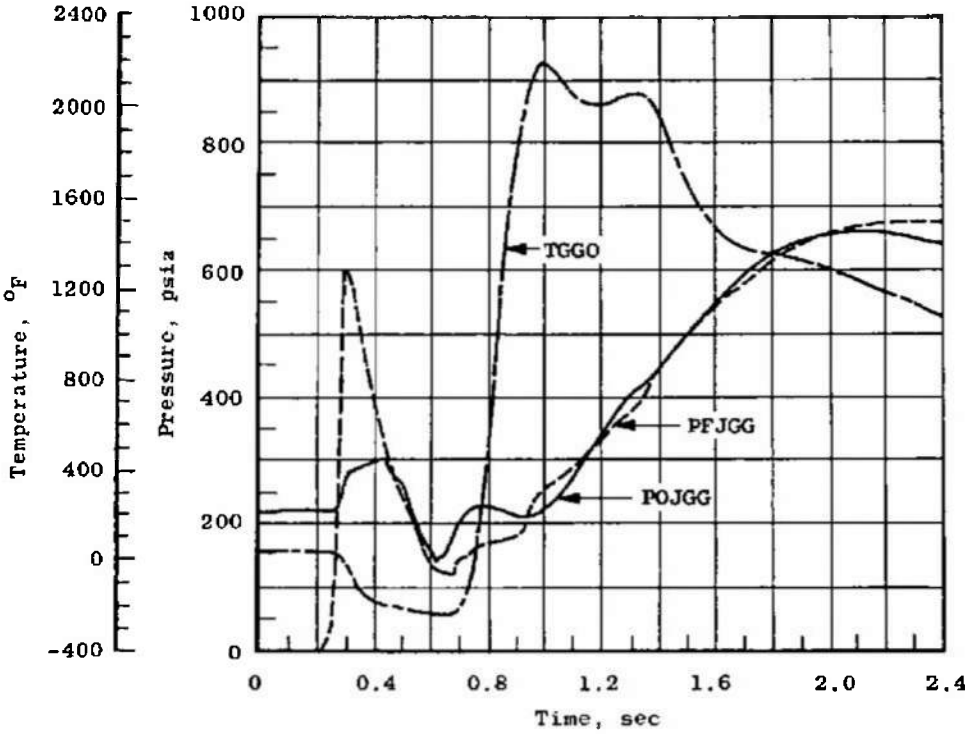

b. Gas Generator Start Transient – Test 24D

Fig. 33 Start Transient Comparisons – Tests 23C and 24D

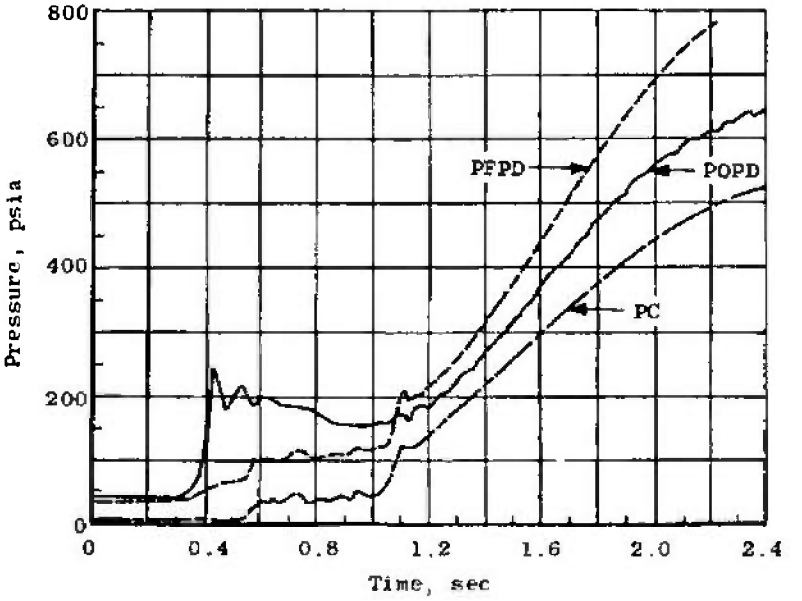

c. Main Chamber Start Transient – Test 23C

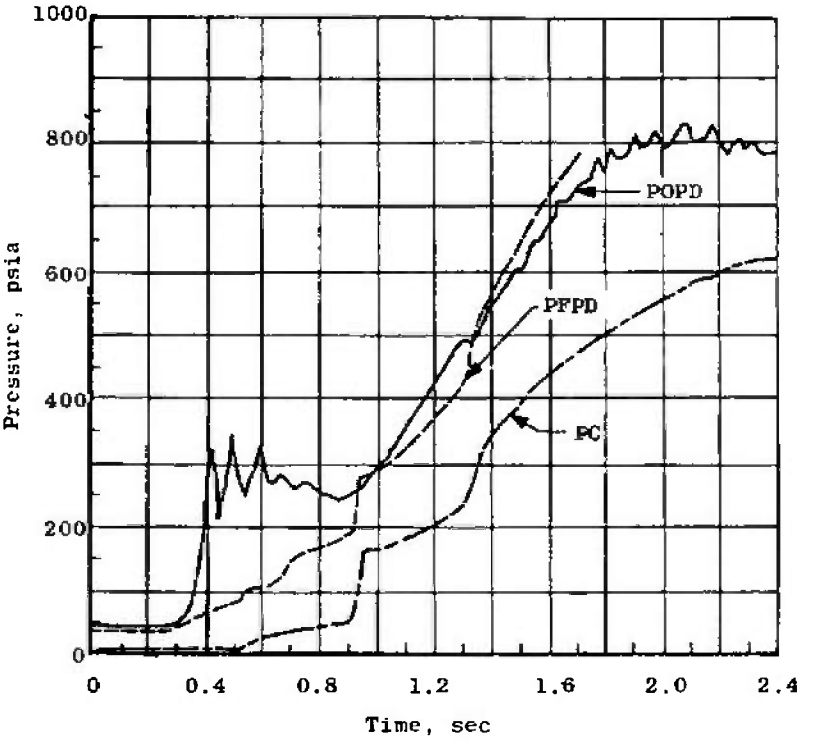

d. Main Chamber Start Transient – Test 24D

Fig. 33 Continued

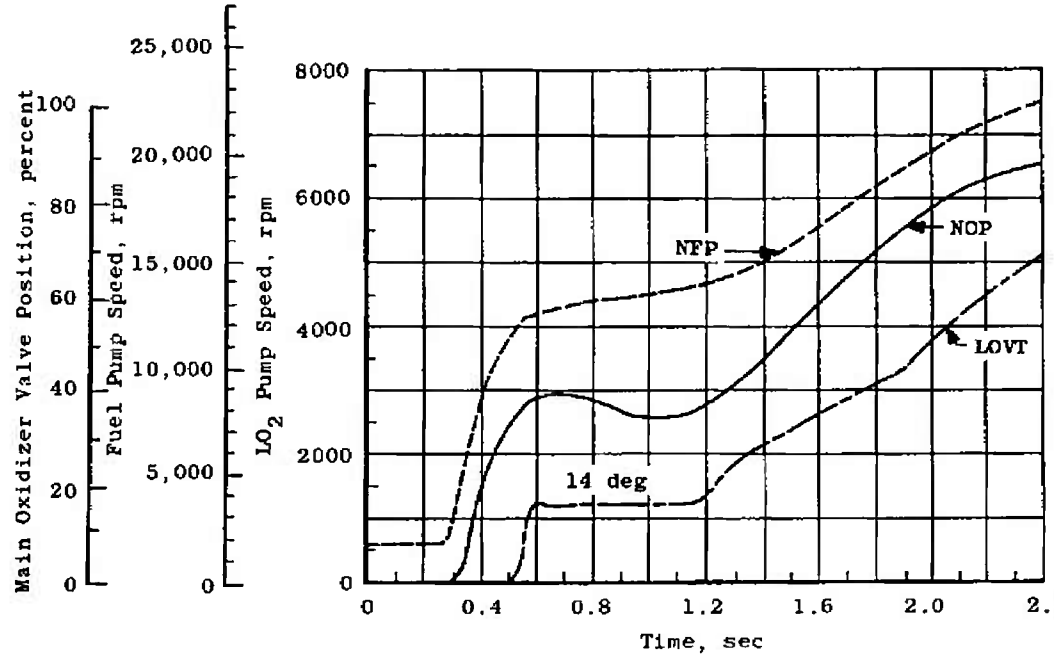

e. Pump Speeds and Main Oxidizer Valve Movement – Test 23C

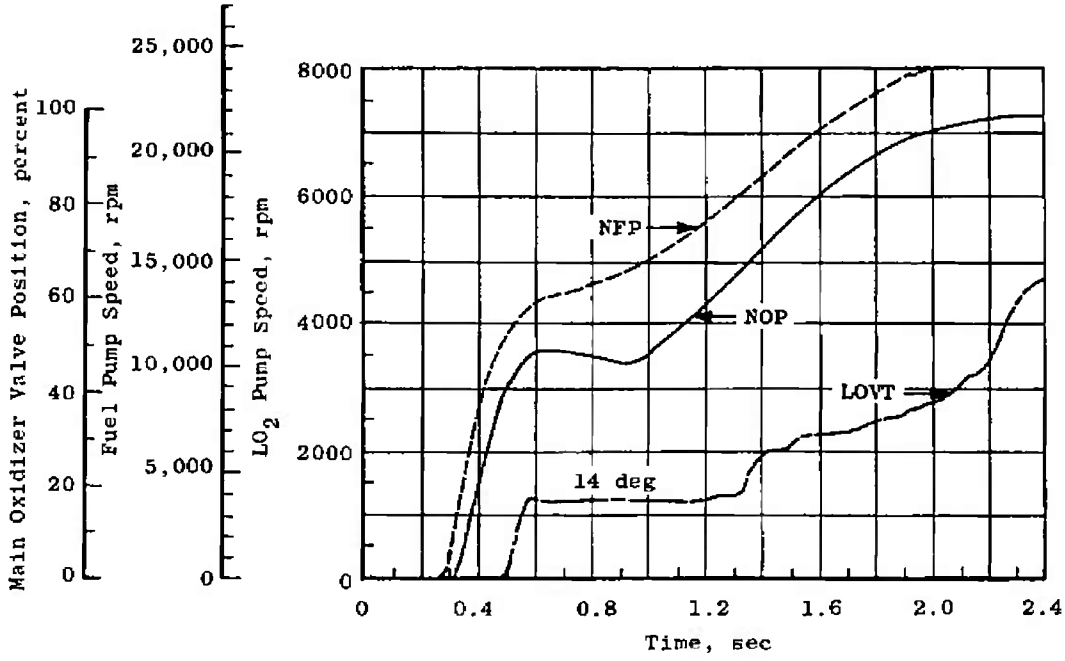

f. Pump Speeds and Main Oxidizer Valve Movement – Test 24D

Fig. 33 Concluded

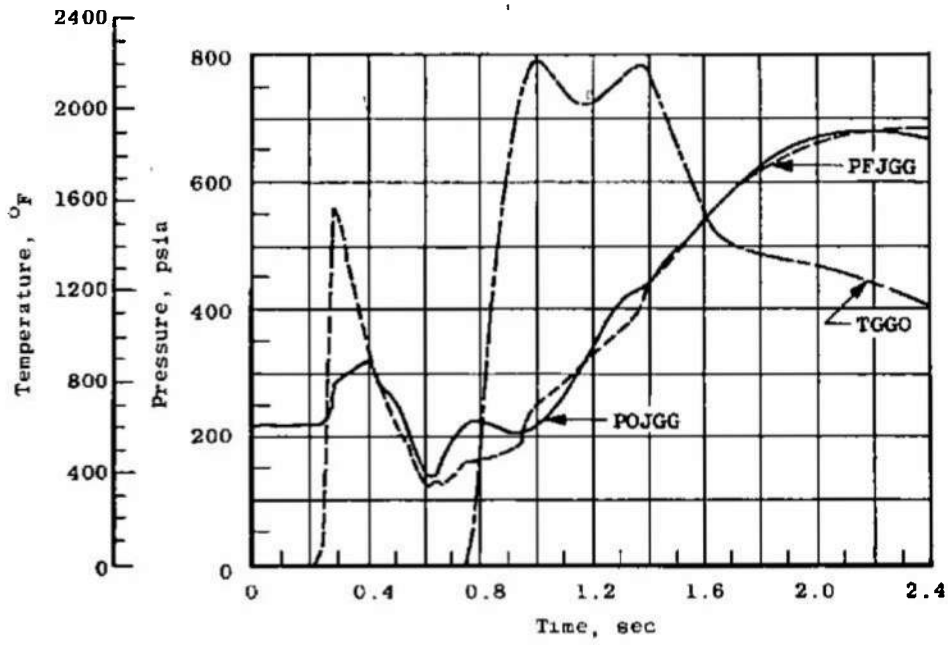

a. Gas Generator Start Transient – Test 25B

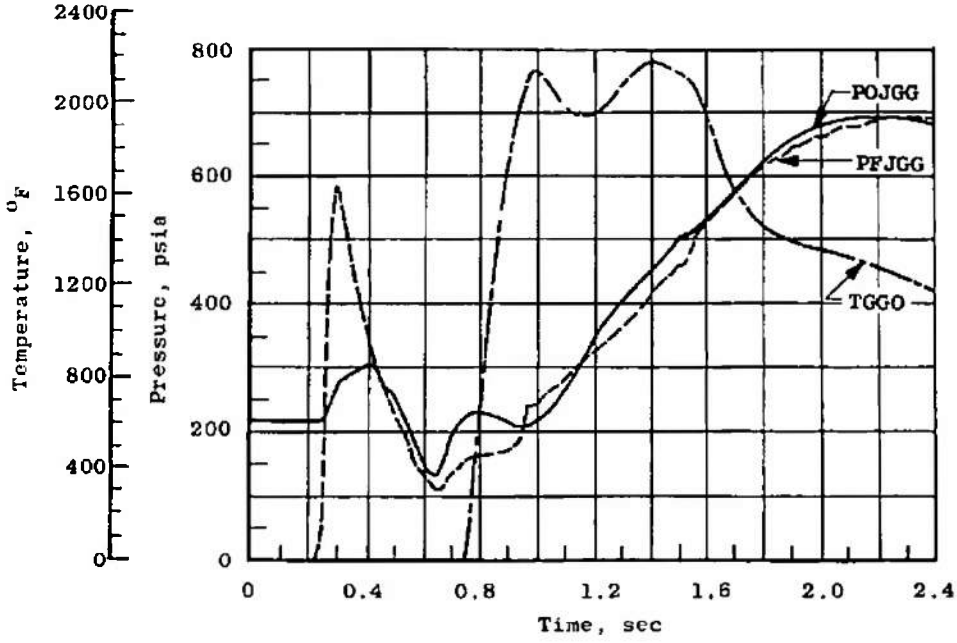

b. Gas Generator Start Transient – Test 25D

Fig. 34 Start Transient Comparisons – Tests 25B and 25D

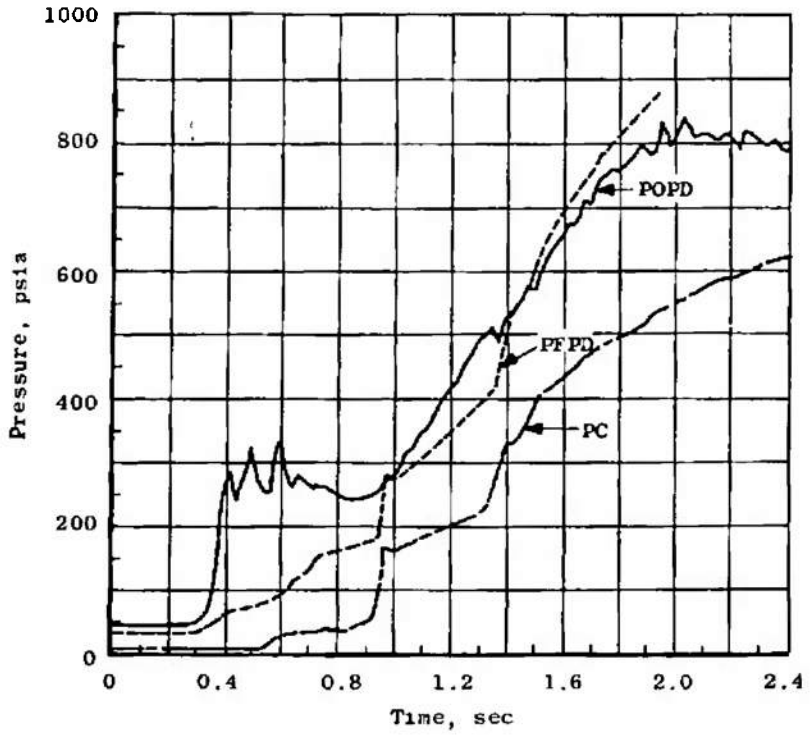

c. Main Chamber Start Transient – Test 25B

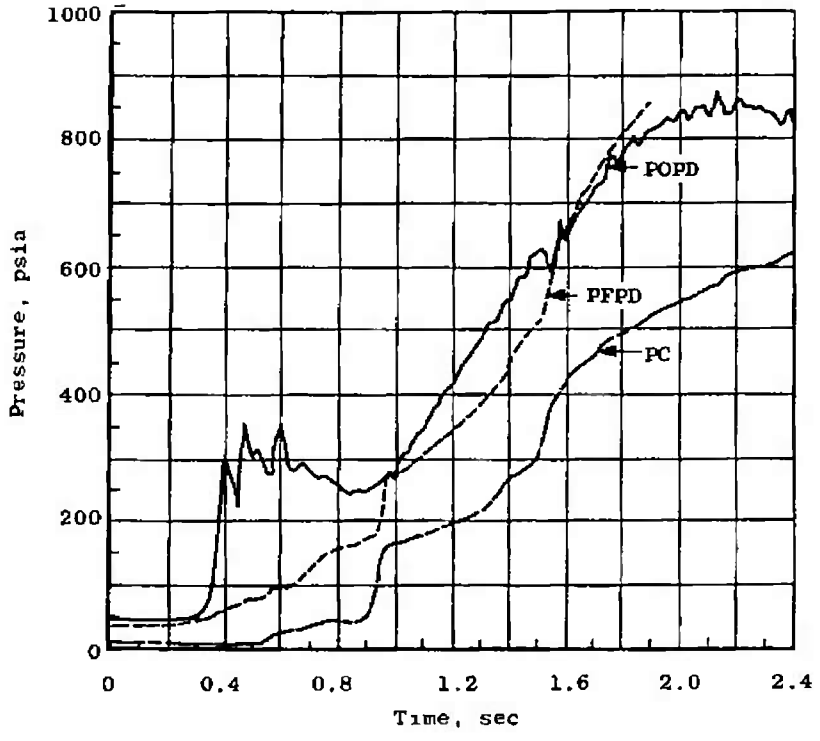

d. Main Chamber Start Transient – Test 25D

Fig. 34 Continued

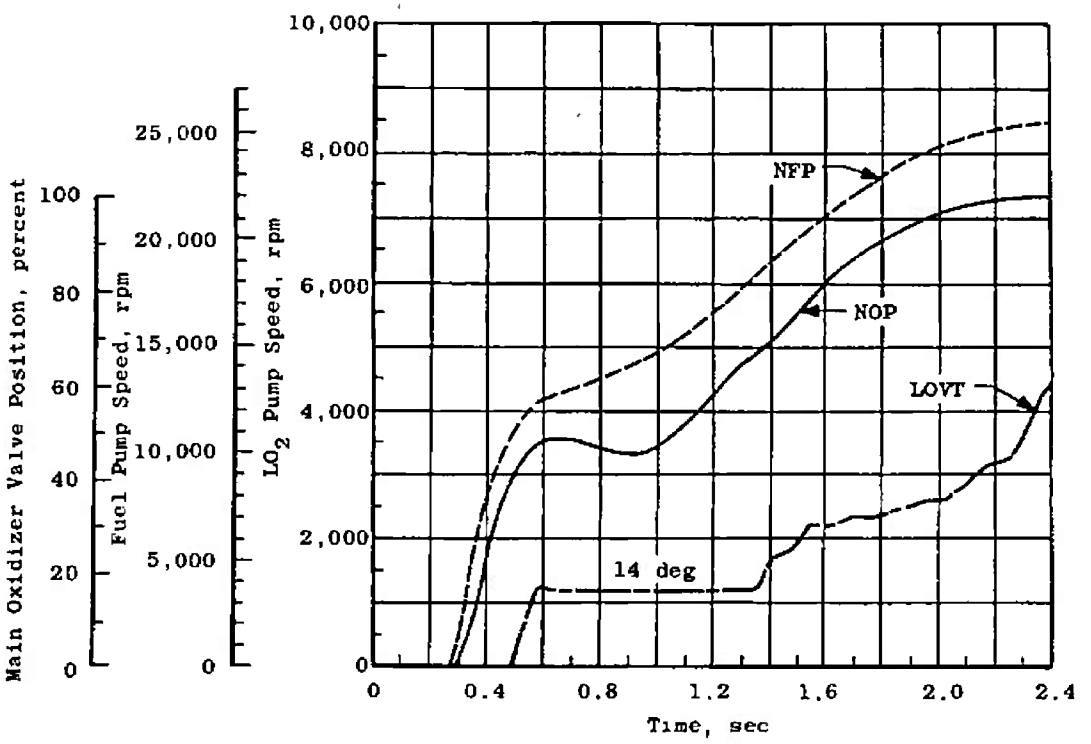

e. Pump Speeds and Main Oxidizer Valve Movement – Test 25B

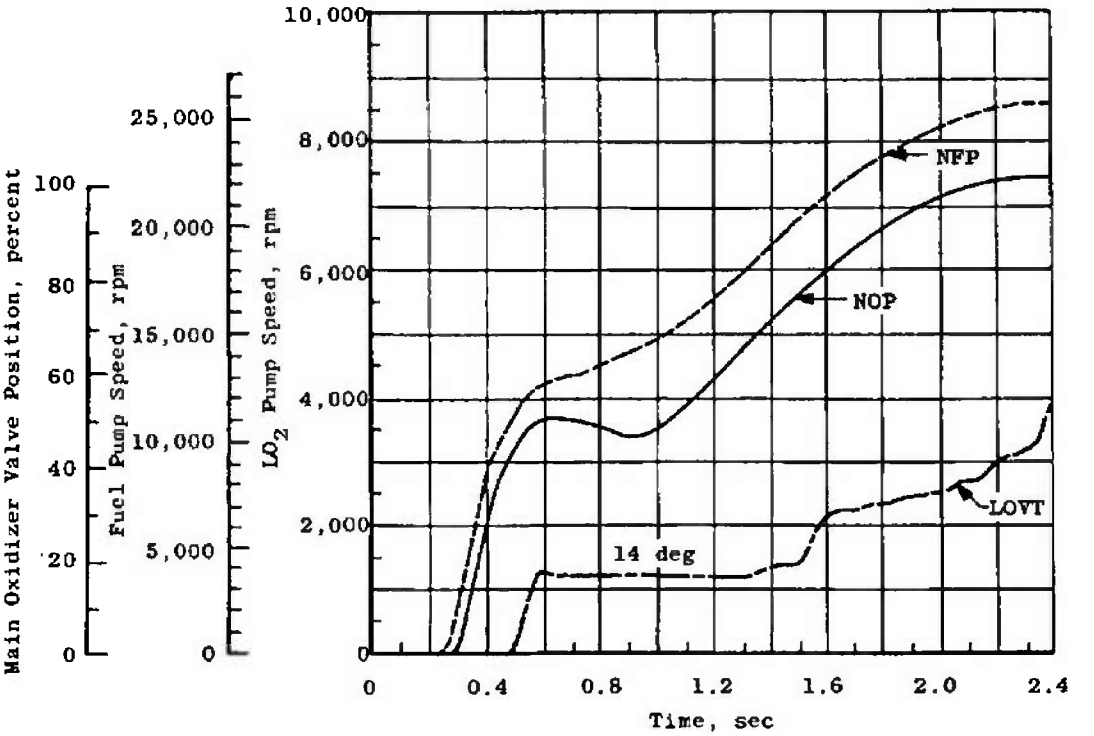

f. Pump Speeds and Main Oxidizer Valve Movement – Test 25D

Fig. 34 Concluded

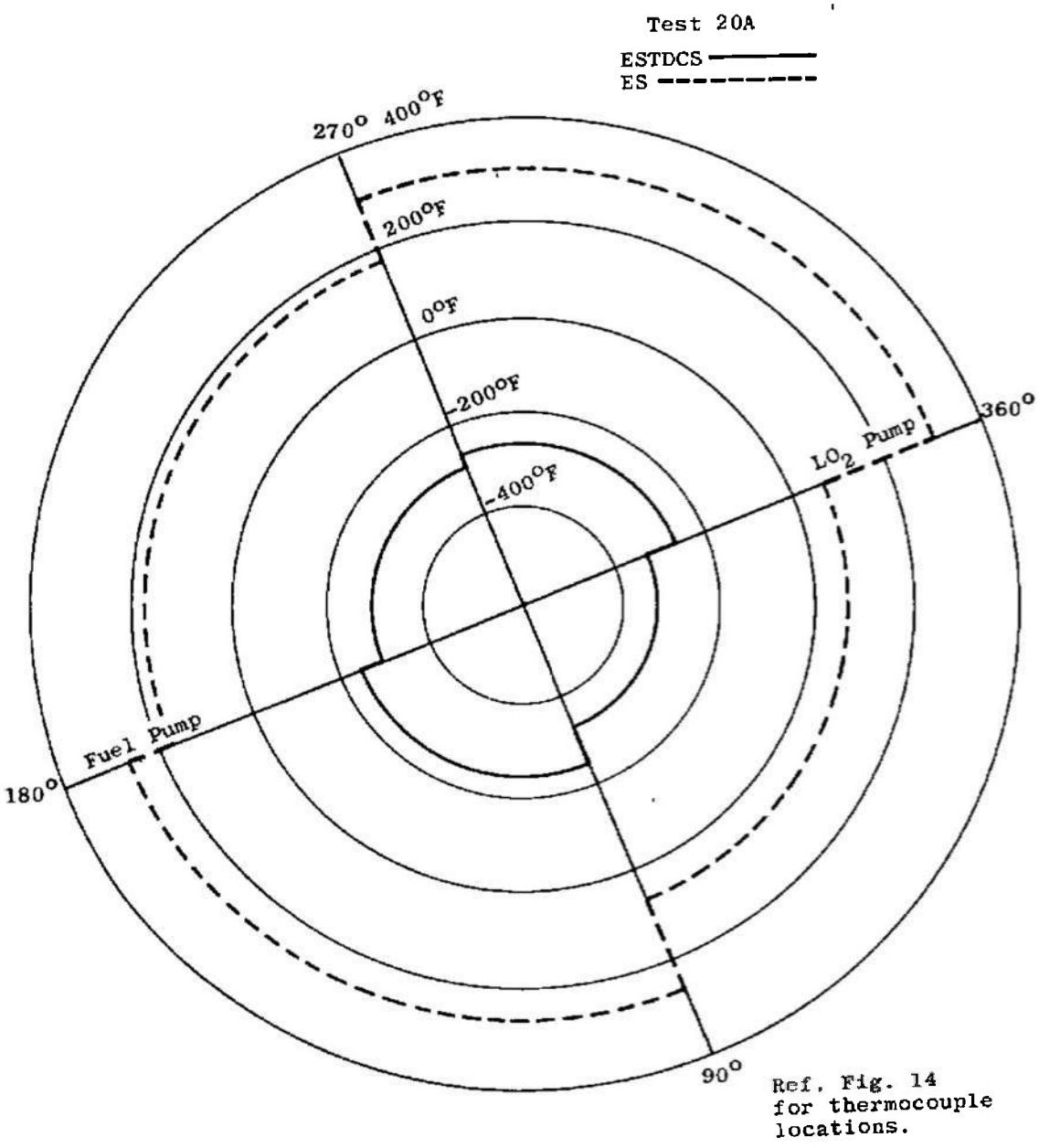

a. Exit Profiles

Fig. 35 Thrust Chamber Temperature Profiles – Test 20A

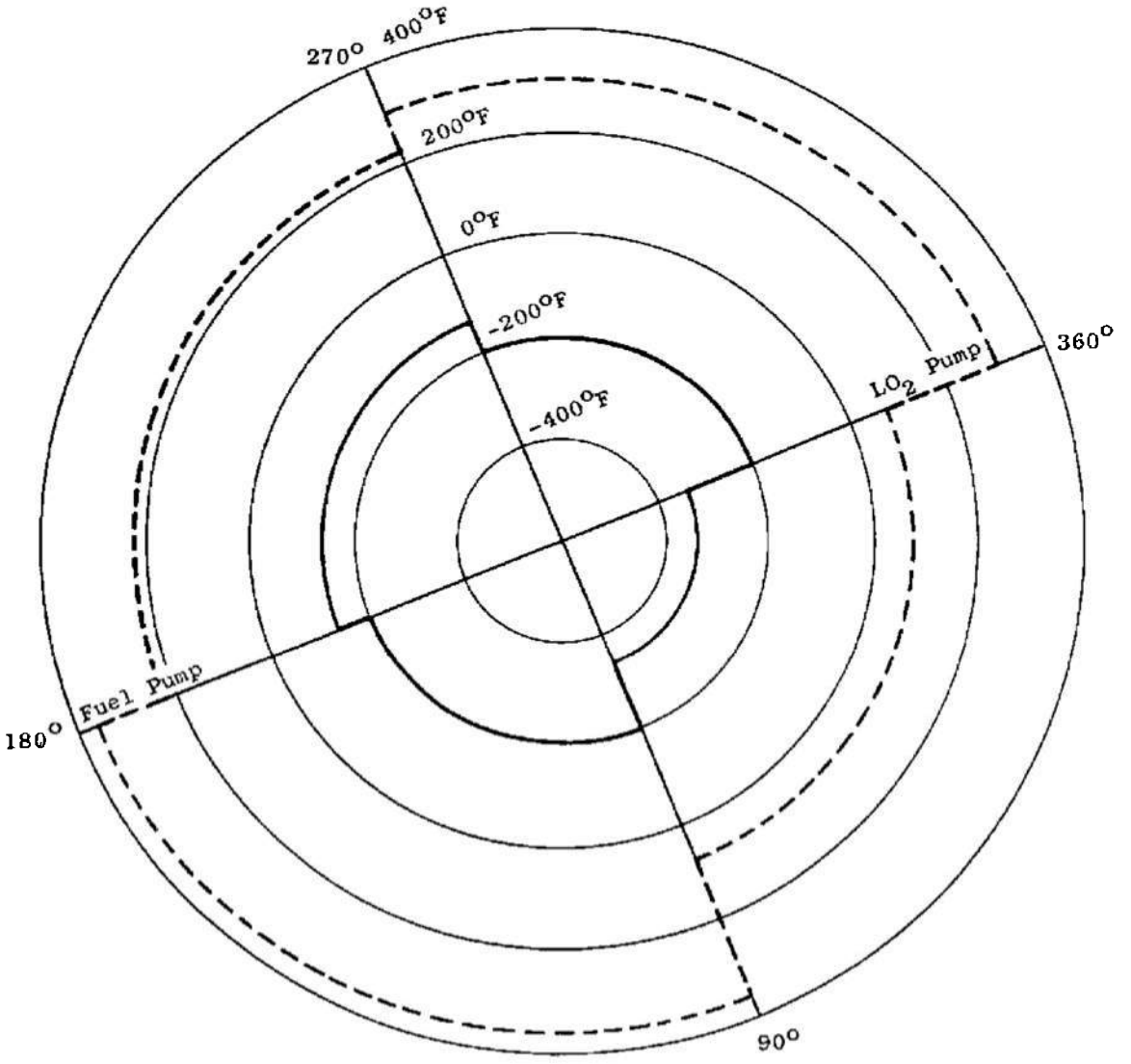

b. 19-in. Profiles

Fig. 35 Continued

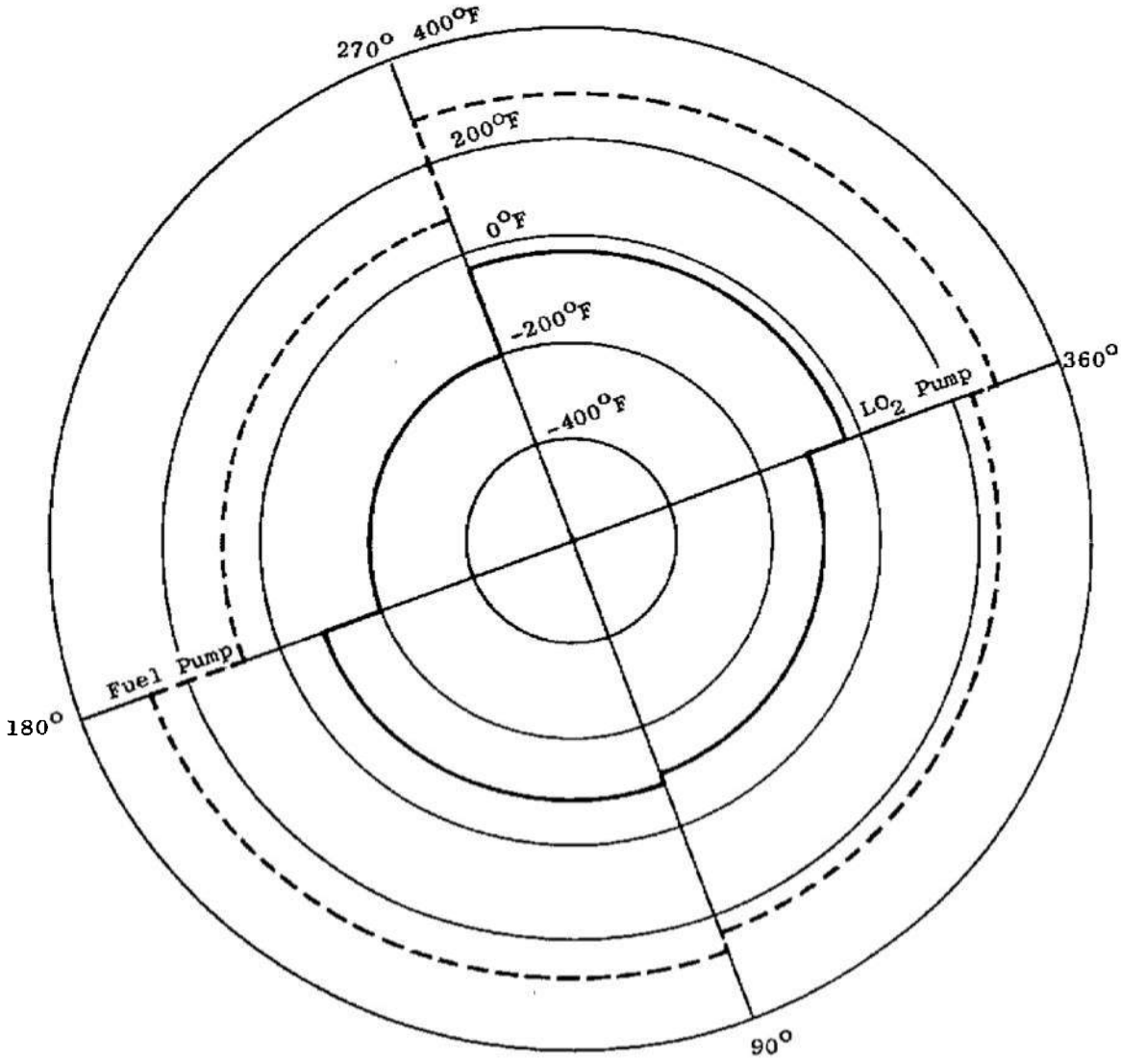

c. 27-in. Profiles

Fig. 35 Continued

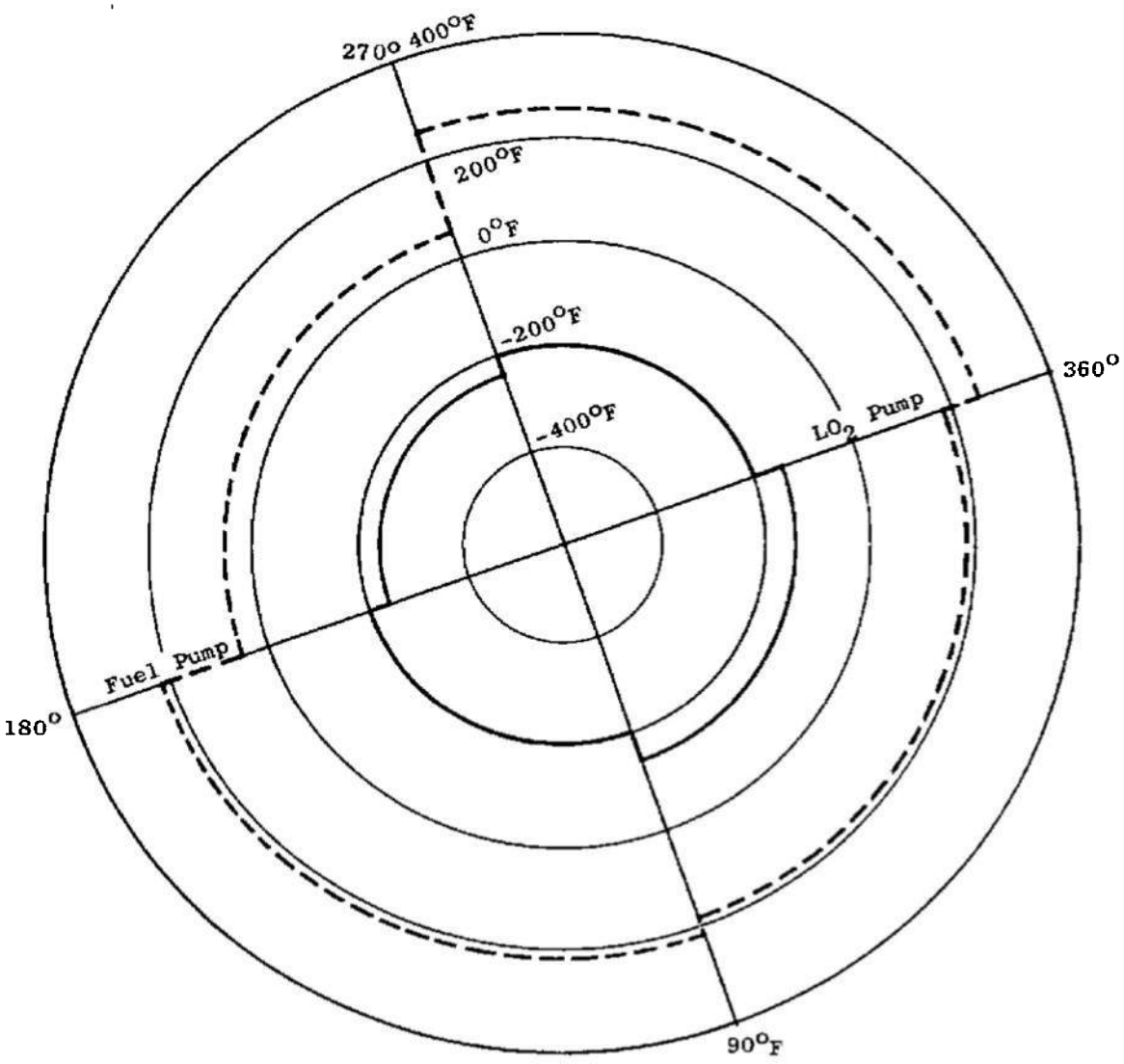

d. 46-in. Profiles

Fig. 35 Continued

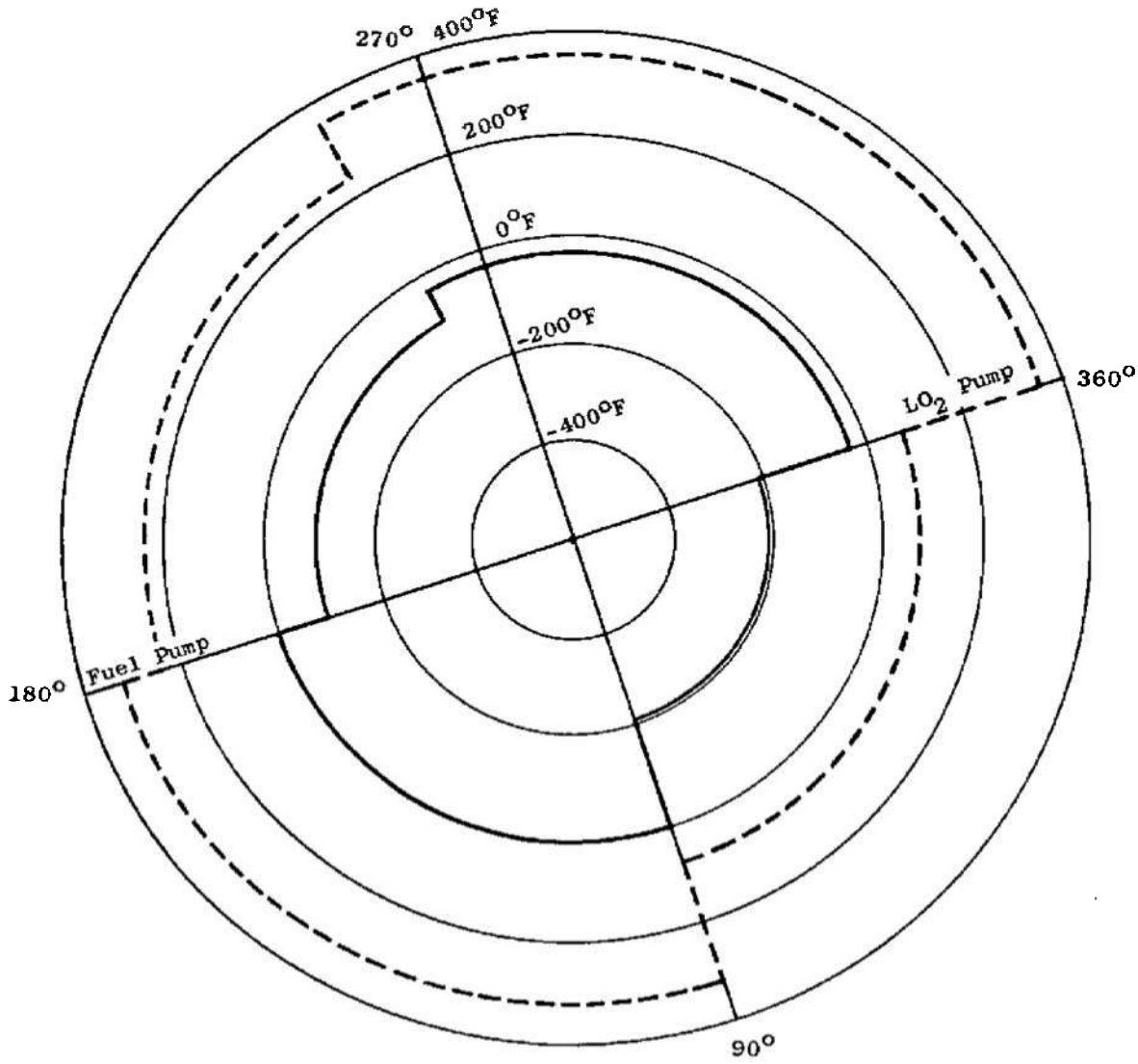

e. 65-in. Profiles

Fig. 35 Continued

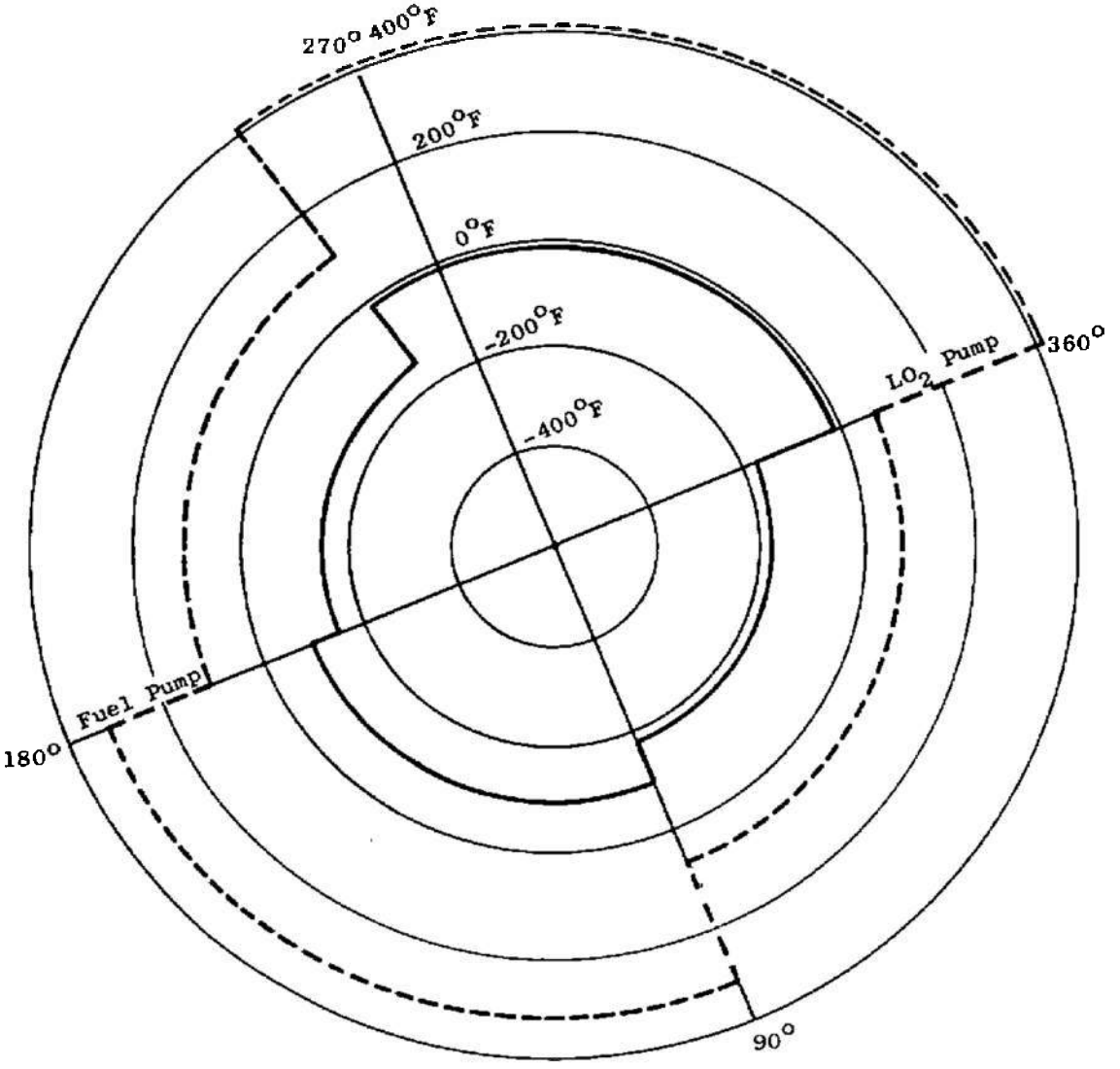

f. Throat Profiles

Fig. 35 Concluded

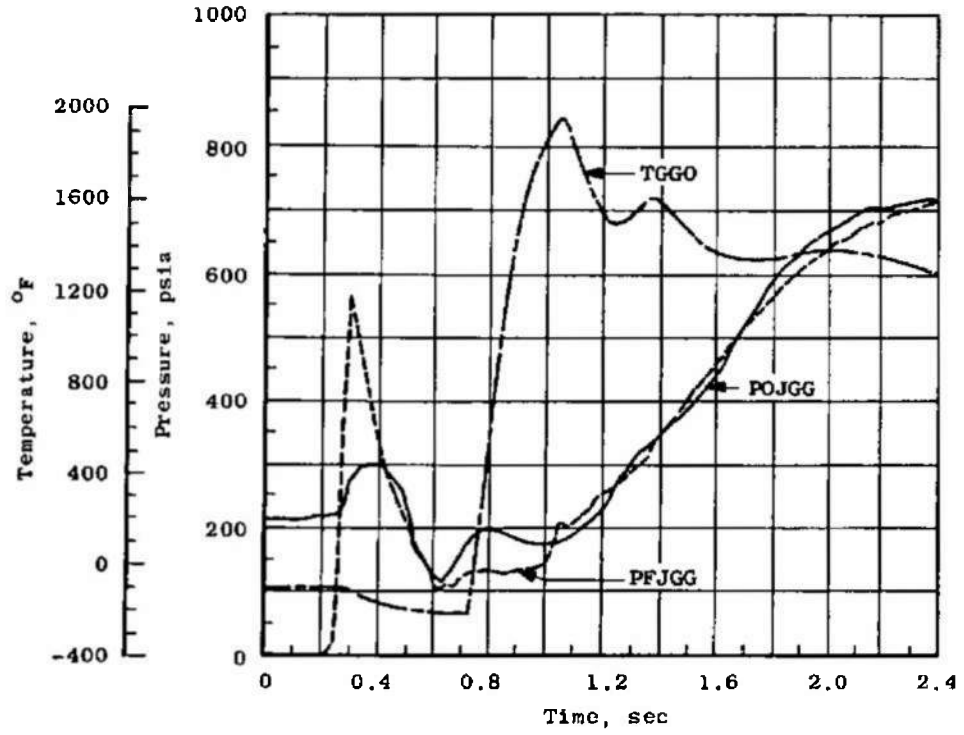

a. Gas Generator Start Transient – Test 26A

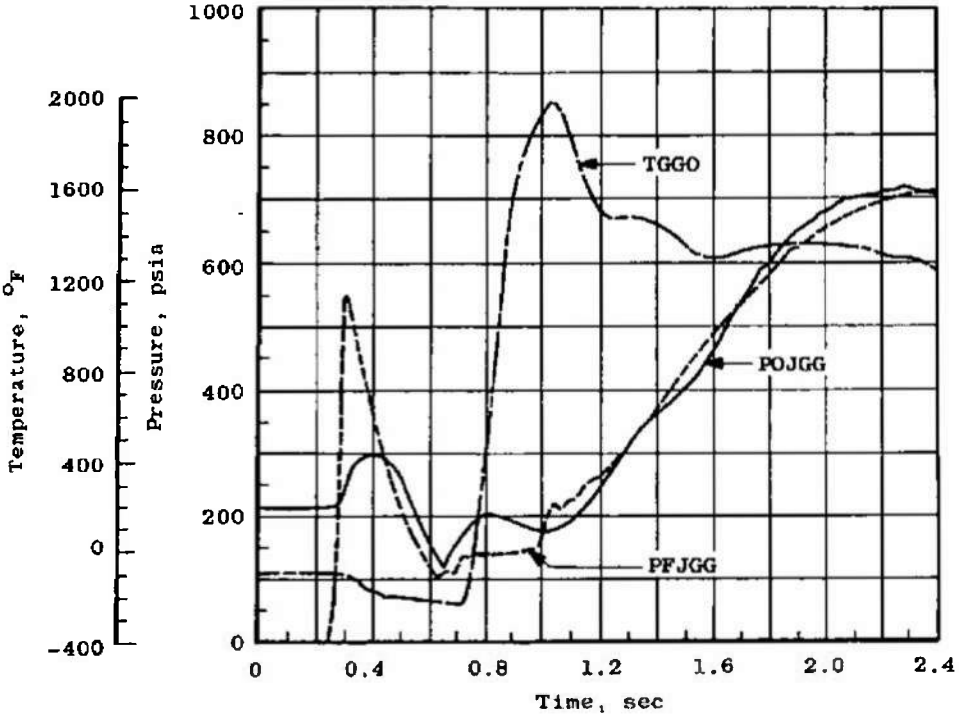

b. Gas Generator Start Transient – Test 26C

Fig. 36 Start Transient Comparisons – Tests 26A and 26C

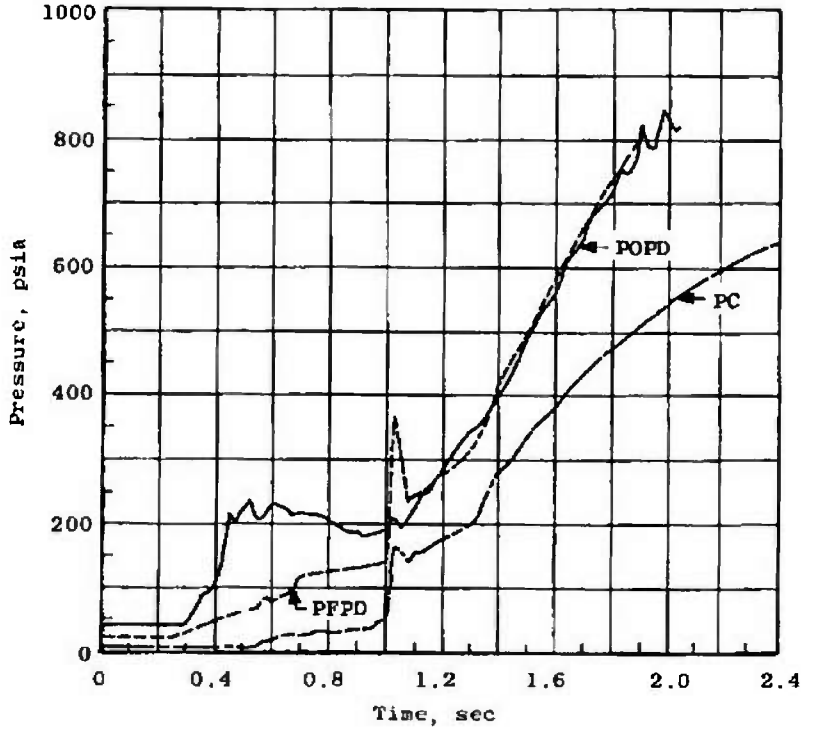

c. Main Chamber Start Transient – Test 26A

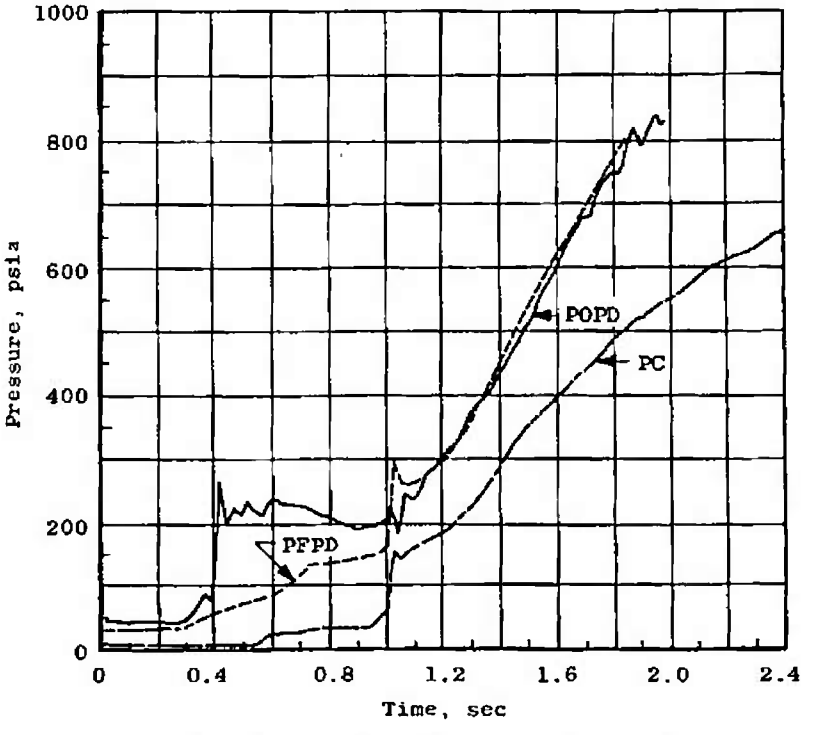

d. Main Chamber Start Transient – Test 26C

Fig. 36 Continued

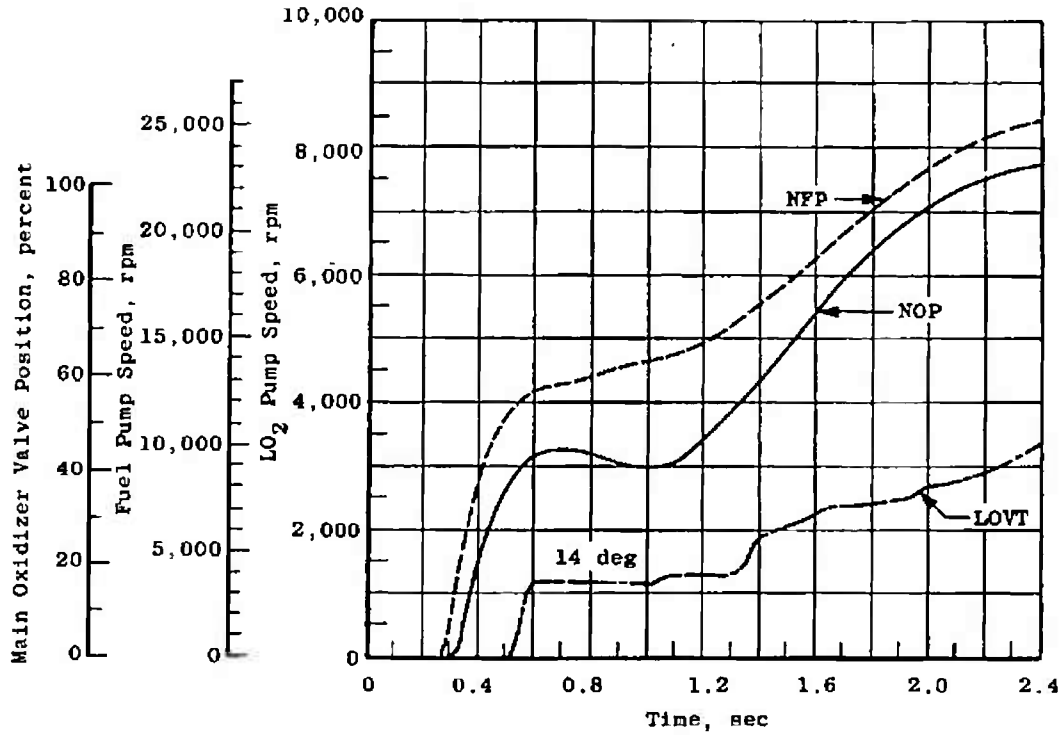

e. Pump Speeds and Main Oxidizer Valve Movement – Test 26A

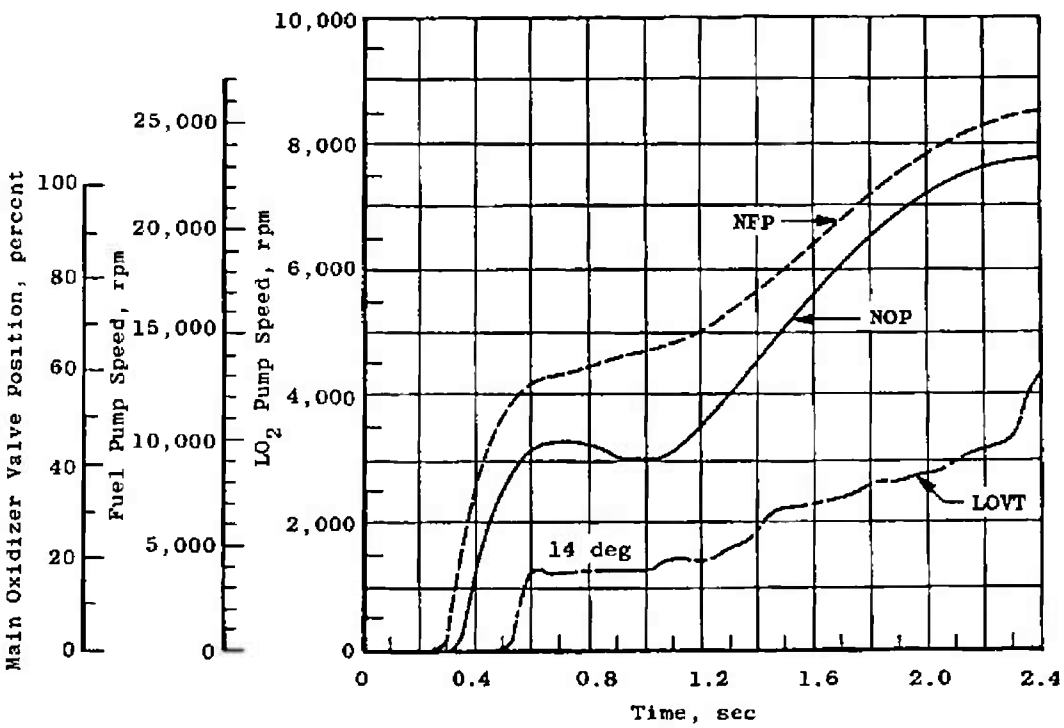

f. Pump Speeds and Main Oxidizer Valve Movement – Test 26C

Fig. 36 Concluded

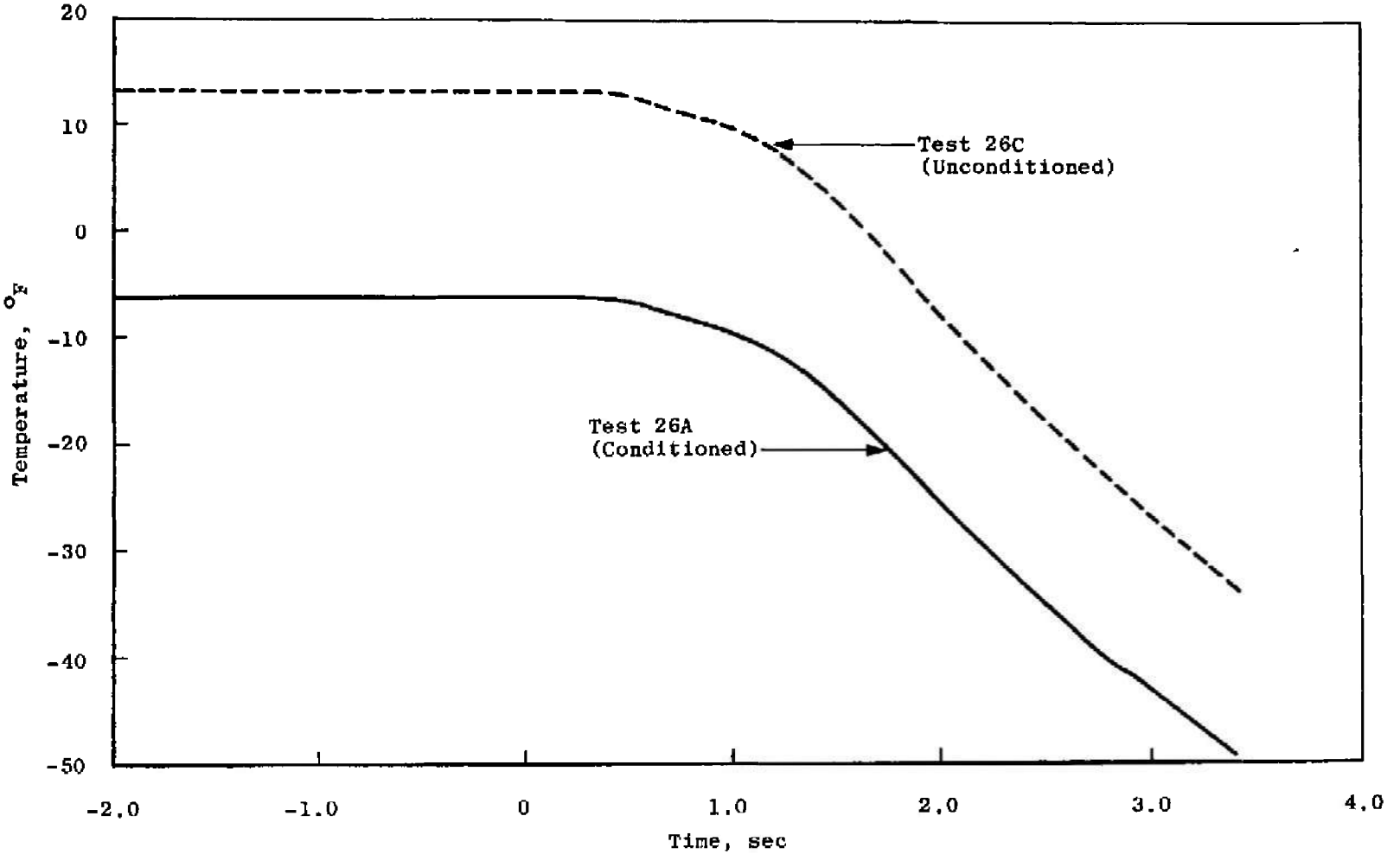

Fig. 37 Gas Generator Liquid Oxygen Supply Line Ground Environment Simulation Test Comparisons

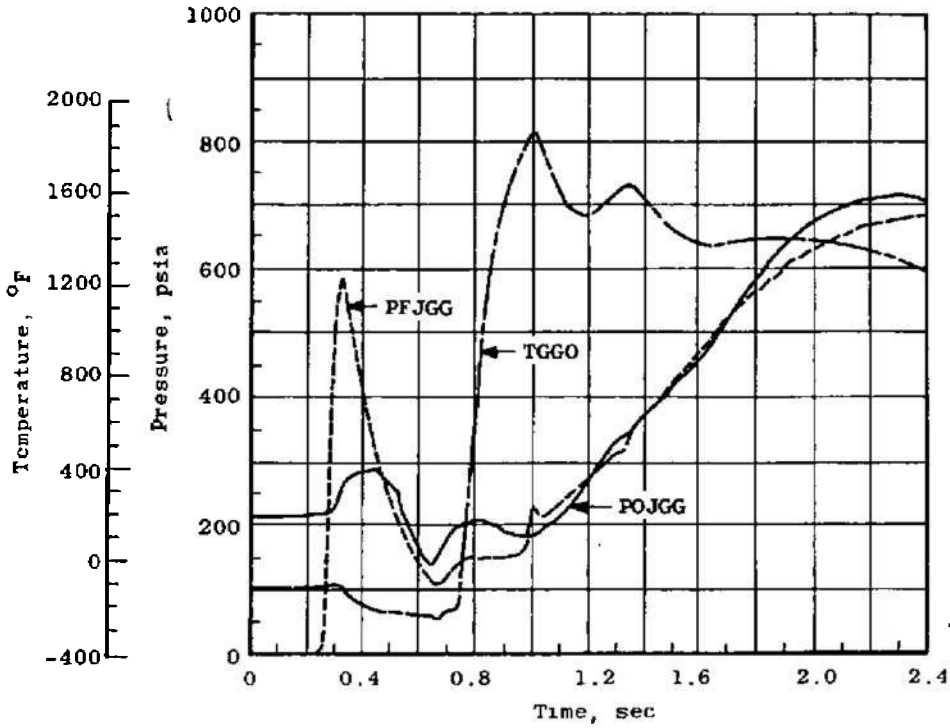

a. Gas Generator Start Transient – Test 21C

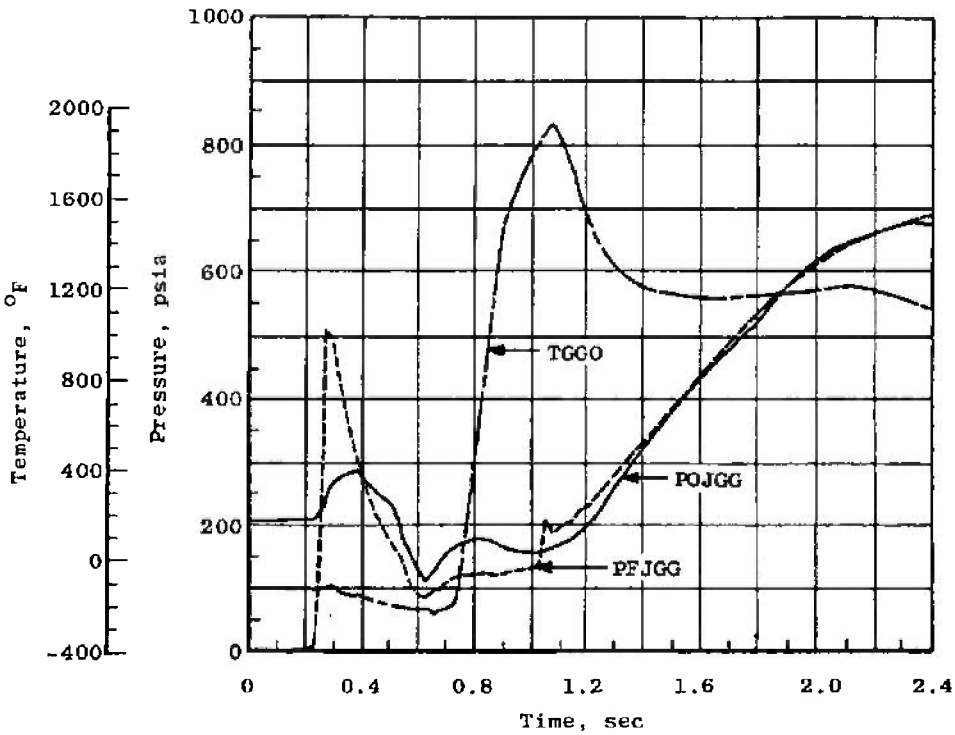

b. Gas Generator Start Transient – Test 24C

Fig. 38 Start Transient Comparisons – Tests 21C and 24C

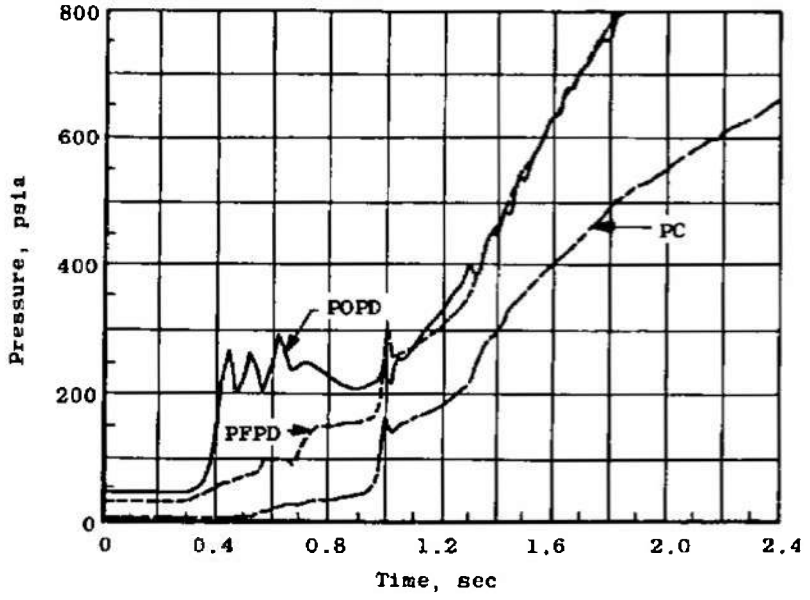

c. Main Chamber Start Transient – Test 21C

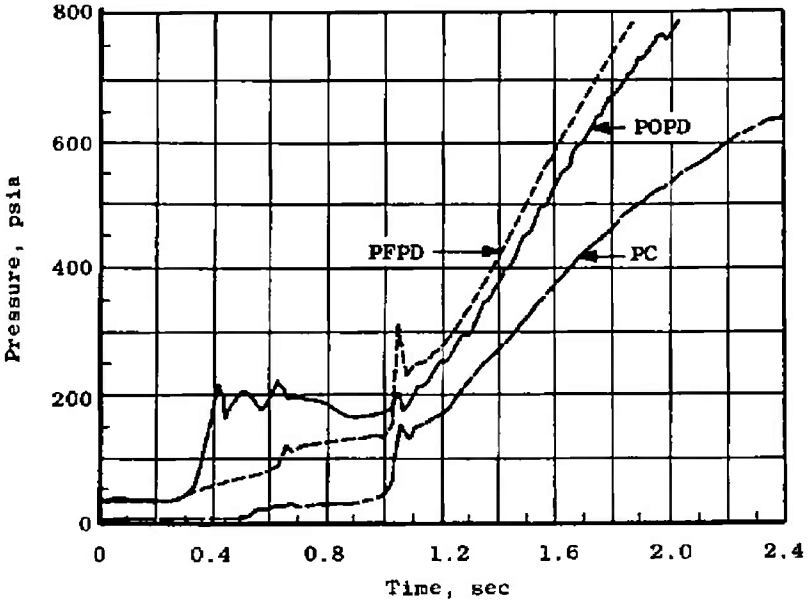

d. Main Chamber Start Transient – Test 24C

Fig. 38 Continued

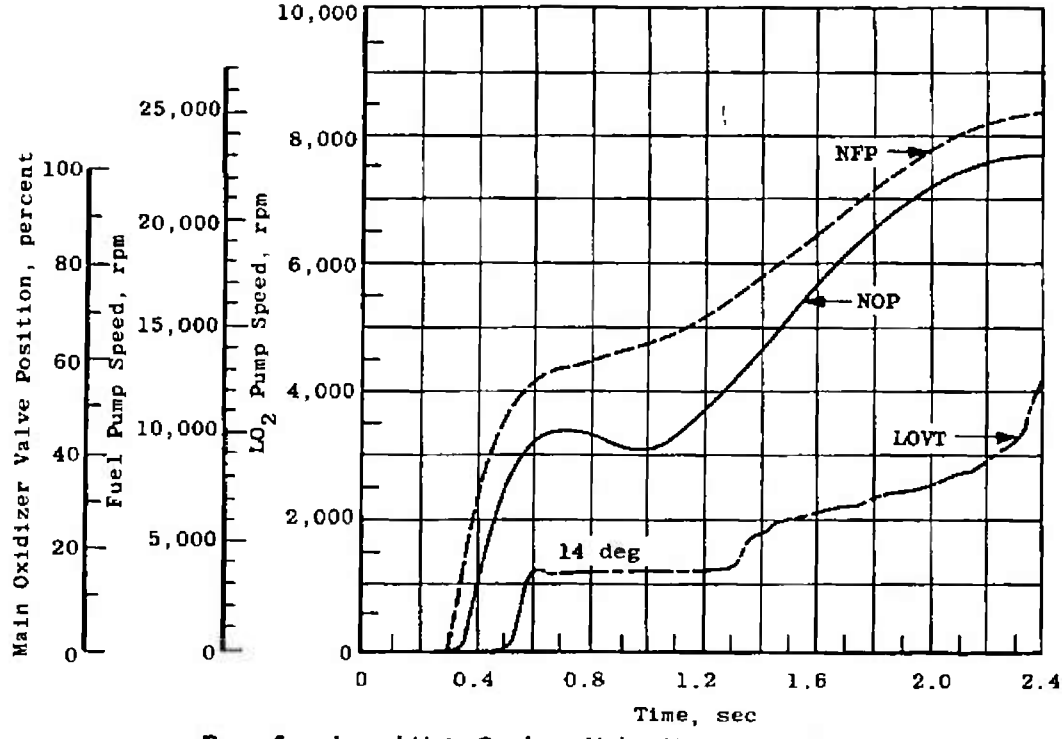

e. Pump Speeds and Main Oxidizer Valve Movement – Test 21C

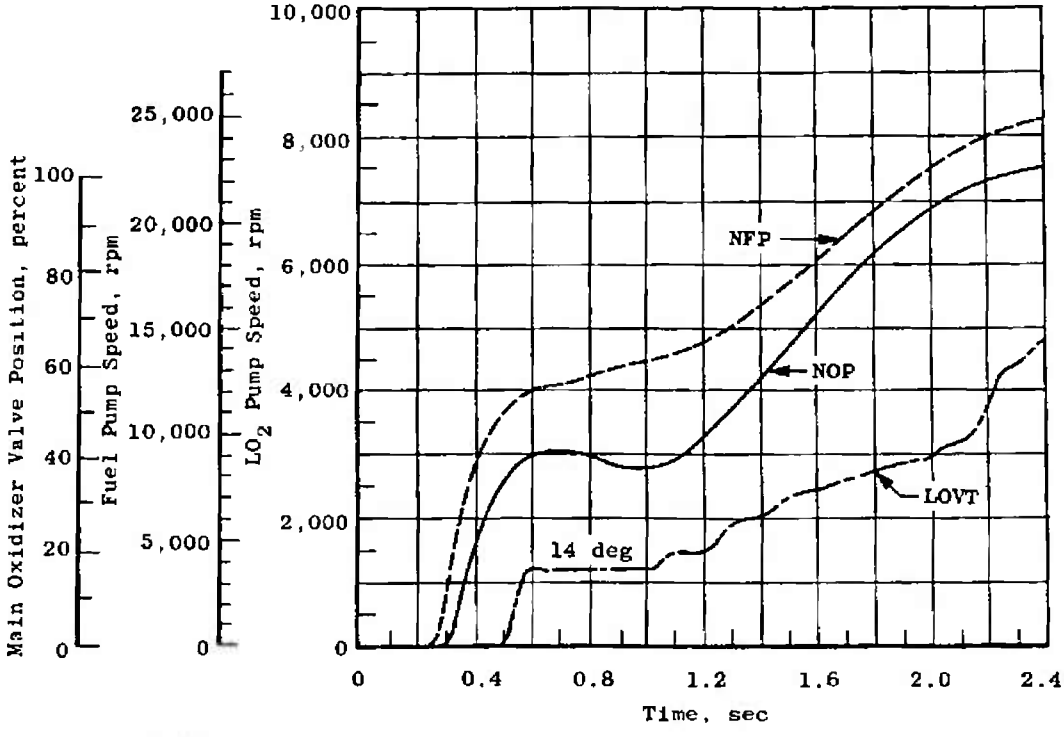

f. Pump Speeds and Main Oxidizer Valve Movement – Test 24C

Fig. 38 Concluded

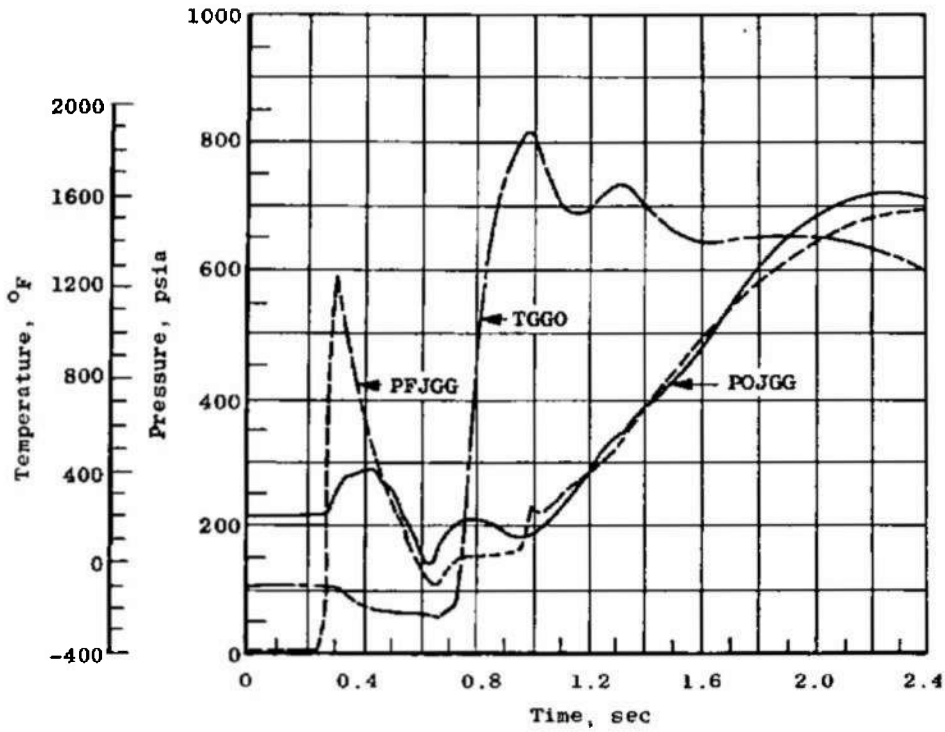

a. Gas Generator Start Transient – Test 21C

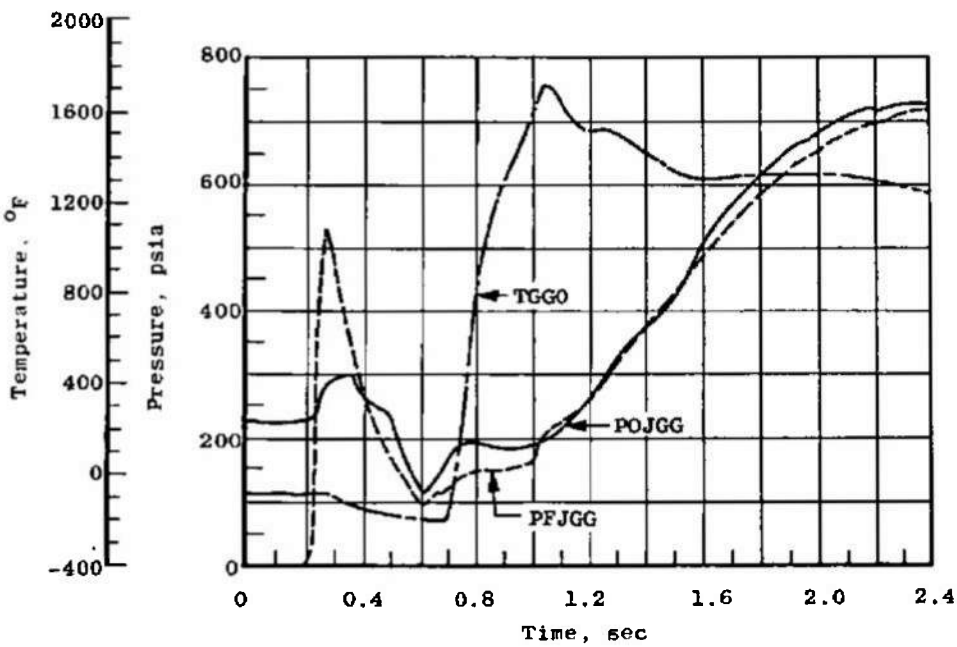

b. Gas Generator Start Transient – Test 22A

Fig. 39 Start Transient Comparisons – Tests 21C and 22A

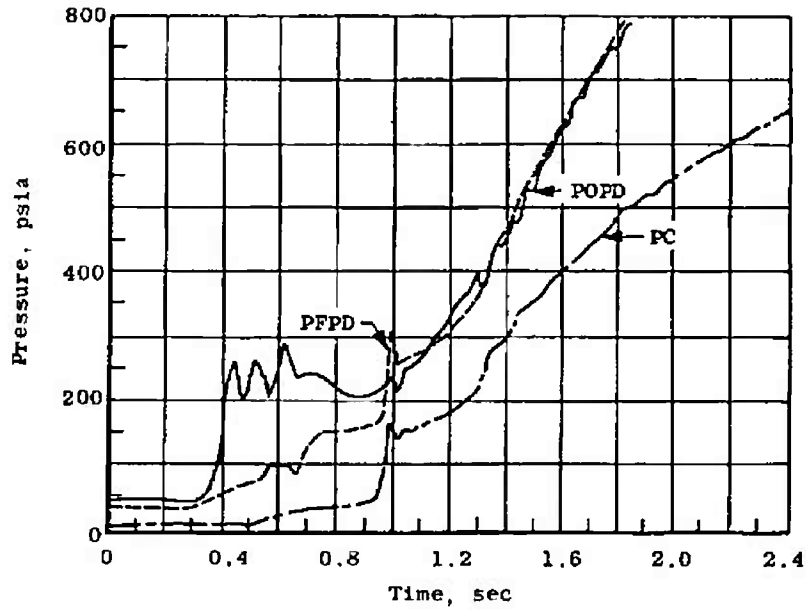

c. Main Chamber Start Transient – Test 21C

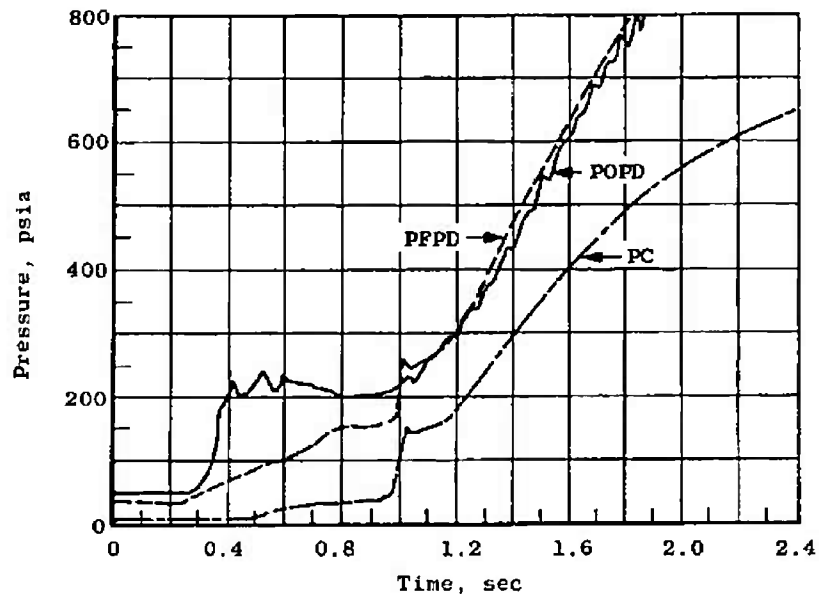

d. Main Chamber Start Transient – Test 22A

Fig. 39 Continued

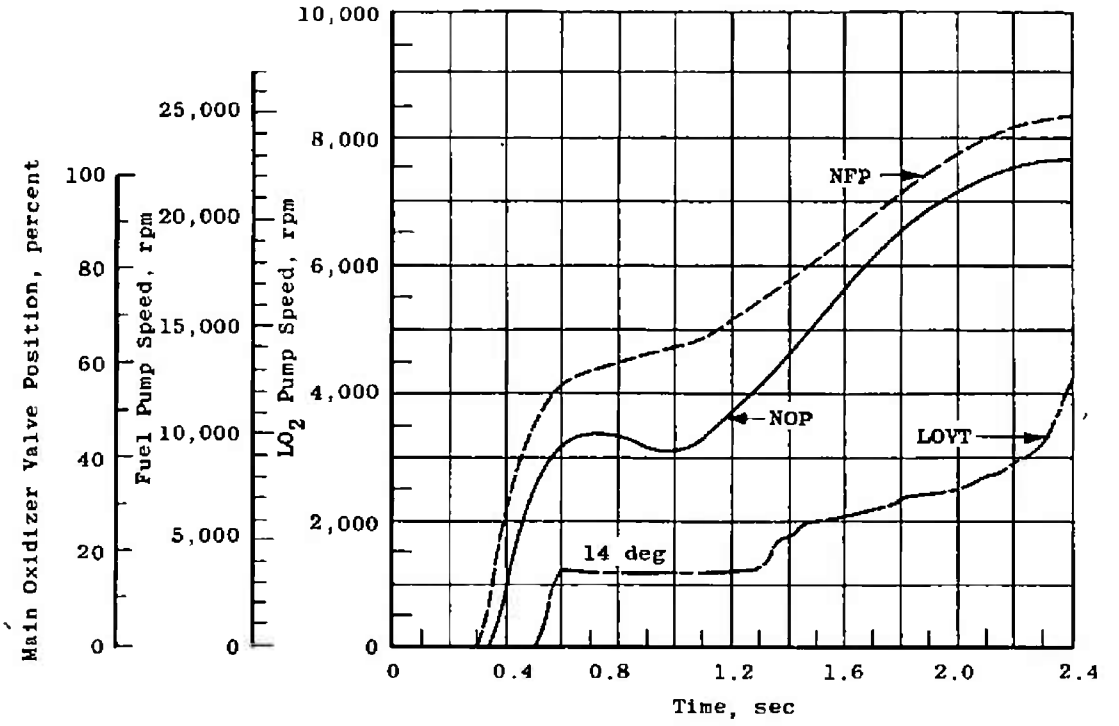

e. Pump Speeds and Main Oxidizer Valve Movement – Test 21C

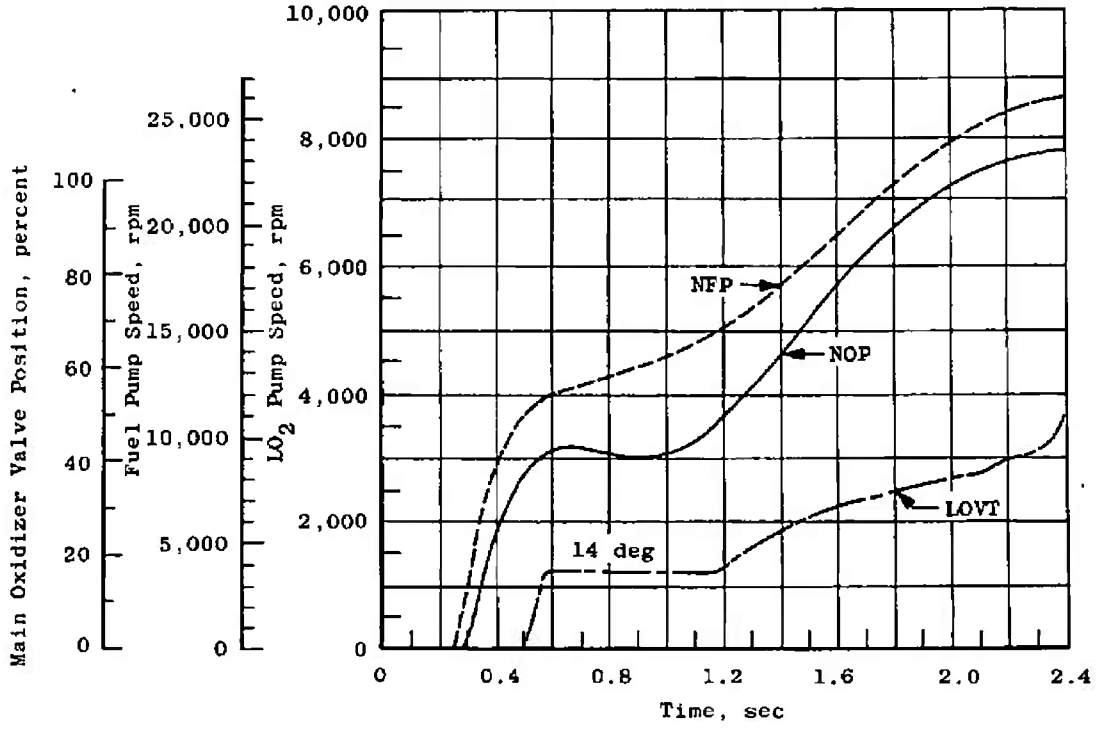

f. Pump Speeds and Main Oxidizer Value Movement – Test 22A

Fig. 39 Concluded

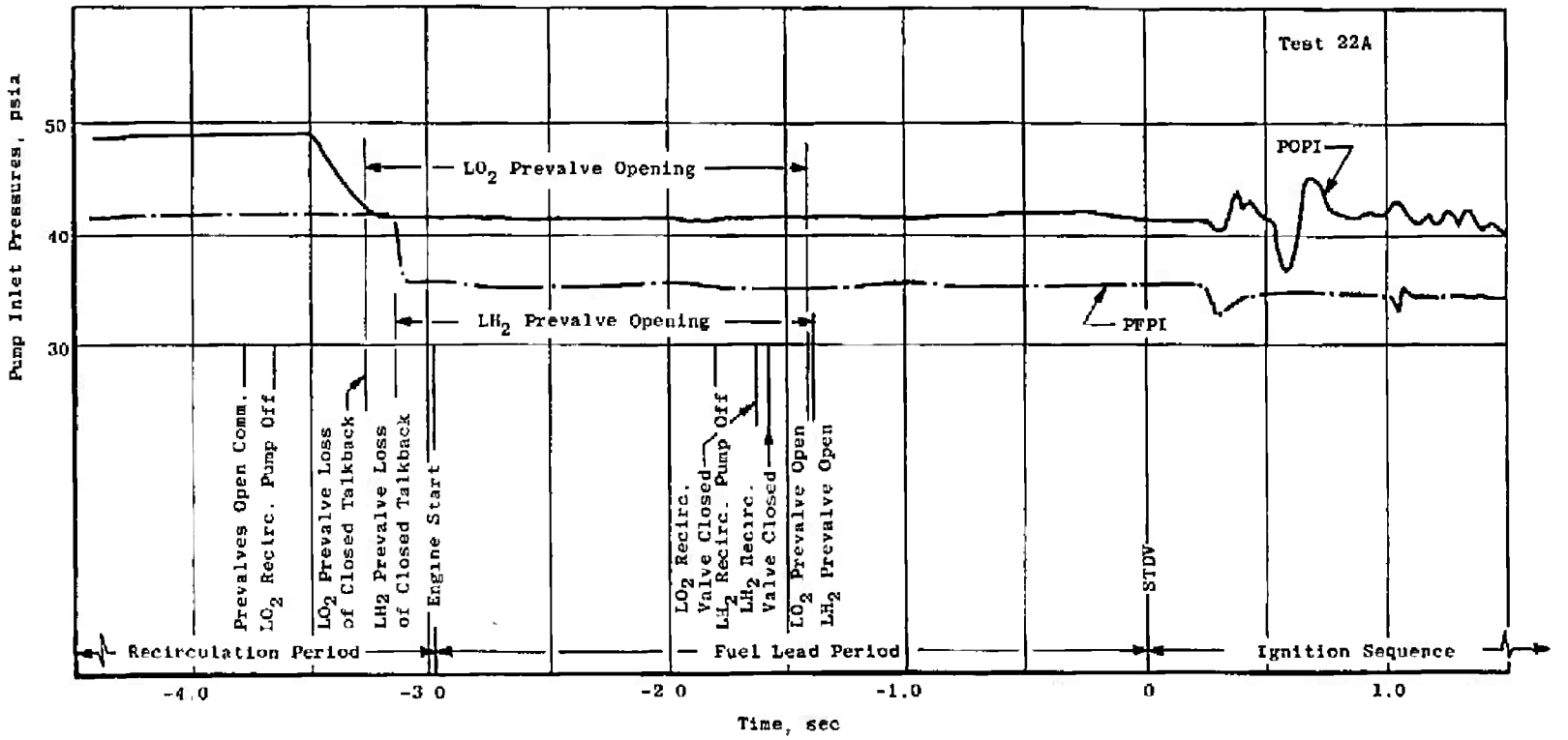

Fig. 40 Saturn V (501)/S-IVB First-Burn Prevalve Sequencing Effect on Pump Inlets

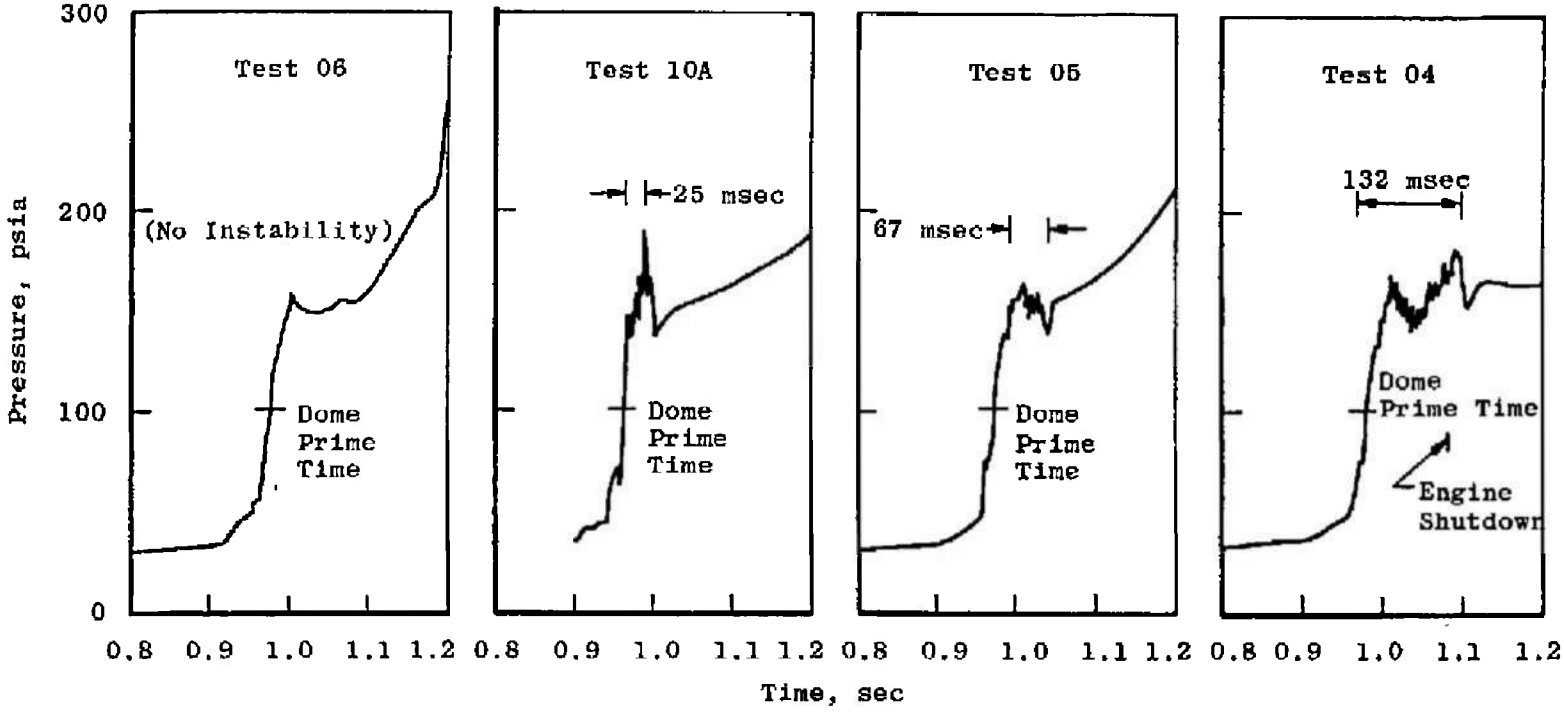

Fig. 41 Typical Thrust Chamber Pressure Traces with Dome Prime Vibration

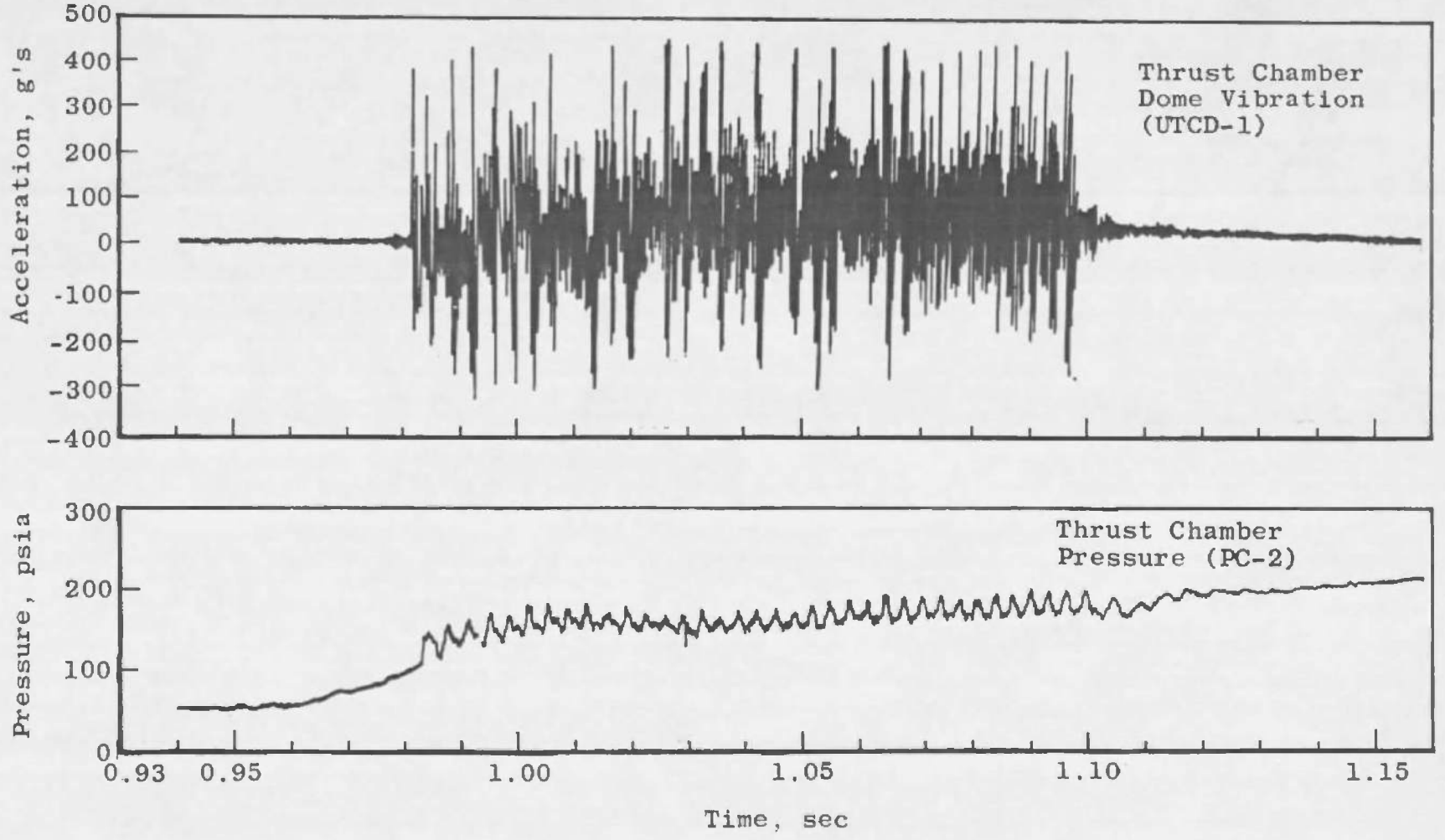

a. Acceleration and Pressure versus Time

Fig. 42 Thrust Chamber Vibration Data – Test 21A

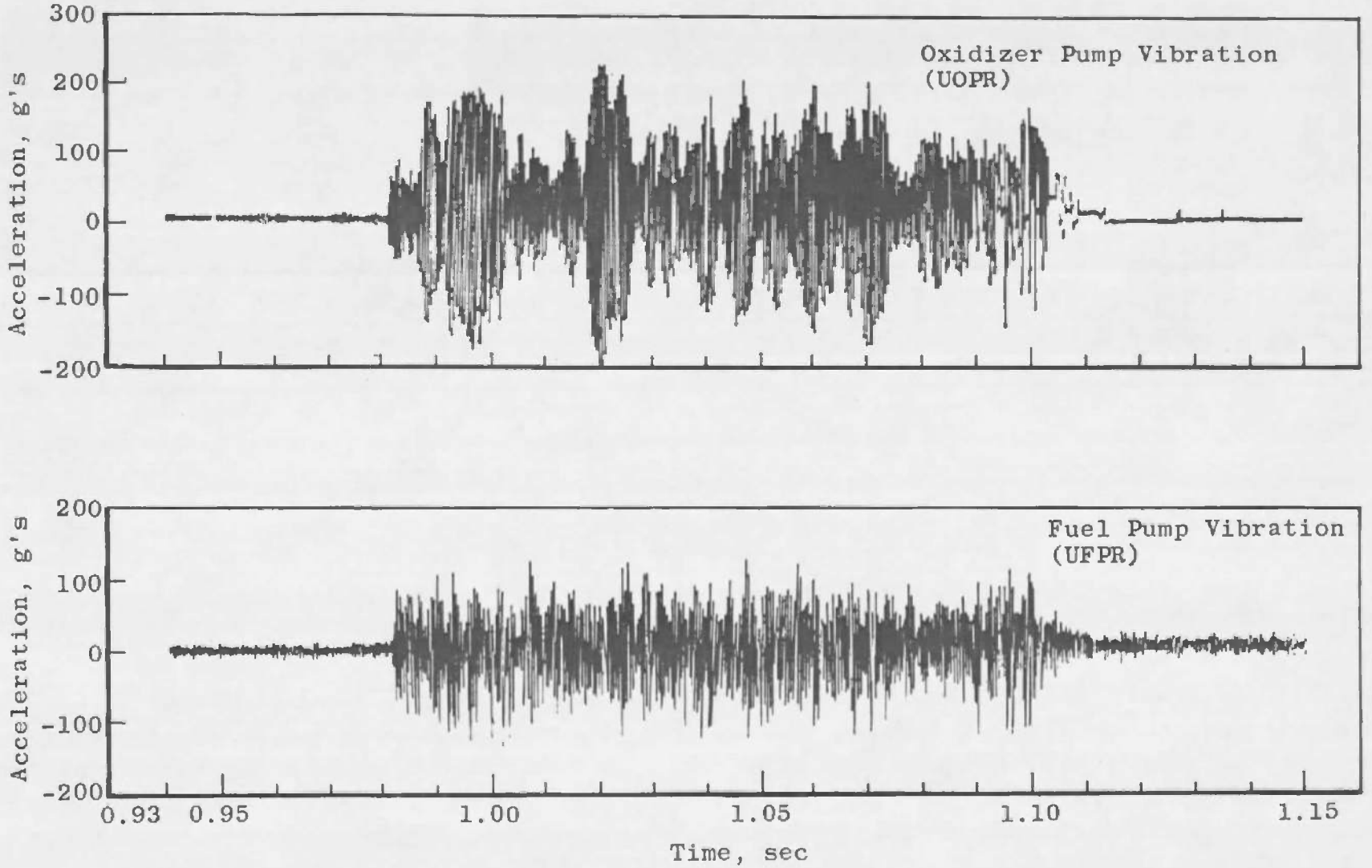

Fig. 42c Concluded

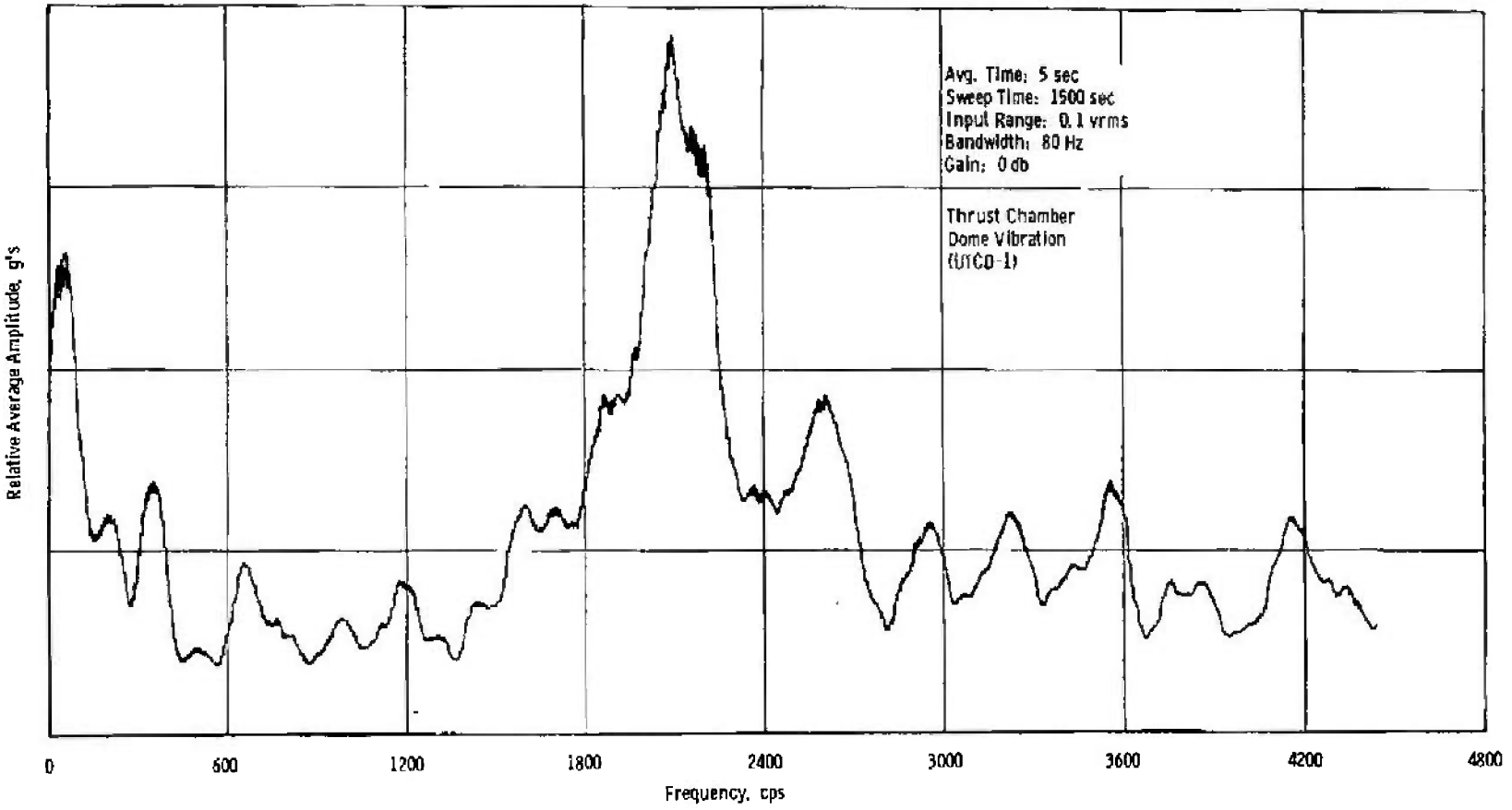

b. Amplitude Spectrum

Fig. 42 Continued

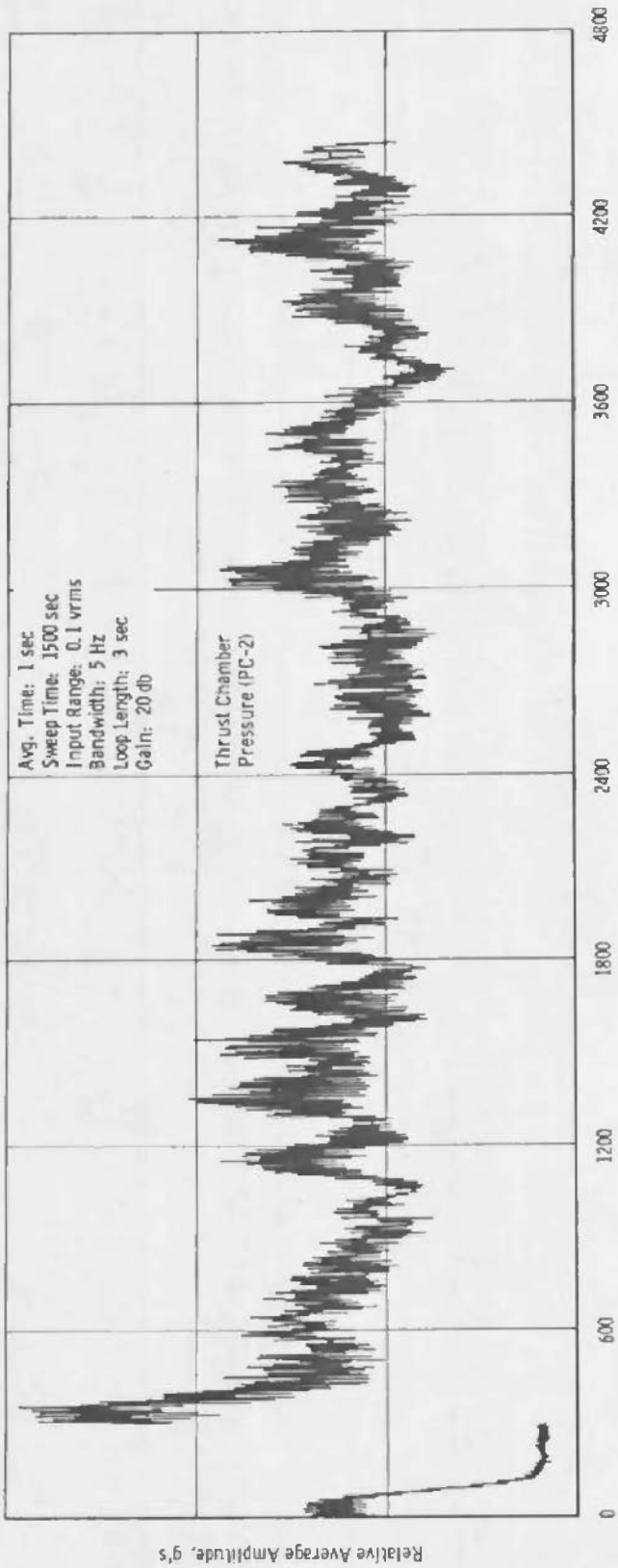

Fig. 42b Continued

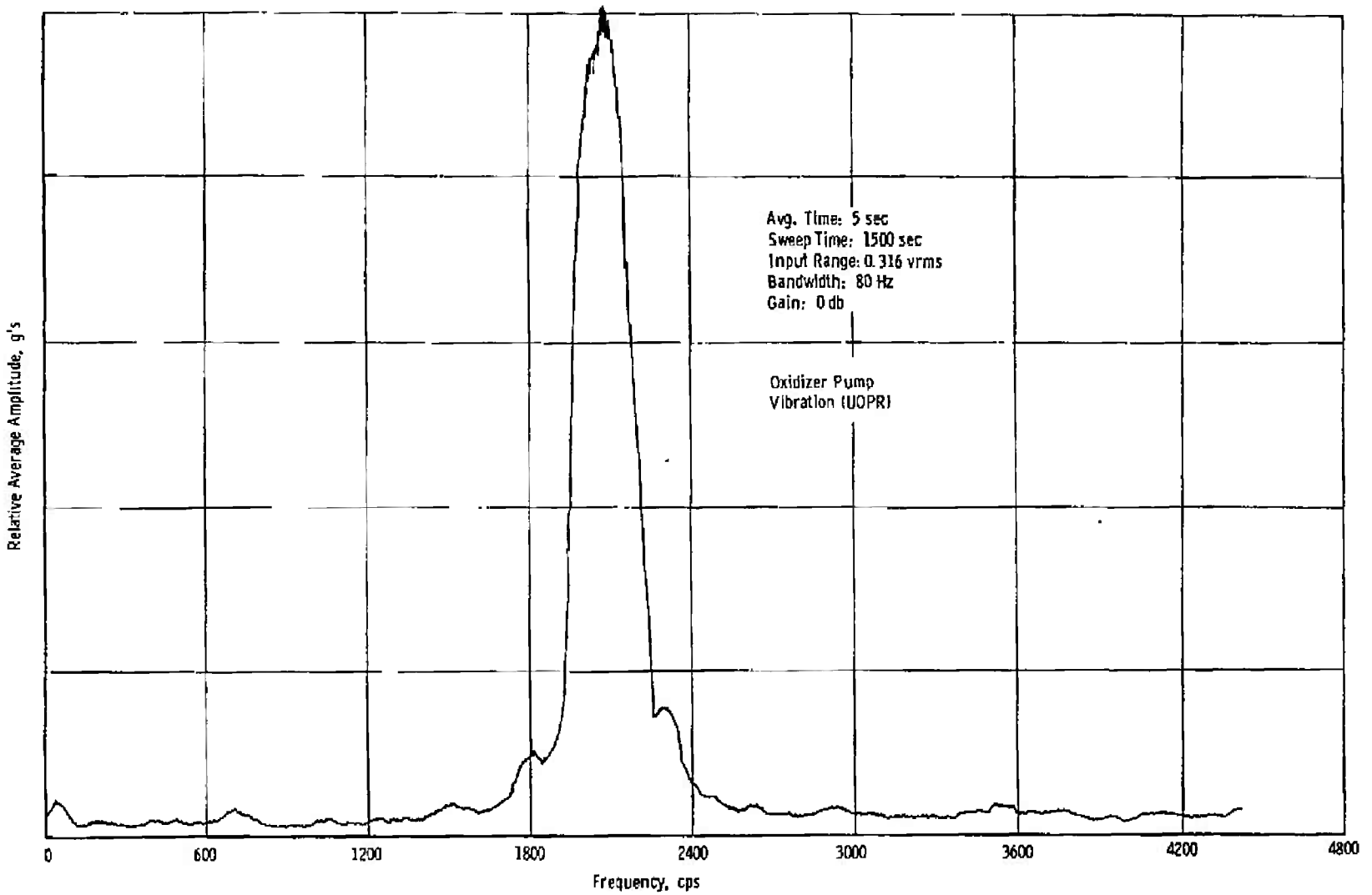

Fig. 42b Continued

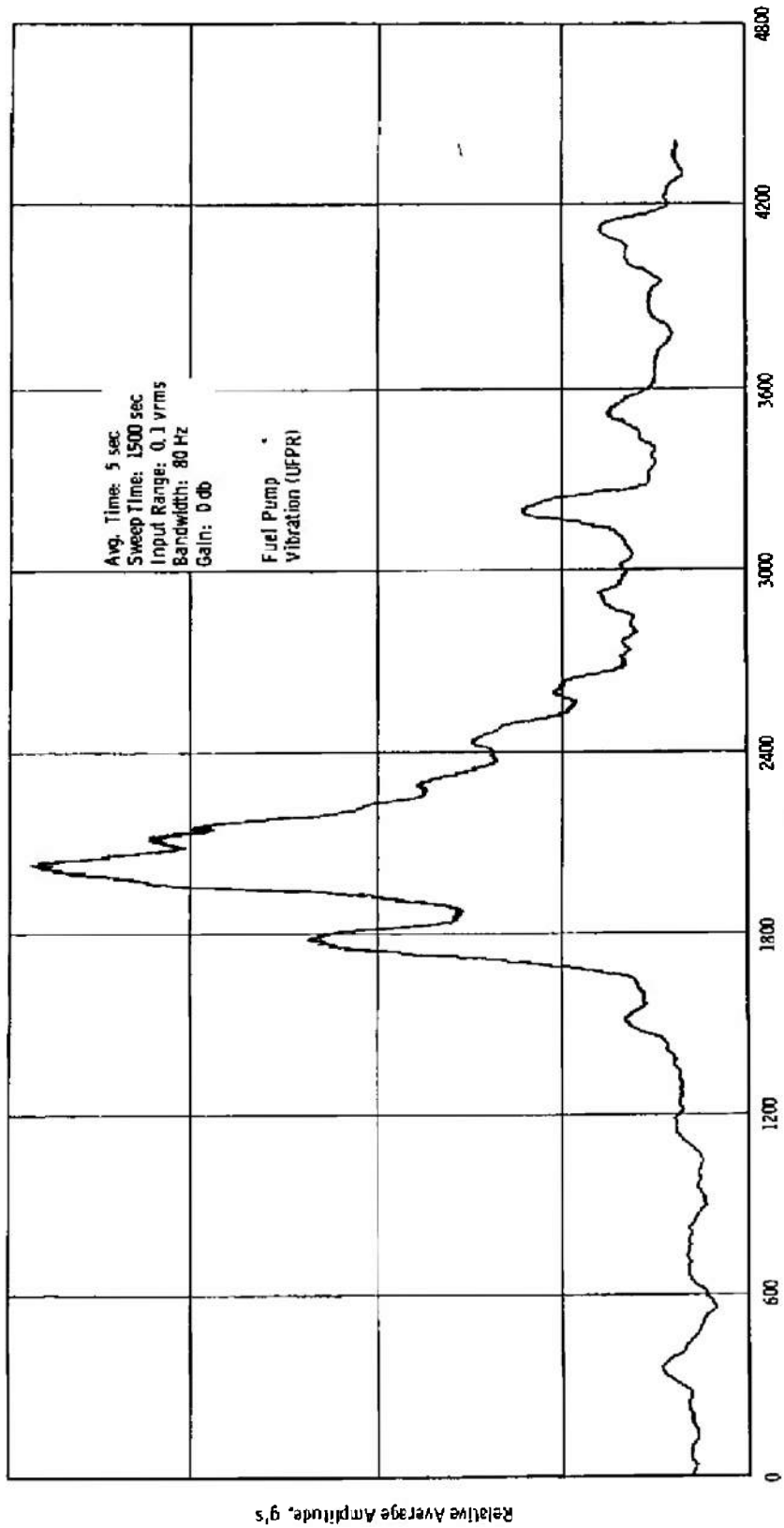

Fig. 42b Concluded

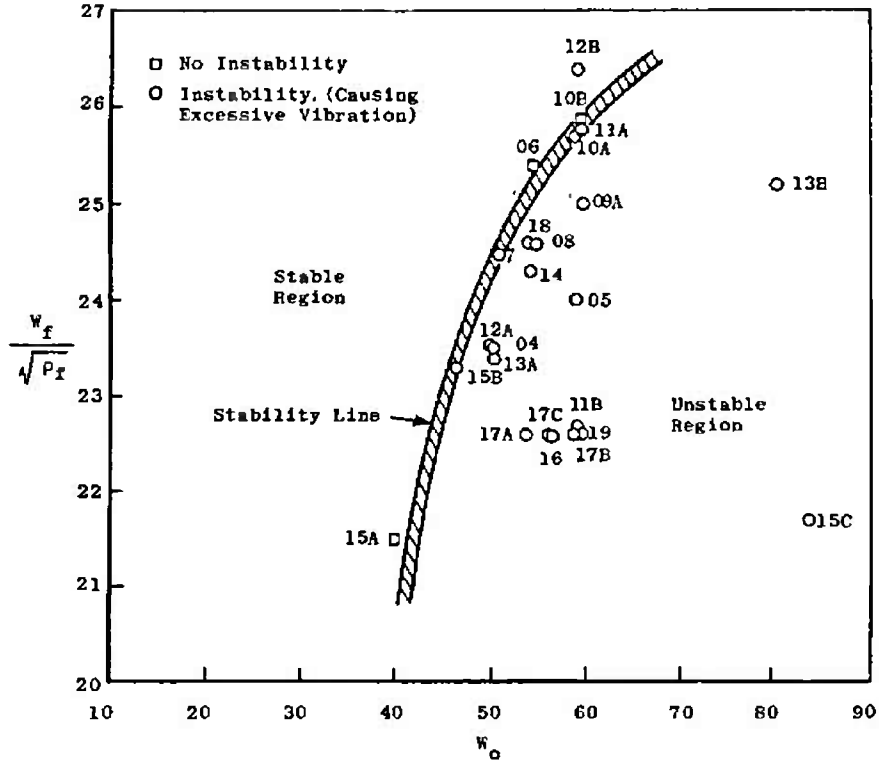

a. Original Injector – S/N 407189

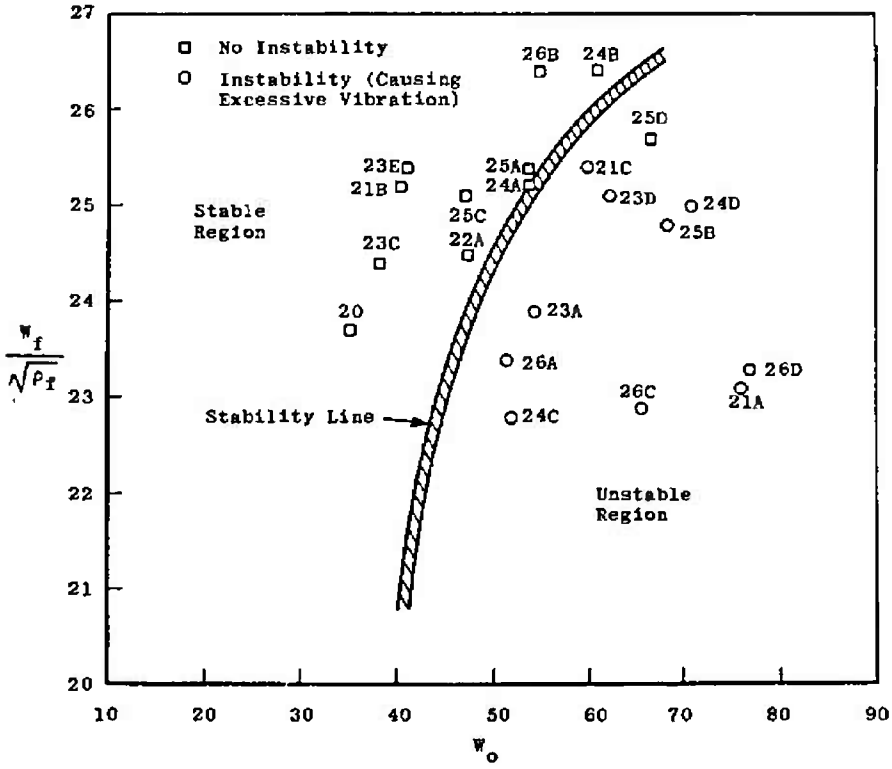

b. Replacement Injector – S/N 4084917

Fig. 43 Combustion Stability Map at Oxidizer Dome Prime Time

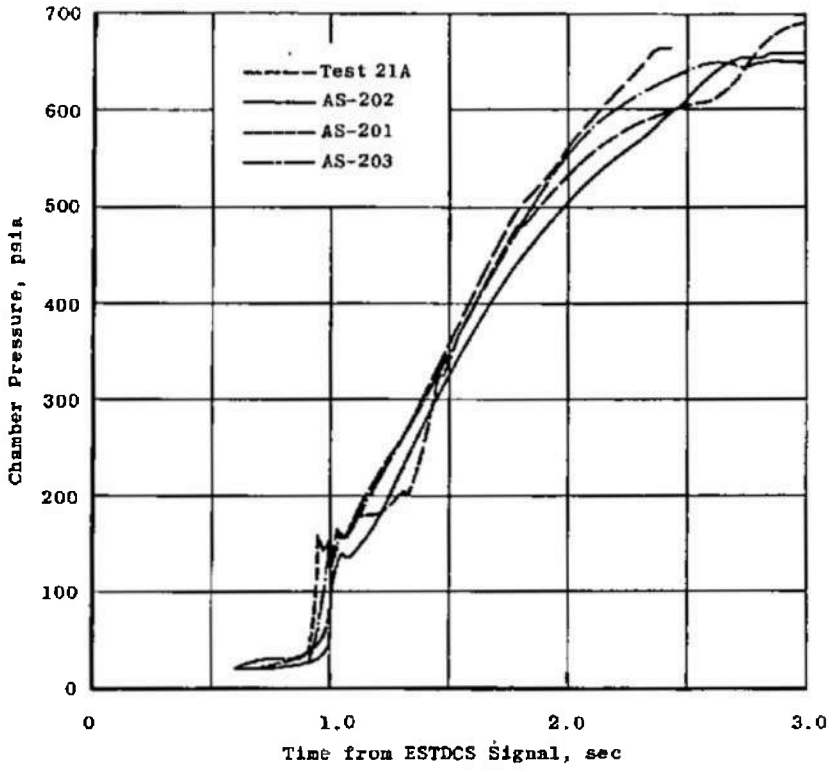

a. Chamber Pressure Buildup Transients

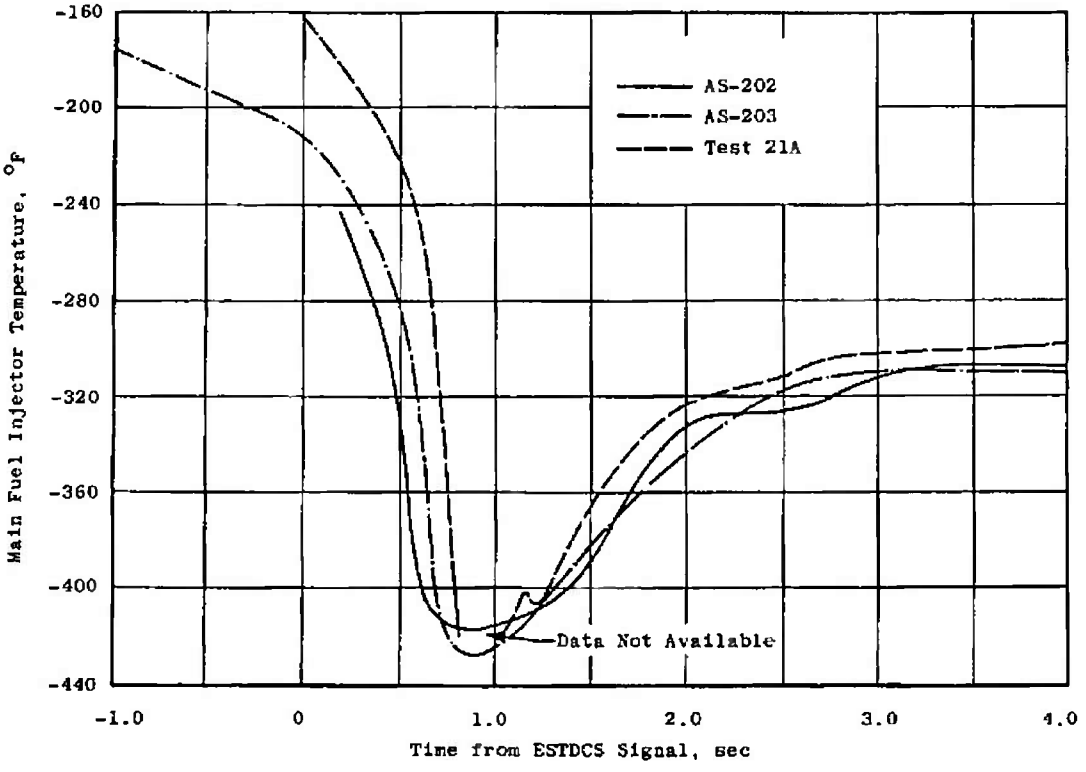

b. Fuel Injection Temperature Comparisons

Fig. 44 AEDC Test and Flight Data Comparisons

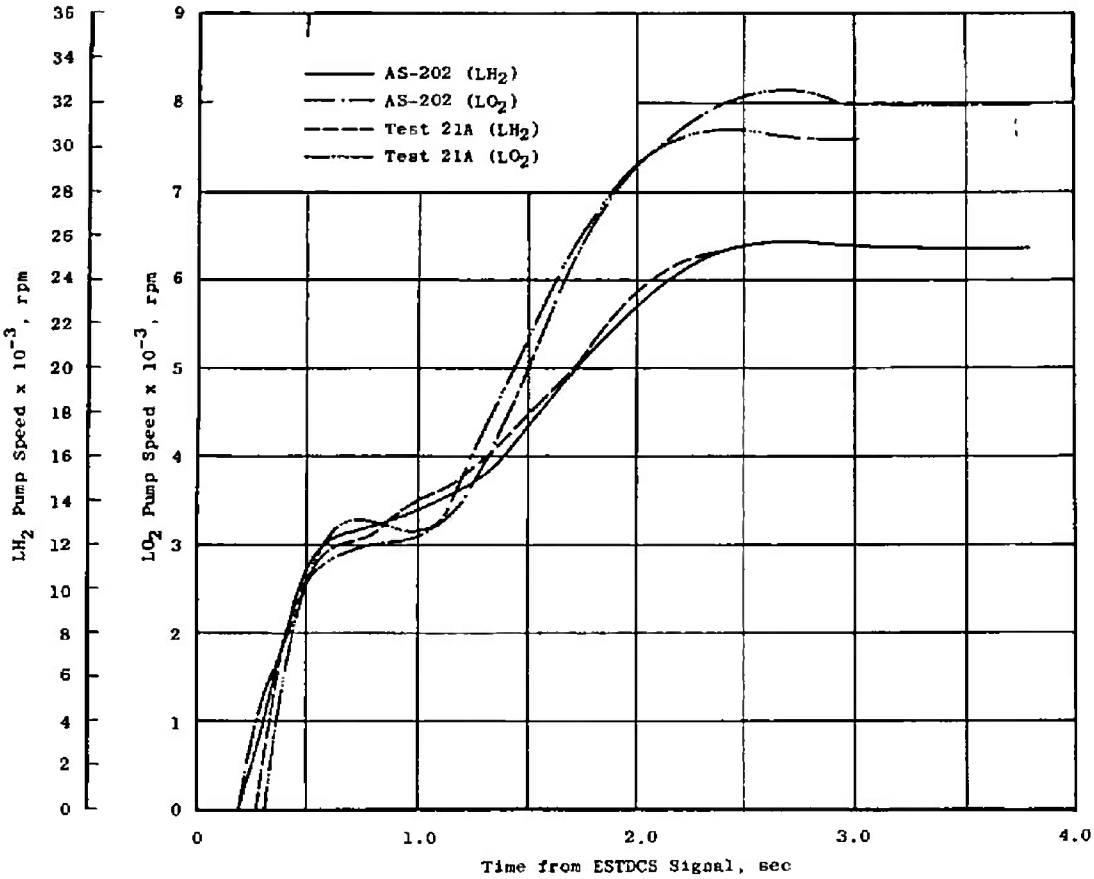

c. Pump Speed Transients

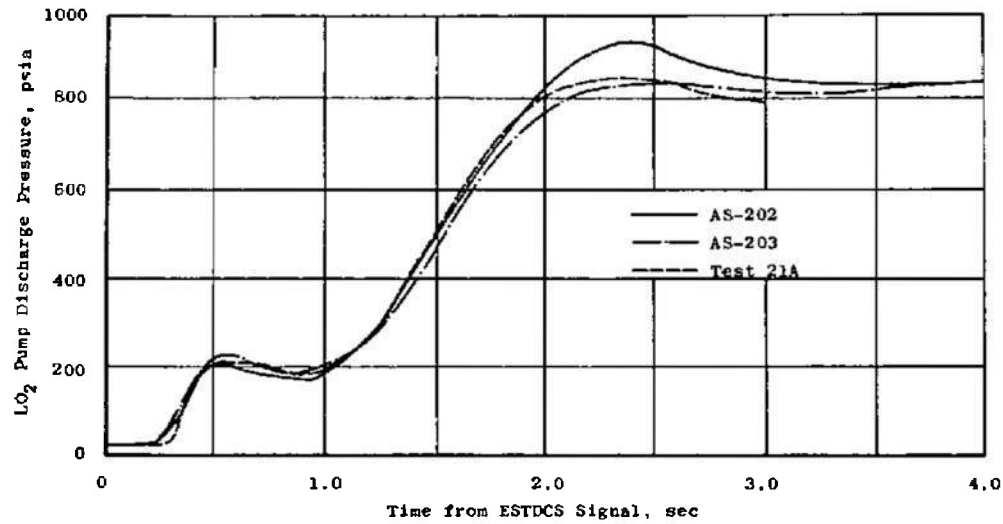

d. Oxidizer Pump Discharge Pressure Transients

Fig. 44 Continued

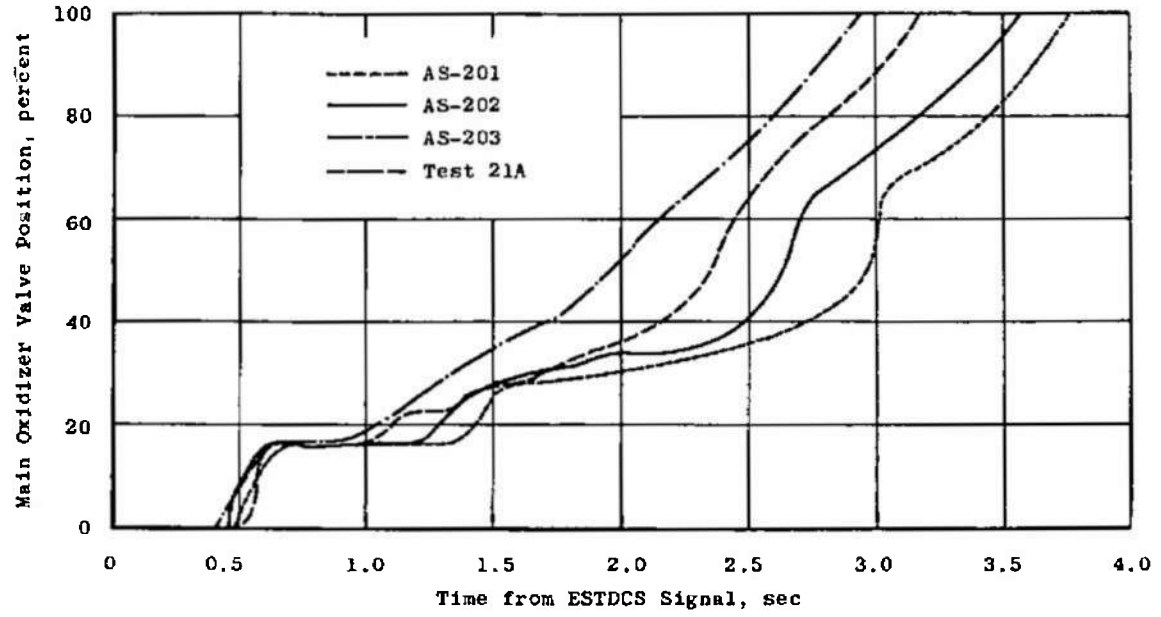

e. Main Oxidizer Valve Position Traces

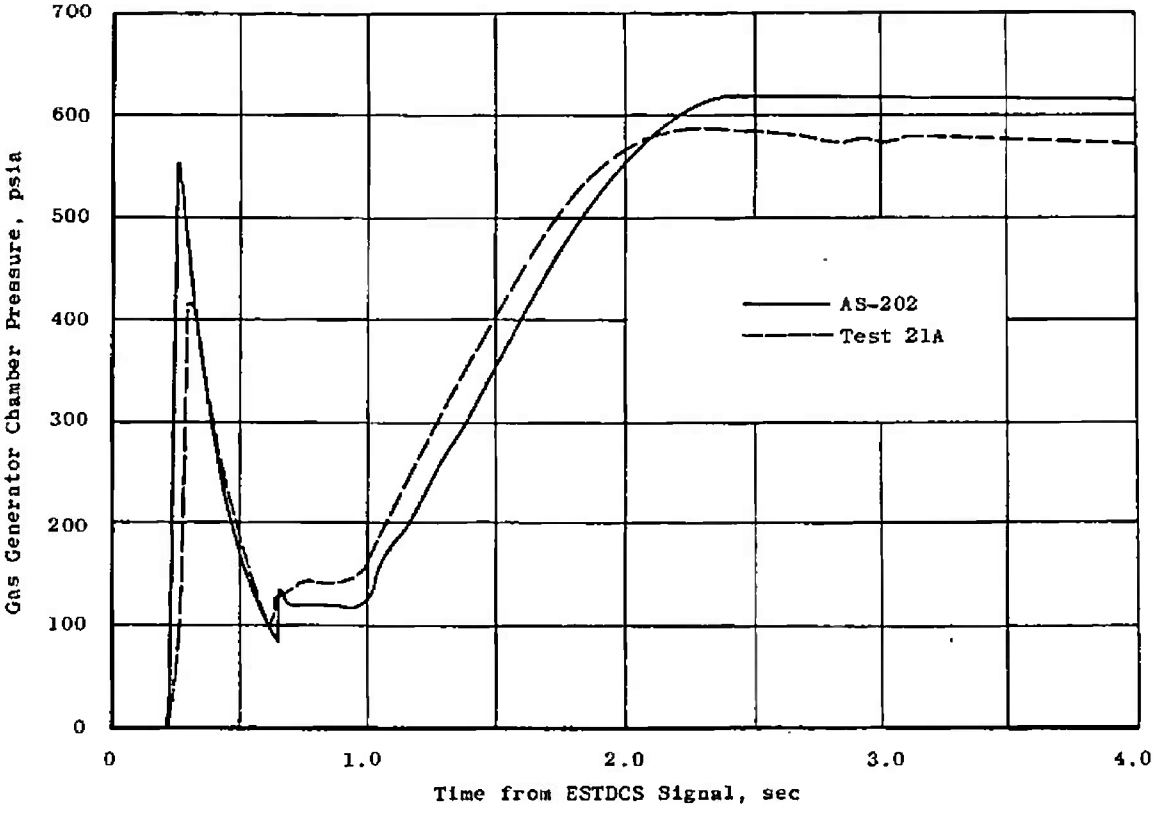

f. Gas Generator Chamber Pressure Transients

Fig. 44 Concluded

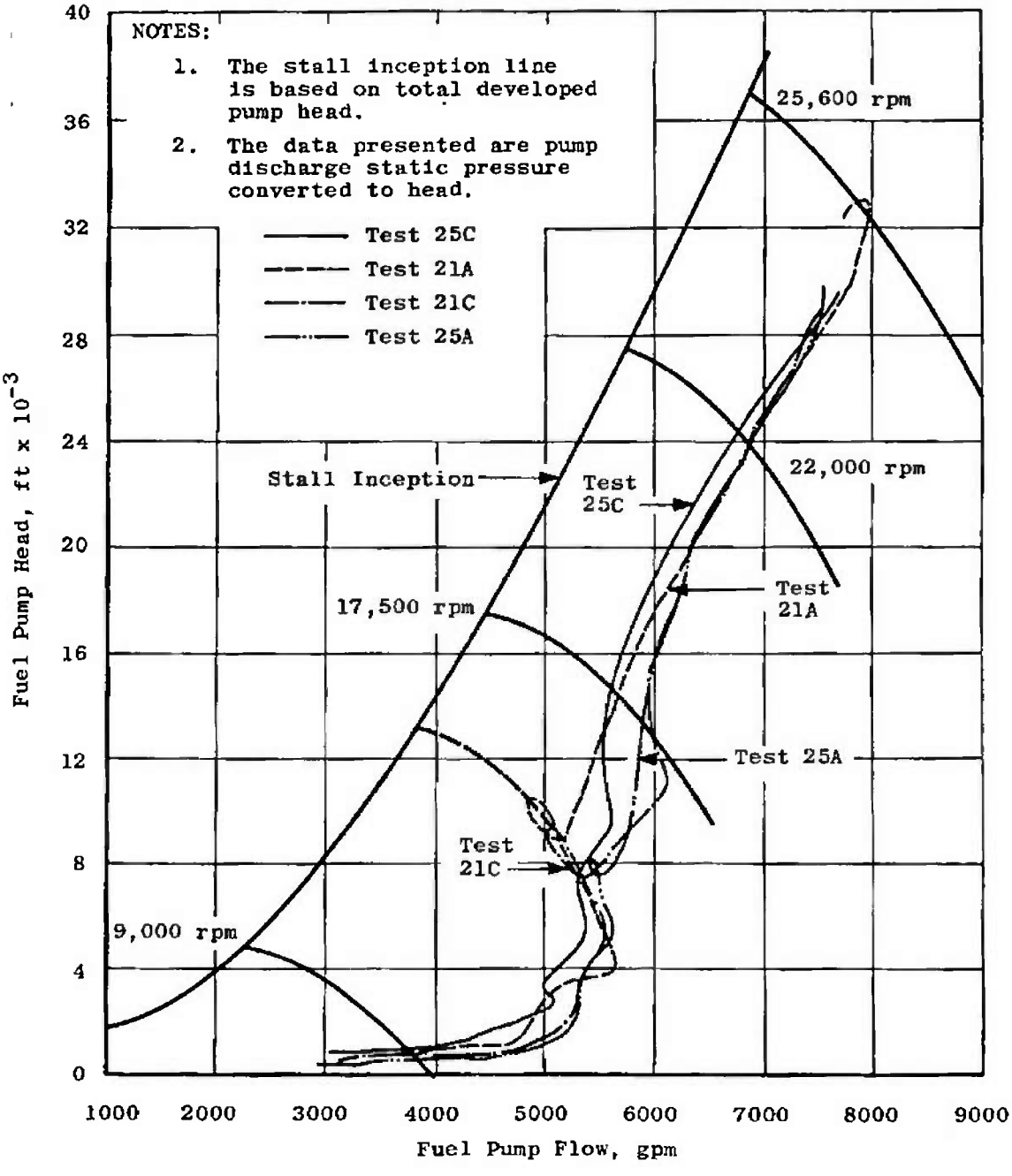

Fig. 45 Fuel Pump Start Transient Performance—Tests 21A, 21C, 25A, and 25C

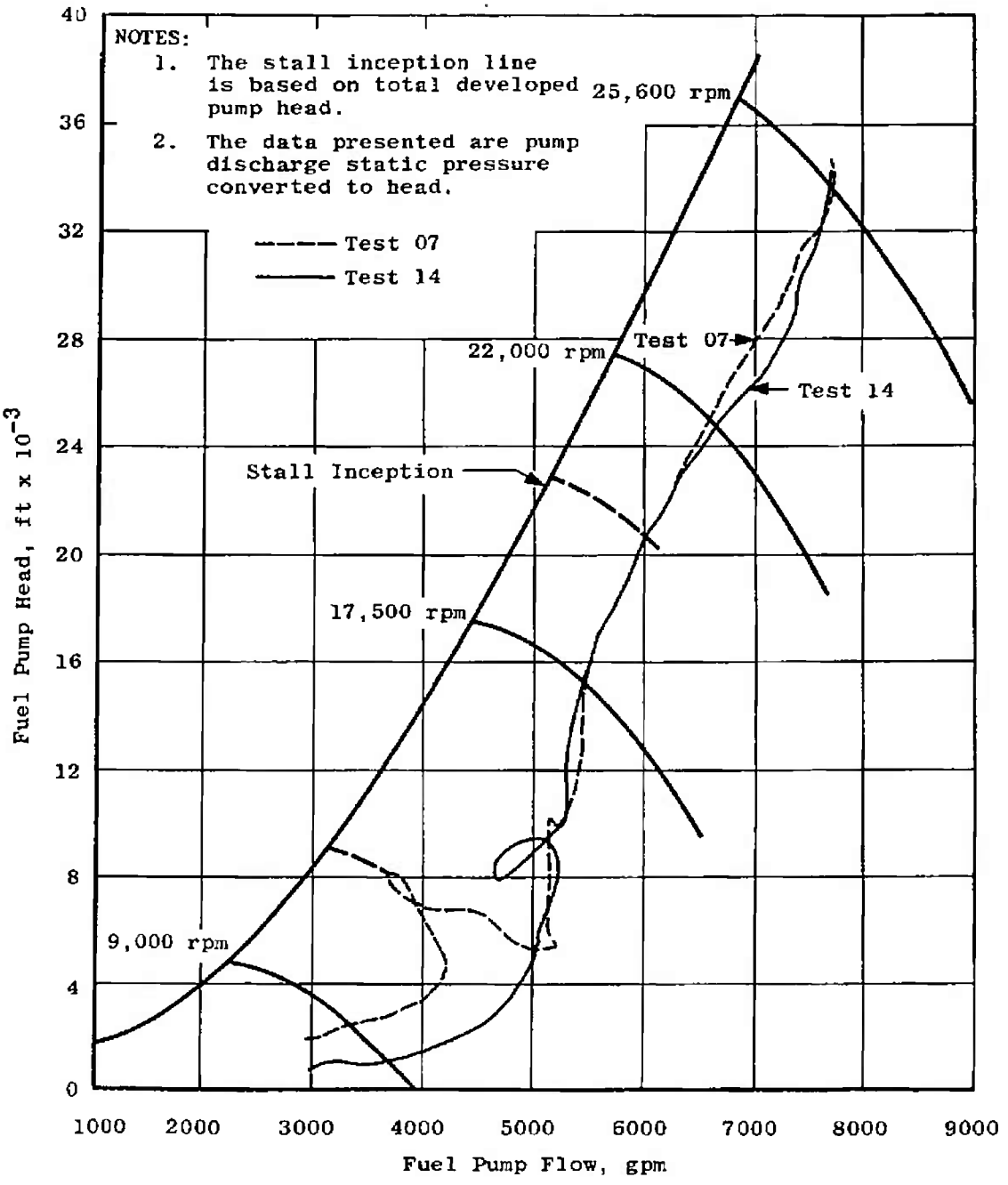

Fig. 46 Fuel Pump Start Transient Performance – Tests 07 and 14

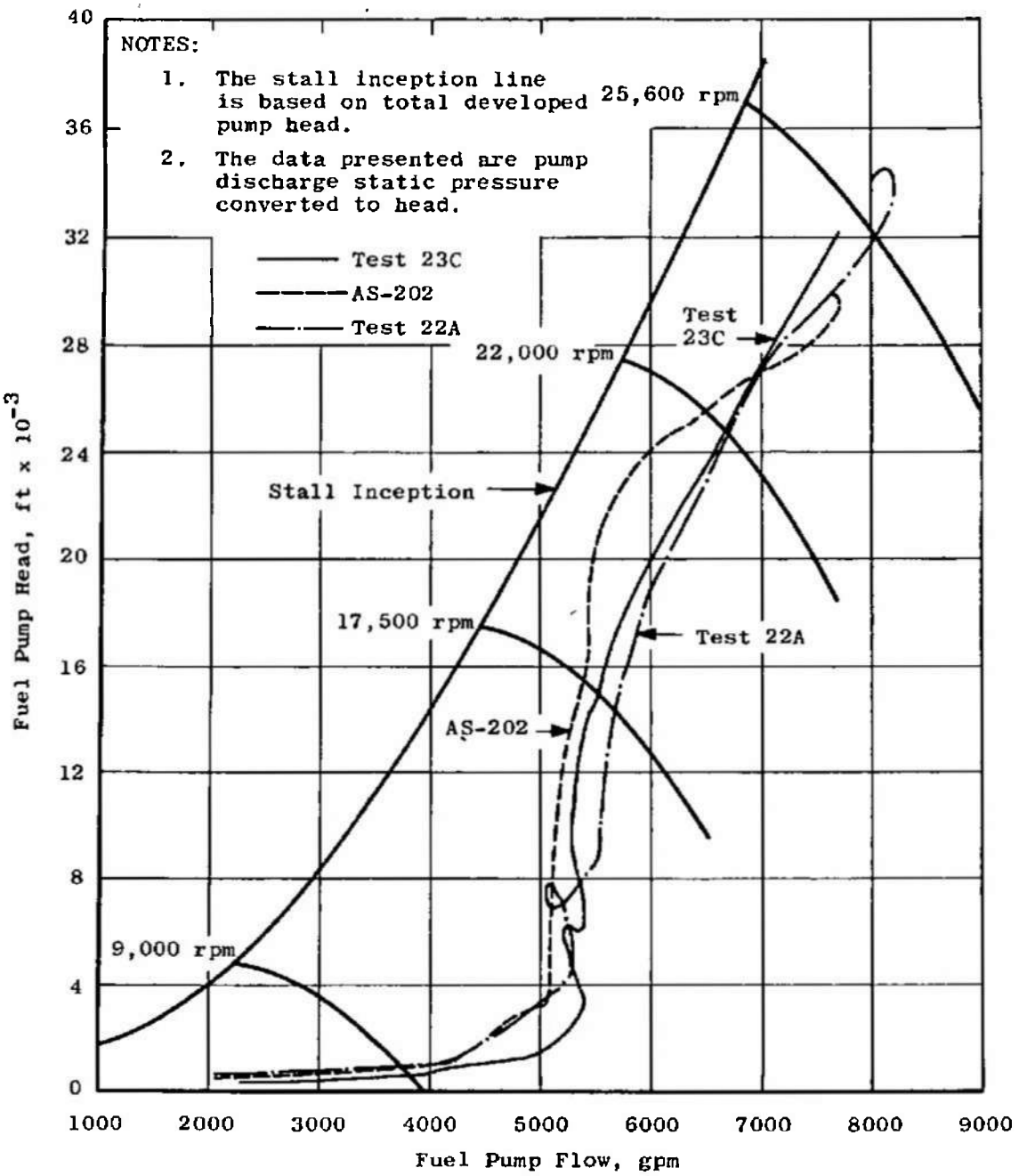

Fig. 47 Fuel Pump Start Transient Performance – Tests 22A, 23C, and AS-202

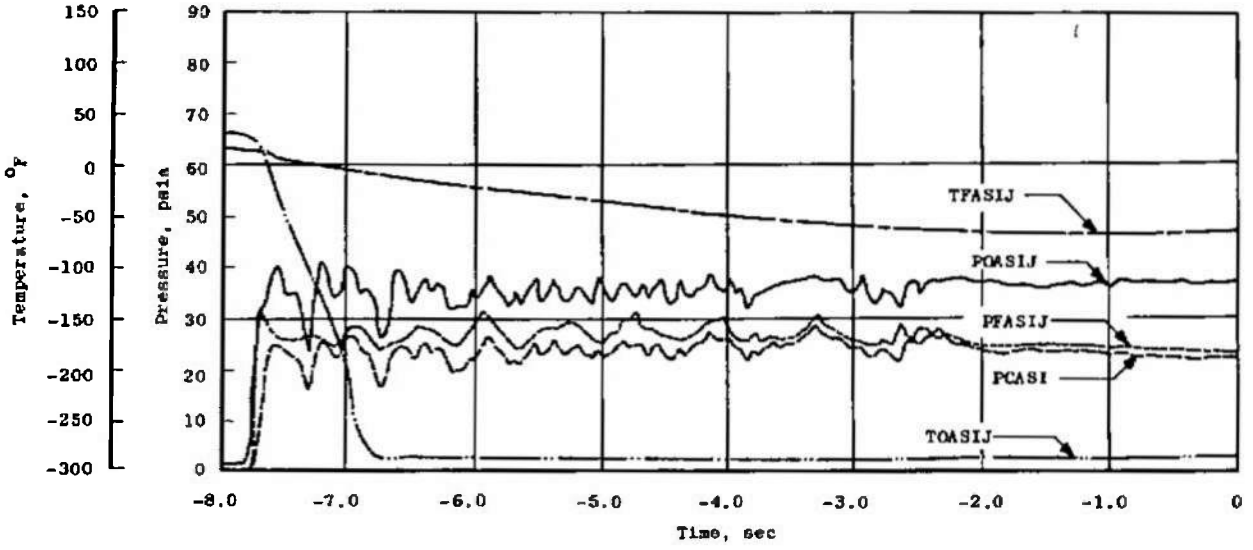

a. ASI Fuel and Oxidizer Conditions–Test 23E

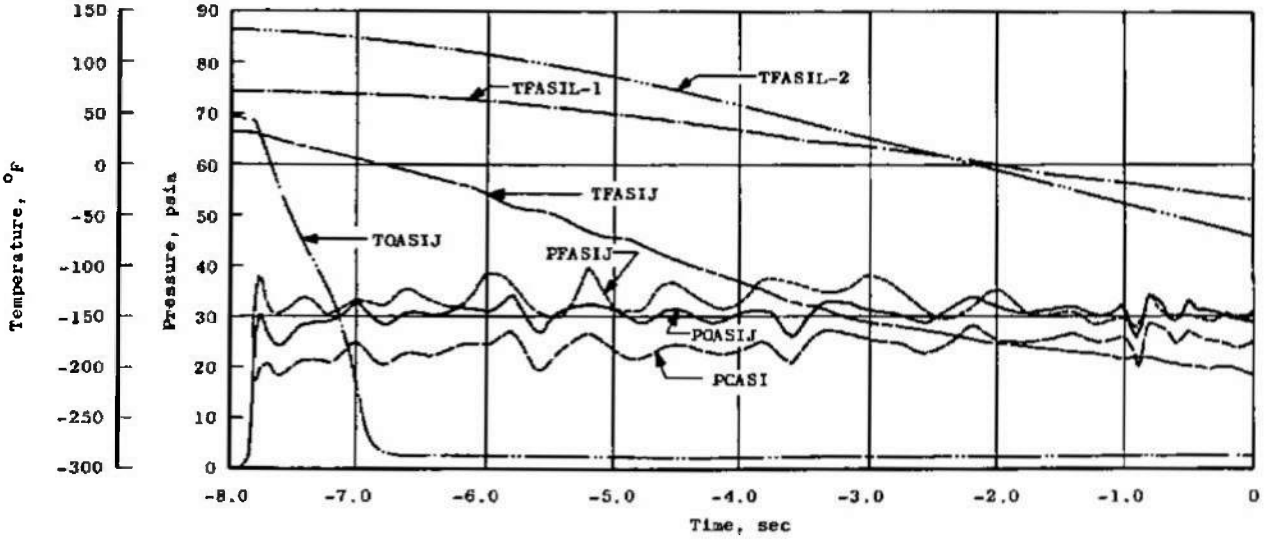

b. ASI Fuel and Oxidizer Conditions–Test 24A

Fig. 48 Augmented Spark Igniter Chamber Conditions – Tests 23E and 24A

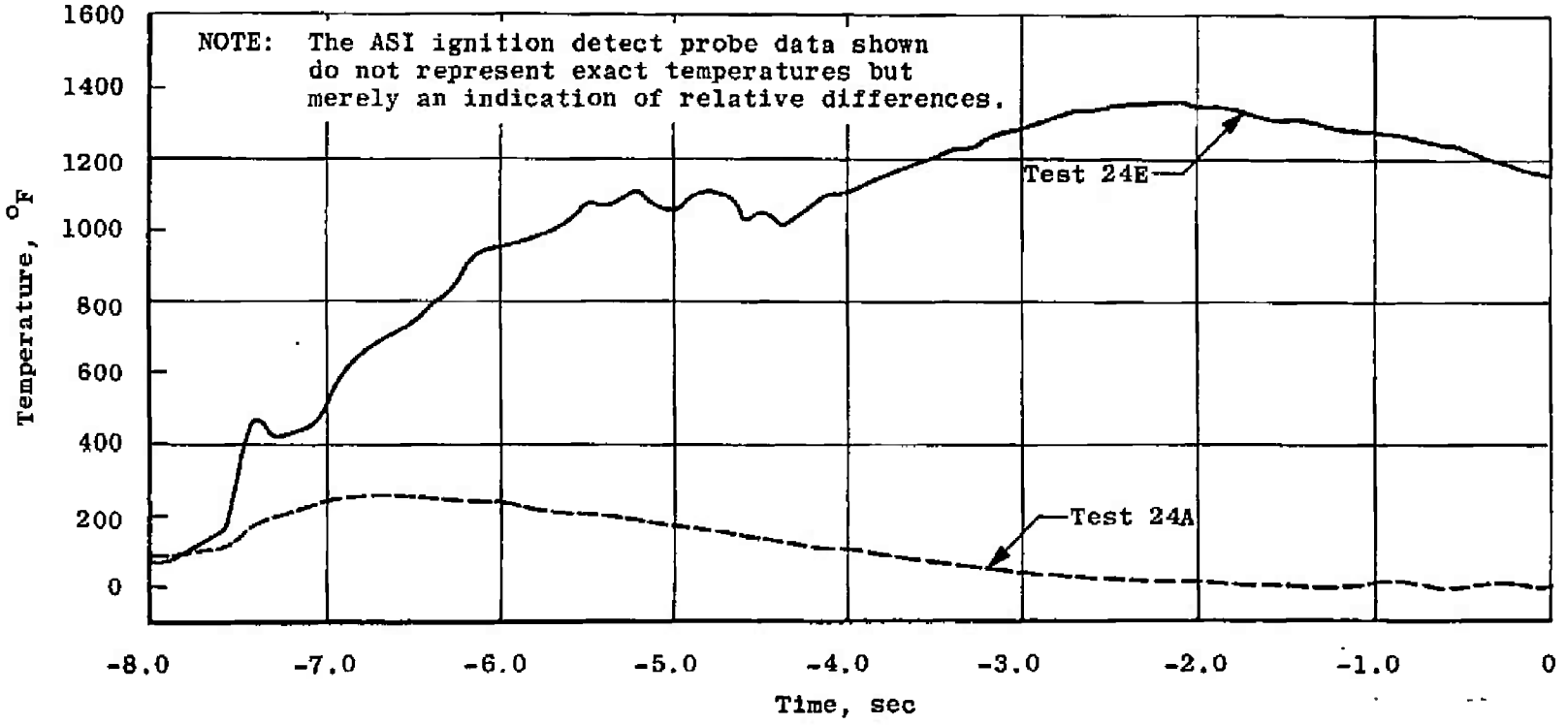

Fig. 49 Augmented Spark Igniter Chamber Temperature – Tests 23E and 24A

TABLE I
MAJOR J-2 ENGINE S/N J-2052 COMPONENTS (EFFECTIVE TEST J4-1554-20)

Part Name	P/N	S/N
Thrust Chamber Body	206600-31	4076553
Thrust Chamber Injector Assembly	208021-11	4084917
Fuel Turbopump Assembly	459000-121	4078258
Oxidizer Turbopump Assembly	458175-71	6623549
Start Tank	303439	0064
Augmented Spark Igniter	206280-21	3661349
GG Fuel Injector and Combustor	308360-11	2008734
Pneumatic Control Assembly	556947	4079720
Electrical Control Package	502670	4078604
Primary Flight Instr. Package	703685	4078716
Auxiliary Flight Instr. Package	703680	4078718
Main Fuel Valve	409920	4078041
Main Oxidizer Valve	410431	4087228
GG Control Valve	309040	4055754
Start Tank Discharge Valve	306875	4079062
Oxidizer Turbine Bypass Valve	409930	4081832
Prop. Utilization Valve	251351-11	4068944
Mainstage Control Valve	558069	8313568
Ignition Phase Control Valve	558069	8313422
Helium Control Valve	106012000	342270
Start Tank Vent and Relief Valve	557828-X2	4046446
Helium Tank Vent Valve	106012000	342277
Fuel Bleed Valve	309034	4077749
Oxidizer Bleed Valve	309029	4077746
ASI Oxidizer Valve	308880	4077205
P/A Purge Control Valve	557823	4068834
Start Tank Fill/Refill Valve	558000	4079001
Fuel Flowmeter	251225	4077752
Oxidizer Flowmeter	251216	4074114
Fuel Injector Temp. Transducer	NA5-27441	12775
Restartable Ignition Detect Probe	NA5-27298T1	201

TABLE II
LIST OF ENGINE MODIFICATIONS PERFORMED

Rocketdyne Field Directive Number	RFD Date	Description of the Change	Test Effectivity
AEDC 12-67	Feb. 7, 1967	Wiring Harness Assembly Repair	20
AEDC 13-67	Feb. 8, 1967	Replacement of Oxidizer Dome Assembly	20
AEDC 14-67	Feb. 9, 1967	Replacement of ASI Oxidizer Orifice	20
AEDC 15-67	Feb. 10, 1967	Addition of ASI Oxidizer Line Purge	20
AEDC 16-67	Feb. 10, 1967	Addition of Hot Gas Duct Chill System	20
AEDC 17-67	Feb. 10, 1967	Retiming of Main Oxidizer Valve	20
AEDC 18-67	Feb. 10, 1967	Replacement of Thrust Chamber Heater Blanket	20
AEDC 19-67	Feb. 13, 1967	Inspection of Helium Control Bottle Weld	20
AEDC 20-67	Feb. 22, 1967	Additional Requirements for ASI Instrumentation	21
AEDC 21-67	Feb. 22, 1967	Reorificing of Engine System	22
AEDC 22-67	Feb. 28, 1967	Insulation of Electrical Control Assembly	22
AEDC 23-67	March 10, 1967	Installation of ASI Fuel Line Heater	24
AEDC 24-67	March 10, 1967	Increase Timer Setting of Vibration Safety Cutoff System	24
AEDC 25-67	March 11, 1967	Addition of Oxidizer GG Bootstrap Line Thermocouple	24
AEDC 26-67	March 11, 1967	Addition of Oxidizer Turbine Inlet Thermocouple	24 and 25
AEDC 27-67	March 13, 1967	Insulation of Primary Flight Instrumentation Package	24
AEDC 28-67	March 13, 1967	Replacement of Flight Instrumentation Console Circuit Board	24
AEDC 29-67	March 11, 1967	Change of Main Oxidizer Valve Opening Time	25
AEDC 30-67	March 20, 1967	Addition of Fuel and Oxidizer Turbine Shroud Thermocouples	25
AEDC 31-67	March 27, 1967	Addition of Oxidizer Pump Discharge Line Thermocouple	26
AEDC 32-67	March 27, 1967	Installation of GG Oxidizer Bootstrap Line Conditioning System	26

TABLE III
LIST OF ENGINE SYSTEM COMPONENT REPLACEMENTS

Rocketdyne Report Number	UCR Date	Item Replaced	Test Effectivity
UCR-004123	Feb. 20, 1967	Restart Probe	21
UCR-004128	Feb. 20, 1967	Ignition Phase Control Valve	21
UCR-004131	Feb. 23, 1967	#2 Mainstage O.K. Pr. Switch	21
UCR-004130	Feb. 25, 1967	GG Purge Check Valve	21
UCR-007901	March 6, 1967	ASI Ignition Detector Temperature Probe	22
UCR-004195	March 5, 1967	Main Fuel Valve	22
UCR-007902	March 8, 1967	Fuel Injection Temperature Transducer Probe	23
UCR-007903	March 13, 1967	ASI Ignition Detector Temperature Probe	24
UCR-007904	March 16, 1967	ASI Ignition Detector Temperature Probe	25
UCR-007907	March 16, 1967	Oxidizer Turbine Bypass Valve	25
UCR-007908	March 27, 1967	Transducer, Oxidizer Pump Bearing Coolant Pressure	26
UCR-007909	March 27, 1967	Transducer, GG Fuel Injection Pressure	26
UCR-007910	March 27, 1967	Transducer, Fuel Pump Interstage Pressure	26
UCR-007911	March 27, 1967	Transducer, Fuel Pump Discharge Pressure	26
UCR-007912	March 27, 1967	Transducer, Thrust Chamber Pressure	26
UCR-007914	April 3, 1967	Pressure Actuated Purge Control Valve	26

UCR - Unsatisfactory Condition Report

TABLE IV
INSTRUMENTATION SUMMARY

AEDC Code	Parameter	Tap No.	Range	Micro-radio	Magnetic Tape	Oscillo-graph	Strip Chart	X-Y Plotter
	Current		Amp					
ICC	Control		0 to 30	x		x		
IIC	Ignition		0 to 30	x		x		
	Event							
EECL	Engine Cutoff Lockin		on/off	x		DF/x		
EECO	Engine Cutoff Signal		on/off	x	x	x		
EES	Engine Start Command		on/off	x		x		
EFJT	Fuel Injector Temperature OK		on/off	x		x		
EFPV C/O	Fuel Prevalve Closed/Open Limit		closed/open	x		DF		
EHCS	Helium Control Solenoid		on/off	x		DF/x		
EID	Ignition Detected		on/off	x		DF/x		
EIPCS	Ignition Phase Control Solenoid		on/off	x		x		
EMCS	Mainstage Control Solenoid		on/off	x		x		
EOPVC	Oxidizer Prevalve Closed Limit		closed	x		x		
EOPVO	Oxidizer Prevalve Open Limit		open	x		x		
ESTDCS	Start Tank Discharge Control Solenoid		on/off	x	x	DF/x		
	Flows		gpm					
QF-1A	Fuel	PFF	9000	x		DF/x		
QF-2	Fuel	PFFA	9000	x	x	x		
QF-2SD	Stall Approach Monitor Fuel		9000	x		DF		
QFRP	Fuel Recirculation		150	x				
QO-1A	Oxidizer	POF	3000	x		DF/x		

TABLE IV (Continued)

AEDC Code	Parameter	Tap No.	Range	Micro-radic	Magnetic Tape	Oscillo-graph	Strip Chart	X-Y Plotter
QO-2	Oxidizer	POFA	3000	x	x	x		
QORP	Oxidizer Recirculation		50	x			x	
	Forces		lbf					
FSP-1	Side Load (Pitch)		±20,000	x		x	x	
FSP-3	Side Load (Pitch)		±20,000	x				
FSY-1	Side Load (Yaw)		±20,000	x		x	x	
FSY-3	Side Load (Yaw)		±20,000	x				
	Position		% Open					
LFVT	Main Fuel Valve		0 to 100	x		DF x		
LGGVT	Gas Generator Valve		0 to 100	x		DF x		
LOTBVT	Oxidizer Turbine Bypass Valve		0 to 100	x		DF x		
LOVT	Main Oxidizer Valve		0 to 100	x		DF x		
LPUTOP	Propellant Utilization Valve		0 to 100	x		x	x	
LSTDVT	Start Tank Discharge Valve		0 to 100	x		DF x		
	Pressure		psia					
PA1	Test Cell		0.5	x		x		
PA2	Test Cell		1.0	x	x			
PA3	Test Cell		5.0	x			x	
PC-1P	Thrust Chamber	CG1	1000	x			x	
PC-2	Thrust Chamber	CG1	1000		x	x		
PC-3	Thrust Chamber	CG1A	1000	x		DF x		

TABLE IV (Continued)

AEDC Code	Parameter	Tap No.	Range	Micro-sadic	Magnetic Tape	Oscillo-graph	Strip Chart	X-Y Plotter
PCASI-2	Augmented Spark Igniter Chamber	IG1	1000	x				
PCGG-1P	Gas Generator Chamber	GG1	1000	x	x	x		
PCGG-2	Gas Generator Chamber	GG1A	1000	x				
PFASIJ	Augmented Spark Igniter Fuel Injection		1000	x				
PFJ-1A	Main Fuel Injection	CF2	1000	x		x		
PFJ-2	Main Fuel Injection	CF2A	1000	x	x			
PFJGG-1A	Gas Generator Fuel Injection	GF4	1000	x	x			
PFJGG-2	Gas Generator Fuel Injection	GF4	1000	x		DF/x		
PFMI	Fuel Jacket Inlet Manifold	CF1	2000	x				
PFPD-1P	Fuel Pump Discharge	PF3	1500	x				
PFPD-2	Fuel Pump Discharge	PF2	1500	x	x	x		
PFPI-1	Fuel Pump Inlet		100	x				x
PFPI-2	Fuel Pump Inlet		200	x				x
PFPI-3	Fuel Pump Inlet		200		x	DF/x		
PFRPO	Fuel Recirculation Pump Outlet		60	x				
PFRPR	Fuel Recirculation Pump Return		50	x				
PFST-1P	Fuel Start Tank	TF1	1500	x		x		
PFST-2	Fuel Start Tank	TF1	1500	x				x
PFTO	Fuel Turbine Outlet	TG2	200	x				
PFUT	Fuel Tank Ullage		100	x				
PHET-1P	Helium Tank	NN1	3500	x		x		
PHET-2	Helium Tank	NN1	3500	x				x
PHRO-1A	Helium Regulator Outlet	NN2	750	x				
PHRO-2	Helium Regulator Outlet	NN2	750	x				

TABLE IV (Continued)

AEDC Code	Parameter	Tap No.	Range	Micro-sadic	Magnetic Tape	Oscillo-graph	Strip Chart	X-Y Plotter
POASIJ	Augmented Spark Igniter Oxidizer Injection		1000	x				
POBSC	Oxidizer Bootstrap Conditioning		50	x				
POBV	Gas Generator Oxidizer Bleed Valve	GO2	2000	x				
POIJ-1A	Main Oxidizer Injection	CO3	1000	x				
POIJ-2	Main Oxidizer Injection	CO3A	1000	x	x	x		
POIJGG-1A	Gas Generator Oxidizer Injection	GO5	1000	x	x	x		
POIJGG-2	Gas Generator Oxidizer Injection	GO5	1000	x				
POPD-1P	Oxidizer Pump Discharge	PO3	1500	x				
POPD-2	Oxidizer Pump Discharge	PO2	1500	x	x	x		
POPI-1	Oxidizer Pump Inlet		100	x				x
POPI-2	Oxidizer Pump Inlet		200	x				x
POPI-3	Oxidizer Pump Inlet		200			DF / x		
PORPO	Oxidizer Recirculation Pump Outlet		115	x				
PORPR	Oxidizer Recirculation Pump Return		100	x				
POTI-1A	Oxidizer Turbine Inlet	TG3	200	x				
POTO-1A	Oxidizer Turbine Outlet	TG4	100	x				
POTO-2	Oxidizer Turbine Outlet	TG4	100	x				
POUT	Oxidizer Tank Ullage		100	x				
POVCC	Main Oxidizer Valve Closing Control		500	x				
PTCFJP	Thrust Chamber Fuel Jacket Purge		100	x				
	Spark Rates							
RASIS-1	Augmented Spark Igniter No. 1					DF / x		
RASIS-2	Augmented Spark Igniter Spark No. 2					DF / x		

TABLE IV (Continued)

AEDC Code	Parameter	Tap No.	Range	Micro-radic	Magnetic Tape	Oscillo-graph	Strip Chart	X-Y Plotter
RGGS-1	Gas Generator Spark No. 1					DF x		
RGGS-2	Gas Generator Spark No 2					DF x		
	Speeds		rpm					
NFP-1P	Fuel Pump	PFV	30,000	x	x	x		
NFRP	Fuel Recirculation Pump		15,000	x				
NOP-1P	Oxidizer Pump	POV	12,000	x	x	x		
NORP	Oxidizer Recirculation Pump		15,000	x				
	Temperatures		°F					
TA1	Test Cell (North)		-50 to +800	x				
TA2	Test Cell (East)		-50 to +800	x				
TA3	Test Cell (South)		-50 to +800	x				
TA4	Test Cell (West)		-50 to +800	x				
TAIP-1A	Auxiliary Instrument Package		-300 to +200	x				
TBHR-1	Helium Regulator Body (north side)		-100 to + 50	x			x	
TBHR-2	Helium Regulator Body (south Side)		-100 to + 50	x			x	
TECP-1P	Electrical Controls Package	NST1A	-300 to +200	x			x	
TECP-2	Electrical Controls Package	NST1B	-300 to +200	x				
TFASIJ	Augmented Spark Igniter Fuel Injection	IFT1	-425 to +100	x		x		
TFASIL-1	Augmented Spark Igniter Fuel Line		-300 to +200	x			x	
TFASIL-2	Augmented Spark Igniter Fuel Line		-300 to +200	x			x	

TABLE IV (Continued)

AEDC Code	Parameter	Tap No.	Range	Micro-sadic	Magnetic Tape	Oscillo-graph	Strip Chart	X-Y Plotter
TFBV-1A	Fuel Bleed Valve	GFT1	-425 to -375	x				
TFJ-1P	Main Fuel Injection	CFT2	-425 to -100	x	x	x		
TFPD-1P	Fuel Pump Discharge	PFT1	-425 to -400	x	x	x		
TFPD-2	Fuel Pump Discharge	PFT1	-425 to -400	x				
TFPDD	Fuel Pump Discharge Duct		-320 to +300	x				
TFPI-1	Fuel Pump Inlet		-425 to -400	x				x
TFPI-2	Fuel Pump Inlet		-425 to -400	x				x
TFRPO	Fuel Recirculation Pump Outlet		-425 to -410	x				
TFRPR	Fuel Recirculation Pump Return Line		-425 to -250	x				
TFRT-1	Fuel Tank		-425 to -410	x				
TFRT-2	Fuel Tank		-425 to -410	x				
TFST-1P	Fuel Start Tank	TFT1	-350 to +100	x				
TFST-2	Fuel Start Tank	TFT1	-350 to +100					x
TFTD-1	Fuel Turbine Discharge Duct		-200 to +800	x				
TFTD-2	Fuel Turbine Discharge Duct		-200 to +800	x				
TFTD-3	Fuel Turbine Discharge Duct		-200 to +1000	x			x	
TFTD-4	Fuel Turbine Discharge Duct		-200 to +1000	x			x	
TFTD-5	Fuel Turbine Discharge Duct		-200 to +800	x				
TFTD-6	Fuel Turbine Discharge Duct		-200 to +800	x				
TFTD-7	Fuel Turbine Discharge Duct		-200 to +800	x				
TFTD-8	Fuel Turbine Discharge Duct		-200 to +800	x				
TFTI-1P	Fuel Turbine Inlet	TFT1	0 to 1800	x			x	
TFTO	Fuel Turbine Outlet	TFT2	0 to 1800	x				
TGGO-1A	Gas Generator Outlet	GGT1	0 to 2000	x	x	DF / x		

TABLE IV (Continued)

AEDC Code	Parameter	Tap No.	Range	Micro-sadic	Magnetic Tape	Oscillo-graph	Strip Chart	X-Y Plotter
THET-1P	Helium Tank	NNT1	-350 to +100	x				x
TOASIJ	Augmented Spark Igniter Oxidizer Injection	ICT1	-300 to +100	x		x		
TOBS-1	Oxidizer Bootstrap Line		-300 to +250	x				
TOBS-2	Oxidizer Bootstrap Line		-300 to +250	x				
TOBSCI	Oxidizer Bootstrap Conditioning Inlet		0 to 100	x				
TOBSCO	Oxidizer Bootstrap Conditioning Outlet		0 to 100	x				
TOBV-1A	Oxidizer Bleed Valve	GOT2	-300 to -250	x				
TOBV-2	Oxidizer Bleed Valve	GOT2	-300 to -250	x				
TOPD-1P	Oxidizer Pump Discharge	POT3	-300 to -250	x	x	x	x	
TOPD-2	Oxidizer Pump Discharge	POT3	-300 to -250	x				
TOPDS	Oxidizer Pump Discharge Skin		-300 to -100	x				
TOPI-1	Oxidizer Pump Inlet		-310 to -270	x				x
TOPI-2	Oxidizer Pump Inlet		-310 to -270	x				x
TORPO	Oxidizer Recirculation Pump Outlet		-300 to -250	x				
TORPR	Oxidizer Recirculation Pump Return		-300 to -140	x				
TORT-1	Oxidizer Tank		-300 to -287	x			x	
TORT-3	Oxidizer Tank		-300 to -287	x				
TOTI-1P	Oxidizer Turbine Inlet	TGT3	0 to 1200	x			x	
TOTO-1P	Oxidizer Turbine Outlet	TGT4	0 to 1000	x				
TPIP-1P	Primary Instrument Package		-350 to +500	x				
TSC-1E	Thrust Chamber Skin		-350 to +500	x				
TSC-2E	Thrust Chamber Skin		-350 to +500	x				
TSC-3E	Thrust Chamber Skin		-350 to +500	x				
TSC-4E	Thrust Chamber Skin		-350 to +500	x				

TABLE IV (Continued)

AEDC Code	Parameter	Tap No.	Range	Micro-sadic	Magnetic Tape	Oscillo-graph	Strip Chart	X-Y Plotter
TSC-5E	Thrust Chamber Skin		-350 to +500	x				
TSC-6E	Thrust Chamber Skin		-350 to +500	x				
TSC-7E	Thrust Chamber Skin		-350 to +500	x			x	
TSC-8E	Thrust Chamber Skin		-350 to +500	x				
TSC-1T	Thrust Chamber Skin		-350 to +500	x				
TSC-3T	Thrust Chamber Skin		-350 to +500	x				
TSC-4T	Thrust Chamber Skin		-350 to +500	x				
TSC-5T	Thrust Chamber Skin		-350 to +500	x				
TSC-6T	Thrust Chamber Skin		-350 to +500	x				
TSC-8T	Thrust Chamber Skin		-350 to +500	x				
TSC9-1	Thrust Chamber Skin		-350 to +500	x				
TSC9-2	Thrust Chamber Skin		-350 to +500	x				
TSC9-3	Thrust Chamber Skin		-350 to +500	x				
TSC10-1	Thrust Chamber Skin		-350 to +500	x				
TSC10-2	Thrust Chamber Skin		-350 to +500	x				
TSC10-3	Thrust Chamber Skin		-350 to +500	x				
TSC11-1	Thrust Chamber Skin		-350 to +500	x				
TSC11-2	Thrust Chamber Skin		-350 to +500	x				
TSC11-3	Thrust Chamber Skin		-350 to +500	x				
TSC12-1	Thrust Chamber Skin		-350 to +500	x				
TSC12-2	Thrust Chamber Skin		-350 to +500	x				
TSC12-3	Thrust Chamber Skin		-350 to +500	x				
TSC13-1	Thrust Chamber Skin		-350 to +500	x				
TSC13-2	Thrust Chamber Skin		-350 to +500	x				

TABLE IV (Concluded)

AEDC Code	Parameter	Tap No.	Range	Micro-sadic	Magnetic Tape	Oscillo-graph	Strip Chart	X-Y Plotter
TSC13-3	Thrust Chamber Skin		-350 to +500	x				
TSC14-1	Thrust Chamber Skin		-350 to +500	x				
TSC14-2	Thrust Chamber Skin		-350 to +500	x				
TSC14-3	Thrust Chamber Skin		-350 to +500	x				
TSC-15	Thrust Chamber Skin		-400 to +600	x				
TSC-16	Thrust Chamber Skin		-400 to +600	x				
TSC-17	Thrust Chamber Skin		-400 to +600	x				
TSC-18	Thrust Chamber Skin		-400 to +600	x				
TSOVAL-1	Oxidizer Valve Closing Control Line		-200 to +100	x			x	
TSOVAL-2	Oxidizer Valve Closing Control Line		-200 to +100	x				
TTC-1P	Thrust Chamber Jacket (Control)	CS1	-425 to +100	x			x	
TTC-2	Thrust Chamber Jacket	CS1A	-425 to +100	x				
	Vibrations		G's					
UFPR	Fuel Pump Radial 90°		±200		x			
UOPR	Oxidizer Pump Radial 90°		±200	x				
UTCD-1	Thrust Chamber Dome		±500		x	x		
UTCD-2	Thrust Chamber Dome		±500		x	x		
UTCD-3	Thrust Chamber Dome		±500		x	x		
U1VSC	No. 1 Vibration Safety Counts		on/off			DF x		
U2VSC	No. 2 Vibration Safety Counts		on/off			x		
	Voltage		Volts					
VCB	Control Bus		0 to 36	x		x		
VIB	Ignition Bus		0 to 36	x		x		

TABLE V
ENGINE SEQUENCE

Test Number	Start																
	Main Fuel Valve Open		Start Tank Discharge Valve Open		Start Tank Discharge Valve Closed		Main Oxidizer Valve, First Stage Open		Main Oxidizer Valve, Second Stage Open		Gas Generator Fuel Poppet Open		Gas Generator Oxidizer Poppet Open		Oxidizer Turbine ③ Bypass Valve Closed		① Ignition Phase Timer
	Valve ① Delay Time, msec	Valve Opening Time, msec	Valve ② Delay Time, msec	Valve Opening Time, msec	Valve ③ Delay Time, msec	Valve ③ Closing Time, msec	Valve ③ Delay Time, msec	Valve Opening Time, msec	Valve ③ Delay Time, msec	Valve Opening Time, msec	Valve ③ Delay Time, msec	Valve Opening Time, msec	Valve ③ Delay Time, msec	Valve Opening Time, msec	Valve Delay Time, 80%, msec	Valve Delay Time, Fully Closed, msec	
20	59	64	153	141	98	260	57	56	749	*	106	27	178	70	431	483	435
21A	60	70	152	136	102	268	55	53	548	2060	106	30	185	75	455	508	441
21B	58	45	160	158	99	283	50	51	820	1768	107	30	188	76	422	480	444
21C	57	60	161	151	95	259	51	55	837	1847	110	25	183	71	446	508	441
22A	51	62	146	131	93	252	52	57	713	1968	105	28	175	68	423	471	443
22B	53	59	—	—	—	—	—	—	—	—	—	—	—	—	—	—	—
23A	53	70	149	135	96	258	54	60	600	2200	111	25	182	70	445	501	442
23C	51	60	153	133	100	257	49	53	700	1820	100	30	178	67	446	500	441
23D	52	62	163	152	97	257	50	54	804	1765	110	30	185	84	411	503	442
23E	51	55	160	150	107	253	47	51	710	1830	101	31	178	70	427	513	440
24A	49	62	153	138	100	262	49	50	710	1814	96	29	170	70	427	480	442
24B	51	57	164	156	98	259	46	49	842	1712	100	31	182	77	414	507	442
24C	55	68	152	141	98	261	55	52	585	2024	112	28	180	73	451	501	440
24D	54	60	164	154	95	261	49	53	762	1829	107	26	186	76	421	552	442
25A	52	67	152	148	80	247	48	51	687	1930	102	30	174	67	427	487	441
25B	53	59	157	147	94	256	48	52	738	1885	105	25	181	80	427	480	441
25C	47	55	150	140	98	258	45	41	737	1861	95	29	171	77	436	488	442
25D	51	58	153	147	95	254	48	53	880	1780	105	30	185	86	423	469	441
26A	54	66	150	138	93	255	53	51	557	2128	105	27	181	71	443	493	445
26B	55	64	155	145	100	260	51	50	757	1810	117	28	180	75	435	480	440
26C	52	70	158	144	100	268	55	60	549	2107	110	30	185	72	448	507	445
26D	50	63	163	148	100	280	50	55	788	1770	105	27	185	75	435	485	441

① Measured from ignition phase control solenoid energized.

② Measured from start tank discharge control solenoid energized

③ Measured from mainstage control solenoid energized

Note - Engine sequence times shown are actual "Hot-Firing" data.

TABLE V (Concluded)

Test Number	Shutdown									
	Main Oxidizer Valve, Closed		Main Fuel Valve, Closed		Gas Generator Oxidizer Poppet, Closed		Gas Generator Fuel Poppet, Closed		Oxidizer Turbine Bypass Valve, Open	
	Valve④ Delay Time, msec	Valve Closing Time, msec	Valve④ Delay Time, msec	Valve Closing Time, msec	Valve④ Delay Time, msec	Valve Closing Time, msec	Valve④ Delay Time, msec	Valve Closing Time, msec	Valve Delay Time, msec	Valve④ Opening Time, msec
20	*	130	**	330	*	12	*	67		728
21A	84	203	131	347	33	13		67		955
21B	64	178	112	304	37	14		64		751
21C	92	198	125	329	32	15		65		870
22A	82	183	121	308	31	13		66		843
22B	—	—	106	303	—	—		—		—
23A	58	209	128	345	34	14		65		857
23C	81	164	112	287	32	12		60		861
23D	65	183	114	309	35	15		55		714
23E	79	164	112	296	34	12		64		906
24A	75	168	110	285	30	13		56		847
24B	66	165	106	293	35	14		55		803
24C	92	209	134	345	31	14		74		913
24D	65	187	113	322	35	15		66		853
25A	85	189	120	351	29	14		58		846
25B	67	175	113	320	34	14		60		783
25C	76	158	104	281	31	16		58		891
25D	62	178	110	309	36	14		60		810
26A	71	190	125	343	35	15		67		798
26B	65	168	111	300	35	15		67		800
26C	88	195	128	344	30	16		70		834
26D	65	185	111	320	40	15		65		770

④Measured from engine cutoff lockin (except Test 20)

*Mainstage control solenoid de-energized

**Ignition phase control solenoid de-energized

Note - Engine sequence times shown are actual "Hot-Firing data

TABLE VI
MAIN OXIDIZER VALVE DRY SEQUENCE TIMING

Test Number	Opening Time			
	First Stage		Second Stage	
	Delay, msec	Travel, msec	Delay, msec	Travel, msec
20	47 48	46 46	544 556	1650 1642
21	50 47	50 46	570 563	1642 1630
22	48 49	48 44	550 560	1672 1648
23	48 47	44 46	532 547	1655 1643
24	47 50	47 43	547 540	1647 1630
25	47 46	47 43	562 552	1710* 1693*
26	48 45	42 42	470 478	1700* 1670*

Second Stage Travel Desired: 1650 ± 40 msec

$*1700 \begin{smallmatrix} + & 0 \\ - & 25 \end{smallmatrix}$ msec

Notes:

1. The valve times appearing first for each test were obtained during the full facility verification sequence checks approximately 24 hr preceding the firing series.
2. The valve times appearing second for each test were obtained during the final engine verification sequence check on the day of firing.

*3. Prior to Test 25, the 8.65-scfm orifice in the main oxidizer valve closing control line was replaced with an 8.433-scfm orifice to re-time the main oxidizer valve.

4. Fuel lead time was 1 sec for each sequence check for valve time verification.

TABLE VII
ENGINE PURGE SEQUENCE AT AEDC

		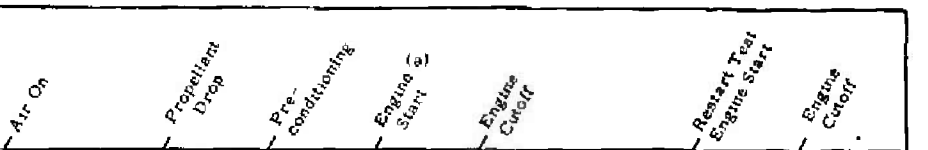
Turbopump and Gas Generator (Purge Manifold System)	Helium, 82 - 125 psia, 50° - 200°F at Customer Connect, 6 scfm Nominal	
Oxidizer Dome and Gas Generator LO_2 Injector (Engine Pneumatic System)	Helium, 400 ± 25 psig at Engine Pneumatic Package Outlet, 50° to 200°F at Helium Fill Customer Connect, 230 scfm Nominal	
Oxidizer Dome (Facility Line to Instrumentation Port CO3A)	Nitrogen, 400 - 450 psig, 100° - 200°F at Facility Check Valve, 200 scfm Minimum	
Oxidizer Turbopump Intermediate Seal Cavity (Engine Pneumatic System)	Helium, 400 ± 25 psig at Engine Pneumatic Package Outlet, Engine Ambient Temperature, 2500 - 7000 scfm	
Thrust Chamber Jacket (Purge and Preconditioning through Customer Connect Line)	Helium, 40 - 50 psig, 50° - 200°F at Customer Connect Panel, 60 scfm Nominal	
	Helium, 12 - 14 psig, 50° - 200°F at Customer Connect Panel, 10 scfm Nominal	
	Helium, 1000 psig at Customer Connect Panel, 10 - 20 lb_m/min	

(a) Normal post-test purge procedures shall be used following an aborted test

(b) May be turned on any time after stabilized mainstage is obtained

TABLE VIII
SPECIFIC TEST OBJECTIVES

Test Number	Specific Test Objectives
20	Minimum start tank energy second orbit S-IVB restart with the PU valve open and the thrust chamber asymmetrically heated to the warmest expected.
21A	AS-200 Series first-burn simulation for AEDC correlation
21B	S-IVB restart with maximum start tank energy, an asymmetrically heated thrust chamber, and a 10-min propellant system chilldown.
21C	S-IVB first burn with maximum start tank energy and warmest thrust chamber prechill to evaluate low-level stall and valve sequence overlap with engine start.
22A	S-IVB first-burn verification of .ight 501 prevalve sequencing effects on engine start
22B	S-IVB restart evaluation using s .art tank V & R setting selected for engine S/N 2031 on S501, 10-min propellant system chilldown.
23A	S-IVB first burn to evaluate "light off" characteristics of the ASI with a 0.125-in. ASI oxidizer orifice
23C	Slowest S-IVB restart with 10-min propellant system chilldown and simulated GG valve leak.
23D	S-IVB 2nd orbit restart worst-case GGOT (exception: MOV timing of 25 msec faster than planned for engine S/N 2031 on S501), 10-min propellant system chilldown.
23E	S-IVB restart evaluation with possible ASI burnout due to high mixture ratio.
24A	S-IVB restart worst-case GGOT test with minimum start tank energy and an asymmetrically heated thrust chamber.
24B	S-IVB restart with maximum start tank energy and asymmetrically heated thrust chamber.
24C	Slowest expected S-IVB first-burn start investigation.
24D	S-IVB 2nd Orbit restart with start conditions for worst-case GGOT and possible ASI erosion
25A	S-IVB maximum buildup rate restart investigation for possible low-level stall with a symmetrically heated thrust chamber and high start tank energy.
25B	S-IVB restart evaluation for the effect of the lowered maximum start tank V & R setting on GGOT.
25C	S-IVB minimum buildup rate restart investigation for possible low-level stall with a symmetrical heated thrust chamber and low start tank energy.
25D	Demonstration of 1st orbit (90-min) S-IVB restart without crossover duct cooling purge as contemplated for flight.
26A	S-IVB first-burn nominal buildup rate start investigation with simulated ground environmental conditions on the oxidizer GG bootstrap line.
26B	S-IVB nominal buildup rate restart investigation.
26C	S-IVB first-burn nominal buildup rate start investigation without simulated oxidizer GG bootstrap line environmental conditions. (Comparison with Test 26A)
26D	S-IVB 2nd orbit restart with conditions set for worst-case GGOT using the shaved start tank V & R limit selected for flight S501.

TABLE IX
TEST MATRIX

Test Number		20	21A	21B	21C	22A	22B	23A	23C	23D	23E	24A	24B	24C	24D	25A	25B	25C	25D	26A (K)	26B	26C	26D
Test Date		2-18-67	2-26-67	2-26-67	2-26-67	3-6-67	3-6-67	3-10-67	3-10-67	3-10-67	3-10-67	3-16-67	3-16-67	3-16-67	3-16-67	3-23-67	3-23-67	3-23-67	3-23-67	4-4-67	4-4-67	4-4-67	4-4-67
Firing Duration, sec		30	30	5	30	30	5	30	30	5	30	30	5	30	5	40	5	30	5	5	5	30	5
Fuel Pump Inlet Conditions at E. S.	Pressure, psia	31 ± 1	41 ± 1	35 ± 1	35 ± 1(B)	35 ± 1(B)	37 ± 1	37^{+1}_{-0}(B)	35 ± 1	37 ± 1	30^{+1}_{-0}	37^{+1}_{-0}	37 ± 1	35 ± 1(B)	30^{+1}_{-0}	35 ± 1	37 ± 1	35 ± 1	37 ± 1	35 ± 1 (B)	35 ± 1	35 ± 1 (B)	37 ± 1
	Temperature, °F	-420.4 ± 0.4	-422.2 ± 0.4	-420.4 ± 0.4	(B) -420.4 ± 0.4	(B) -420.4 ± 0.4	-421.1 ± 0.4	(B) -421.1 ± 0.4	-420.4 ± 0.4	-421.1 ± 0.4	-421.0 ± 0.4	-422.2 ± 0.4	-422.2 ± 0.4	(B) -420.4 ± 0.4	-421.0 ± 0.4	-420.0 ± 0.4	-420.0 ± 0.4	-420.0 ± 0.4	-420.0 ± 0.4	(B) -421.1 ± 0.4	-421.1 ± 0.4	(B) -421.1 ± 0.4	-419.6 ± 0.4
Oxidizer Pump Inlet Conditions at E. S.	Pressure, psia	38 ± 1 (C)	41 ± 1	41 ± 1	41 ± 1(B)	41 ± 1(B)	41 ± 1	38^{+0}_{-1}(C) (B)	41 ± 1 (C)	41 ± 1	41^{+1}_{-0}	38 ± 1(C)	41 ± 1	38 ± 1 (C) (B)	41 ± 1	41 ± 1	41 ± 1	41 ± 1	41 ± 1	40 ± 1 (C) (B)	40 ± 1	40 ± 1 (B)	41 ± 1
	Temperature, °F	-290.4 ± 0.4	-295.3 ± 0.4	-294.9 ± 0.4	(B) -295.6 ± 0.4	(B) -295.6 ± 0.4	-294.9 ± 0.4	(B) -290.4 ± 0.4	-294.0 ± 0.4	-294.9 ± 0.4	-294.9 ± 0.4	-295.3 ± 0.4	-295.3 ± 0.4	(B) -295.3 ± 0.4	-295.3 ± 0.4	-295.3 ± 0.4	-295.3 ± 0.4	-295.3 ± 0.4	-295.3 ± 0.4	(B) -293.0 ± 0.4	-293.0 ± 0.4	(B) -293.0 ± 0.4	-295.6 ± 0.4
Start Tank Conditions at E. S.	Pressure, psia	1250 ± 10	1270 ± 10	1380 ± 10	1400 ± 10	1250 ± 10	1300 ± 10	1250 ± 10	1250 ± 10	1380 ± 10	1380 ± 10	1250 ± 10	1385 ± 10	1250 ± 10	1385 ± 10	1380 ± 10	1300 ± 10	1250 ± 10	1315 ± 10	1325 ± 10	1300 ± 10	1325 ± 10	1300 ± 10
	Temperature, °F	-140 ± 10	-170 ± 10	-275 ± 10	-200 ± 10	-140 ± 10	-210 ± 10	-140 ± 10	-140 ± 10	-225 ± 10	-225 ± 10	-140 ± 10	-225 ± 10	-140 ± 10	-225 ± 10	-225 ± 10	-210 ± 10	-140 ± 10	-225 ± 10	-170 ± 10	-190 ± 10	-170 ± 10	-210 ± 10
Thrust Chamber Temperature Conditions at E. S., °F	Throat	(I)	-220 ± 10	(I)	-80 ± 10(D)	-80 ± 10(D)	50^{+0}_{-50} (H)	-80 ± 10 (D)	-100 ± 10(D)	50^{+0}_{-50} (H)	50^{+0}_{-50} (H)	(I)	(I)	-200 ± 10(D)	50^{+0}_{-50} (H)	(J)	50^{+0}_{-50} (H)	(J)	50^{+0}_{-50} (H)	-160 ± 10(D)	50^{+0}_{-50} (H)	-160 ± 10	50^{+0}_{-50} (H)
	Exit		-180		-80 ± 10(D)	-80 ± 10(D)	50^{+0}_{-50} (H)	-80 ± 10 (D)	-100 ± 20(D)	50^{+0}_{-50} (H)	50^{+0}_{-50} (H)			-200 ± 10(D)	50^{+0}_{-50} (H)		50^{+0}_{-50} (H)		50^{+0}_{-50} (H)	-160 ± 10(D)	50^{+0}_{-50} (H)	-160 ± 10	50^{+0}_{-50} (H)
Fuel Lead Time, sec		8	1	8	3	3	8	3	8	8	8	8	8	3	8	8	8	8	8	3	8	3	8
Fuel in Engine Time, min		60	150	10	60	60	10	60	10	10	30	20	10	60	10	60	10	10	10	60	10	60	10
Oxidizer in Engine Time, min		60	150	10	60	60	10	60	10	10	30	20	10	60	10	60	10	10	10	60	10	60	10
Propellant Recirculation, min		10	17	10	10	10	10	10	10	10	10	10	10	10	10	10	10	10	10	10	10	10	10
Propellant Utilization Valve Position, deg	Engine Start	-29	0	-29	0	0	-29	0	-29	-29	-29	-29	-29	0	-29	-29	-29	-29	-29	0	-29	0	-29
	Mainstage	33.3	33.3	-29	33.3	33.3	-29	33.3	33.3	-29	33.3	33.3	-29	33.3	-29	33.3	-29	33.3	-29	33.3	-29	33.3	-29
	Excursion Time	10	10	None	10	10	None	10	10	None	10	10	None	10	None	10	None	10	None	10	None	10	None
Prevalve Sequencing Logic		Restart	Restart	Restart	First Burn	First Burn	Restart	First Burn	Restart	Restart	Restart	Restart	Restart	First Burn	Restart	Restart	Restart	Restart	Restart	First Burn	Restart	First Burn	Restart
MOV Closing Control Line Temperature, °F		-50^{+25}_{-0} (F)	-150^{+25}_{-0}(F)	-150^{+25}_{-0}	-100^{+25}_{-0}(F)	20^{+0}_{-25}(F)	-150^{+25}_{-0}	-20 ± 10(F)	50^{+0}_{-25}	-150^{+25}_{-0}	Ambient	-50 ± 25 (F)	-150 ± 25	-20 ± 10 (F)	-150 ± 25	-150^{+25}_{-0}(F)	-150^{+25}_{-0}	-150^{+25}_{-0}(F)	-150^{+25}_{-0}	75 ± 15(F)	-80 ± 15	-75 ± 15 (F)	150^{+25}_{-0}
Pneumatic Control Package Temperature, °F		-50^{+25}_{-0} (F)	-150^{+25}_{-0} (F)	-150^{+25}_{-0}	-100^{+25}_{-0}(F)	-20^{+0}_{-25}(F)	-150^{+25}_{-0}	-20 ± 10(F)	50^{+0}_{-25}	-150^{+25}_{-0}	Ambient	-50 ± 25 (F)	-150 ± 25	-20 ± 10(F)	-150 ± 25	-150^{+25}_{-0} (F)	-150^{+25}_{-0}	-150^{+25}_{-0}(F)	-150^{+25}_{-0}	-75 ± 15 (F)	-80 ± 15	-75 ± 15 (F)	-150^{+25}_{-0}
Crossover Duct Temperature, °F		-50^{+25}_{-0} (F)	-75 ± 15 (F)	125 ± 10	-100^{+25}_{-0}(F)	-100^{+25}_{-0}(F)	125 ± 10	-100 ± 15(F)	-100 ± 15 (F)	125 ± 10	Ambient	-100 ± 15(F)	125 ± 10	-100 ± 15 (F)	125 ± 10	Ambient	125^{+15}_{-0}	Ambient	165^{+15}_{-0}	75 ± 15 (F)	50 ± 25	-75 ± 15 (F)	125^{+15}_{-0}
ASI Fuel Supply Line Temperature, °F		N/A	N/A	N/A	N/A	N/A	N/A	N/A	N/A	N/A	60 ± 10(H)	N/A	Lower 145 ± 15 / Upper 25 ± 25 (H)	N/A	Lower 145 ± 15 / Upper 25 ± 25 (H)	N/A	50^{+0}_{-50} (H)	N/A	50^{+0}_{-50} (H)	N/A	50^{+0}_{-50} (H)	N/A	50^{+0}_{-50} (H)
Time between Multiple Tests, min		N/A	(E)	(G)	150 (E)	(E)	(G)	(E)	(E)	(G)	150	(E)	(G)	150 (E)	(G)	(E)	(G) & (E)	150 (E)	(G) & (E)	(E)	(H)	150 (E)	(G)

Thrust Chamber Heating Guide Line, 125°F

TSC10-1	TSC10-2	TSC15	TSC11-1	TSC11-2	TSC16	TSC13-1	TSC13-2	TSC17	TSC14-1	TSC14-2	TSC18	TSC8-T	TSC5-T	Profile
150	175	175	325	275	375	350	175	175	375	275	325	375	325	Asymmetric
250	250	250	250	250	250	250	250	250	250	250	250	250	250	Symmetric

Comments

(A) The oxidizer vehicle tank level should be 30 percent or greater prior to engine start when using GN_2 as pressurant
(B) Pump inlet conditions are to be met after the prevalves come open
(C) At mainstage OK signal, increase propellant tank pressure as required to maintain adequate NPSH for engine operation at 5.5 mixture ratio.
(D) Monitor exit thermocouple TSC-7E and throat thermocouple TTC-1P, the warmer location to be within the specified limits
(E) Close prevalves and recirculation valves after engine cutoff and purge inlet ducts, if required, to remove all propellant from the engine by T + 15 min.
(F) These components should be conditioned for approximately one hour at their respective target temperatures.
(G) Adjust the coast time for engine restart to attain the required crossover duct temperature
(H) Use 40- to 50-psig thrust chamber helium purge and thrust chamber and ASI fuel line heaters as required to attain the specified temperatures for engine restart
(I) Using the thrust chamber heaters, condition the thrust chamber at the required asymmetric profile for a minimum of 30 min prior to engine start.
(J) Using the thrust chamber heaters, condition the thrust chamber at the required symmetric profile for a minimum of 30 min prior to engine start.
(K) Condition the oxidizer GG bootstrap line with ambient temperature GN_2 for a minimum of one hour prior to engine start

TABLE X
SUMMARY OF TEST CONDITIONS AND RESULTS

Test Number		20(A)(B)	21A(B)	21B(A)(B)	21C(A)(B)	22A(B)	22B(B)	23A	23C	23D	23E	24A	24B	24C	24D	25A(B)	25B	25C(B)	25D	26A	26B	26C	26D
Test Date		2-18-67	2-26-67	2-26-67	2-26-67	3-6-67	3-6-67	3-10-67	3-10-67	3-10-67	3-10-67	3-16-67	3-16-67	3-16-67	3-16-67	3-23-67	3-23-67	3-23-67	3-23-67	4-4-67	4-4-67	4-4-67	4-4-67
Pressure Altitude at E. S., ft		100,000	95,000	105,000	105,000	97,000	100,000	104,000	107,000	110,000	109,000	105,000	111,000	109,000	110,000	104,000	108,000	108,000	109,000	107,000	107,000	107,000	108,000
Firing Duration, sec		2.03	30.08	5.08	30.08	30.05	—	3.90	30.08	5.05	30.05	30.08	5.08	30.07	5.07	30.07	5.07	30.07	5.07	5.07	5.07	30.07	5.07
Fuel Pump Inlet Conditions at E. S.	Pressure, psia	30.4	41.0	34.5	36.0	35.9	36.9	37.9	35.1	36.9	30.4	37.8	37.2	35.7	31.2	35.6	37.1	35.4	37.6	35.6	34.7	35.8	36.7
	Temperature, °F	-420.7	-421.8	-420.7	-420.7	-420.2	-420.2	-421.2	-419.8	-421.1	-421.1	-421.5	-421.6	-420.7	-420.7	-420 0	-419.7	-418.8	-419.9	-421.4	-420.9	-421.3	-419.4
Oxidizer Pump Inlet Conditions at E. S.	Pressure, psia	38.6	41.3	41.1	40.9	40.8	46.8	37.4	41.4	41.8	42.0	38.0	41.1	38.5	41.4	41.2	40.9	41.9	41.4	40.0	40.4	40.3	40.0
	Temperature, °F	-290.8	-295.7	-295.0	-295.9	-296.0	-294.3	-290.1	-293.5	-294.2	-294.9	-295.3	-295.7	-295.8	-295.5	-295.6	-295.6	-295.8	-295.4	-293.7	-293.4	-293.1	-295.4
Start Tank Conditions at E. S.	Pressure, psia	1243	1285	1385	1410	1252	1319	1253	1252	1384	1387	1255	1390	1244	1384	1376	1292	1247	1319	1327	1303	1330	1306
	Temperature, °F	-141	-170	-216	-203	-133	-207	-145	-145	-222	-227	-147	-228	-145	-231	-224	-207	-141	-217	-173	-194	-179	-215
Helium Tank Conditions at E. S.	Pressure, psia	3100	3068	3073	2878	3173	3233	3146	3098	3260	3130	3114	3081	3075	3152	3224	3081	3093	3118	3236	3040	3176	3163
	Temperature, °F	-149	-179	-224	-217	-139	-215	-151	-155	-232	-236	-163	-235	-152	-239	-228	-225	-154	-228	-177	-207	-194	-218
Thrust Chamber Temperature Conditions at E. S., °F	TTC-1P Throat	See p. 153	-197	See p. 153	-122	-108	48	-184	-153	47	30	See p. 153	See p. 153	-194	17	See p. 153	31	See p. 153	30	-174	45	-164	20
	1SC-7E Exit		-132		-107	-58	15	-138	-164	23	55			-186	17		54		23	-162	46	-149	22
Average Thrust Chamber Temperature at S1DV, °F		-160	-193	-182	-238	-206	-340	-271	-354	-288	-251	-208	-170	-305	-270	-238	-277	-236	-286	-292	282	-280	-298
Fuel Lead Time, sec		7.95	1.00	7.93	3.00	3.00	13.35	2.88	7.98	7.90	7.85	7.92	7.90	2.97	7.89	8.00	8.00	8.00	8.00	3.00	7.98	3.00	7.98
Fuel in Engine Time, min		42	287	17	60	61	10	128	11.5	16.5	35	20.5	10.0	116	10.5	112	10	12	15	123	10	123	11
Oxidizer in Engine Time, min		42	287	17	60	61	10	128	11.5	16.5	35	20.5	10.0	116	10.5	112	10	12	15	123	10	123	11
Propellant Recirculation Time, min		10	21	17	11	10	10	11	11.5	16.5	16	10	10.0	10	10.5	10	10	12	15	10	10	10	11
VSC Duration Time, msec		None	120	None	23	None	—	12	None	20	None	None	None	26	4	None	3	None	None	42	None	30	3 and 3
Gas Generator Temperature, °F	Initial Peak	1435	2050	1869	1884	1719	—	1624	1595	2097	1870	1111	1891	1931	2196	1667	2204	1585	2154	1954	1505	1990	2220
	Second Peak		1356	1896	1646	1320	—	1139	None	1915	1422	948	1899	1211	2057	1189	2179	1439	2184	1608	1488	1469	2028
Oxidizer Dome Prime Time, sec		1.031	0.998	0.962	0.978	1.004	—	1.055	1.078	0.935	0.961	1.015	0.949	1.027	0.931	0.987	0.954	0.991	0.940	1.017	1.007	1.010	0.957
MOV Second Stage Movement Delay, sec		1.175	0.992	1.264	1.275	1.163	—	1.043	1.136	1.250	1.151	1.162	1.325	1.026	1.293	1.130	1.305	1.187	1.317	1.006	1.208	1.000	1.237
Mainstage OK Signal No. 2, sec		1.915	1.650	1.687	1.714	1.721	—	1.750	1.959	1.651	1.789	1.885	1.636	1.770	1.644	1.744	1.623	1.792	1.678	1.705	1.726	1.704	1.630
550-psia Chamber Pressure Attained, sec		—	1.961	2.052	2.007	1.980	—	2.095	2.549	1.983	2.118	2.347	2.001	2.043	1.974	2.120	1.994	2.133	2.019	2.002	2.142	1.993	1.993
Crossover Duct Temperature, °F	TFTD-3	-42	-53	66	-93	-55	116	-107	-93	126	47	-102	104	-133	115	61	120	54	160	-28	65	-22	130
	TFTD-4	-44	-55	68	-94	-53	121	-109	-94	128	46	-100	107	-127	118	61	124	53	164	-34	63	-24	130
Oxidizer Turbine Inlet Temperature, °F		-26	-57	185	-76	-63	251	-106	-81	254	+27	-89	226	-109	254	42	268	62	323	-54	76	-55	277
Propellant Utilization Valve Position, deg	Engine Start	-29	0	-29	0	0	-29	0	-29	-29	-29	-29	-29	0	-29	-29	-29	-29	-29	0	-29	0	-29
	Mainstage	-29	33.3	-29	33.3	33.3	—	—	33.3	-29	33.3	33.3	-29	33.3	-29	33.3	-29	33.3	-29	0	-29	33.3	-29
	Excursion Time, sec	None	10.5	None	10	5.5	None	None	10.5	None	10	12	None	11.5	None	10	None	10	None	None	None	11	None
Prevalve Sequencing Logic		Restart	Restart	Restart	First Burn	First Burn	Restart	First Burn	Restart	Restart	Restart	Restart	Restart	First Burn	Restart	Restart	Restart	Restart	Restart	First Burn	Restart	First Burn	Restart
MOV Closing Control Line Temperature, °F		-59	-154	-158	-138	-24	-170	-42	-9	-122	-120	-53	-164	-19	-131	-140	-168	-166	-133	-71	-92	-80	-151
Pneumatic Control Package Temperature, °F		-51	-145	-147	-99	-20	-159	-34	-21	-112	-134	-73	-155	-31	-151	-150	-156	-156	-145	-70	-86	-64	-153
MOV Actuator Cap Temperature, °F		-172	-140	-106	-155	-77	-87	-154	-55	-115	-51	-44	-73	-177	-128	-118	-90	-13	-82	-138	78	-135	-117
CG Oxidizer Supply Line Temperature, °F		-29	-86	-99	-68	10	-91	-9	-8	-65	-57	30	15	-11	-5	26	20	21	5	1	16	11	8
ASI Fuel Supply Line Temperature, °F	TFASIL-1	N/A	N/A	N/A	N/A	N/A	N/A	N/A	N/A	N/A	N/A	71	61	-164	63	-36	35	-31	36	-155	24	-145	24
	TFASIL-2	N/A	N/A	N/A	N/A	N/A	N/A	N/A	N/A	N/A	N/A	132	112	-133	15	130	37	125	3	-115	27	-105	34
Time between Multiple Tests, min		N/A	N/A	59	343	N/A	41	N/A	190	42	297	N/A	49	266	41	N/A	38	178	25	N/A	59	148	37

(A) Stall Approach Monitor Enabled for Engine Cutoff

(B) Prechill Controller Activated

TABLE X (Concluded)

Heated Thrust Chamber Conditions

Test Number	TSC10 -1	TSC10 -2	TSC15	TSC11 -1	TSC11 -2	TSC16	TSC13 -1	TSC13 -2	TSC17	TSC14 -1	TSC14 -2	TSC18	TSC8 -T	TSC5 -T
20	52	185	63	316	211	356	355	48	254	307	255	306	419	307
21B	71	185	239	304	192	331	275	177	245	266	275	298	287	228
24A	91	175	294	176	242	406	150	239	149	147	213	387	145	151
24B	114	222	300	268	274	420	493	250	295	439	333	382	225	201
25A	100	222	91	169	201	111	352	80	166	281	98	65	197	94
25C	96	23	87	150	250	114	317	82	133	259	96	56	96	90

TABLE XI
TEST OPERATIONS SUMMARY

Test		Remarks
AEDC Test 20	A	Saturn 501/S-IVB restart of scheduled 30 sec. Mainstage and ignition phase control solenoids de-energized prematurely resulting in a 2.045-sec firing.
	B	A short in the ECA caused by a loose piece of safety wire was the cause and resulted in the following test cancellations. Cancelled
	C	Cancelled
	D	Cancelled
AEDC Test 21	A	Successful 30-sec firing.
	B	Successful 5-sec firing. Thrust chamber approximately 65°F cooler than desired.
	C	Successful 30-sec firing.
	D	Cancelled because of excessive cooldown rate of the crossover duct. An alternate test was cancelled because of a suspected fuel low pressure duct leak.
AEDC Test 22	A	Successful 30-sec firing.
	B	An automatic test termination resulted because of the failure to complete the fuel lead chilldown sequence caused by failure of the prechill controller circuitry.
	C	Cancelled. The ignition detect probe resistance was high (outside specifications). LO_2 recirculation system malfunctioned because of iced system screen.
	D	Cancelled
	E	Cancelled
AEDC Test 23	A	Terminated at T + 3.9 sec by LO_2 observer (scheduled 30 sec). Start initiated with LO_2 inlet conditions too near safe run region low limit.
	B	Rescheduled after -23E because of fast crossover duct cooldown post -23A. Later cancelled because of an "open" ignition detect probe indication
	C	Successful 30-sec firing.
	D	Successful 5-sec firing.
	E	Duration re-scheduled to 30 sec; successfully completed.
AEDC Test 24	A	Successful 30-sec firing.
	B	Successful 5-sec firing.
	C	Successful 30-sec firing.
	D	Successful 5-sec firing.
AEDC Test 25	A	Successful 30-sec firing.
	B	Successful 5-sec firing.
	C	Successful 30-sec firing.
	D	Successful 5-sec firing.
AEDC Test 26	A	Successful 5-sec firing.
	B	Successful 5-sec firing.
	C	Successful 30-sec firing.
	D	Successful 5-sec firing.

TABLE XII
ENGINE J-2052 VIBRATION DATA AT AEDC

	Test Number	First or Second Burn Simulation	VSC Duration	Oxidizer Dome Prime	VSC Period	Fuel Lead Period	Thrust Chamber Conditions at E. S.	Thrust Chamber Temperature at STDV	Time* TFJ-1P Reaches -425°F	NOP at** Dome Prime	NFP at** Dome Prime	PC Peak as Dome Primes
			msec	sec	sec	sec	°F	°F	sec	rpm	rpm	psia
Thrust Chamber Prechilled, 1-sec Fuel Lead	02	1st	30	1.034	1.031-1.061	1.0	-224 Throat -165 Exit	-236 Throat -229 Exit	0.75	3035	13977	129
	03	1st	12	0.997	0.992-1.004	1.1	-199 Throat -188 Exit	-218 Throat -245 Exit	0.72	3151	13995	136
	04	1st	132	0.979	0.969-1.101	1.0	-215 Throat -209 Exit	-236 Throat -263 Exit	0.67	3252	14027	159
	05	1st	67	0.973	0.964-1.031	1.0	-198 Throat -215 Exit	-219 Throat -264 Exit	0.67	3316	14424	162
	06	1st	0	0.970	None	1.1	-156 Throat -178 Exit	-179 Throat -234 Exit	0.77	3374	14390	159
	07	1st	30	0.978	0.970-1.000	1.1	- 89 Throat - 70 Exit	- 82 Throat -146 Exit	0.92	3422	14192	160
	08	1st	15	0.990	0.999-1.004	1.0	-183 Throat - 61 Exit	-180 Throat -159 Exit	0.80	3274	14141	149
	09A	1st	3	0.984	0.987-0.990	1.0	-177 Throat -154 Exit	-195 Throat -218 Exit	0.80	3310	14206	150
	10A	1st	25	0.962	0.965-0.990	1.0	-191 Throat -153 Exit	-202 Throat -218 Exit	0.77	3334	14522	175
	11A	1st	83	0.956	0.943-1.026	1.0	-153 Throat -132 Exit	-170 Throat -214 Exit	0.77	3455	14786	177
	13A	1st	90	0.971	0.963-1.053	1.0	-196 Throat -214 Exit	-213 Throat -262 Exit	0.72	3235	14433	169
	21A	1st	120	0.997	0.981-1.101	1.0	-184 Throat -129 Exit	-190 Throat -210 Exit	0.77	3100	14005	165
Thrust Chamber Prechilled, Fuel Lead 2- to 2-1/2-sec	14	1st	15	1.003	1.009-1.024	1.85	-126 Throat -117 Exit	-163 Throat -235 Exit	0.77	3251	13850	169
	17A	1st	35	0.974	0.978-1.013	2.6	-143 Throat -144 Exit	-241 Throat -283 Exit	0.62	3160	14297	146
	17C	1st	30	0.965	0.952-0.982	2.6	- 86 Throat -100 Exit	-169 Throat -235 Exit	0.80	3400	14607	173
	19	1st	6	1.007	1.006-1.012	2.5	-177 Throat -130 Exit	-244 Throat -280 Exit	0.67	2969	13548	144
Thrust Chamber Prechilled, 3-sec Fuel Lead	12A	1st	40	0.990	0.995-1.035	3.1	-118 Throat -172 Exit	-222 Throat -301 Exit	0.65	3157	13913	161
	12B	1st	15	0.994	0.995-1.010	3.1	-208 Throat -224 Exit	-334 Throat -359 Exit	-0.75	3135	14500	152
	15C	1st	20	0.982	1.083-1.103	3.1	-215 Throat -227 Exit	-343 Throat -360 Exit	-0.87	3125	14100	138
	21C	1st	23	0.979	0.961-0.984	3.0	-133 Throat -109 Exit	-228 Throat -306 Exit	0.67	3153	14276	165
	23A	1st	12	1.052	1.030-1.042	3.1	-175 Throat -139 Exit	-270 Throat -328 Exit	0.37	2933	13525	150
	24C	1st	26	1.027	1.021-1.047	3.0	-192 Throat -190 Exit	-306 Throat -354 Exit	-0.07	2795	13471	156
	26A	1st	42	1.017	0.930-1.032	3.0	-161 Throat -169 Exit	-291 Throat -345 Exit	-0.50	2971	13998	162
	26C	1st	30	1.010	0.985-1.015	3.0	-169 Throat -155 Exit	-276 Throat -343 Exit	0.25	3005	14099	156
	22A	1st	0	1.004	None	3.0	-111 Throat - 59 Exit	-190 Throat -276 Exit	0.70	3097	13784	156
S-1B/S-IVB Flights to Date	AS-201	1st	30	0.92	—	1.0	-212 Throat -235 Exit	—				
	AS-202	1st	30	1.02	—	1.0	-220 Throat -220 Exit	—				
	AS-203	1st	60	0.96	0.94-1.00	1.0	-205 Throat -220 Exit	—				

*An indication of whether or not fuel injection flow was liquid at dome prime

**Relative pump speeds give indication of whether "hard" or "soft" dome prime

Note. The three flights to date are presented for comparison

TABLE XII (Concluded)

	Test Number	First or Second Burn Simulation	VSC Duration	Oxidizer Dome Prime	VSC Period	Fuel Lead Period	Thrust Chamber Conditions at E. S.	Thrust Chamber Temperature at STDV	Time* TFJ-1P Reaches -425°F	NOP at** Dome Prime	NFP at** Dome Prime	PC Peak as Dome Primes
			msec	sec	sec	sec	°F	°F	sec	rpm	rpm	psia
Thrust Chamber Prechilled, Fuel Lead 4-1/2-sec	10B	1st	0	0.973	None	4.60	41 Throat 27 Exit	+141 Throat -254 Exit	0.68	3490	14884	170
	15A	1st	0	0.964	None	4.44	50 Throat 48 Exit	-141 Throat -213 Exit	0.80	3533	14542	163
	13B	2nd	40	0.918	0.910- 0.950	4.72	16 Throat 72 Exit	+154 Throat -248 Exit	0.73	3961	14680	192
	15B	2nd	35	0.931	0.925- 0.964	4.40	32 Throat 0 Exit	-155 Throat -232 Exit	0.75	3713	14501	179
Thrust Chamber Ambient or Prechilled, 8-sec Fuel Lead	11B	2nd	20	0.957	0.870- 0.880	8.13	65 Throat 43 Exit	-280 Throat -345 Exit	-1.62	2559	14870	110
	16	1st	21	0.998	0.995- 1.016	8.07	38 Throat 46 Exit	-271 Throat -296 Exit	-0.95	3047	14142	144
	17B	2nd	8	0.945	0.949- 0.957	8.31	48 Throat 19 Exit	-305 Throat -323 Exit	-2.05	3430	14662	163
	18	1st	15	1.037	1.039- 1.054	7.97	57 Throat 58 Exit	-227 Throat -267 Exit	0.50	2840	13410	150
	23C	2nd	0	1.079	None	7.98	-163 Throat -159 Exit	-365 Throat -368 Exit	-4.75	2582	13663	127
	23D	2nd	20	0.934	0.924- 0.954	7.90	80 Throat 31 Exit	-271 Throat -345 Exit	-1.32	3392	14702	182
	23E	2nd	0	0.962	None	7.85	57 Throat 61 Exit	-221 Throat -325 Exit	0.55	3081	14282	156
	24D	2nd	4	0.931	0.818- 0.822	7.89	70 Throat 29 Exit	-241 Throat -339 Exit	0.50	3384	14565	178
	25B	2nd	4	0.954	0.839- 0.841	8.00	76 Throat 41 Exit	-264 Throat -340 Exit	-0.85	3381	14416	174
	25D	2nd	0	0.940	None	8.00	72 Throat 25 Exit	-262 Throat -346 Exit	-1.20	3405	14241	177
	26B	2nd	0	1.007	None	7.98	61 Throat 43 Exit	-267 Throat -343 Exit	-0.82	3043	14191	160
	26D	2nd	3 3	0.957	0.622- 0.625 0.846- 0.849	7.98	75 Throat 25 Exit	-245 Throat -351 Exit	-1.80	3309	14089	171
Thrust Chamber Heated, 8-sec Fuel Lead	20	2nd	0	1.032	None	7.95	Heated	+104 Throat +269 Exit	0.58	2959	13615	146
	21B	2nd	0	0.962	None	7.93	Heated	+154 Throat +285 Exit	0.48	3366	14721	168
	24A	2nd	0	1.016	None	7.92	Heated	+217 Throat +290 Exit	—	2942	13646	152
	24B	2nd	0	0.949	None	7.90	Heated	+175 Throat +274 Exit	—	3414	14630	179
	25A	2nd	0	0.997	None	8.00	Heated	+247 Throat +313 Exit	0.18	3107	14584	158
	25C	2nd	0	0.986	None	8.00	Heated	+244 Throat +315 Exit	0.40	2988	13881	156

*An indication of whether or not fuel injection flow was liquid at dome prime.

**Relative pump speeds give an indication of whether "hard" or "soft" dome prime.

TABLE XIII
NORMALIZED ENGINE PERFORMANCE SUMMARY

Test Number		21A	21C	22A	23C	23E	24A	24C	25A	25C	26C
Data Time Slice, sec		29.5	29.5	29.5	29.5	29.5	29.5	29.5	29.5	29.5	29.5
Overall Engine Performance	Chamber Pressure, psia	743.5	739.4	754.6	746.7	743.1	746.5	753.8	758.9	757.8	760.5
	Mixture Ratio	5.647	5.625	5.501	5.487	5.485	5.512	5.489	5.523	5.526	5.499
	Total Weight Flow, lb/sec	523.51	521.71	528.59	522.76	523.14	522.61	525.22	527.81	526.42	528.34
Thrust Chamber Performance	Mixture Ratio	5.871	5.849	5.723	5.713	5.711	5.742	5.715	5.740	5.745	5.723
	Total Weight Flow, lb/sec	516.59	514.79	521.40	515.62	516.05	515.46	518.02	520.65	519.26	521.11
	Characteristic Velocity, ft/sec	7889.1	7872.9	7932.3	7937.6	7892.2	7937.8	7975.6	7989.2	7999.7	7998.7
Fuel Turbopump Performance	Pump Efficiency	0.724	0.720	0.714	0.715	0.722	0.726	0.726	0.722	0.721	0.725
	Pump Speed, rpm	26280.7	26204.9	26890.6	26500.9	26559.5	26471.6	26680.1	26777.8	26823.3	26716.5
	Turbine Efficiency	0.581	0.579	0.588	0.570	0.589	0.583	0.589	0.582	0.585	0.586
	Turbine Pressure Ratio	7.37	7.42	7.62	7.60	7.58	7.62	7.58	7.52	7.45	7.62
	Turbine Inlet Temperature, °F	1189.0	1180.2	1158.1	1115.5	1097.1	1107.7	1129.5	1221.1	1210.4	1154.7
	Turbine Weight Flow, lb/sec	6.92	6.92	7.19	7.14	7.09	7.15	7.21	7.16	7.15	7.23
Oxidizer Turbopump Performance	Pump Efficiency	0.803	0.802	0.802	0.802	0.802	0.802	0.802	0.802	0.802	0.803
	Pump Speed, rpm	8428.3	8412.5	8502.6	8423.8	8408.9	8397.9	8430.8	8505.6	8479.9	8476.9
	Turbine Efficiency	0.460	0.459	0.467	0.454	0.462	0.444	0.446	0.463	0.401	0.462
	Turbine Pressure Ratio	2.62	2.63	2.63	2.66	2.66	2.68	2.65	2.66	2.67	2.65
	Turbine Inlet Temperature, °F	758.5	746.4	724.4	693.5	679.5	724.3	739.5	783.8	759.9	729.0
	Turbine Weight Flow, lb/sec	6.17	6.17	6.31	6.27	6.23	6.30	6.37	6.28	7.16	6.36
Gas Generator Performance	Mixture Ratio	0.933	0.928	0.915	0.890	0.879	0.885	0.898	0.952	0.946	0.913
	Chamber Pressure, psia	650	648.8	672.0	662.3	655.9	663.1	670.5	675.6	674.8	675.7

APPENDIX III
PERFORMANCE PROGRAM EQUATIONS

NOMENCLATURE

A	Area, $in.^2$
B	Horsepower, hp
C*	Characteristic velocity, ft/sec
C_p	Specific heat at constant pressure, Btu/lb/°F
D	Diameter, in.
H	Head, ft
h	Enthalpy, Btu/lb_m
M	Molecular weight
N	Speed, rpm
P	Pressure, psia
Q	Flow rate, gpm
R	Resistance, $sec^2/ft^3\text{-}in.^2$
r	Mixture ratio
T	Temperature, °F
TC*	Theoretical characteristic velocity, ft/sec
W	Weight flow, lb/sec
Z	Pressure drop, psi
β	Ratio
γ	Ratio of specific heats
η	Efficiency
θ	Degrees
ρ	Density, lb/ft^3

SUBSCRIPTS

A	Ambient
AA	Ambient at thrust chamber exit

B	Bypass nozzle
BIR	Bypass nozzle inlet (Rankine)
BNI	Bypass nozzle inlet (total)
C	Thrust chamber
CF	Thrust chamber, fuel
CO	Thrust chamber, oxidizer
CV	Thrust chamber, vacuum
E	Engine
EF	Engine fuel
EM	Engine measured
EO	Engine oxidizer
EV	Engine, vacuum
e	Exit
em	Exit measured
F	Thrust
FIT	Fuel turbine inlet
FM	Fuel measured
FY	Thrust, vacuum
f	Fuel
G	Gas generator
GF	GG fuel
GO	GG oxidizer
H1	Hot gas duct No. I
H1R	Hot gas duct No. 1 (Rankine)
H2R	Hot gas duct No. 2 (Rankine)
IF	Inlet fuel
IO	Inlet oxidizer
ITF	Isentropic turbine fuel
ITO	Isentropic turbine oxidizer
N	Nozzle

NB	Bypass nozzle (throat)
NV	Nozzle, vacuum
O	Oxidizer
OC	Oxidizer pump calculated
OF	Outlet fuel pump
OFIS	Outlet fuel pump isentropic
OM	Oxidizer measured
OO	Oxidizer outlet
PF	Pump fuel
PO	Pump oxidizer
PUVO	PU valve oxidizer
RNC	Ratio bypass nozzle, critical
SC	Specific, thrust chamber
SCV	Specific thrust chamber, vacuum
SE	Specific, engine
SEV	Specific, engine vacuum
T	Total
TEF	Turbine exit fuel
TEFS	Turbine exit fuel (static)
TF	Fuel turbine
TIF	Turbine inlet fuel (total)
TIFM	Turbine inlet, fuel, measured
TIFS	Turbine inlet fuel isentropic
TIO	Turbine inlet oxidizer
T_O	Turbine oxidizer
t	Throat
V	Vacuum
v	Valve
XF	Fuel tank repressurant
XO	Oxidizer tank repressurant

TEST MEASUREMENTS REQUIRED BY PERFORMANCE PROGRAM

Fuel and Oxidizer Engine Inlet Pressures, psia

Fuel and Oxidizer Engine Inlet Temperatures, °F

Fuel and Oxidizer Flowmeter Speeds, cps

Fuel and Oxidizer (Main Valves) Temperatures, °F

Fuel and Oxidizer Pump Discharge Pressures, psia

Fuel and Oxidizer Pump Speeds, rpm

Fuel* and Oxidizer Turbine Inlet Pressure, psia

Fuel and Oxidizer Turbine Inlet Temperature, °F

Gas Generator (Bootstrap Line at Bleed Valve) Temperature, °F

Gas Generator Chamber Pressure, psia

Oxidizer Turbine Discharge Pressure, psia

Oxidizer Turbine Discharge Temperature, °F

PU Valve Center Tap Voltage, v

PU Valve Position, v

Thrust Chamber Fuel and Oxidizer Injection Pressure, psia

Thrust Chamber Fuel Injection Temperature, °F

Thrust Chamber (Injector Face) Pressure, psia

---

*At AEDC, fuel turbine inlet pressure is estimated from gas generator chamber pressure.

PERFORMANCE PROGRAM EQUATIONS

MIXTURE RATIO

Engine

$$r_E = \frac{W_{EO}}{W_{EF}}$$

$$W_{EO} = W_{OM} - W_{XO}$$

$$W_{EF} = W_{FM} - W_{XF}$$

$$W_E = W_{EO} + W_{EF}$$

Thrust Chamber

$$r_C = \frac{W_{CO}}{W_{CF}}$$

$$W_{CO} = W_{OM} - W_{XO} - W_{GO}$$

$$W_{CF} = W_{FM} - W_{XF} - W_{GF}$$

$$W_{XO} = 0.8 \text{ lb/sec}$$

$$W_{XF} = 1.8 \text{ lb/sec}$$

$$W_{GO} = W_T - W_{GF}$$

$$W_{GF} = \frac{W_T}{(1 + r_G)}$$

$$W_T = \frac{P_{TIF} A_{TIF} K_7}{TC^*_{TIF}}$$

$$K_7 = 32.174$$

$$W_C = W_{CO} + W_{CF}$$

CHARACTERISTIC VELOCITY

Thrust Chamber

$$C^* = \frac{K_7 P_C A_t}{W_C}$$

$$K_7 = 32.174$$

DEVELOPED PUMP HEAD

Flows are normalized by using the following inlet pressures, temperatures, and densities.

$P_{IO} = 39$ psia

$P_{IF} = 30$ psia

$\rho_{IO} = 70.79$ lb/ft^3

$\rho_{IF} = 4.40$ lb/ft^3

$T_{IO} = -295.212°F$

$T_{IF} = -422.547°F$

Oxidizer

$$H_O = K_4 \left(\frac{P_{OO}}{\rho_{OO}} - \frac{P_{IO}}{\rho_{IO}}\right)$$

$K_4 = 144$

ρ = National Bureau of Standards Values f(P,T)

Fuel

$$H_F = 778.16\ \Delta h_{OFIS}$$

$$\Delta h_{OFIS} = h_{OFIS} - h_{IF}$$

$$h_{OFIS} = f(P,T)$$

$$h_{IF} = f(P,T)$$

PUMP EFFICIENCIES

Fuel, Isentropic

$$\eta_f = \frac{h_{OFIS} - h_{IF}}{h_{OF} - h_{IF}}$$

$$h_{OF} = f(P_{OF}, T_{OF})$$

Oxidizer, Isentropic

$$\eta_O = \eta_{OC}\, Y_O$$

$$\eta_{OC} = K_{40} \left(\frac{Q_{PO}}{N_O}\right)^2 + K_{50} \left(\frac{Q_{PO}}{N_O}\right) + K_{60}$$

$K_{40} = 5.0526$

$K_{50} = 3.8611$

$K_{60} = 0.0733$

$Y_O = 1.000$

TURBINES

Oxidizer, Efficiency

$$\eta_{TO} = \frac{B_{TO}}{B_{ITO}}$$

$$B_{TO} = K_5 \frac{W_{PO}\ H_O}{\eta_O}$$

$K_5 = 0.001818$

$$W_{PO} = W_{OM} + W_{PUVO}$$

$$W_{PUVO} = \sqrt{\frac{Z_{PUVO}\ \rho_{OO}}{R_v}}$$

$$Z_{PUVO} = A + B\,(P_{OO})$$

$$A = -1597$$

$$B = 2.3818$$

If $P_{OO} - 1010$

set $P_{OO} = 1010$

$$\ln R_v = A_3 + B_3\,(\theta_{PUVO}) + C_3(\theta_{PUVO})^3 + D_3\,(e)^{\frac{\theta_{PUVO}}{7}} + E_3\,\theta_{PUVO}\,(e)^{\frac{\theta_{PUVO}}{7}} + F_3\left[(e)^{\frac{\theta_{PUVO}}{7}}\right]^2$$

$A_3 = 5.5659 \times 10^{-1}$
$B_3 = 1.4997 \times 10^{-2}$
$C_3 = 7.9413 \times 10^{-6}$
$D_3 = 1.2343$
$E_3 = -7.2554 \times 10^{-2}$
$F_3 = 5.0691 \times 10^{-2}$
$\theta_{PUVO} = 16.5239$

Fuel, Efficiency

$$\eta_{TF} = \frac{B_{TF}}{B_{ITF}}$$

$$B_{ITF} = K_{10}\,\Delta h_F\,W_T$$

$$\Delta h_f = h_{TIF} - h_{TEF}$$

$$B_{TF} = B_{PF} = K_5\left(\frac{W_{PF}\,H_F}{\eta_f}\right)$$

$$W_{PF} = W_{FM}$$

$$K_{10} = 1.4148$$

$$K_5 = 0.001818$$

Oxidizer, Developed Horsepower

$$B_{TO} = B_{PO} + K_{56}$$

$$B_{PO} = K_5\left(\frac{W_{PO}\,H_O}{\eta_O}\right)$$

$$K_{56} = -15$$

Fuel, Developed Horsepower

$$B_{TF} = B_{PF}$$

$$B_{PF} = K_5 \left(\frac{W_{PF} \; H_f}{\eta_f} \right)$$

$$W_{PF} = W_{FM}$$

Fuel, Weight Flow

$$W_{TF} = W_T$$

Oxidizer, Weight Flow

$$W_{TO} = W_T - W_B$$

$$W_B = \left[\frac{2K_7 \quad H2}{\gamma_{H2}-1} \; (P_{RNC})^{\frac{2}{\gamma_{H2}}} \right]^{\frac{1}{2}} \left[1 - (P_{RNC})^{\frac{\gamma_{H2}-1}{\gamma_{H2}}} \right]^{\frac{1}{2}} \quad \frac{A_{NB} \; P_{BNI}}{(R_{H_2} T_{BIR})^{\frac{1}{2}}}$$

$$P_{RNC} = f \; (\beta_{NB}, \gamma_{H_2})$$

$$\beta_{NB} = \frac{D_{NB}}{D_B}$$

$$\gamma_{H2}, \; M_{H2} = f(T_{H2R}, R_C)$$

$$A_{NB} = K_{13} \; D_{NB}$$

$$K_{13} = 0.7854$$

$$T_{BIR} = T_{TIO} + 460$$

$$P_{BNI} = P_{TEFS}$$

$$P_{TFFS} = \text{Iteration of } P_{TEF}$$

$$P_{TEF} = P_{TEFS} \left[1 + K_8 \left(\frac{W_T}{P_{TEFS}} \right)^2 \frac{T_{H2R}}{D^4_{TEF} \; M_{H2}} \left(\frac{\gamma_{H2}-1}{\gamma_{H2}} \right) \right] \frac{\gamma_{H2}}{\gamma_{H2}-1}$$

$$K_8 = 38.8983$$

GAS GENERATOR

Mixture Ratio

$$r_G = D_1 (T_{H1})^3 + C_1 (T_{H1})^2 + B_1 (T_{H1}) + A_1$$

$A_1 = 0.2575$

$B_1 = 5.586 \times 10^{-4}$

$C_1 = -5.332 \times 10^{-9}$

$D_1 = 1.1312 \times 10^{-11}$

$T_{H1} = T_{TIFM}$

Flows

$$TC^*_{TIF} = D_2 (T_{H1})^3 + C_2 (T_{H1})^2 + B_2 (T_{H1}) + A_2$$

$A_2 = 4.4226 \times 10^3$

$B_2 = 3.2267$

$C_2 = -1.3790 \times 10^{-3}$

$D_2 = 2.6212 \times 10^{-7}$

$$P_{TIF} = P_{TIFS} \left[1 + K_8 \left(\frac{W_T}{P_{TIFS}} \right)^2 \frac{T_{H1R}}{D^4_{TIF} M_{H1}} \left(\frac{\gamma_{H1}-1}{\gamma_{H1}} \right) \right]^{\frac{\gamma_{H1}}{\gamma_{H1}-1}}$$

$K_8 = 38.8983$

NOTE: P_{TIF} is determined by iteration

$T_{HIR} = T_{TIF}$

$M_{H1}, Y_{H1}, C_p, r_{H1} = f (T_{HIR}, r_C)$

APPENDIX IV
FUEL INJECTION TEMPERATURE DATA ACQUISITION

A data acquisition problem with fuel injection temperature (TFJ-1P) below -423°F stems from the RTT resistance-temperature curve fit equation:

$$T = a_0 + a_1x + a_2x^2 + a_3x^3 + a_4x^4 + a_5x^5 + a_6x^6 *$$

where $a_0 = -423.57°F$

and x = ohms, resistance

Using this equation, as $x \to 0$, the transducer temperature reading $T \to -423.57°F$. The flight instrumentation console (FIC) amplifier is calibrated such that the output is zero when the bridge sensing resistance is equivalent to the RTT input resistance at the minimum point in the operating range. For "sea-level" testing, this equation allows fuel temperature to be measured to a limit corresponding to saturated LH_2 at one atmosphere barometric pressure. For both fuel injection RTT probes (TFJ-1P and the fuel injection temperature OK probe), the -423°F corresponds to approximately 6.1 ohms and liquid helium temperature, -452°F, corresponds to approximately 1 ohm. At an ambient pressure of approximately 0.1 psia, it is feasible that hydrogen may exist as liquid at temperatures somewhat colder than -423°F, the limit of the TFJ-1P data. A probe resistance of 3 ohms corresponds to approximately -430°F.

---

*Rocketdyne R-5711, "Flight Instrumentation Transducers Calibration and Usage," 29 June 1964.

UNCLASSIFIED
Security Classification

DOCUMENT CONTROL DATA - R & D

(Security classification of title, body of abstract and indexing annotation must be entered when the overall report is classified)

1. ORIGINATING ACTIVITY (Corporate author)
Arnold Engineering Development Center
ARO, Inc., Operating Contractor
Arnold Air Force Station, Tennessee

2a. REPORT SECURITY CLASSIFICATION
UNCLASSIFIED

2b. GROUP
N/A

3. REPORT TITLE
ALTITUDE TESTING OF THE J-2 ROCKET ENGINE IN PROPULSION ENGINE TEST CELL (J-4) (TESTS J4-1554-20 THROUGH J4-1554-26)

4. DESCRIPTIVE NOTES (Type of report and inclusive dates)
Interim Report - February 18 - April 4, 1967

5. AUTHOR(S) (First name, middle initial, last name)
M. R. Collier and N. S. Dougherty, Jr., ARO, Inc.

6. REPORT DATE	7a. TOTAL NO. OF PAGES	7b. NO OF REFS
October 1967	176	8

8a. CONTRACT OR GRANT NO	9a. ORIGINATOR'S REPORT NUMBER(S)
AF40(600)-1200 b. PROJECT NO 9194 c. System 921E d.	AEDC-TR-67-145 9b. OTHER REPORT NO(S) (Any other numbers that may be assigned this report) N/A

10. DISTRIBUTION STATEMENT Subject to special export controls; transmittal to foreign governments or foreign nationals requires approval of NASA Marshall Space Flight Center (I-E-J), Huntsville, Alabama. Transmittal outside of DoD requires approval of NASA Marshall Space Flight Center (I-E-J), *

11. SUPPLEMENTARY NOTES	12. SPONSORING MILITARY ACTIVITY
Available in DDC	NASA Marshall Space Flight Center (I-E-J), Huntsville, Alabama

13. ABSTRACT

Twenty-two start and restart transient tests of the Rocketdyne J-2 rocket engine were conducted at pressure altitudes from 95,000 to 111,000 ft in Propulsion Engine Test Cell J-4 of the Large Rocket Facility, Arnold Engineering Development Center. A flight configuration J-2 engine (S/N J-2052) and S-IVB battleship vehicle were used. Engine restarts were made at crossover duct and turbine hardware conditions predicted for coast periods of both one and two orbits. Engine starts were made at both S-IB/S-IVB and S-V/S-IVB predicted flight conditions. Firing durations were programmed for 5 or 30 sec, and the accumulated firing time for the test period was 352.26 sec. This test series completed the orbital restart problem investigation and demonstrated successful engine restart at simulated orbital conditions.

This document is subject to special export controls and each transmittal to foreign governments or foreign nationals may be made only with prior approval of NASA Marshall Space Flight Center (I-E-J), Huntsville, Alabama.

This [illegible] public release; its distribution is unlimited.

per AF Letter
dtd 12 July 74
signed William O. Cole

* Huntsville, Alabama.

DD FORM 1 NOV 65 1473

UNCLASSIFIED
Security Classification

UNCLASSIFIED
Security Classification

14 KEY WORDS	LINK A		LINK B		LINK C	
	ROLE	WT	ROLE	WT	ROLE	WT
J-2 rocket engine						
liquid-propellant rocket engines						
orbital restart						
Apollo Saturn						
vibration						
performance						

1. Rocket motors -- J-2
2. " " -- Vibration
3 " " -- Performance
4 " " -- Restart

16 - 3

UNCLASSIFIED
Security Classification